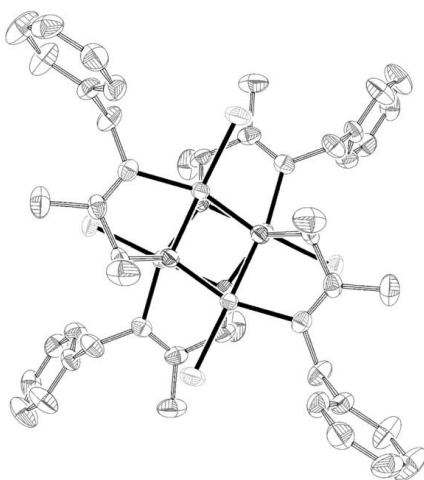




Justus-Liebig-Universität Gießen
Institut für Anorganische und
Analytische Chemie

Fachbereich
Biologie und
Chemie

Synthesis, Characterization and Reactivity of Copper Cluster Complexes



Inaugural-Dissertation zur Erlangung des
Doktorgrades der Naturwissenschaften

vorgelegt von Sabine Löw aus Wetzlar

Die vorliegende Arbeit wurde von April 2011 bis Januar 2014 am Institut für Anorganische und Analytische Chemie der Justus-Liebig-Universität Gießen unter der Betreuung von Prof. Dr. Siegfried Schindler durchgeführt.

Der Kernteil dieser Arbeit besteht aus in englischer Sprache verfassten, wissenschaftlichen Publikationen. Diese wurden bereits in Fachzeitschriften veröffentlicht oder sind in Vorbereitung zur Einreichung. Aus diesem Grund ist der wissenschaftliche Teil meiner Dissertation in englischer Sprache verfasst.

Erklärung

Ich habe die vorgelegte Dissertation selbständig und ohne unerlaubte fremde Hilfe und nur mit den Hilfen angefertigt, die ich in der Dissertation angegeben habe. Alle Textstellen, die wörtlich oder sinngemäß aus veröffentlichten Schriften entnommen sind, und alle Angaben, die auf mündlichen Auskünften beruhen, sind als solche kenntlich gemacht. Bei den von mir durchgeführten und in der Dissertation erwähnten Untersuchungen habe ich die Grundsätze guter wissenschaftlicher Praxis, wie sie in der „Satzung der Justus-Liebig-Universität Gießen zur Sicherung guter wissenschaftlicher Praxis“ niedergelegt sind, eingehalten.

Gießen, den 28.01.14

.....
Sabine Löw

Danksagung

Zuerst möchte ich mich ausdrücklich bei Herrn Prof. Dr. Siegfried Schindler bedanken, nicht nur für die interessante Aufgabenstellung, sondern vor allem auch für das entgegengebrachte Vertrauen und die Freiheit bei der Entscheidung in welche Richtung das Thema voran getrieben wird. Außerdem möchte ich mich für die große und stets gewährte Unterstützung während der letzten Jahre bedanken, dieses auch in finanzieller Hinsicht.

Ein weiteres großes Dankeschön gilt meinen Kollegen und ehemaligen Kollegen der Arbeitsgruppe Schindler für die nicht langweilig werdenden, wissenschaftlichen Diskussionen und das gute Arbeitsklima: Dr. Alexander Beitat, Dr. Jörg Müller, Dr. Anja Henß, Dr. Sabrina Schäfer, Dr. Christian Würtele, Dr. Sandra Kisslinger, Dr. Thomas Nebe, Jonathan Becker, Melanie Jopp, Lars Valentin, Janine Will, Stefan Schaub, Tobias Hoppe, Manfred Steinbach, Frank Mehlich, Natascha Kempf, Cornelius Brombach, Andreas Miska, Jolanthe Lintl und Miriam Wern. Hierbei möchte ich mich insbesondere bei Dr. Christian Würtele bedanken, der mir nicht nur geduldig die Geheimnisse der Kristallographie näher gebracht hat, sondern auch während meiner Doktorandenzeit immer ein offenes Ohr für mich hatte.

Auch möchte ich mich herzlich bei Prof. Dr. Ulrich Behrens bedanken, der mir bei allen Kristallographieproblemen unter die Arme gegriffen hat und ohne den große Teile dieser Arbeit im Unklaren geblieben wären.

Des Weiteren möchte ich mich auch bei den Mitarbeitern des Fachbereiches 08 bedanken, insbesondere denen der Analytikabteilung. Mein Dank gilt hier besonders Herrn Dr. Erwin Röcker, für die vielfach gewährte Unterstützung im Rahmen der MS-Analyse.

Ein großes Dankeschön geht zudem an den Verband der chemischen Industrie für die finanzielle Unterstützung im Rahmen des Stipendiums und an unsere Sekretärin Ursula Gorr für die freundliche Zusammenarbeit und die große Hilfe bei den notwendigen Formalien.

Zusätzlich möchte ich mich bei allen meinen ehemaligen Kommilitonen bedanken, die mir nicht nur während des Studiums, sondern auch während der Promotion immer mit Rat und auch viel Humor zur Seite gestanden haben. Unsere Semesteressen werden mir fehlen!

Nicht zu letzt geht ein riesengroßes Dankeschön an Jonathan Becker und meine Familie, die mich während meiner Arbeit immer unterstützt haben und mich auch immer wieder aufgebaut haben, wenn es nicht so lief wie geplant. Vielen Dank!

Wer sich Steine zurechtlegen kann, über die er stolpert, hat Erfolg in Naturwissenschaften.

(Erwin Chargaff)

Für meine Familie

*Für Jonathan,
seine liebevolle Unterstützung und immerwährenden Ermutigungen*

Contents

1. Introduction	1
1.1. Copper in General	1
1.2. Copper Chloride in Industrial Processes and Organic Reactions	2
1.2.1. Copper Chloride as Chlorination Reagent	3
1.2.2. Copper Chloride as Coupling Reagent	3
1.2.3. Copper Chloride as Catalyst in Oxidation Reactions .	4
1.3. Copper Cluster Complexes	7
1.4. Research Goals	10
1.4.1. Reactions of Copper(II) Chloride with Benzylamine .	10
1.4.2. Reactions of Copper(II) Chloride with Derivatives of Benzylamine and Organic Solvents	11
1.4.3. Reactions of Copper(I) Chloride with Benzylamine . .	11
2. Reactions of Copper(II) Chloride with Benzylamine	15
2.1. Reactions of Copper(II) Chloride in Solution: Facile Forma- tion of Tetranuclear Copper Clusters and Other Complexes That Are Relevant in Catalytic Redox Processes	17
2.1.1. Introduction	18
2.1.2. Results and Discussion	19
2.1.3. Conclusion	34
2.1.4. Experimental Section	35
2.1.5. Acknowledgements	39
2.2. Selected Supporting Information and Unpublished Material .	40
2.2.1. Reactivity of Cluster I	40
2.2.2. Cluster I in Oxygenation Reactions	41
2.2.3. Approaches with ZnCl ₂	47
2.2.4. Molecular Structures of the "Solvent Clusters"	49
3. Reactions of Copper(II) Chloride with Derivatives of Benzylamine and Organic Solvents	51
3.1. Investigations Concerning [Cu ₄ OCl ₆ L ₄]-Cluster Formation of CuCl ₂ with Amines and in Organic Solvents	53
3.1.1. Introduction	53
3.1.2. Experimental Section	55

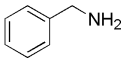
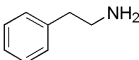
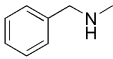
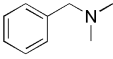
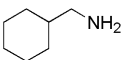
3.1.3.	Results and Discussion	62
3.1.4.	Conclusion	81
3.1.5.	Acknowledgements	82
3.2.	Selected Supporting Information and Unpublished Material	83
3.2.1.	Investigations Concerning the Catalytic Activity of "Solvent Clusters"	83
3.2.2.	Reactivity of Cluster I	84
3.2.3.	Additional Molecular Structures	88
4.	Reactions of Copper(I) Chloride with Benzylamine	91
4.1.	Synthesis, Structure and Reactivity of the Compound [Cu(C ₇ H ₇ NH ₂)Cl] ₄	93
4.1.1.	Introduction	93
4.1.2.	Results and Discussion	94
4.1.3.	Conclusion	103
4.1.4.	Experimental Section	104
4.2.	Selected Supporting Information and Unpublished Material	106
5.	Materials, Methods and Spectroscopy	109
5.1.	Materials and Methods	109
5.1.1.	Chemicals and Solvents	109
5.1.2.	Air Sensitive Compounds	109
5.1.3.	Crystallography	109
5.1.4.	Infrared Spectroscopy	110
5.1.5.	Elemental Analysis	110
5.1.6.	GC-MS Spectrometry	110
5.1.7.	UV-vis Spectroscopy	110
5.2.	Crystallography	111
5.2.1.	Crystallographic Data for Chapter 2	111
5.2.2.	Crystallographic Data for Chapter 3	147
5.2.3.	Crystallographic Data for Chapter 4	187
5.3.	Infrared Spectroscopy and Elemental Analyses	196
5.3.1.	Data for Chapter 2	196
5.3.2.	Data for Chapter 3	209
5.3.3.	Data for Chapter 4	234
6.	Summary/Zusammenfassung	237
6.1.	Summary	237
6.1.1.	Reaction of copper(II) chloride with benzylamine, its derivatives and solvent molecules	238
6.1.2.	Reaction of copper(I) chloride with benzylamine	244
6.2.	Zusammenfassung	245

6.2.1. Reaktionen von Kupfer(II)-Chlorid mit Benzylamin .	246
6.2.2. Reaktionen von Kupfer(I)-Chlorid mit Benzylamin . .	252
7. List of Figures	255
8. List of Tables	261
9. Bibliography	265
A. Publications	275
B. Curriculum Vitae	277

Table of abbreviations

dcm	dichloromethane
dmf	dimethylformamide
dmsO	dimethylsulfoxide
EtOH	ethanol
GC-MS	gas chromatography with mass spectrometry
IR	infrared
LMCT	ligand to metal charge transfer
Me	methyl
MeOH	methanol
p. a.	pro analysis
RT	room temperature
thf	tetrahydrofuran
UV-vis	ultraviolet and visible (light)

Table of ligands

L^1		benzylamine	$C_7H_7NH_2$ 107.15 g/mol
L^2		phenethylamine	$C_8H_9NH_2$ 121.18 g/mol
L^3		N-methylbenzylamine	$C_7H_7NH(CH_3)$ 121.18 g/mol
L^4		N,N-dimethylbenzylamine	$C_7H_7(CH_3)_2$ 135.21 g/mol
L^5		cyclohexylamine	$C_6H_{11}NH_2$ 99.17 g/mol
L^6		cyclohexanemethylamine	$C_7H_{13}NH_2$ 113.20 g/mol

1. Introduction

1.1. Copper in General

The earth crust contains 0.005 % copper. Barrel copper is found in North America, Chile and Australia as nuggets or dendrites. But usually copper is found as copper ore in the lithosphere. Among these ores sulfides, oxides and carbonates are most common.[1]



Figure 1.1.: Overview of the most common copper ores. [2]

Copper has always been important to mankind throughout history. But it plays an even more important role in biochemical processes. With the begin of photosynthesis ca. 2.5 billion years ago copper became an important bio-essential element. Photosynthesis led to a dramatic increase of oxygen concentration in the atmosphere and thus to the extinction of most living species on earth. However this so-called "oxygen catastrophe" was the beginning of a new form of life. The oxygen formed an oxidizing atmosphere which changed the solubility of many chemical compounds, especially iron and copper compounds. Until then copper had mostly been found as copper(I) halogenides and chalcogenides. But with an increasing

1. Introduction

oxygen concentration the copper(I) compounds were oxidized and soluble copper(II) salts occurred.[3] Due to the altered solubility of the copper salts copper became bio-available for new organisms. Copper possesses a wide redox potential for the transition $\text{Cu}^{II}/\text{Cu}^I$ and Cu^I/Cu^0 . Additionally it has a strong tendency towards single electron transfer reactions. These properties resulted in incorporation of copper ions in the active site of many enzymes.[4], [5] Today copper is known as a very important bio-element. It is often found in the active site of oxygenases, which catalyze redox reactions of organic substrates. Here laccases are important examples. They are widely spread in nature and often are of fungal origin. Fungal laccases for example are involved in lignin degradation and thus play an important role in the ecosystem.[6] Another major task of copper enzymes is the activation of oxygen and its transfer to organic molecules. An important example is tyrosinase which catalyzes the hydroxylation of phenols and thus is involved in the browning of vegetables when cut.[7] Furthermore copper enzymes play an important role in the transport, regulation and storage of copper. The group of copper enzymes is quite complex: The incorporation of copper ions into the active sites is observed from one single copper ion in azurin [8] to two copper ions in tyrosinase [9] and furthermore to multi nuclear copper centers with four copper ions per active site in laccases.[10], [11]

1.2. Copper Chloride in Industrial Processes and Organic Reactions

High reactivity, selectivity and easy handling make enzymes perfect catalysts. Some of them have already been tested in industrial applications. Laccases for example are used in pulp bleaching, textile dye decolorization, detergents, bioglueing and detoxification.[12] Besides complex copper enzymes simple copper compounds are often used as well. Among these salts such as copper(I) and copper(II) chlorides are widely used in industrial processes as well as in organic synthesis. There are three major applications for copper chloride:

1. As chlorination reagent
2. As coupling reagent
3. And as catalyst in oxidation reactions

A selection of important and interesting reactions is reported below.

1.2.1. Copper Chloride as Chlorination Reagent

Copper halogenides are often used as halogenation reagents. A prominent example for a chlorination reaction with CuCl is the Sandmeyer reaction (see Figure 1.2).[13] It describes the conversion of a diazonium salt to an arylhalogenide and so is a powerful tool to introduce electron withdrawing groups in aromatic systems. The reaction is catalyzed by CuCl but also runs with CuBr and other anions. A radical mechanism is proposed for the reaction.

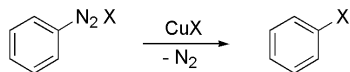
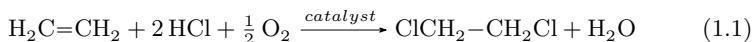


Figure 1.2.: General reaction equation for the Sandmeyer reaction.

Another example for copper chloride as chlorination reagent is the industrial chlorination of acetylene:



The reaction requires a high temperature and pressure (190-250 °C, 3-5 bar). A mixture of CuCl₂ and Al₂O₃ is used as a catalyst.[14] The product dichloroethane is obtained in 98-99% yield.

1.2.2. Copper Chloride as Coupling Reagent

Copper chloride is widely used as a coupling reagent as well. Here the Glaser reaction is very famous and for this reason has been extensively reviewed.[15] In this reaction two terminal alkynes are linked to give a symmetrical 1,3-diyne (see Figure 1.3).

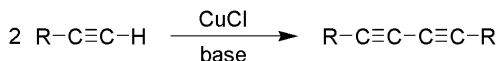


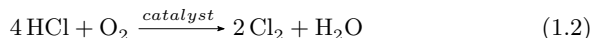
Figure 1.3.: General reaction equation for the Glaser reaction.

Glaser discovered this reaction in 1869.[16] Since then many improvements have been made which includes the use of CuCl₂ instead of CuCl (Eglinton coupling).[17] Apart from this reaction many other coupling reactions are catalyzed by CuCl₂ or CuCl as well.[18]

1. Introduction

1.2.3. Copper Chloride as Catalyst in Oxidation Reactions

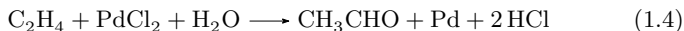
Another broad field of application is the use as a catalyst in oxygenation reactions. Already in the 1860s Henry Deacon discovered the activity of CuCl_2 as a catalyst in the oxidation of HCl . [19] His idea became known as Deacon process and describes the reaction of HCl with oxygen and copper(II) chloride to give chlorine and water:



Although it is an easy chemical way to oxidize HCl , the practical implementation suffered from many difficulties which prevented a long-lasting industrial realization of this process. More recently these difficulties have been pointed out in regard to modify this process by the use of new catalysts. [20] Another industrial process which makes use of CuCl_2 in an oxidation reaction is the synthesis of acetaldehyde: [21]



This process which uses a mixture of PdCl_2 and CuCl_2 as catalyst is known as the Wacker-Hoechst-Process. It was developed at the beginning of the 1960s and was one of the first processes which used alkenes as educts. The reaction conditions are comparatively harsh, high temperatures and pressure (120-130 °C, 3-5 bar) are required. The actual catalyst is PdCl_2 which is reduced to elemental palladium during the reaction:



CuCl_2 converts the resulting palladium back into PdCl_2 . This step leads to copper(I) chloride which is oxidized by oxygen to CuCl_2 again.



The reaction mechanism is not yet fully clarified. A proposed mechanism is shown in Figure 1.4.

1.2. Copper Chloride in Industrial Processes and Organic Reactions

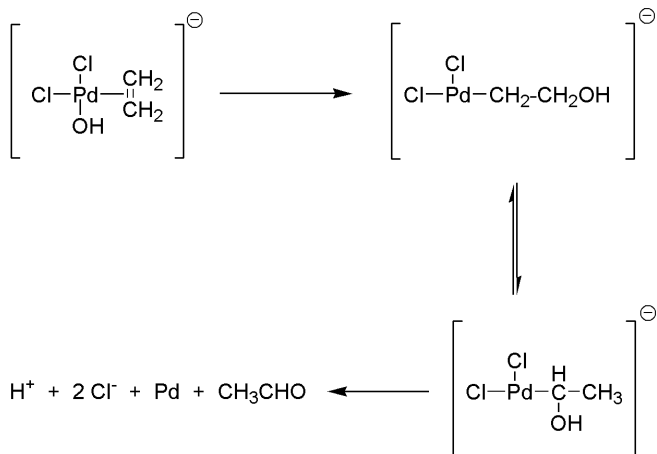


Figure 1.4.: Proposed mechanism for the Wacker-Hoechst-Process: Acetylene is coordinated and a hydroxido- π -acetylene-palladium-complex is formed. Due to rearrangement the σ -complex is formed which decomposes to the final products.

The complexation of acetylene as a first step to give a hydroxido- π -acetylene-palladium-complex is very likely. This complex rearranges to a σ -complex which then decomposes to the final products. Copper chloride furthermore is used as a catalyst for synthetic applications in organic chemistry as well.[18] An interesting example is the oxidation of benzene to phenol.[22] The stability of the aromatic C-H-bond makes benzene very unreactive and thus difficult to activate. However phenols are important basic materials for industrial processes. It is a future goal to develop inexpensive catalysts that convert benzene with oxygen as a green oxidant to phenol. For this purpose CuCl has been tested as well as a potential catalyst. The reaction is performed at room temperature in aqueous H_2SO_4 (see Figure 1.5) and gives a mixture of phenol and hydroquinone.

1. Introduction

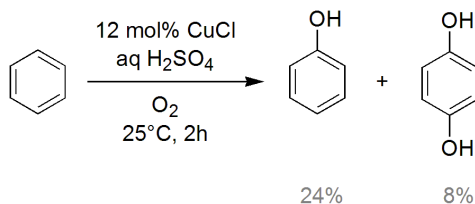


Figure 1.5.: Equation for the oxidation of benzene according to [22].

Phenol itself may be oxidized again. Tyrosinase (as already described above) is a natural example of a catalyst that both hydroxylates and oxidizes phenols. Since the incorporation of copper ions in the active site of tyrosinase it is not very surprising that copper compounds show similar activity in the oxidation of phenols. Takehira and co-workers reported the oxygenation of phenols to *p*-quinones with a pyridine-CuCl₂-complex in dmsO (see Figure 1.6).[23] Immobilization of this complex onto a solid phase resulted in similar yields.

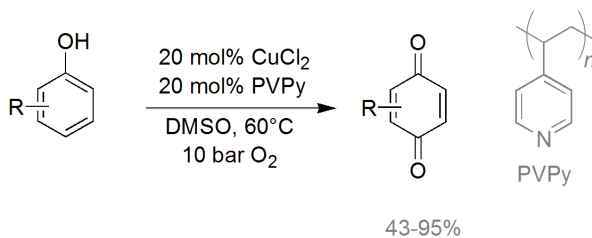


Figure 1.6.: Equation for the oxidation of phenol according to [23].

Another synthetic difficulty is the selective hydroxylation of aliphatic C-H-bonds. Aliphatic C-H-bonds are very strong as well and so it is very challenging to attack them via a radical process which is typical for oxygenation with copper compounds and oxygen. This leads to low selectivity and low yields. So usually a mixture of alcohols and ketones is obtained. Comparatively good yields are obtained by using CuCl₂, 18-crown-6, acetaldehyde and oxygen (see Figure 1.7), but still a mixture of products is obtained.[24], [25]

1.3. Copper Cluster Complexes

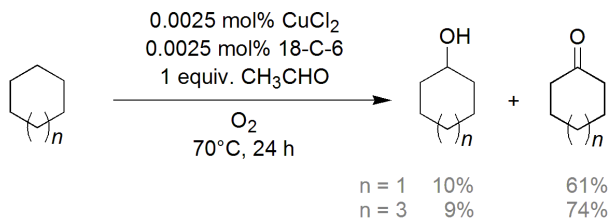


Figure 1.7.: Equation for the oxygenation of alkanes according to [24], [25].

Copper chloride (both CuCl and CuCl₂) seems to be a potential catalyst for a broad range of reactions. Its application as industrial catalyst as well as in many organic reactions emphasizes its importance as catalyst. However in most cases the reaction mechanisms are not clear, very little is known about the active species. Many of the described reactions involve more than one electron transfer (generally 2 or 4 electrons are transferred). This makes copper chloride very unlikely as active species because it can only store/provide one electron per molecule due to only one copper ion per molecule. In nature complex redox reactions with more than one electron transfer are carried out by either multi nuclear copper centered enzymes or by the use of an organic co-factor which may store/provide one additional electron.[10], [26] This concept is rather difficult to assign to simple copper salts such as CuCl and CuCl₂. In some cases ligands which may act as an organic co-factor have been added to the reaction. However mostly that is not the case - and the reaction mechanism cannot be explained easily.

1.3. Copper Cluster Complexes

As described above simple copper salts undergo a variety of different oxidation reactions. However the reaction mechanisms are not always clarified. In view of this it would be interesting to consider multinuclear copper compounds concerning their reaction behavior. Multinuclear copper compounds are - in contrast to simple copper salts - able to store/provide more than one electron during redox reactions. Hence they can be seen as potential model systems for multinuclear copper enzymes, which makes them interesting for organic synthesis. There are two prominent structure types of multinuclear copper(II) compounds, both are shown in Figure 1.8.

1. Introduction

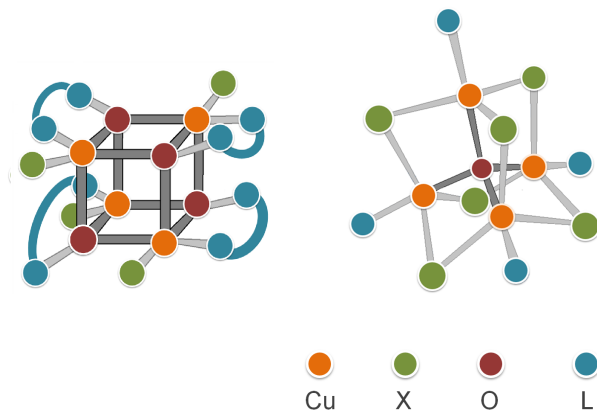


Figure 1.8.: Schematic presentation of the cubane unit $\text{Cu}_4\text{O}_4\text{L}_4\text{X}_4$ (*left*) and $\text{Cu}_4\text{OX}_6\text{L}_4$ (*right*)(e.g., X = chloride).

Both cluster types are known since the 1960s. The first cluster of the $\text{Cu}_4\text{OCl}_6\text{L}_4$ type was synthesized by J. A. Bertrand et al.[27] The central oxygen is tetrahedrally coordinated by four copper ions which are coordinated themselves by additional ligands. The ligands may be of organic nature or halogenides. They can influence the geometry of the Cu_4O -core so that ideal tetrahedrons as well as distorted tetrahedrons have been observed. There are two synthetic routes to prepare copper clusters of the $\text{Cu}_4\text{OCl}_6\text{L}_4$ type. The easiest way is to heat CuO , CuCl_2 and the ligand in absolute methanol under reflux.[28] The synthesis must be carried out under inert conditions and good yields are obtained. An alternative donor for the central oxygen in the Cu_4O -core is NaOH . Additionally traces of water may also provide the central oxygen.[29] Some of these obtained copper clusters showed interesting properties concerning magnetism and structural motifs. This led to a strong increase of publications about copper clusters of this type during the 1960s and 1970s.[27]-[41] But all compounds suffered from instability towards moisture. This and lacking applications led to a strong decrease of interest in the 1980s. However more recently there is a growing number of reports about copper clusters of this type which were found by accident, only few examples are given in the references.[42]-[48] In 1989 the mineral ponomarevite, which was found at the volcano Tolbachik (Kamchatka, Russia), was structurally characterized for the first time.[49] It turned out to be a copper cluster of the chemical formula $\text{K}_4[\text{Cu}_4\text{OCl}_{10}]$, which was identical with the in 1972 synthesized copper cluster by J. de Boer et al.[34] Ponomarevite is

found at volcanic fumaroles, where it is formed at high temperatures between 280-450 °C. Just as the synthetic compounds ponomarevite is sensitive towards moisture and decomposes to $K_2CuCl_4 \cdot 2H_2O$ (mitscherlichite) in air (see Figure 1.9).



Figure 1.9.: *Left:* Crystalline ponomarevite [50]: The red ponomarevite decomposes in air to turquoise mitscherlichite. *Right:* The volcano Tolbachik in Kamchatka, where ponomarevite was found. [51]

The synthesis of the second prominent copper cluster, $Cu_4O_4Cl_4L_4$ (cubane structure), occurs through self-arrangement of the ligand system with copper salts. Simple ligands as acetylacetonate-derivatives form cubane copper compounds with the corresponding copper salt.[37] However in some cases syntheses of these compounds can be quite a challenge.[52] Just as the copper clusters of the kind $Cu_4OCl_6L_4$ the cubane clusters were investigated because of interesting magnetic properties. But a lack of applications as well as synthetic problems led again to a decrease of interest in the 1990s.

Although multinuclear copper clusters seem to be promising candidates in catalytic reactions, the activity of such copper clusters remained undetected for several years. Only in 2002 the catalytic activity of a cubane cluster was discovered.[38] Further success was made by Kirillov et al. when they used a tetranuclear copper cluster and H_2O_2 to oxidize aliphatic C-H-bonds.[53], [54] In the last years there have been further reports about the catalytic activity of cubane clusters.[39], [40] In addition catalyses with other tetranuclear copper clusters were reported.[38], [41], [53]-[57] The hydroxylation of methane is probably most interesting among these reports.[57] Although there are many promising experiments the synthesis of an optimized copper catalyst remains a challenge in many cases.

1.4. Research Goals

As described above copper compounds (and simple copper salts as copper chloride especially) are very useful in catalysis. This is emphasized by a broad field of applications among industrial processes as well as in organic synthesis. However it is difficult to explain the catalytic activity of simple copper salts in many cases because of the discrepancy between the ability and the need for storing/providing electrons in catalytic redox reactions. Multinuclear copper compounds can store/provide more electrons than mononuclear copper salts and hence seem to be even more promising candidates than copper chloride in catalytic redox reactions. However in both cases reaction mechanisms are not clarified yet. Hence it is an important task to investigate the reactivity of both - simple copper salts and multinuclear copper compounds - in order to obtain a better understanding of catalytic reactions with copper compounds. This in turn is important for the modification, use and development of existing and new copper catalysts. The topic of the present work hence is the investigation and comparison of the catalytic activity of copper(II) chloride and the multinuclear copper cluster complex "cluster I" in redox reactions. Cluster I is a μ_4 -oxido cluster of the formula $2[\text{Cu}_4\text{OCl}_6\text{L}^1_4] \cdot [\text{CuL}^1_2\text{Cl}_2]$ ($\text{L}^1 = \text{benzylamine}$) and was obtained during my master thesis.[58] Cluster I is characterized by a simple synthetic route, low educt costs and an enormous stability in air towards moisture.[58] These features made cluster I a perfect candidate for a potential application as catalyst in redox reactions.

In order to gain more insight into the reactivity and mode of operation of the copper compounds described above several redox reactions were analyzed using the copper cluster as well as copper chloride as catalysts. Thus it was essential to investigate the reactivity of the copper compounds in solution due to complex equilibria with additional copper species. For clarity the results are presented in three parts.

1.4.1. Reactions of Copper(II) Chloride with Benzylamine

Chapter 2 describes the reactivity of cluster I and copper chloride in comparison. The following results are discussed in detail:

- Cluster I was in a complex chemical equilibrium with other copper compounds. After a large number of experiments it was finally possible to characterize most of these colorful compounds. Their molecular structures are presented and the role of cluster I during the formation

of these compounds is discussed.

- The catalytic activity of cluster I and copper(II) chloride was investigated. Therefore both compounds were tested in the oxygenation of cyclohexane and n-hexane and the selective oxidation of *p*-chlorobenzylalcohol.
- Based on copper(II) chloride the synthesis and structural characterization of several so-called "solvent clusters" of the type $[\text{Cu}_4\text{OCl}_6\text{L}_4]$ ($\text{L} = \text{MeOH}$, acetonitrile, dmf, dmsO) was performed. The connection between cluster I, copper chloride and the "solvent clusters" as possible connectors is discussed.

1.4.2. Reactions of Copper(II) Chloride with Derivatives of Benzylamine and Organic Solvents

Chapter 3 describes structural modifications of cluster I including the ligand, the halogenide and the central oxygen. As described above clusters of the type $\text{Cu}_4\text{OCl}_6\text{L}_4$ are found most often by accident if organic molecules are mixed with copper chloride. Little is known about the cluster formation itself and it seems to be impossible to predict occurrence of a cluster instead of a simple complex. The understanding of the cluster formation based on copper chloride in solution is important in order to understand the catalytic activity of copper chloride. Thus many experiments concerning cluster formation were carried out. The following results are discussed in detail:

- The modification of the ligand, halogenide and the central oxygen did not always lead to cluster formation. Instead the formation of copper complexes or simple copper salts was observed. The influence of the modifications named above is discussed in more detail.
- In order to investigate the reactivity of $\text{CuCl}_2 \cdot 2\text{H}_2\text{O}$ towards organic solvents, it was recrystallized in diverse organic solvents. The compounds obtained are discussed in more detail.
- The catalytic activity of cluster I and the compounds obtained was tested and compared. The results are discussed in more detail.

1.4.3. Reactions of Copper(I) Chloride with Benzylamine

Chapter 4 describes the reaction of copper(I) salts towards benzylamine. As described in chapter 2 cluster I was in a chemical equilibrium with copper(I)

1. Introduction

species. Hence it was important to investigate the reactivity of copper(I) salts towards benzylamine as well. In addition the reactivity of the obtained compound $[\text{Cu}_4\text{Cl}_4\text{L}^1_4]$ ($\text{L}^1 = \text{benzylamine}$) towards dioxygen was investigated. The results are discussed in more detail:

- The synthesis and structure of $[\text{Cu}_4\text{Cl}_4\text{L}^1_4]$ ($\text{L}^1 = \text{benzylamine}$) is reported. Additionally the reaction of CuBr , CuI and CuCl towards benzylamine under atmospheric conditions was investigated.
- The reactivity of $[\text{Cu}_4\text{Cl}_4\text{L}^1_4]$ ($\text{L}^1 = \text{benzylamine}$) towards dioxygen and as a catalyst in oxidation reactions was investigated.

2. Reactions of Copper(II) Chloride with Benzylamine

This chapter contains one publication that was published in the journal "Chemistry - A European Journal" previously. Selected parts of the Supporting Information and unpublished results are shown additionally. The complete Supporting Information can be found in the online library of the journal (<http://onlinelibrary.wiley.com/journal/10.1002/%28ISSN%291521-3765/issues>).

Contribution of the co-authors:

Except Andreas Miska, who crystallized the compounds **4a** and **7**, the co-authors solved several of the crystal structures, to detail:

- J. Becker: **4a**, $\text{HC}_{13}\text{H}_{19}\text{NOCl}$ and "MeOH-cluster"
- C. Würtele: Cluster I and bromide version of cluster I
- C. Kleeberg: Support in the determination of cluster II
- U. Behrens: **2**, **3**, cluster II, **7** and $[\text{Cu}(\text{MeOH})_2\text{Cl}_2]$
- O. Walter: $[\text{Cu}(\text{aniline})_2\text{Cl}_2]$ and $[\text{Zn}(\text{benz}_2\text{dba})\text{Cl}_2]$

2.1. Reactions of Copper(II) Chloride in Solution: Facile Formation of Tetranuclear Copper Clusters and Other Complexes That Are Relevant in Catalytic Redox Processes

This work has been published previously in "Chemistry - A European Journal".

Sabine Löw, Jonathan Becker, Christian Würtele, Andreas Miska, Christian Kleeberg, Ulrich Behrens, Olaf Walter and Siegfried Schindler

Chem. Eur. J. **2013**, 19, 5342-5351

Mixing $\text{CuCl}_2 \cdot 2\text{H}_2\text{O}$ with benzylamine in alcoholic solutions led to an extremely colorful chemistry caused by the formation of a large number of different complexes. Many of these different species could be structurally characterized. These include relatively simple compounds such as $[\text{CuL}^1_4\text{Cl}_2]$ ($\text{L}^1 = \text{benzylamine}$) and $(\text{HL}^1)_2[\text{CuCl}_4]$. Most interestingly is the easy formation of two cluster complexes, one based on two cluster units $\text{Cu}_4\text{OCl}_6\text{L}^1_4$ connected through one $[\text{Cu}(\text{L}^1)_2\text{Cl}_2]$ complex and one based on a cubane-type ($[\text{Cu}_4\text{O}_4](\text{C}_{11}\text{H}_{14})_4\text{Cl}_4$) cluster. Both clusters proved to be highly reactive in a series of oxidation reactions of organic substrates using air or peroxides as oxidants. Furthermore, it was possible to isolate and structurally characterize $([\text{Cu}(\text{L}^1)\text{Cl}]_3$ and $[\text{Cu}(\text{benz}_2\text{mpa})_2]\text{CuCl}_2$), two copper(I) complexes that formed in solution, demonstrating the high redox activity of the cluster systems. In addition it was possible to solve the molecular structures of the compounds $\text{Cu}_4\text{OCl}_6(\text{MeOH})_4$, $[\text{Cu}(\text{MeOH})_2\text{Cl}_2]$, $[\text{Cu}(\text{aniline})_2\text{Cl}_2]$ and an organic side product ($\text{HC}_{13}\text{H}_{19}\text{NOCl}$). In fact all determined structures are of a known type but the chemical relation between these compounds could be explained for the first time. The paper describes these different compounds and their chemical equilibria. Some of these complexes seem to be relevant in catalytic oxidation reactions and their reactivity is discussed in more detail.

2.1.1. Introduction

Copper complexes that form clusters of the type $\text{Cu}_4\text{OX}_6\text{L}_4$ ($\text{X} = \text{halogen}$, $\text{L} = \text{ligand}$ or X) or $\text{Cu}_4\text{O}_4\text{L}_4\text{X}_4$ (cubane-type structure) are already known since the 1960s.[27]-[41] Both basic structural units are shown in Figure 2.1. Such multicopper compounds have been investigated especially in regard to their magnetic properties.[27], [33], [37], [39], [40], [60]-[66] However, synthesis of such compounds in some cases can be quite a challenge. Furthermore, several compounds of the formula $\text{Cu}_4\text{OX}_6\text{L}_4$ were sensitive towards moisture and/or oxygen and therefore difficult to handle.[28], [29], [31]

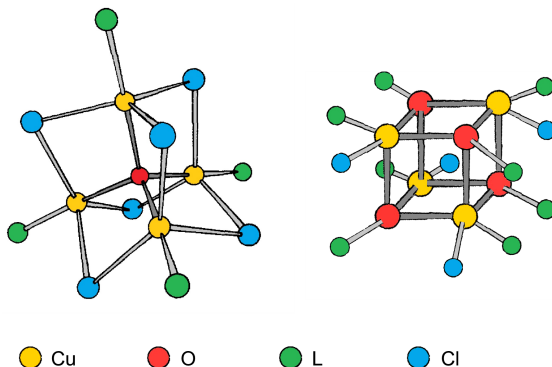


Figure 2.1.: Schematic presentation of the $\text{Cu}_4\text{OX}_6\text{L}_4$ and cubane unit $\text{Cu}_4\text{O}_4\text{L}_4\text{X}_4$ (e. g. $\text{X} = \text{chloride}$).

A lack of applications and the described synthetic difficulties led to a strong decrease of interest in these compounds during the last decades. Finally, in 2002 catalytic properties of the cubane element in redox reactions were recognized.[38] Since then multicopper compounds have been used as catalysts for oxidation reactions such as hydroxylation of CH -bonds and oxidation of catechol.[39], [40], [53]-[57] However, so far there is no detailed understanding of the reactivity of these compounds. This is quite unfortunate because multicopper systems have the advantage to provide/accept more than one electron in a redox reaction, a concept that is well known in nature from the active site in a large number of metalloenzymes.[67]

Here we describe the facile preparation of both cluster types in solution from $\text{CuCl}_2 \cdot 2\text{H}_2\text{O}$ and benzylamine. Especially cluster I seems to be quite useful

in catalytic oxidation reactions. During our investigations on the reactivity of cluster I we observed the formation of a large number of copper complexes strongly depending on reaction conditions. Most of these complexes could be structurally characterized and the chemical relationship between these compounds could be explained.

2.1.2. Results and Discussion

Due to our interest in copper complexes and their reactivity towards dioxygen [68]-[72] we had started to investigate the reaction of copper(II) salts with different amines. When reacting $\text{CuCl}_2 \cdot 2\text{H}_2\text{O}$ with benzylamine (L^1) we expected to obtain $[\text{Cu}(\text{L}^1)_2\text{Cl}_2]$ a simple copper amine complex that had been structurally described previously.[73] However, when characterizing our product we observed that by chance a polynuclear copper complex had formed similar to previous investigations on different systems.[29], [33] While expected $[\text{CuL}^1_2\text{Cl}_2]$ still formed, it co-crystallized with two $\text{Cu}_4\text{OCl}_6\text{L}^1_4$ cluster units (the outcome of the reaction is strongly dependent on reaction conditions, see below). The molecular structure of what we call "cluster I" is shown in Figure 2.2.

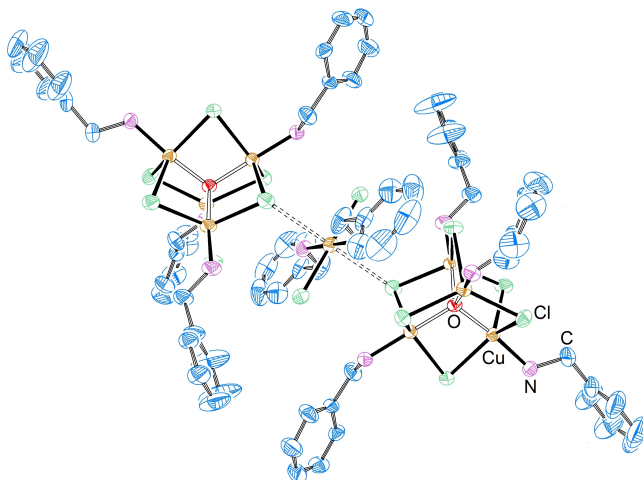


Figure 2.2.: Molecular structure of cluster I (hydrogen atoms and crystallized solvent molecules are omitted for clarity. Ellipsoids are drawn at the 50% probability level.).

2. Reactions of Copper(II) Chloride with Benzylamine

Crystallographic data, bond lengths and angles of cluster I $\cdot 2\text{CH}_3\text{OH}$ are reported in the Supporting Information. When reacting CuBr_2 instead of $\text{CuCl}_2 \cdot 2\text{H}_2\text{O}$ with benzylamine the same structural unit formed, the $[\text{CuL}^1_2\text{Br}_2]$ complex co-crystallized with two $\text{Cu}_4\text{OBr}_6\text{L}^1_4$ cluster units (see SI). Cluster I is formed without any problems in large quantities as an olive green powder (Figure 2.3) that deposited immediately after the reaction is completed (a few seconds).

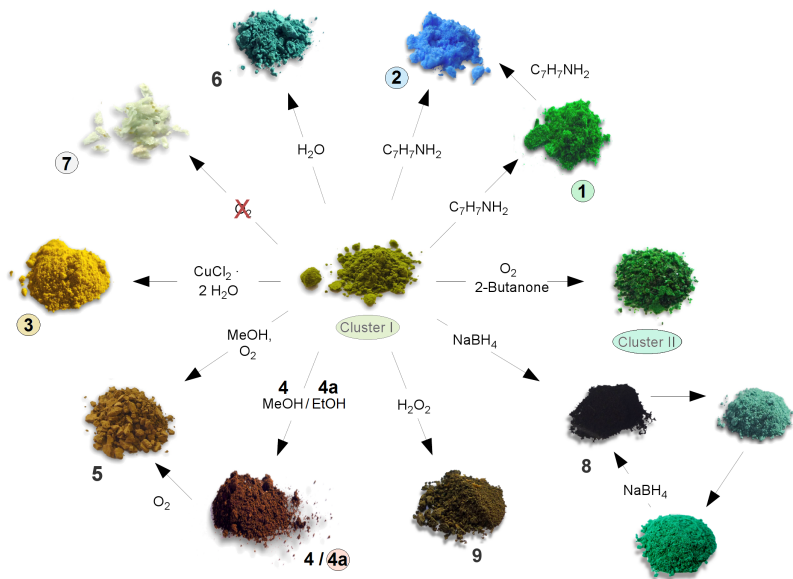


Figure 2.3.: Overview of the color range of cluster I and related compounds (compounds that have been structurally characterized are encircled).

In contrast to other clusters of the type $\text{Cu}_4\text{OX}_6\text{L}_4$ cluster I is not sensitive towards air which is mirrored in the facile synthesis of cluster I. The molecular structure is quite interesting because it formed a cluster dimer that is "connected" through a $[\text{CuL}^1_2\text{Cl}_2]$ unit (Cu5-Cl14 distance 3.06 Å compared to Cu1-Cl11 bond lengths of 2.44 Å in the cluster unit and 2.32 Å (Cu5-Cl17) in the complex). Interestingly, so far we could not detect formation of $\text{Cu}_4\text{OCl}_6\text{L}^1_4$ alone, only cluster I formed in all our samples. The central oxide ion in these complex units is tetrahedrally coordinated to four cop-

2.1. Reactions of Copper(II) Chloride in Solution

per(II) ions as described above. The oxygen atom derives from water present in solution. [27], [29], [35]

Especially interesting was the observation that depending on concentrations and solvents solutions with a huge color range were obtained. Furthermore, in most cases color changes occurred while standing. If the samples were not stirred, strong color gradients within particular samples were observed as shown for a Schlenk tube in Figure 2.4. Especially this finding tempted us to investigate the chemistry of these complexes further, however it also clearly demonstrated the complexity of the system.

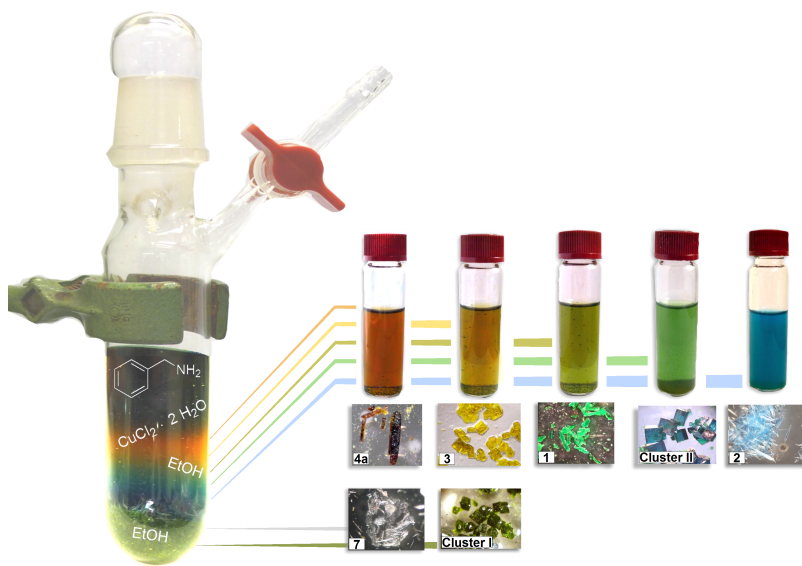


Figure 2.4.: Detailed view of a section in a flask containing a mixture of benzylamine (0.2 mol/L), $\text{CuCl}_2 \cdot 2 \text{H}_2\text{O}$ (0.1 mol/L) in denatured ethanol (contains 2-butanone); the mixture wasn't stirred for a day so that the whole color gradient became visible. The different species could be isolated and crystallized as described in the text.

To the best of our knowledge investigations on the reactivity of clusters of the type $\text{Cu}_4\text{OX}_6\text{L}_4$ have not been reported so far. Furthermore, we are only aware of one important report by Fenton and co-workers where similar color

2. Reactions of Copper(II) Chloride with Benzylamine

changes due to cluster formation were reported for copper(II) complexes with the ligand teed (teed = N,N,N',N'-tetraethylethylenediamine).[74] The authors already were quite successful in understanding the reactivity of this complex system, however, here the situation is even more complicated due to an additional radical reaction of teed with copper(II) ions leading to ligand decomposition.

Adding benzylamine in slight excess to cluster I first led to a green material (compound **1**, Figure 2.3) that could be structurally characterized. As primarily expected $[\text{CuL}^1_2\text{Cl}_2]$ (**1**) is formed that has been described previously.[73] If benzylamine was added in a large excess compound **2** formed, a blue complex (Figure 2.3) that could be structurally characterized and turned out to be octahedral $[\text{CuL}^1_4\text{Cl}_2]$. Its molecular structure is shown in Figure 5.5 (crystallographic data are reported in the Supporting Information).

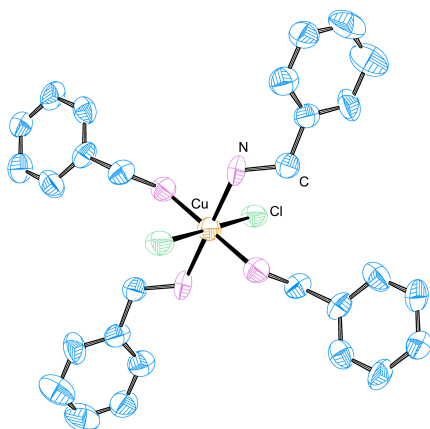


Figure 2.5.: Molecular structure of $[\text{CuL}^1_4\text{Cl}_2]$ (**2**), hydrogen atoms are omitted for clarity. Ellipsoids are drawn at the 50% probability level.

In contrast, if the amount of $\text{CuCl}_2 \cdot 2\text{H}_2\text{O}$ was increased a very pretty golden compound, **3** (Figure 2.3), was formed that turned out to be $(\text{HL}^1)_2[\text{CuCl}_4]$. The molecular structure of **3** is shown in Figure 2.6 (crystallographic data are reported in the Supporting Information). Here benzylamine is protonated with $[\text{CuCl}_4]^{2-}$ as an anion. Complex salts of this type are well known in the literature.[75], [76] Together with water cluster I reacted to a turquoise

powder (compound **6**, Figure 2.3) that so far could not be characterized.

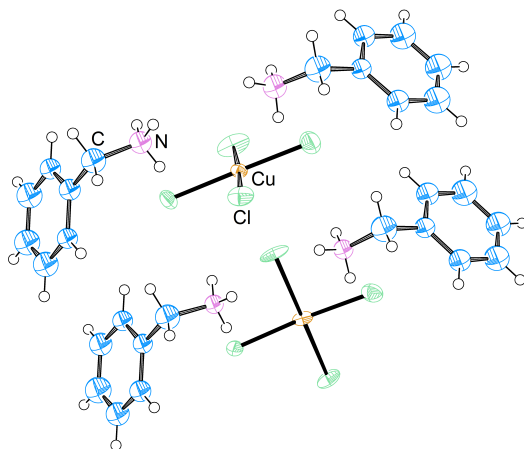


Figure 2.6.: Molecular structure of $(\text{HL}^1)_2[\text{CuCl}_4]$ (**3**). Ellipsoids are drawn at the 50% probability level.

Very surprising was our observation that leaving suspensions/solutions of cluster I in methanol (as well as in other solvents) caused a color change from green to red and a red brown powder (compound **4**) could be isolated. Enforcing the reaction by bubbling air through the solution allowed us to isolate an orange brown solid (compound **5**, Figure 2.3). Unfortunately, so far despite much effort neither **4** or **5** could not be identified when obtained from solutions in methanol. In this context it is very important to distinguish between methanolic and ethanolic solutions because of the butanone in ethanolic solutions (see below). Butanone is present in ethanol because it is added to commercial ethanol to avoid its usage as drinking alcohol (declared in Germany as denatured ethanol).

Most exciting however was the finding that a suspension of cluster I in denatured ethanol caused the formation of a second different cluster ("cluster II") of the cubane type (Figure 2.1). The dark green colored crystals that had formed (Figure 2.3) could be structurally characterized and the molecular structure of cluster II is shown in Figure 2.7 (crystallographic data are reported in the Supporting Information).

2. Reactions of Copper(II) Chloride with Benzylamine

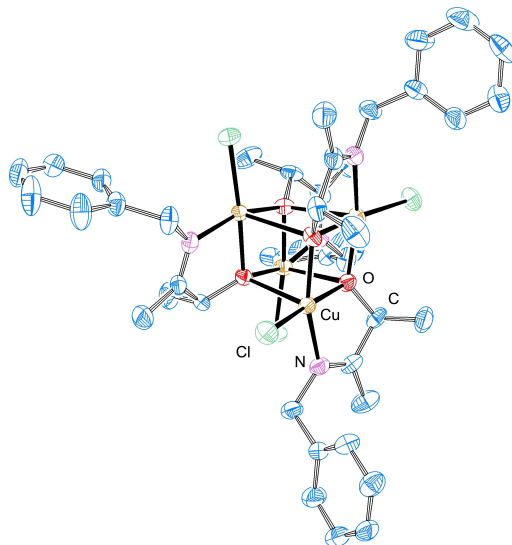
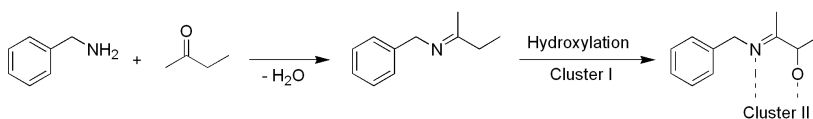


Figure 2.7.: Molecular structure of cluster II ($[\text{Cu}_4\text{O}_4](\text{C}_{11}\text{NH}_{14})_4\text{Cl}_4$), hydrogen atoms omitted for clarity. Ellipsoids are drawn at the 50 % probability level.

The new ligand is obviously formed by condensation between benzylamine and 2-butanone and selective hydroxylation of this compound by cluster I according to the following equation:



Again cluster II can be easily prepared and is obtained reproducibly in acceptable yields. This seems to be the first time that such a cluster could be obtained in a self-assembly reaction caused by a selective oxidation reaction of an in situ formed ligand. Here it is very important to point out that while hydroxylation reactions are common during the reaction of copper(I) complexes with dioxygen, to the best of our knowledge such a reaction so far

2.1. Reactions of Copper(II) Chloride in Solution

has never been observed starting with a copper(II) compound. This indicates that it is most likely that redox reactions cause formation of copper(I) complexes that afterwards will lead to ligand hydroxylation in the presence of dioxygen. Support for the formation of copper(I) complexes was obtained when cluster I was kept overnight in denatured ethanol excluding air. Again, the solution turned to a red color, however this time a colorless material crystallized in good yields (compound **7**, Figure 2.3) instead of formation of cluster II. These colorless crystals are very sensitive towards air and moisture and turn to a green color under air. Despite the fact that it was very difficult to obtain suitable crystals for structural analysis (due to crystallization in a layered structure), we were able to determine the molecular structure of this complex (Figure 2.8, crystallographic data are reported in the Supporting Information). The structure shows that $[\text{Cu}(\text{L}^1)\text{Cl}]_3$, a trimer, has formed.

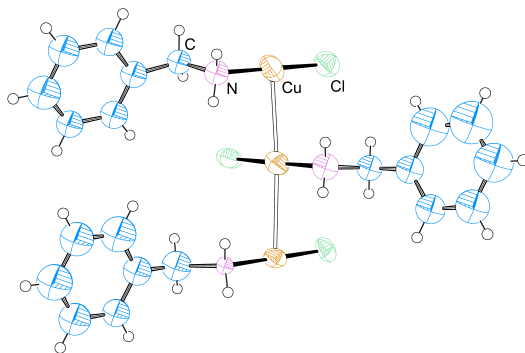


Figure 2.8.: Molecular structure of compound **7**. Ellipsoids are drawn at the 50 % probability level.

It is obvious that this trimer is only a small piece of a long linear polymeric chain in the crystals, explaining the layered structure. It is important to point out that here weak unsupported $\text{Cu}^I \cdots \text{Cu}^I$ interactions are observed that are documented with distances of 2.88 and 2.93 Å between the copper ions. Structures of this type are interesting with regard to the $\text{Cu}^I \cdots \text{Cu}^I$ interactions that are not enforced by the ligand environment.[77]-[80] The reason for this behavior is not quite clear and has been discussed previously in literature.[79] Unsupported $\text{Cu}^I \cdots \text{Cu}^I$ interactions have been reported with distances in the range of 2.65-3.02 Å in comparison to the sum of the van der Waals radii (2.80 Å).[80]

Efforts to obtain this copper(I) species by reducing cluster I with NaBH_4

2. Reactions of Copper(II) Chloride with Benzylamine

in methanol were not successful. First, a black powder was obtained, then after prolonged stirring (10-20 min) a turquoise/bluish compound formed that turned green afterwards (Figure 2.3). This cycle could be repeated several times, however, phases to reach the different colors became longer. Again, so far these compounds could not be characterized.

Further evidence for the presence of a copper(I) species in solution was obtained when red crystals could be isolated together with compound **7** from a red-colored ethanolic (denatured) solution of cluster I. Especially here it was important to find the right conditions and timing to isolate these crystals from the red solution. It took a lot of time and a large number of attempts to finally crystallize this species. The amount of dioxygen available has a huge influence on the outcome of the reaction (species and hence, color). If no or only a small amount of dioxygen was available the solution turned to a red color and colorless crystals formed (compound **7**). If dioxygen is present, for example, due to air entering the open flask, the solution again turned to a red color, however this time dark green crystals formed (cluster II). In both cases it was possible only after many attempts to obtain a few red crystals co-crystallized with colorless crystals (compound **7**). Usually the red compounds did not crystallize leading only to intensively red-colored solutions. The molecular structure of the red compound **4a** is presented in Figure 2.9 (crystallographic data are reported in the Supporting Information).

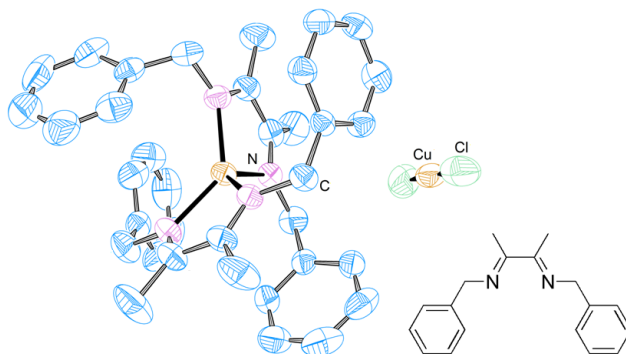
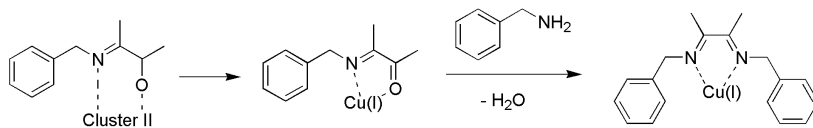


Figure 2.9.: Molecular structure of $[\text{Cu}(\text{benz}_2\text{mpa})_2]\text{CuCl}_2$ (compound **4a**, benz_2mpa = benzyl-(2-benzylimino-1-methyl-propylidene)-amine), hydrogen atoms are omitted for clarity. Ellipsoids are drawn at the 50% probability level. An additional Lewis structure of the ligand is presented for clarity.

2.1. Reactions of Copper(II) Chloride in Solution

The ligand of **4a** is probably formed by oxidation of the ligand of cluster II and consecutive condensation with benzylamine according to the following equation:



The oxidation of the alcoholate leads to a copper(I) species, which may now form a copper(I) complex with the new Schiff base ligand benzyl-(2-benzylimino-1-methyl-propylidene)-amine and CuCl_2^- as anion. It is remarkable that the compound **7**, cluster II and the red material **4a** ($[\text{Cu}(\text{benz}_2\text{mpa})_2]\text{CuCl}_2$ described above) always seem to occur together in solution. This strongly indicates the existence of a redox equilibrium between these species. Although in the case of denatured ethanol we were able to identify the red species (compound **4a**) we cannot assign this structure to the red species (compound **4**) in other solvents due to lacking of 2-butanone in solution. But it is most likely that similar redox reactions take place, which will lead to related copper(I) complexes.

The strong redox activities of cluster I as well as of cluster II were further demonstrated in a series of experiments:

1. It was observed that storing either of the clusters in denatured ethanol led to selective oxidation of some of the solvent to acetaldehyde. Acetic acid was not detected.
2. Cluster I showed activity in oxidation of catechol and derivatives such as 2-aminophenol. Adding a small amount of cluster I to a solution of catechol in DMF under atmospheric conditions immediately led to the formation of the red-colored corresponding quinone. UV/Vis-measurements confirmed these observations (for spectra see the Supporting Information). Investigations of the detailed reaction mechanism are in progress.
3. Furthermore, cluster I can support hydroxylation of aliphatic C-H bonds with dihydrogen peroxide as a co-reagent. Mixing a suspension of cluster I in acetonitrile with cyclohexane or hexane and H_2O_2 will lead to the according alcohols and side products (Figure 2.10).

2. Reactions of Copper(II) Chloride with Benzylamine

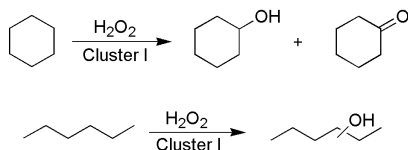


Figure 2.10.: Hydroxylation of cyclohexane and n-hexane by cluster I.

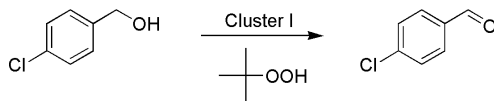
During this reaction overall yields for the oxidation of cyclohexane up to 18% and a turnover of 72 could be reached. For the oxidation of n-hexane overall yields of 6% and a turnover of 24 could be observed (no regioselectivity was observed). In contrast to the oxidation of cyclohexane the dihydroxylated product could also be found; which is about 30% of the product. This behavior resembles a multicopper system found by Kirillov et al.[81] Similar to these authors we could also observe the formation of an activated copper(I) system by the addition of H₂O₂. As proposed in the mechanism by Kirillov et al. we could also observe a strong evolution of molecular oxygen, indicating the reduction of the copper(II) species and hence, formation of an activated copper(I) system. Additionally, the reaction mixture turned red. As suspected we could confirm the formation of the copper(I) system due to the strong reaction with cuproine, which is a highly selective detection reagent for copper(I) ions. Investigations of the detailed reaction mechanism and studies on increasing yields are in progress. Preliminary results are presented in Table 2.1.

Table 2.1.: Hydroxylation of cyclohexane with H₂O₂ and cluster I.

Catalyst (amount [μmol])	Starting material (amount [mmol])	H ₂ O ₂ [mmol]	Yield alcohol [%]	Yield ketone [%]	Turn- over
cluster I (25)	cyclohexane (10)	10	7	3	40
cluster I (25)	cyclohexane (10)	20	14	4	72
CuCl ₂ · 2 H ₂ O (41)	cyclohexane (10)	20	7	4	27
-	cyclohexane (10)	20	0	0	-
cluster I (25)	n-hexane (10)	10	6	0	24

2.1. Reactions of Copper(II) Chloride in Solution

4. When dihydrogen peroxide was added to a suspension of cluster I in acetonitrile without substrate a violent reaction occurred and a brown material, compound **9**, could be isolated (Figure 2.3). So far, this compound could not be characterized. By using tert-butylhydroperoxide instead of dihydrogen peroxide allowed us to selectively oxidize p-chlorobenzyl alcohol catalytically to the according aldehyde in excellent yields (yields up to 90%, turnover of 360, for details, see the Supporting Information) according to the following equation:



Another quite interesting reaction was observed when cluster I was dissolved in acetone. The solution turned to a red color within a few hours and colorless crystals could be separated from the mixture. The molecular structure of this compound is shown in Figure 2.11 (crystallographic data are reported in the Supporting Information).

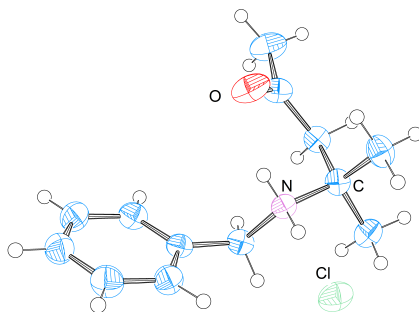


Figure 2.11.: Molecular structure of the salt benzyl-(1,1-dimethyl-3-oxobutyl)- ammonium chloride, HC₁₃H₁₉NOCl. Ellipsoids are drawn at the 50% probability level.

Obviously the cluster facilitated an aldol condensation (Figure 2.12 (a)) followed by a Michael addition reaction (Figure 2.12 (b)).

This reactivity is quite unusual, because aldol condensations are usually observed either with rather CH-acidic compounds or due to catalysis with

2. Reactions of Copper(II) Chloride with Benzylamine

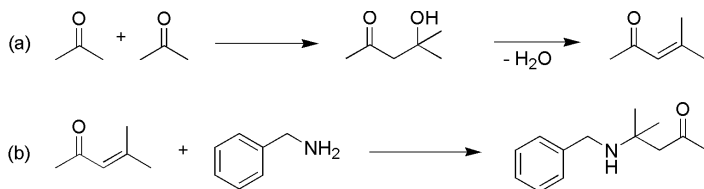


Figure 2.12.: Proposed (a) aldol condensation and (b) Michael addition for the formation of $\text{HC}_{13}\text{H}_{19}\text{NOCl}$.

strong bases such as KOH. In our case neither acetone is very CH acidic nor is benzylamine a strong base. It is quite interesting to compare this reaction with the reaction of cluster I with 2-butanone described above. The only difference between 2-butanone and acetone is a methyl group. Thus, it is surprising to observe such a different behavior. However, both reactions have in common that the products may be isolated in good and reproducible yields. Kinetic studies are in progress to obtain detailed information on the reaction mechanisms, however, these investigations are complicated and time consuming (see below).

Furthermore, an analogous reaction behavior could be observed by using zinc chloride instead of copper(II) chloride. Colorless crystals could be isolated in good yields from the solution and were structurally characterized. As observed for the reaction with copper chloride zinc chloride also seems to facilitate an aldol condensation and a following Michael addition (see the Supporting Information for a detailed description of this reaction).

It is important to point out that both CuCl_2 as well as ZnCl_2 seem to allow reactions to proceed at room temperature that normally only may be achieved under much harsher conditions. It is an interesting future goal to investigate if zinc chloride can form cluster units analogous to $\text{Cu}_4\text{OCl}_6\text{L}_4$ as well. The reactivity of these clusters should be different with regard to the non-redox behavior of the zinc ion in contrast to the observed $\text{Cu}^I/\text{Cu}^{II}$ redox couple. This would allow to separately investigate all reactions that do not include changes in the redox state of the metal ion.

During our investigations we went back to original literature reports on clusters of the type $\text{Cu}_4\text{OX}_6\text{L}_4$. Although most of these complexes have been studied thoroughly by spectroscopy only few crystal structures were reported such as $[\text{Cu}_4\text{OX}_6(\text{py})_4]$ (py = pyridine).[32] At this point it is important to clarify that not all co-ligands seem to support formation of such cluster units. When we used aniline instead of benzylamine the expected copper

2.1. Reactions of Copper(II) Chloride in Solution

complex $[\text{Cu}(\text{aniline})_2\text{Cl}_2]$ immediately formed and here we could not observe cluster units confirming previous results by tom Dieck et al.[29] So far we do not have an explanation for this observation. The molecular structure of $[\text{Cu}(\text{aniline})_2\text{Cl}_2]$ is presented in Figure 5.10 (crystallographic data are reported in the Supporting Information).

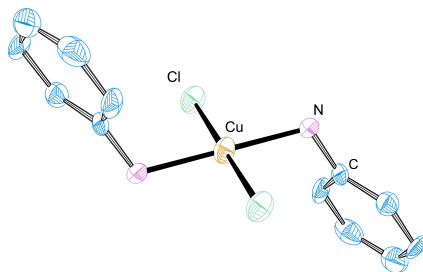


Figure 2.13.: Molecular structure of the compound $[\text{Cu}(\text{aniline})_2\text{Cl}_2]$. Hydrogen atoms omitted for clarity. Ellipsoids are drawn at the 50 % probability level.

However, most interestingly to us seemed the cluster $[\text{Cu}_4\text{OX}_6(\text{MeOH})_4]$ in which the solvent molecules form the additional ligands in the cluster unit. We could easily prepare this cluster under inert conditions according to the procedure published previously by tom Dieck et al. and obtained crystals suitable for crystallographic characterization.[28] The molecular structure presented in Figure 2.14 (crystallographic data are reported in the Supporting Information) confirmed the original postulation including the two solvent molecules, which co-crystallized with the cluster. The yellow crystals are sensitive towards air and moisture and therefore have to be kept under argon. As for the other clusters of this type the central oxygen atom is coordinated tetrahedrally to four copper(II) ions, whereas the six chloride ions form the typical cage for these structures. Every copper ion is coordinated to three chloride anions, the central oxygen atom and one ligand (in this case methanol), which results in a trigonal-bipyramidal coordination for each copper ion. Similar to methanol other solvents can be used and we successfully could structurally characterize $\text{Cu}_4\text{OCl}_6\text{L}_4$ (L = acetonitrile, dmsO, and dmf). The molecular structures of these compounds are presented in the Supporting Information.

2. Reactions of Copper(II) Chloride with Benzylamine

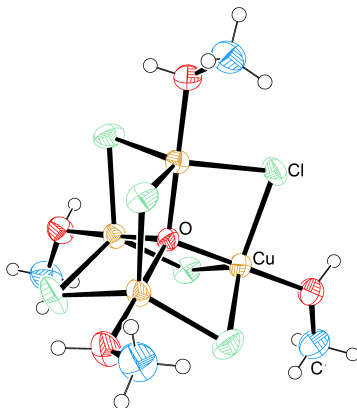


Figure 2.14.: Molecular structure of the compound $[\text{Cu}_4\text{OCl}_6\text{L}_4]$ (L = methanol). Solvent molecules are omitted for clarity. Ellipsoids are drawn at the 50% probability level.

We think that these "solvent cluster complexes" are quite important for the general understanding of stoichiometric and catalytic reactions using copper(I/II) chloride as an active compound. Most likely there are no simple copper(II) or copper(I) ions present in solution in the presence of chloride ions (or bromide ions). Formation of different cluster units will occur in the majority of these reactions (see below). Depending on the reaction conditions copper chloride can easily form the $[\text{Cu}_4\text{OX}_6(\text{MeOH})_4]$ cluster in methanol. Complete or partial substitution of coordinated methanol through other ligands is facile and actually was used to obtain some of the other "solvent clusters". [28] As a result of the molecular formula the presence of oxygen (e.g., in form of H_2O) is indispensable for the formation of these clusters. To get an idea which complexes copper chloride can form in methanol when an oxygen source is excluded, we carried out an experiment where CuS (instead of CuO) and CuCl_2 were heated to reflux in dry methanol (experimental conditions analogous to the synthesis of $[\text{Cu}_4\text{OCl}_6(\text{MeOH})_4]$). Crystals could be isolated in very good yields from the solution and the molecular structure of this compound is presented in Figure 2.15 (crystallographic data are reported in the Supporting Information).

The structure shows a square-planar-coordinated copper(II) ion with a staggered trans formation of the ligands chloride and methanol. Few complexes with solvent molecules have been crystallized so far. Among these

2.1. Reactions of Copper(II) Chloride in Solution

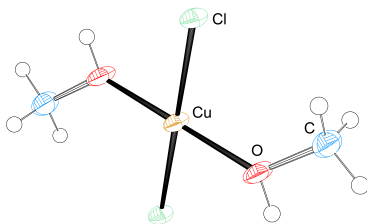


Figure 2.15.: Molecular structure of the complex $[\text{Cu}(\text{MeOH})_2\text{Cl}_2]$. Ellipsoids are drawn at the 50% probability level.

complexes the structure motif $[\text{Cu}(\text{MeOH})_2\text{Cl}_2]$ is most common and was found quite often to co-crystallize with other compounds.[82]-[85] However, so far it was not possible to crystallize $[\text{Cu}(\text{MeOH})_2\text{Cl}_2]$ alone (only co-crystallizations were accomplished). A second "solvent complex" is the complex $[\text{Cu}(\text{dmsO})_2\text{Cl}_2]$.[86] Complexes with other solvents as acetonitrile, dmf, acetone or thf of the formula $[\text{Cu}(\text{L}_2)\text{Cl}_2]$ (L = solvent molecule) are not known yet.

We always tested the catalytic activity of cluster I in comparison by simply adding $\text{CuCl}_2 \cdot 2\text{H}_2\text{O}$ alone in all of our experiments. Similar to previous results we observed that $\text{CuCl}_2 \cdot 2\text{H}_2\text{O}$ is catalytically active in most of these reactions as well (only some selected examples are given in the references).[87]-[92] However, this is not surprising because as discussed above there is no simple CuCl_2 in solution. Different clusters can be formed and even the solvent can act as a ligand. Thus, CuCl_2 can form $\text{Cu}_4\text{OX}_6\text{L}_4$ with L = solvent. Here, the solvent can be easily replaced by other stronger coordinating ligands, such as amines or chloride ions.[28]

Despite the fact that we could synthesize cluster I - or that in general cluster units of the type $\text{Cu}_4\text{OX}_6\text{L}_4$ (X = halogen, L = ligand or X) can be isolated - it is still questionable if these species are really the active catalysts. Excellent detailed and complicated kinetic studies by Davis and coworkers in the past have demonstrated that in solution quite a large number of equilibria between different cluster units (or cluster parts) can be observed (as one example the chloride only cluster $\text{Cu}_4\text{OCl}_{10}$ should be mentioned) that actually may become the reactive species.[93], [94] To really understand these reactions in detail will need a lot of more research efforts in that area. However, we think with combining the previous excellent results of different research groups and our new findings that we moved one step closer to a better understanding of these reactions.

2.1.3. Conclusion

We have obtained a useful catalytic system from copper(II) chloride and benzylamine. By using cluster units derived from this system we were able to perform a series of interesting reactions, that is:

1. Selective oxidation of ethanol
2. Oxidation of catechol and derivatives
3. Hydroxylation of aliphatic C-H bonds with H₂O₂
4. Selective oxidation of *p*-chlorbenzylic alcohol with *tert*-butylhydroperoxide.

In addition we could show that the cluster units are highly reactive and show a huge affinity towards carbonyl compounds such as 2-butanone or acetone. We could observe different types of reactions starting with the formation of a Schiff base. As consecutive reactions we could observe selective hydroxylation of aliphatic C-H bonds as well as an aldol condensation and Michael addition under mild conditions.

It is clear from our work and literature reports that the behavior of simple copper(II) compounds in solution can be quite complex. Many times our understanding of CuCl₂ in solution seems to be oversimplified (organic chemists tend to write CuCl₂ in chemical equations just above the reaction arrow; only some examples are given in the references).[87]-[92], [95]-[98] Although not discussed in detail, several of our findings should be relevant to reactions supported by CuCl as well.[96], [99], [100]. The redox reactions as described above lead to formation of Cu^I from Cu^{II} and vice versa. In some publications it is mentioned that either CuCl or CuCl₂ can be used.[95]

It is important to note that an "outstanding" copper catalyst should always be compared to simply adding copper(II) chloride (or copper(I) chloride). As discussed above this might show the same reactivity due to the formation of active species in solution (sometimes most likely leading to the same intermediate that is formed with the catalyst). In contrast, copper(II) salts such as sulphate or triflate in the absence of chloride ions may not be very effective for many catalytic reactions.

Furthermore, it should be pointed out that the complex behavior described above for our copper benzylamine cluster is not restricted to this system but will occur with other metal ions and ligands as well. Although we cannot say that we have completely understood these reactions yet, we have provided new insight into the formation and reactivity of a CuCl₂/ligand system. It

is clear that a better and more detailed understanding of these reactions will allow the development of optimized and new copper catalytic systems.

2.1.4. Experimental Section

Analytical data (elemental analyses, IR spectra, and crystallographic data [101]) are summarized in the Supporting Information.

Preparation of cluster I

$\text{CuCl}_2 \cdot 2\text{H}_2\text{O}$ (15.3 g, 90 mmol) was dissolved in methanol (ca. 50 mL) and benzylamine (10.7 g, 100 mmol) was added dropwise to the solution under stirring. The mixture was stirred for approximately 10 min and the resulting olive green precipitate was filtered off and dried to give cluster I (15.5 g, 7.13 mmol, 71 %). The preparation of the bromide analogue of cluster I was performed accordingly except that CuBr_2 was used instead of $\text{CuCl}_2 \cdot 2\text{H}_2\text{O}$. The target compound was obtained in 80 % yield.

Preparation of cluster II

2-Butanone (0.72 g, 10 mmol) was dissolved in ethanol (100 mL) and benzylamine (1.1 g, 10 mmol) was added dropwise to the stirred solution. Afterwards, $\text{CuCl}_2 \cdot 2\text{H}_2\text{O}$ (0.85 g, 5.0 mmol) was added. The solution was stirred for a few minutes under air and then allowed to stand until crystallization occurred. The flask was opened every day and shaken slightly. After a few days the solution turned to a red color and green crystals could be obtained in good yields from the solution.

Preparation of compound 1

$\text{CuCl}_2 \cdot 2\text{H}_2\text{O}$ (0.85 g, 5.0 mmol) was dissolved in methanol (ca. 20 mL) and benzylamine (2.1 g, 20 mmol) was added dropwise to the stirred solution. The solution was stirred for approximately 10 min and the precipitate was filtered off. The filtrate was added to diethyl ether (ca. 40 mL) to precipitate the rest of compound 1 (1.4 g, 4.0 mmol, 80 %).

2. Reactions of Copper(II) Chloride with Benzylamine

Preparation of compound 2

$\text{CuCl}_2 \cdot 2\text{H}_2\text{O}$ (0.51 g, 3.0 mmol) was dissolved in methanol (ca. 15 mL) and benzylamine (3.2 g, 30 mmol) was added dropwise to the stirred solution. The resulting blue solution was added to diethyl ether (ca. 50 mL) and allowed to stand until crystallization occurred. The crystals were isolated and washed with little portions of diethyl ether to give compound **2** (1.4 g, 2.4 mmol, 81 %).

Preparation of compound 3

$\text{CuCl}_2 \cdot 2\text{H}_2\text{O}$ (3.4 g, 20 mmol) was dissolved in methanol (ca. 20 mL) and benzylamine (0.54 g, 5.0 mmol) was added dropwise to the stirred solution. The solution was stirred for 5 min and then added to diethyl ether (ca. 40 mL) to precipitate compound **3**. The precipitate was isolated and washed with small portions of diethyl ether to give compound **3** (0.93 g, 2.20 mmol, 88 %).

Preparation of compound 4

Cluster I was prepared as described above in ethanol but this time it was not isolated. The solution turned to a red color after two days. Then the precipitate was filtered off and the red-colored filtrate was evaporated in a rotary evaporator. The resulting red-colored oil was dissolved in ethanol (1-2 mL) and added to diethyl ether (ca. 350 mL). The red-colored precipitate was filtered off. Compound **4** is slightly sensitive towards air and therefore was stored under argon. It is possible to use methanol or acetonitrile as well to prepare a red-colored solid as described.

Preparation of compound 5

As described above cluster I was prepared in ethanol but again not isolated. After the solution turned to a red color, air was bubbled through the suspension for approximately 30 min until the solution turned to an orange color. Similar to the preparation of compound **4** the precipitate was now filtered off and the filtrate was evaporated in a rotary evaporator. The orange-colored oil obtained was dissolved in ethanol (1-2 mL) and added to diethyl ether (ca. 350 mL). The orange-brown-colored precipitate was then isolated. Compound **5** is slightly sensitive towards air and therefore was stored under argon.

Preparation of compound 6

Preparation was performed similar to the preparation of cluster I except that 20 % of the solvent was replaced by water.

Preparation of compound 7

2-Butanone (0.72 g, 10 mmol) was dissolved in ethanol (100 mL) and benzylamine (1.1 g, 10 mmol) was added dropwise to the stirred solution. Afterwards $\text{CuCl}_2 \cdot 2\text{H}_2\text{O}$ (0.85 g, 5.0 mmol) was added. The obtained suspension was stirred for a few minutes in a closed flask. The flask was not opened for a few days. During this time the solution has turned to a red color and the olive-colored precipitate turned to colorless crystals. The resulting crystals were sensitive towards air and therefore were stored under argon.

Preparation of compound 8

A small portion of cluster I was suspended in methanol and solid NaBH_4 was slowly added to the suspension until a colorless solution and black precipitate formed. The solid was isolated and dried in air.

Preparation of compound 9

Compound **9** was prepared in situ by reducing a mixture of cluster I in acetonitrile with a 30 % aqueous solution of H_2O_2 . The brown-red-colored precipitate was filtered off. Compound **9** is highly sensitive towards air and unstable at room temperature.

Oxidation of ethanol

A small portion of cluster I (or cluster II) was suspended in denatured ethanol (ca. 5-10 mL) and allowed to stand for a day. Acetaldehyde was detected by GC-MS and exact mass detection.

Oxidation of catechol derivatives

A small amount of o-aminophenol (or catechol) was dissolved in DMF and a tip of a spatula of cluster I was added. The solution immediately turned

2. Reactions of Copper(II) Chloride with Benzylamine

to a red color and was investigated by UV/Vis measurements.

Hydroxylation of cyclohexane and n-hexane

Cluster I (54 mg, 25 mmol) was suspended in acetonitrile (10 mL) and cyclohexane (0.84 g, 10 mmol) was added. A dihydrogen peroxide solution (30 %, 2 mL, ca. 20 mmol H₂O₂) was added dropwise to the stirred solution. A reflux condenser was attached to the flask to prevent evaporation of cyclohexane due to the reaction heat. The solution was stirred until gas evolution stopped and was investigated by GC-MS. Hydroxylation of *n*-hexane was investigated in the same way.

Oxidation of *p*-chlorbenzylic alcohol

Cluster I (54 mg, 25 mmol) was suspended in dichloromethane (10 mL) and *p*-chlorbenzylic alcohol (1.4 g, 10 mmol) was added. To the stirred solution either *tert*-butylhydroperoxide (28.5 %, 3 mL 10 mmol) dissolved in dichloromethane or *tert*-butylhydroperoxide (70 %, 1.5 mL, ca. 10 mmol) dissolved in water was added. The solution was stirred for a defined time and then the cluster was removed through a chromatography column and the yield of the corresponding aldehyde was determined by GC-MS. The results are presented in the Supporting Information.

Preparation of C₁₃H₂₀NOCl

A saturated solution of cluster I in acetone was prepared and left in the fridge for crystallization. The solution dyed red after 1-2 h and colorless crystals were obtained in good yields.

Preparation of methanol cluster

The synthesis was performed according to literature [28]: CuCl₂ (54 g, 0.4 mol) and CuO (11 g, 0.14 mol) were suspended in dry methanol (100 mL) and heated to reflux under inert conditions for 2 h. Afterwards the hot reaction mixture was filtrated and the filtrate was left in the fridge for crystallization. The crystals were isolated and dried in vacuum to remove the crystal methanol to give the target cluster (61 g, 0.1 mol, 74 %).

Preparation of acetonitrile, dmsol, and dmf cluster

According to the literature [28] the methanol cluster (2.5 g) was dissolved in either acetonitrile, dmf, or dmf (5 mL) and heated to reflux under inert conditions for 30 min. The solvent was then removed in vacuum and the pure products were achieved in 95 % yield.

Preparation of $[\text{Cu}(\text{MeOH})_2\text{Cl}_2]$

CuS (6.7 g, 0.07 mmol) and CuCl_2 (27 g, 0.2 mmol) were suspended in dry methanol (50 mL) and heated to reflux under inert conditions for 2 h. Afterwards the hot reaction mixture was filtrated and the filtrate was left in the fridge for crystallization to give $[\text{Cu}(\text{MeOH})_2\text{Cl}_2]$ (31 g, 0.16 mmol, 79 %).

Preparation of $[\text{Cu}(\text{aniline})_2\text{Cl}_2]$

$\text{CuCl}_2 \cdot 2\text{H}_2\text{O}$ (0.85 g, 5.0 mmol) was dissolved in methanol (ca. 20 mL) and aniline (0.52 g, 5.6 mmol) dissolved in a small portion of methanol was added dropwise to the stirred solution. The suspension was stirred for approximately 5 min and the precipitate was then isolated and washed with small portions of methanol. The product was dried in air (0.74 g, 2.3 mmol, 46 %).

2.1.5. Acknowledgements

S. Löw and S. Schindler are thankful to the Stiftung Stipendienfonds der Chemischen Industrie e.V. for providing a Ph.D. scholarship to S. Löw. Furthermore, we appreciate private communications from Prof. Dr. Heindirk tom Dieck and Dr. Hans-Peter Brehm.

2.2. Selected Supporting Information and Unpublished Material

2.2.1. Reactivity of Cluster I

Preparation of cluster II



Figure 2.16.: Color change of cluster I in denatured ethanol: The solution turned from blue to red-brown within a day. The olive colored solid disappeared and cluster II could be obtained as emerald green crystals.

Preparation of compound 7



Figure 2.17.: Comparison of cluster I in denatured ethanol before and after color change: The original green color vanished and a deeply purple colored solution with colorless crystals was formed. In addition the diluted solutions and the solid compounds are shown.

Chlorination of 2-butanone

As a byproduct of the oxidation of ethanol the chlorination of 2-butanone was observed (see Figure 2.18).

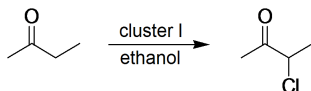


Figure 2.18.: Chlorination of 2-butanone supported by cluster I.

The compound was determined via GC-MS and was found in samples of suspended cluster I in denatured ethanol. The yield could not be determined because of complications with the formation of cluster II and compound **4a** as byproducts. Reference samples with copper(II) chloride instead of cluster I gave the chlorinated compound as well. Since copper chloride is often used as a chlorination reagent this side reaction is not very surprising. However this side reaction may give hint for the hydroxylation of 2-butanone, which occurred at the same position. Regarding the chlorination of 2-butanone an alternative hydroxylation process is possible. Here water or hydroxyl ions (both present in solution) could attack the chlorinated carbon atom via an S_N mechanism. However this is very unlikely because chloride is only a poor leaving group. In addition the reaction takes place in a protic solvent, which is very unfavorable for a nucleophilic attack of either OH^- or H_2O . However the chlorination of 2-butanone could play a role in the hydroxylation of 2-butanone and hence should be considered for future investigations.

2.2.2. Cluster I in Oxygenation Reactions

If not mentioned otherwise all catalytic reactions were performed at room temperature. A reflux condenser was mounted on top of the vessel to avoid evaporating of the solvent and reactants. After adding the dihydrogen peroxide the samples were stirred for 16 h. Then the catalyst was removed through a mini chromatography column from the homogeneous phase. The yield of the obtained solutions was determined via GC-MS without before extracting the organic products. No internal standard was used.

2. Reactions of Copper(II) Chloride with Benzylamine

Oxygenation of cyclohexane and n-hexane

54 mg (25 μ mol) of cluster I were suspended in 10 mL acetonitrile and 10 mmol cyclohexane or n-hexane were added. To the stirred solution were added either 1 mL 30 % aqueous H₂O₂ (10 mmol) or 2 mL (20 mmol). The solution was stirred for 16 h and then the catalyst was removed through a chromatography column and the yield of the corresponding alcohol and aldehyde determined via GC-MS.

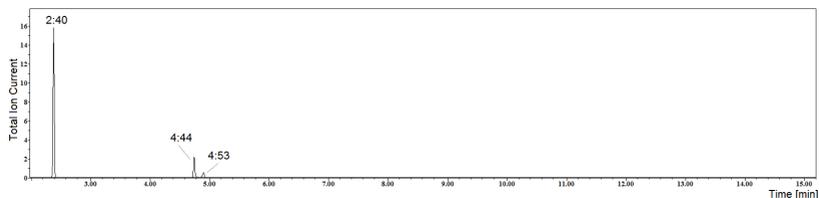


Figure 2.19.: Gas chromatogram of the oxygenation of cyclohexane.

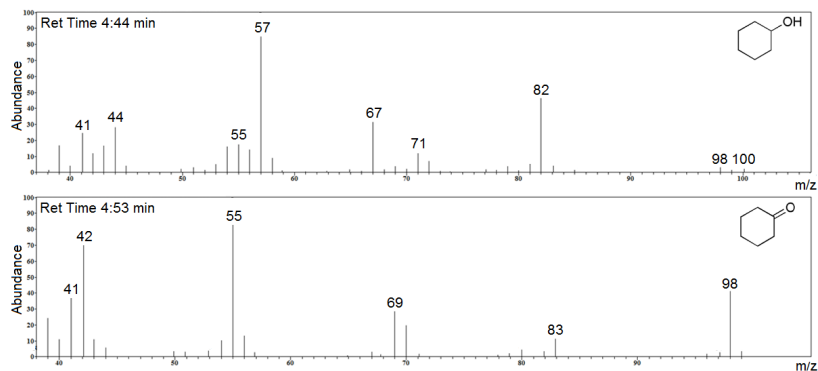


Figure 2.20.: MS spectra of cyclohexanol and cyclohexanone.

In order to increase the yield diverse variations of the reaction conditions were tested. Hence all reaction parameters were hold constant and only one reaction parameter was changed. Increase of the reaction temperature only led to a minor increase of the yield. The variation of the H₂O₂ amount added led to different results. Obviously an amount of 20 mmol to 25 μ mol catalyst

2.2. Selected Supporting Information and Unpublished Material

was ideal. 10 mmol H₂O₂ divided the yield in halves while further increase of the H₂O₂ amount led to a strong decrease of the yield. The addition of more than 30 mmol H₂O₂ led to strong color changes and a very strong time delayed gas evolution. No oxygenation reaction was observed in these experiments. The greatest influence of the yield had the amount of catalyst. With increasing catalyst a yield up to 100 % could be achieved. Table 2.2 shows the reaction results.

Table 2.2.: Results of the oxygenation of cyclohexane with increasing amounts of cluster I as catalyst.

n(catalyst) [μmol]	alcohol [%]	ketone [%]	turnover
25	14	6	81
50	16	5	41
100	9	2	11
200	23	3	13
250	16	1	7
500	66	—	13
750	70	—	9
1000	100	—	10

Interestingly the more catalyst was added the more selective the reaction was. An amount of 25 μ mol cluster I led to a mixture of alcohol and ketone. In contrast greater amounts of cluster I led to formation of cyclohexanol and only traces of cyclohexanone. However the more cluster I was added the more benzaldehyde (up to 40 %) was formed as a side product resulting from oxidation of the ligand benzylamine. The increase of the yield was especially interesting concerning the reaction mechanism. Cluster I was only slightly soluble in acetonitrile. Hence reactions with even only 25 μ mol of catalyst took place in suspensions of cluster I and not in a homogeneous mixture. So increasing the amount of cluster I could not increase the dissolved amount of cluster I. Thus the strong increase of the yield obtained due to increasing the amount of cluster I would speak for an heterogeneous catalysis. However the solvent itself had a huge influence on the outcome. Solvents as dichloromethane for example did not support the oxygenation reaction. This again would argue for a homogeneous mechanism. An explanation for these contradictory observations could be that the active species (which is formed from cluster I and H₂O₂) was soluble in acetonitrile indeed. However it is not clear if the reaction proceeded via a homogeneous or heterogeneous mechanism or if it was a mixture of both. Figure 2.21 shows a

2. Reactions of Copper(II) Chloride with Benzylamine

photograph of the reaction solutions after the oxygenation reaction.



Figure 2.21.: Photograph of the reaction solutions after the oxygenation reactions (*concentration of cluster I increases from left to right*). The color change from yellow or red to bluish solutions was noticeable. This indicated the decomposition of cluster I which is consistent with the finding of benzaldehyde as byproduct with increasing amount of cluster I.

Since copper(II) chloride catalyzed this reaction as well, control experiments with increasing amounts of $\text{CuCl}_2 \cdot 2\text{H}_2\text{O}$ were carried out, too. However no increase of the amount of cyclohexanol/cyclohexanone was observed. This was surprising because copper(II) chloride catalyzed the oxygenation of cyclohexane nearly as good as cluster I if added in small amounts. Phase separation during the reaction might have been responsible for these rather bad results. With higher amounts of copper(II) chloride the phases separated within addition of H_2O_2 . This problem did not occur when cluster I was used as a catalyst. So probably due to deficient mixing of the reactants the reaction was not efficient.

Oxygenation of toluene

54 mg ($25\mu\text{mol}$) of cluster I were suspended in 10 mL acetonitrile and toluene (10 mmol) was added. To the stirred solution were added 2 mL 30 % aqueous H_2O_2 (20 mmol). The solution was stirred for 16 h and then the catalyst was removed through a chromatography column and the yield of the corresponding alcohol and aldehyde determined via GC-MS.

Only traces or yields up to a maximum of ca. 2 % of benzylalcohol or benzaldehyde could be found. The reaction was tested with several other copper compounds such as cluster II, $\text{CuCl}_2 \cdot 2\text{H}_2\text{O}$, $[\text{CuL}^1_2\text{Cl}_2]$, $[\text{CuL}^1_4\text{Cl}_2]$,

(HL¹)₂[CuCl₄] (L¹ = benzylamine), CuBr₂, Cu(NO₃)₂ · 3 H₂O and Cu(SO₄) · 5 H₂O, but the yield did not increase. In addition determination of the yield was complicated due to the oxidation of benzylamine to benzaldehyde which can occur at too high H₂O₂ concentrations.

Oxidation of *p*-chlorobenzylalcohol

54 mg (25 μmol) of cluster I were suspended in 10 mL dcm and 1.4 g (10 mmol) *p*-chlorobenzylalcohol were added. To the stirred solution were added either 3 mL 28,5 % tert-butylhydroperoxide (10 mmol) dissolved in dcm or 1.5 mL 70 % tert-butylhydroperoxide (ca. 10 mmol) dissolved in water. The solution was stirred for a defined time and then the cluster was removed through a chromatography column and the yield of the corresponding aldehyde determined via GC-MS. The average results are presented in table 2.3.

Table 2.3.: Average results of selective oxidation of *p*-chlorbenzylic alcohol with tert-butylhydroperoxide to the corresponding aldehyde.

n(catalyst) ([μmol])	n(educt) [mmol]	n(peroxide) [mmol]	reaction time	yield [%]	turn- over
cluster I, 25	10	10 in dcm	18 h	77	310
			60 h	81	344
CuCl ₂ · 2 H ₂ O, 25	10	10 in dcm	18 h	32	128
			60 h	71	320
—	10	10 in dcm	4 d	7	—
			10 in H ₂ O	18 h	56
cluster I, 25	10	10 in H ₂ O	60 h	90	360
			18 h	12	49
CuCl ₂ · 2 H ₂ O, 25	10	10 in H ₂ O	60 h	20	81
			4 d	3	—

Oxidation of 2-aminophenol

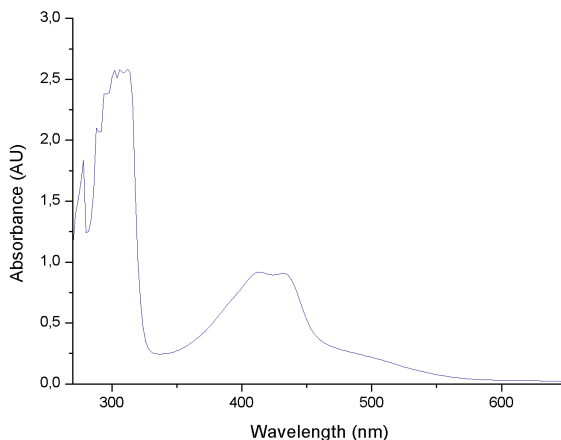


Figure 2.22.: UV-vis spectrum of the oxidation of 2-aminophenol, $\lambda_{max} \approx 312$ nm; $\lambda_{max} = 414$ nm and 432 nm. The unusual high concentration was chosen in order to show the maxima at 414 and 432 nm.

A solution of 2-aminophenol in dmf (ca. 1 mmol/L) was prepared and a small tip of a spatula of cluster I was added. The solution turned immediately deep red and UV-vis data were collected. The maxima are according to literature typical for 2-aminophenoxazine-3-one [102], the corresponding quinone to 2-aminophenol.

Other oxidation reactions

The activity of cluster I as catalyst in oxidation reactions was also tested in the oxidation of allyl alcohol and norbornene. The reactions were performed analogous to the oxygenation of cyclohexane. In the case of allyl alcohol the corresponding aldehyde and acid could be observed, but with a yield below 1%. The reaction with $\text{CuCl}_2 \cdot 2\text{H}_2\text{O}$ did not lead to any oxidation products. Concerning norbornene three oxidation products could be observed (see Figure 2.23), but again the yield was below 1%. Once again $\text{CuCl}_2 \cdot 2\text{H}_2\text{O}$ did not support the oxidation reaction.

2.2. Selected Supporting Information and Unpublished Material

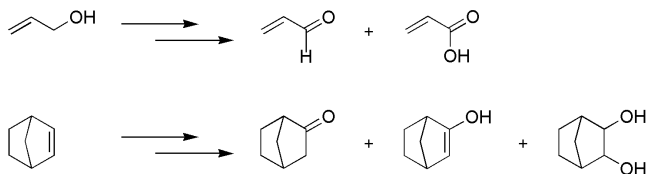


Figure 2.23.: Oxidation products of allyl alcohol and norbornene.

In addition the oxidation of trilostane, glucose, adamantane-1-ol and 3-phenyl-pent-4-en-1-ol was tested. However attempts to oxidize these substrates were not successful.

2.2.3. Approaches with ZnCl_2

Preparation of $[\text{Zn}(\text{benz}_2\text{dba})\text{Cl}_2]$

0.62 g (4.2 mmol) of a 40 % glyoxal solution in water and 0.58 mg (4.5 mmol) $\text{ZnCl}_2 \cdot 2\text{H}_2\text{O}$ were dissolved in ca. 15 mL ethanol. Benzylamine (0.91 g, 8.5 mmol) was added dropwise to the stirred solution. The solution was stirred for ca. 5 min and the colorless precipitate isolated. A small tip of a spatula was dissolved in 1 ml acetone and left for crystallization.

$\text{Zn}(\text{benz}_2\text{dba})\text{Cl}_2$ could be isolated from the solution as large crystals, the molecular structure is shown in Figure 2.24.

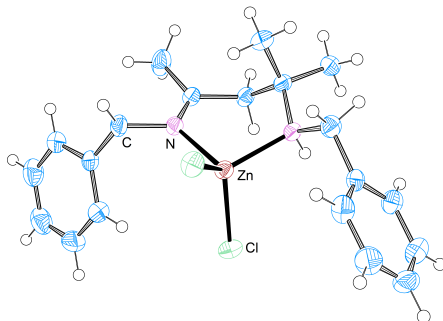


Figure 2.24.: Molecular structure of $[\text{Zn}(\text{benz}_2\text{dba})\text{Cl}_2]$. Ellipsoids are drawn at the 50 % probability level.

2. Reactions of Copper(II) Chloride with Benzylamine

Formation of [Zn(benz₂dba)Cl₂]

As observed for the reaction with copper chloride zinc chloride also seemed to facilitate an aldol condensation and a following Michael addition. But in contrast to the reaction with CuCl₂ shown in the paper (Scheme 2, steps (a) and (b)) an additional reaction step formed a Schiff base that then coordinated to the zinc chloride. The proposed mechanism is shown here:

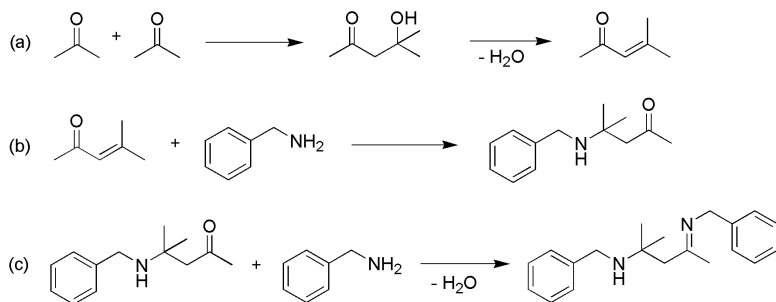


Figure 2.25.: Proposed mechanism of the formation of benz₂dba: As first step an aldol condensation occurred (a) followed by a Michael addition (b). This product then underwent an additional Schiff base reaction with benzylamine to form the final ligand (c).

Preparation of [Zn(L¹)₂Cl₂]

ZnCl₂ · 2 H₂O (930 mg, 5.40 mmol) was dissolved in methanol (ca. 20 mL) and benzylamine (642 mg, 6.00 mmol) was added dropwise to the solution under stirring. The mixture was stirred for approximately 10 min and the resulting colorless precipitate was filtered off and dried to give 707 mg (1.8 mmol, 61 %) of the target compound.

[Zn(L¹)₂Cl₂] in oxygenation reactions

[Zn(L¹)₂Cl₂] was tested in several oxygenation reactions. In all cases oxygenation products were not observed and [Zn(L¹)₂Cl₂] remained unreactive as catalyst.

2.2.4. Molecular Structures of the "Solvent Clusters"

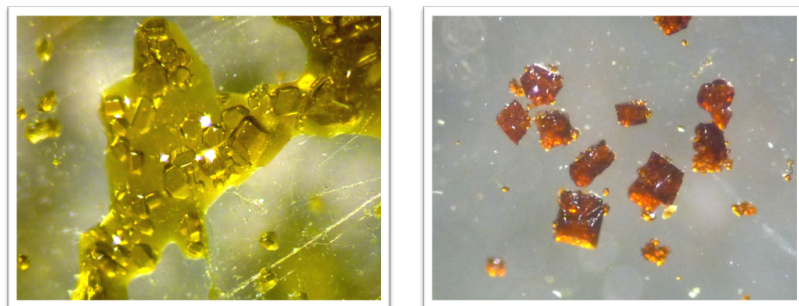


Figure 2.26.: Photographs of the crystals obtained from the "methanol cluster" (*left*) and the "acetonitrile cluster" (*right*).

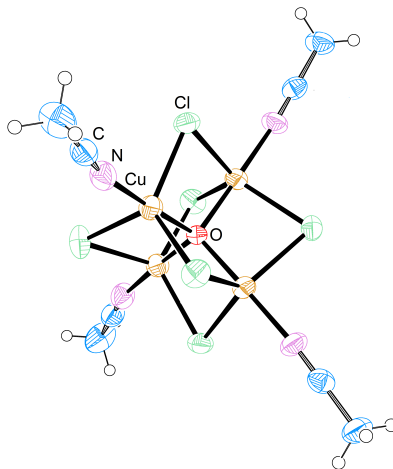


Figure 2.27.: Molecular structure of the "acetonitrile cluster", thermal ellipsoids are set at 50% probability. Solvent molecules are not shown.

2. Reactions of Copper(II) Chloride with Benzylamine

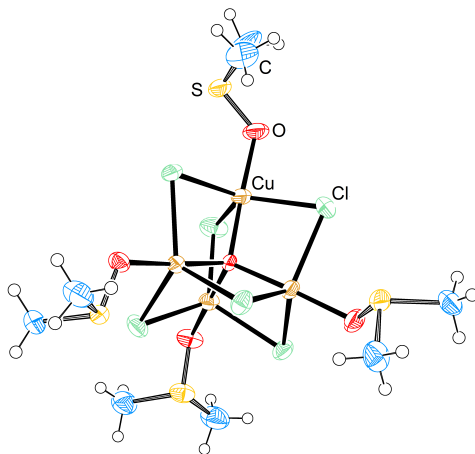


Figure 2.28.: Molecular structure with thermal ellipsoids set at 50% probability of the "dmsoligand". Solvent molecules and disorder are not shown.

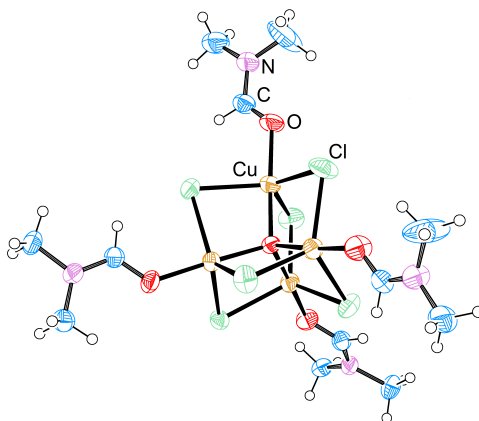


Figure 2.29.: Molecular structure with thermal ellipsoids set at 50% probability of the "dmfoligand".

3. Reactions of Copper(II) Chloride with Derivatives of Benzylamine and Organic Solvents

This chapter includes one manuscript that is going to be submitted to the journal "*Inorganic Chemistry*".

Contribution of the co-authors:

The co-authors solved several of the crystal structures, to detail:

- J. Becker: **11**
- U. Behrens: Cluster IV, $[\text{CuL}^5_4]\text{Cl}_2$, **3d, 7, 9, 10** and **12**

3.1. Investigations Concerning $[\text{Cu}_4\text{OX}_6\text{L}_4]$ -Cluster Formation of CuCl_2 with Amines and in Organic Solvents

This work is to be submitted to "Inorganic Chemistry".

Sabine Löw, Jonathan Becker, Ulrich Behrens and Siegfried Schindler

The following work describes investigations concerning the stability and formation of copper clusters of the formula $[\text{Cu}_4\text{OX}_6\text{L}_4]$ (X = halogenide, L = amine ligand). The reactivity of $\text{CuCl}_2 \cdot 2\text{H}_2\text{O}$ with several simple amine ligands was investigated, which led to an extremely colorful chemistry. In this context the crystal structures of the copper complexes and clusters $[\text{Cu}_4\text{OCl}_6\text{L}^2_4] \cdot [\text{CuL}^2_2\text{Cl}_2]$ (L^2 = phenethylamine), $[\text{CuL}^3_2\text{Cl}_2]$ (L^3 = *N*-methylbenzylamine), HL^4Cl , $[\text{Cu}_4\text{OCl}_6\text{L}^4_4]$ (L^4 = *N,N*-dimethylbenzylamine), $[\text{CuL}^5_4\text{Cl}_2]$ (L^5 = cyclohexylamine) and $[\text{Cu}_4\text{OCl}_6\text{L}^6_4] \cdot 1.5 [\text{CuL}^6_2\text{Cl}_2]$ (L^6 = cyclohexanemethylamine) are reported. Furthermore the influence of the halogenide during cluster formation was investigated and it was tried to exchange the central oxide with sulfide. During these attempts some interesting copper(I) and copper(II) compounds were obtained whose molecular structures could be determined as following: $[\text{Cu}(\text{acetonitrile})_4][\text{CuBr}_4]$, $[\text{Cu}(\text{acetonitrile})\text{Br}]$ and $[\text{Cu}(\text{acetonitrile})\text{Br}_2]$. In addition the reactivity of $\text{CuCl}_2 \cdot 2\text{H}_2\text{O}$ towards organic solvents was explored and if multinuclear copper clusters were formed if $\text{CuCl}_2 \cdot 2\text{H}_2\text{O}$ was dissolved in these solvents. Recrystallization of $\text{CuCl}_2 \cdot 2\text{H}_2\text{O}$ in those solvents led to the compounds $[\text{CuCl}_2] \cdot \text{H}_2\text{O} \cdot 0.5$ acetone, $[\text{Cu}_3(\text{acetonitrile})_2\text{Cl}_6]$ and the salt $(\text{H}_2\text{N}(\text{CH}_3)_2)_2[\text{CuCl}_3]$. When NaO^tBu was added in addition the "solvent cluster" $[\text{Cu}_4\text{OCl}_6(\text{MeOH})_4]$ was obtained. The formation of such "solvent clusters" may play an important role in elucidating the mechanism of copper chloride catalyzed reactions. This is discussed in more detail.

3.1.1. Introduction

Ponomarevite is the natural mineral $\text{K}_4[\text{Cu}_4\text{OCl}_{10}]$. It is found in volcanic fumaroles where it is formed at higher degrees between 280-450°C. The molecular structure and a schematic representation are shown in Figure 3.1.[49]

3. Reactions of CuCl_2 with Derivatives of Benzylamine

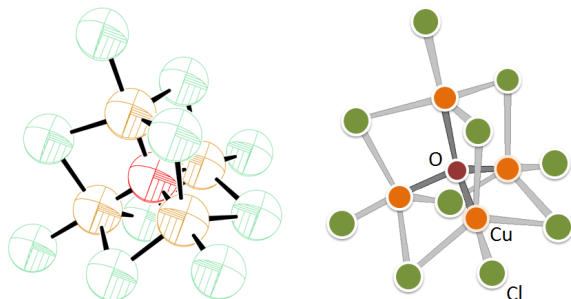


Figure 3.1.: Molecular structure of the mineral ponomarevite (K^+ is omitted for clarity). Ellipsoids are drawn at the 5% probability level. A schematic representation is provided for clarity. The crystals were collected in Kamchatka (Russia) after the Great Tolbachik Fissure in 1975/6.[49]

The first artificial synthesis of a copper cluster complex with the structural motif Cu_4OCl_6 was carried out by Bertrand et al. in 1966.[27] During the next decade many copper clusters of this type were reported and especially investigated concerning their magnetic and structural properties.[27]-[41], [33], [60]-[66] In most of these cases syntheses had to be carried out under inert conditions and the resulting products were sensible towards moisture just as their natural relative.[28], [29], [31]. These difficulties and a lack of applications led to a strong decrease of interest during the last decades. Nevertheless there are many publications describing the accidental formation of such a copper cluster (only few are given in the references).[32], [42]-[48] Therein the formation of the Cu_4OCl_6 motif occurred when copper(II) chloride (or less often CuCl) was used to either catalyze a reaction or to synthesize a complex. In many cases the desired product differed much from the obtained copper cluster. The reported clusters show an astonishing variety concerning the ligand system. There are simple amines like dimethylamine as well as steric challenging ligands or even tripodal ligands. Figure 3.2 shows a small selection of ligands which unexpectedly formed clusters.

Recently we reported a cluster system that we found by chance as well.[103] The molecular structure already was shown in Figure 2.2. This cluster (cluster I) could easily be prepared by mixing $\text{CuCl}_2 \cdot 2\text{H}_2\text{O}$ and benzylamine at air.[103] Interestingly cluster I showed a huge color range if stored in solution and so tempted us to investigate the system further. Although many of the

3.1. Investigations Concerning $[Cu_4OCl_6L_4]$ -Cluster Formation

reactions which took place and led to the color changes could be determined, we still do not fully understand the cluster formation itself.[103]

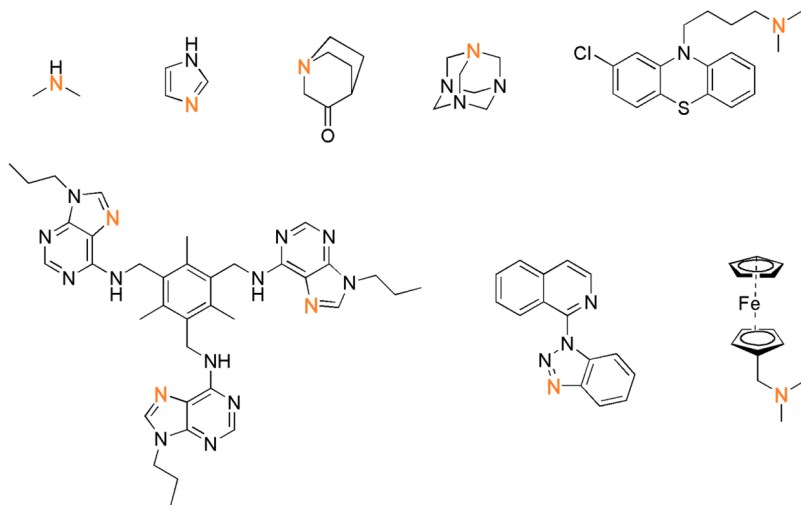


Figure 3.2.: Some ligands that were found by chance to form a cluster with copper(II) chloride, coordinating nitrogen atoms are highlighted.[32], [42]-[48]

There seems to be no special demand to the ligand so that one cannot predict whether the reaction with copper(II) chloride will form a simple complex or a cluster. Because of that, variations concerning the Cu_4OCl_6 unit were investigated to find out if there is a system in cluster formation indeed. In addition the question how $CuCl_2 \cdot 2H_2O$ "looks like" in common solvents was very interesting and if there are multinuclear aggregates/clusters formed, when $CuCl_2 \cdot 2H_2O$ is dissolved in these solvents.

3.1.2. Experimental Section

Materials and Methods

All chemicals used were of p.a. quality and were purchased from either Acros, Aldrich, Fluka or Merck, if not mentioned otherwise (see Supporting

3. Reactions of CuCl_2 with Derivatives of Benzylamine

Information for parameters of used instruments).

Preparation of 2a: $(\text{HL}^2)_2[\text{CuCl}_4]$

$\text{CuCl}_2 \cdot 2\text{H}_2\text{O}$ (512 mg, 3.00 mmol) was dissolved in methanol (ca. 10 mL) and phenethylamine (181 mg, 1.50 mmol) was added dropwise to the solution under stirring. The red-brown solution was stirred for approximately 10 min and then allowed to stand until crystallization occurred. 143 mg (0.318 mmol, 21 %) of the crystalline target compound were obtained.

Preparation of cluster III: $[\text{Cu}_4\text{OCl}_6\text{L}^2_4] \cdot [\text{CuL}^2_2\text{Cl}_2]$ (atmospheric conditions)

$\text{CuCl}_2 \cdot 2\text{H}_2\text{O}$ (852 mg, 5.00 mmol) was dissolved in methanol (ca. 15 mL) and phenethylamine (673 mg, 5.60 mmol) was added dropwise to the solution under stirring. The mixture was stirred for approximately 10 min and the resulting olive green precipitate was filtered off and dried to give cluster III (570 mg, 0.41 mmol, 44 %).

Preparation of cluster III: $[\text{Cu}_4\text{OCl}_6\text{L}^2_4] \cdot [\text{CuL}^2_2\text{Cl}_2]$ (inert conditions)

Synthesis was carried out in a glove box. $[\text{Cu}_4\text{OCl}_6(\text{MeOH})_4]$ (230 mg, 0.375 mmol) was dissolved in absolute acetonitrile (10 mL) and phenethylamine (184 mg, 1.50 mmol) was added to the solution under stirring. The solution was allowed to stand until crystallization occurred. 163 mg (0.117 mmol, 31 %) of the crystalline target compound were obtained.

Preparation of 2d: $[\text{CuL}^2_4\text{Cl}_2]$

$\text{CuCl}_2 \cdot 2\text{H}_2\text{O}$ (256 mg, 1.50 mmol) was dissolved in methanol (10 mL) and phenethylamine (724 mg, 6.00 mmol) was added to the solution under stirring. The solution was allowed to stand until crystallization occurred. 118 mg (0.19 mmol, 13 %) of the microcrystalline target compound was obtained.

Preparation of 3a: $(\text{HL}^3)_2[\text{CuCl}_4] \cdot 1.5 \text{CuCl}_2$

$\text{CuCl}_2 \cdot 2\text{H}_2\text{O}$ (512 mg, 3.00 mmol) was dissolved in methanol (ca. 10 mL) and N-methylbenzylamine (181 mg, 1.50 mmol) was added dropwise to the

3.1. Investigations Concerning $[\text{Cu}_4\text{OCl}_6\text{L}_4]$ -Cluster Formation

solution under stirring. The red-brown solution was stirred for approximately 10 min and then allowed to stand until the solvent was evaporated. Thf (ca. 10 mL) was added to the resulting green-orange solid. The green impurities were dissolved and the orange colored target compound could be filtered off and dried to give 170 mg (0.26 mmol, 35 %). **3a** was contaminated with CuCl_2 , which precipitated as well.

Preparation of **3b**

$\text{CuCl}_2 \cdot 2\text{H}_2\text{O}$ (852 mg, 5.00 mmol) was dissolved in methanol (ca. 20 mL) and N-methylbenzylamine (673 mg, 5.60 mmol) was added dropwise to the solution under stirring. The mixture was stirred for approximately 10 min. The solvent was evaporated to give a green colored solid.

Preparation of **3c/3d**: $[\text{CuL}^3_2\text{Cl}_2]$

$\text{CuCl}_2 \cdot 2\text{H}_2\text{O}$ (256 mg, 1.50 mmol) was dissolved in methanol (ca. 10 mL) and N-methylbenzylamine (724 mg, 6.00 mmol) was added dropwise to the solution under stirring. The mixture was stirred for approximately 10 min and then allowed to stand until crystallization occurred. The target compounds crystallized as violet and blue crystals.

Attempted preparation of $[\text{Cu}_4\text{OCl}_6\text{L}^3_4]$ (inert conditions)

Synthesis was carried out in a glove box. $[\text{Cu}_4\text{OCl}_6(\text{MeOH})_4]$ (115 mg, 0.187 mmol) was dissolved in absolute acetonitrile (10 mL) and N-methylbenzylamine (91 mg, 0.75 mmol) was added to the solution under stirring. The solvent was evaporated to give 30 mg (0.079 mmol, 11 %) of $[\text{CuL}^3_2\text{Cl}_2]$.

Preparation of **4a**: $(\text{HL}^4)_2[\text{CuCl}_4] \cdot \text{CuCl}_2$

$\text{CuCl}_2 \cdot 2\text{H}_2\text{O}$ (512 mg, 3.00 mmol) was dissolved in thf (ca. 20 mL) and N,N-dimethylbenzylamine (202 mg, 1.50 mmol) was added dropwise to the solution under stirring. The red colored precipitate was filtered off and dried to give 317 mg (0.67 mmol, 89 %) of the target compound. **4a** was contaminated with CuCl_2 , which precipitated as well.

3. Reactions of CuCl_2 with Derivatives of Benzylamine

Preparation of **4b**

$\text{CuCl}_2 \cdot 2 \text{H}_2\text{O}$ (256 mg, 1.50 mmol) was dissolved in methanol (ca. 10 mL) and N,N-dimethylbenzylamine (202 mg, 1.50 mmol) was added dropwise to the solution under stirring. The olive colored precipitate was filtered off and dried to give 103 mg of the green colored compound **4b**.

Preparation of cluster IV: $[\text{Cu}_4\text{OCl}_6\text{L}^4_4]$ (atmospheric conditions)

$\text{CuCl}_2 \cdot 2 \text{H}_2\text{O}$ (853 mg, 5.00 mmol) was dissolved in methanol (ca. 20 mL) and N,N-dimethylbenzylamine (1.35 g, 10.0 mmol) was added dropwise to the solution under stirring. The mixture was stirred for approximately 10 min and the resulting orange colored precipitate was filtered off and dried to give 1.24 g (1.21 mmol, 97 %).

Preparation of cluster IV: $[\text{Cu}_4\text{OCl}_6\text{L}^4_4]$ (inert conditions)

Synthesis was carried out in a glove box. $[\text{Cu}_4\text{OCl}_6(\text{MeOH})_4]$ (115 mg, 0.187 mmol) was dissolved in absolute acetonitrile (10 mL) and N,N-dimethylbenzylamine (101 mg, 0.750 mmol) was added to the solution under stirring. The resulting orange colored precipitate was filtered off and dried to give 98 mg (0.10 mmol, 51 %) of the target compound.

Preparation of **5a**: $(\text{HL}^5)_2[\text{CuCl}_4] \cdot 1.5 \text{CuCl}_2$

$\text{CuCl}_2 \cdot 2 \text{H}_2\text{O}$ (850 mg, 5.00 mmol) was dissolved in thf (ca. 40 mL) and cyclohexylamine (248 mg, 2.50 mmol) was added dropwise to the solution under stirring. The larger part of the solvent was evaporated and the resulting red oil was dissolved in a small portion of methanol. This solution was added dropwise to diethylether (ca. 250 mL). The larger part of the solvent was evaporated again and once again the red oil was dissolved in methanol and added dropwise to diethylether. This procedure was repeated until small portions of an orange colored precipitation could be filtered off and dried. 15 mg (0.024 mmol, 2 %) of the target compound was obtained. **5a** was contaminated with CuCl_2 , which precipitated as well.

Preparation of **5b**

$\text{CuCl}_2 \cdot 2\text{H}_2\text{O}$ (852 mg, 5.00 mmol) was dissolved in methanol (ca. 20 mL) and cyclohexylamine (554 mg, 5.60 mmol) was added dropwise to the solution under stirring. The mixture was stirred for approximately 10 min and the resulting olive green precipitate was filtered off and dried to give the green compound **5b** (472 mg).

Preparation of **5e**: $[\text{CuL}^5_2]\text{Cl}_2$

$\text{CuCl}_2 \cdot 2\text{H}_2\text{O}$ (852 mg, 5.00 mmol) was dissolved in methanol (ca. 20 mL) and cyclohexylamine (1.98 g, 20.0 mmol) was added dropwise to the solution under stirring. The mixture was stirred for approximately 10 min and the resulting blue colored precipitate was filtered off and dried to give the target compound (1.35 g, 4.10 mmol, 82%).

Preparation of cluster **V**: $[\text{Cu}_4\text{OCl}_6\text{L}^5_4] \cdot \text{CH}_3\text{CN}$

Synthesis was carried out in a glove box. $[\text{Cu}_4\text{OCl}_6(\text{MeOH})_4]$ (115 mg, 0.187 mmol) was dissolved in absolute acetonitrile (10 mL) and cyclohexylamine (75.0 mg, 0.750 mmol) was added to the solution under stirring. The resulting yellow colored precipitate was filtered off and dried to give 123 mg (0.179 mmol, 96%) of the target compound.

Preparation of **6a**: $(\text{HL}^6)_2[\text{CuCl}_4]$

$\text{CuCl}_2 \cdot 2\text{H}_2\text{O}$ (512 mg, 3.00 mmol) was dissolved in thf (ca. 35 mL) and cyclohexanemethylamine (170 mg, 1.50 mmol) was added dropwise to the solution under stirring. The solvent was evaporated until precipitation occurred. The yellow colored precipitate was filtered off and dried to give 92 mg (0.21 mmol, 28%) of the target compound.

Preparation of **6b**

$\text{CuCl}_2 \cdot 2\text{H}_2\text{O}$ (765 mg, 4.50 mmol) was dissolved in methanol (ca. 15 mL) and cyclohexanemethylamine (565 mg, 5.00 mmol) was added dropwise to the solution under stirring. The mixture was stirred for approximately 10 min and the resulting olive green precipitate was filtered off and dried to give the green compound **6b** (537 mg).

3. Reactions of CuCl_2 with Derivatives of Benzylamine

Preparation of **6c**: $[\text{CuL}^6_2\text{Cl}_2] \cdot 0.5 \text{CuCl}_2$

$\text{CuCl}_2 \cdot 2 \text{H}_2\text{O}$ (32 mg, 0.19 mmol) was dissolved in methanol (ca. 2 mL) and cyclohexanemethylamine (43 mg, 0.38 mmol) was added dropwise to the solution under stirring. The mixture was stirred for approximately 10 min. The solvent was evaporated until precipitation occurred. The resulting green colored precipitate was filtered off and dried to give the target compound (8 mg, 0.04 mmol, 47%). **6c** was contaminated with CuCl_2 which precipitated as well.

Preparation of **6d**: $[\text{CuL}^6_4\text{Cl}_2]$

$\text{CuCl}_2 \cdot 2 \text{H}_2\text{O}$ (16 mg, 0.091 mmol) was dissolved in methanol (ca. 2 mL) and cyclohexanemethylamine (43 mg, 0.38 mmol) was added dropwise to the solution under stirring. The mixture was stirred for approximately 10 min. The solvent was evaporated until crystallization occurred. 35 mg (0.060 mmol, 63%) of the target compound was obtained.

Preparation of cluster **VI**: $[\text{Cu}_4\text{OCl}_6\text{L}^6_4] \cdot 1.5 [\text{CuL}^6_2\text{Cl}_2]$

Synthesis was carried out in a glove box. $[\text{Cu}_4\text{OCl}_6(\text{MeOH})_4]$ (115 mg, 0.187 mmol) was dissolved in absolute acetonitrile (10 mL) and cyclohexanemethylamine (85 mg, 0.75 mmol) was added to the solution under stirring. The resulting olive precipitate was filtered off and dried to give 101 mg (0.070 mmol, 64%) of the target compound.

Preparation of **7, 8 and 9**: $[\text{CuL}_4][\text{CuBr}_4]$, $[\text{CuLBr}]$ and $[\text{CuLBr}_2]$ (**L** = acetonitrile)

Synthesis was carried out under inert conditions. CuBr_2 (8.9 g, 0.040 mmol) and CuS (1.3 g, 0.014 mmol) were suspended in absolute acetonitrile (ca. 10 mL). The mixture was heated under reflux for 1.5 h. The unreacted parts of the reactants were filtered off. The dark green filtrate was allowed to stand in the freezer until crystallization occurred.

Preparation of **10**: $[\text{CuCl}_2] \cdot \text{H}_2\text{O} \cdot 0.5 \text{acetone}$

A spoon full of $\text{CuCl}_2 \cdot 2 \text{H}_2\text{O}$ was suspended in acetone (ca. 20 mL) and heated under reflux for ca. 1 h. The solution was then allowed to stand until

3.1. Investigations Concerning $[\text{Cu}_4\text{OCl}_6\text{L}_4]$ -Cluster Formation

crystallization occurred. The resulting pale orange colored needles could not be isolated because of their high sensibility towards air and moisture. But it was possible to pick some crystals for a crystal structure determination.

Preparation of 11 and 12: $[\text{Cu}_3\text{L}_2\text{Cl}_6]$ and $[\text{Cu}_2\text{L}_2\text{Cl}_4]$ (L = acetonitrile)

A spoon full of $\text{CuCl}_2 \cdot 2\text{H}_2\text{O}$ was suspended in acetonitrile (ca. 20 mL) and heated to reflux for 1 h. The solution was then allowed to stand until crystallization occurred. Red colored crystals were obtained. Storing the red crystals under atmospheric conditions caused decomposition to the yellow colored compound **12** within hours.

Preparation of 13: $(\text{H}_2\text{N}(\text{CH}_3)_2)_2[\text{CuCl}_3]$

A spoon full of $\text{CuCl}_2 \cdot 2\text{H}_2\text{O}$ was suspended in dmf (ca. 20 mL) and heated to 100 °C for 1 h. The solution was then allowed to stand until crystallization occurred. Olive colored crystals were obtained.

Preparation of 14: $[\text{Cu}(\text{dmsO})_2\text{Cl}_2]$

A spoon full of $\text{CuCl}_2 \cdot 2\text{H}_2\text{O}$ was suspended in dmsO (ca. 20 mL) and heated to 100 °C for ca. 1 h. The solution was then allowed to stand until crystallization occurred. The resulting pale green colored crystals were filtered off and dried to give $[\text{Cu}(\text{dmsO})_2\text{Cl}_2]$.

Preparation of 15: $[\text{Cu}_4\text{OCl}_6(\text{MeOH})_4] \cdot \text{MeOH}$

Synthesis was carried out under inert conditions. $\text{CuCl}_2 \cdot 2\text{H}_2\text{O}$ (0.60 g, 3.5 mmol), CuCl_2 (3.2 g, 24 mmol) and NaO^tBu (0.75 g, 7.5 mmol) were dissolved in absolute methanol (ca. 10 mL). The mixture was heated to reflux for ca. 2 h. The unreacted parts of the reactants were filtered off. The solvent was evaporated to give 2.0g (3.1 mmol, 95 %) of the yellow colored compound **15**.

Preparation of $[\text{Cu}(\text{pyridine})_2\text{Cl}_2]$

$\text{CuCl}_2 \cdot 2\text{H}_2\text{O}$ (0.85 g, 5.0 mmol) was dissolved in methanol (ca. 20 mL) and pyridine (0.40 g, 5.0 mmol) was added dropwise to the solution under stirring.

3. Reactions of CuCl_2 with Derivatives of Benzylamine

The mixture was stirred for approximately 10 min and the resulting blue precipitate was filtered off and dried to give $[\text{Cu}(\text{pyridine})_2\text{Cl}_2]$ (0.79 g, 70 %).

3.1.3. Results and Discussion

Apart from changing the metal itself there are three possibilities to diversify the system $[\text{Cu}_4\text{OCl}_6\text{L}_4]$. Figure 3.3 gives an overview of these possibilities: The ligand, the halogenide and the central oxide.

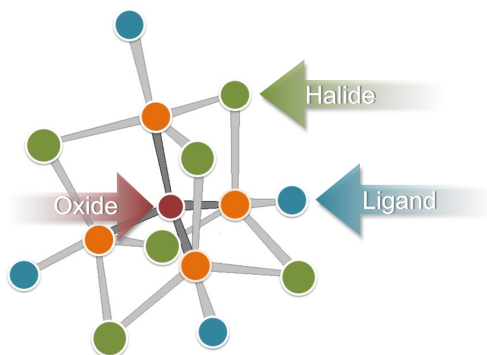


Figure 3.3.: Schematic illustration of $[\text{Cu}_4\text{OCl}_6\text{L}_4]$ with highlighted positions to diversify the system.

Concerning the ligand derivatives of benzylamine were used since cluster formation with benzylamine is fairly easy and led to cluster I in good yields, a system which was investigated in more detail already.[103] Additionally the spectroscopic data of cluster I were already available und thus could be compared to the new ligand system. Figure 3.4 gives an overview of the ligands used. The outcome of the reaction between $\text{CuCl}_2 \cdot 2\text{H}_2\text{O}$ and benzylamine in methanol depended very much on reaction conditions and especially on stoichiometric ratios of the reactants. In solution cluster I was in a chemical equilibrium with many other copper complexes.[103] To find out if cluster formation occurred with the new ligands $\text{L}^2\text{-L}^6$ this chemical equilibrium had to be understood for them as well. Thus many reactions with stoichiometric variations between $\text{CuCl}_2 \cdot 2\text{H}_2\text{O}$ and $\text{L}^2\text{-L}^6$ were carried out. The products of these reactions are shown in Figure 3.5.

3.1. Investigations Concerning $[\text{Cu}_4\text{OCl}_6\text{L}_4]$ -Cluster Formation

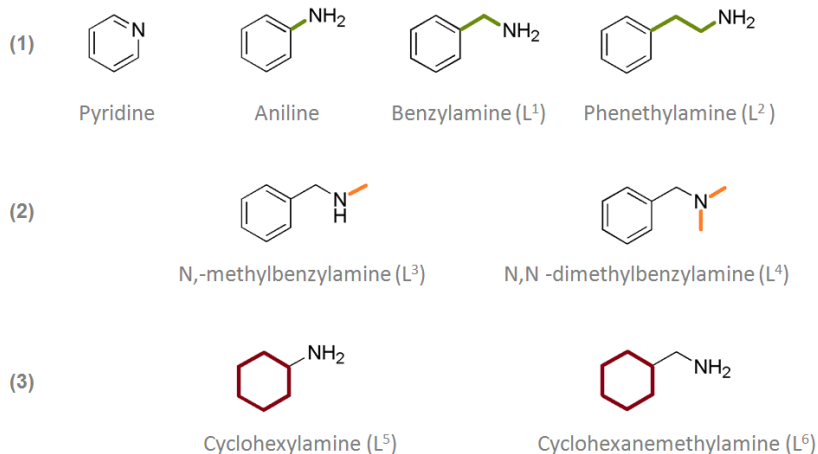


Figure 3.4.: Overview of the ligands which were used to modify cluster I. The focus was on the distance between aromatic residue and amine function (1), steric hindrances of the amine group (2) and influence of the aromatic residue (3).

To investigate the influence of the distance between the benzylic residue and amine function pyridine, aniline, benzylamine (L^1) and phenethylamine (L^2) were chosen. The molecular structures of the pyridine and the aniline compounds have already been reported in literature. Pyridine formed a cluster with the molecular formula $[\text{Cu}_4\text{OCl}_6(\text{pyridine})_4]$.^[32] Here it is important to point out that synthesis of this compound was only possible under inert conditions. Mixing $\text{CuCl}_2 \cdot 2\text{H}_2\text{O}$ and pyridine under air did not form a cluster but the complex $[\text{Cu}(\text{pyridine})_2\text{Cl}_2]$ (see Supporting Information for spectroscopic data). Interestingly it was neither possible to synthesize a cluster with aniline under inert conditions nor under air: We reported the molecular structure of the complex $[\text{Cu}(\text{aniline})_2\text{Cl}_2]$ which formed instead already.^[103] Proceeding the line of the ligands experiments with $\text{CuCl}_2 \cdot 2\text{H}_2\text{O}$ and phenethylamine (L^2) led to a colorful chemistry that resembled the chemistry of $\text{CuCl}_2 \cdot 2\text{H}_2\text{O}$ and benzylamine (L^1) (Figure 3.5). IR measurements and elemental analyses confirmed the nearly identical reaction behavior.

3. Reactions of $\text{CuCl}_2 \cdot 2\text{H}_2\text{O}$ with Derivatives of Benzylamine

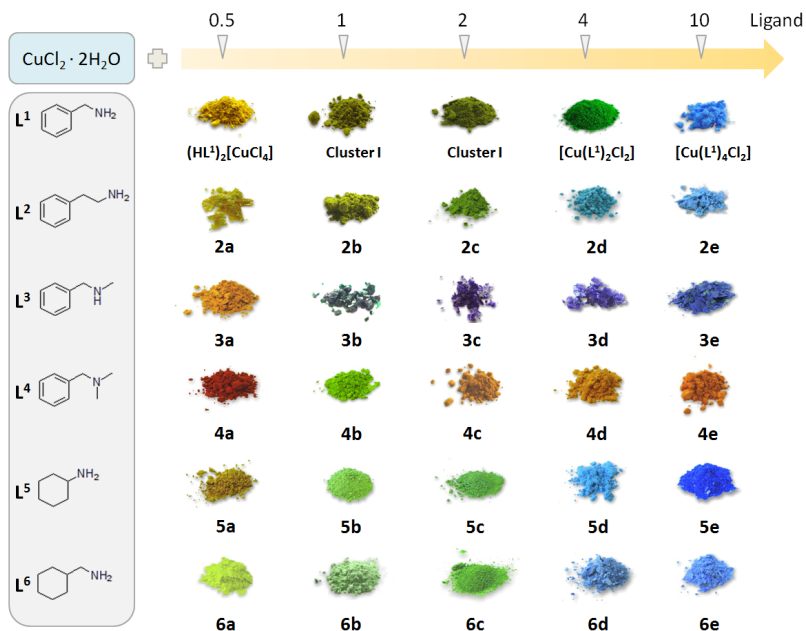


Figure 3.5.: Overview of the products that were obtained by adding L^2 - L^6 to $\text{CuCl}_2 \cdot 2\text{H}_2\text{O}$ in different stoichiometric amounts.

If $\text{CuCl}_2 \cdot 2\text{H}_2\text{O}$ was added in excess, the compound $(\text{HL}^2)_2[\text{CuCl}_4]$ (**2a**, Figure 3.5, see Supporting Information for spectroscopic data) was obtained. The reaction between equal amounts and slight excess of L^2 led to a cluster formation. The molecular structure of this cluster III is shown in Figure 3.6. The cluster unit co-crystallized with the complex $[\text{CuL}^2_2\text{Cl}_2]$. This behavior was already observed for cluster I. It is interesting to note that in both cases cluster formation only occurred with co-crystallization of the simple copper-amine-complex. Both clusters were not sensitive towards air and so needed not to be stored under argon. So far we do not have clear evidence if the co-crystallized complexes are responsible for this extraordinary stability. But due to this co-crystallization the cluster unit is surrounded by complexes which may shelter the cluster unit from water molecules. This might explain the stability towards moisture.

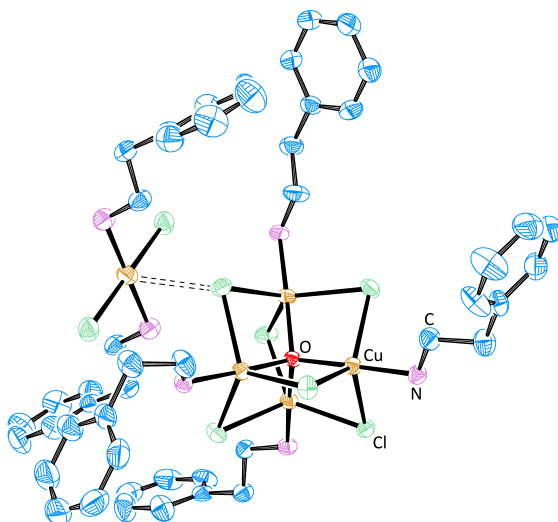


Figure 3.6.: Molecular structure of $[\text{Cu}_4\text{OCl}_6\text{L}_4] \cdot [\text{CuL}_2\text{Cl}_2]$ (cluster III, **2b**, **2c** Figure 3.5) (hydrogen atoms and crystallized solvent molecules are omitted for clarity). Ellipsoids are drawn at the 50 % probability level.

If L^2 was added in huge excess a bluish compound (**2d** and **2e**) was obtained. IR spectroscopy and elemental analysis (see Supporting Information) allowed to determine the compound as $[\text{CuL}_2\text{Cl}_2]$. Interestingly the complex $[\text{CuL}_4\text{Cl}_2]$ was not obtained as in the case of benzylamine (L^1). In summary cluster formation with pyridine, L^1 and L^2 was possible. However a cluster formation with aniline could not be observed. In the cases of benzylamine and phenethylamine cluster formation only occurred with co-crystallization of the simple copper-amine complex. So far one cannot say why aniline has an exceptional position. However it is interesting that L^2 just as L^1 formed a cluster with co-crystallized complex that may be responsible for the stability towards moisture. However it is not clear why with pyridine the cluster crystallizes without a complex. This makes it difficult to find a clear leitmotif in cluster formation concerning the distance benzylic residue - amine function.

To investigate steric hindrance of the donor group, N-methylbenzylamine and N,N-dimethylbenzylamine were chosen (Figure 3.4). By varying stoi-

3. Reactions of CuCl_2 with Derivatives of Benzylamine

chiometric ratios differently colored compounds (Figure 3.5) were obtained. Despite much effort it was not possible to crystallize all of the compounds, but due to IR spectroscopy and elemental analysis it was possible to determine the molecular structures as following: $(\text{HL}^3)_2[\text{CuCl}_4]$ (**3a**) and $[\text{CuL}^3_2\text{Cl}_2]$ (**3c**, **3d**). Again the salt $(\text{HL}^3)_2[\text{CuCl}_4]$ was formed if $\text{CuCl}_2 \cdot 2\text{H}_2\text{O}$ was added in excess. However it was contaminated with copper(II) chloride, which precipitated as well. If equal amounts of the reactants were used a green solution was obtained. It was difficult to get a solid compound from this solution. IR data of this compound showed a very broad absorption in the range of $3445\text{-}1623\text{ cm}^{-1}$. This indicated the formation of basic copper hydroxides. It is known from literature that the cluster unit Cu_4OCl_6 is sensitive towards hydrolysis and forms basic copper hydroxides with water.[28], [29], [31] This raised suspicion that a cluster was formed at first, but was not stable and so was hydrolyzed. Despite many experiments it was not possible to prepare a cluster with L^3 under atmospheric conditions. Further increase of L^3 led to the complex $[\text{CuL}^3_2\text{Cl}_2]$. The molecular structure is shown in Figure 3.7.

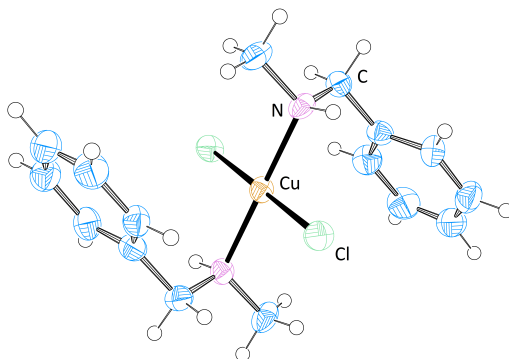


Figure 3.7.: Molecular structure of the complex $[\text{CuL}^3_2\text{Cl}_2]$. Ellipsoids are drawn at the 50 % probability level.

The compound crystallized either as purple crystals in the monoclinic space group $P2_1$ or as bluish compound in the orthorhombic space group Cmc (see Supporting Information for crystal data). The bluish complex was obtained as a major product if the amount of L^3 was increased again. But this time a green side product was formed in traces. IR spectra of the bluish and the green compounds were identical. It is assumed that structural

3.1. Investigations Concerning $[\text{Cu}_4\text{OCl}_6\text{L}_4]$ -Cluster Formation

isomerization occurred because dissolving the bluish compound in methanol always led to a green solution but bluish solid again. Additionally in many cases the protonated ligand (HL^3Cl) formed as a byproduct as well (see Supporting Information for crystal data). The structure of this salt has already been reported in literature.[104]

Adding N,N-dimethylbenzylamine (L^4) to $\text{CuCl}_2 \cdot 2\text{H}_2\text{O}$ led to an intensively red colored compound **4a** if copper(II) chloride was in excess. Compound **4a** could be identified as $(\text{HL}^4)_2[\text{CuCl}_4]$ with traces of contaminating CuCl_2 (see Supporting Information for spectroscopic data). If equal amounts of L^4 and $\text{CuCl}_2 \cdot 2\text{H}_2\text{O}$ were used an olive green solid was obtained. However it was not possible to isolate this compound. During attempts to isolate the solid it dyed green immediately. The IR spectrum of this green compound again showed the formation of a mixture of basic copper hydroxides. This once again suggested a cluster formation by followed hydrolysis. Increasing the amount of L^4 led to orange colored compounds (**4c-4e**, Figure 3.5). After many attempts it was finally possible to crystallize this compound and its molecular structure is shown in Figure 3.8.

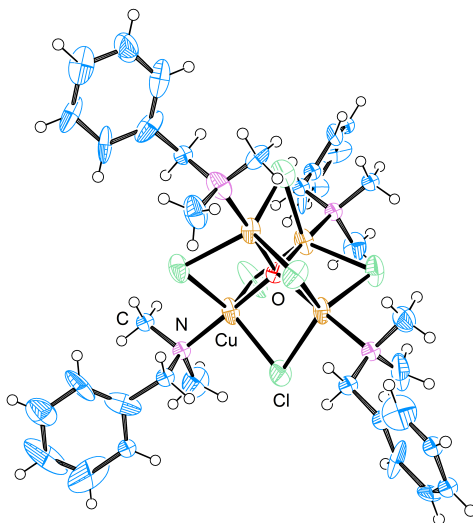


Figure 3.8.: Molecular structure of $[\text{Cu}_4\text{OCl}_6\text{L}_4]$ (cluster IV). Thermal ellipsoids are set at the 50 % probability level.

3. Reactions of CuCl_2 with Derivatives of Benzylamine

IR spectra showed the Cu_4O -vibration at 560 cm^{-1} and elemental analysis proved that always the same product, $[\text{Cu}_4\text{OCl}_6\text{L}^4_4]$ (cluster IV), was formed. However cluster IV was not as stable at air as cluster I or III. If not kept in a closed vessel the color changed to green and IR spectra of the green compound revealed again formation of copper hydroxides. This behavior is responsible for the differences in the theoretical and experimental elemental analyses. Since the analyses were conducted under atmospheric conditions the air moisture already started to hydrolyze the cluster which led to a decrease in the mass-% for C and N. Figure 3.9 shows the decomposition of cluster IV under atmospheric conditions within a week.



Figure 3.9.: Color change caused by hydrolysis of cluster IV if it is stored under atmospheric conditions. The cluster (*left*) is hydrolyzed by air moisture to give basic copper hydroxides (*right*).

The formation of a cluster with L^4 seems to be inconsistent with the findings for L^3 at first sight. However it might be explained with the steric hindrances of the methyl groups. The bulky methyl groups hinder co-crystallization with a complex. Regarding the bond lengths (Cu-Cl : 2.4 \AA , C-N : 1.5 \AA + C-H : 1 \AA) it can be assumed that the methyl group effectively protects the chloride anions of the cluster unit. In addition the methyl groups shield the cluster unit little, but however without a larger, shielding complex this makes the cluster unit easily attackable for water molecules. This might explain the instability of cluster IV at atmospheric conditions. In addition it explains the eye-catching orange color of compound **4c-4f** if compared to that of cluster I or cluster III. The "pure" cluster compounds without co-crystallized complexes are usually described to have a yellow, orange or red color.[28] Assumed that the "pure" clusters with L^1 and L^2 stick to this schemata as well, the olive color is caused by co-crystallization with the green complex $[\text{CuL}_2\text{Cl}_2]$ ($\text{L}=\text{L}^1, \text{L}^2$) probably. If no co-crystallization occurs, the colors should be similar to those of the reported clusters. Of course further investigations and DFG calculations have to be carried out to prove this hypothesis. Again the protonated ligand (HL^4Cl) was formed as a side product (see Supporting Information for crystallographic data).

The last change of the ligand was exchanging the aromatic residue with an aliphatic residue (Figure 3.4). By mixing $\text{CuCl}_2 \cdot 2\text{H}_2\text{O}$ and cyclohexy-

3.1. Investigations Concerning $[\text{Cu}_4\text{OCl}_6\text{L}_4]$ -Cluster Formation

lamine (L^5) the formation of $(\text{HL}^5)_2[\text{CuCl}_4]$ (**5a**, Figure 3.5) was observed with excess of copper(II) chloride again. Once again the compound was contaminated with copper(II) chloride, which precipitated as well. If equal amounts or a slight excess of L^5 were used an olive compound was obtained. Despite careful preparation it was not possible to isolate the solid without a color change to green (**5b**, **5c**, Figure 3.5). As for L^3 and L^4 IR spectra again showed the formation of copper hydroxides. So once again a cluster formation with following hydrolysis is very likely. Adding L^5 in excess led to bluish compounds (**5d**, **5e**, Figure 3.5). In both cases the complex $[\text{CuL}^5_2\text{Cl}_2]$ was formed. In addition it was possible to obtain the compound $[\text{CuL}^5_4]\text{Cl}_2$ as a byproduct when $[\text{Cu}_4\text{OCl}_6(\text{MeOH})_4]$ was used as a precursor in order to obtain a cluster (see below). The molecular structure is shown in Figure 3.10.

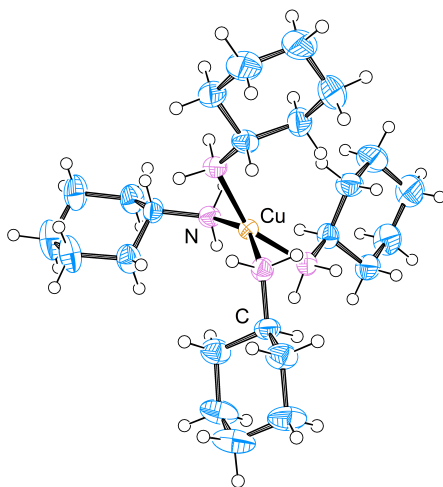


Figure 3.10.: Molecular structure of $[\text{CuL}^5_4]\text{Cl}_2$. The chloride anions are not shown for clarity, thermal ellipsoids are set at the 50% probability level.

A similar compound ($[\text{CuL}^5_4](\text{NO}_3)_2$) has already been reported in literature. [105] As a byproduct the salt of the protonated ligand HL^5Cl was found (as in most cases). Again the crystal structure of this compound already has been reported.[106]-[108] The reaction behavior of L^5 with $\text{CuCl}_2 \cdot 2\text{H}_2\text{O}$ was

3. Reactions of CuCl_2 with Derivatives of Benzylamine

similar to that of L^3 . Again it might be explained with steric hindrances. Because of the lacking possibility to turn the residue away from the cluster unit a co-crystallization with a complex was prohibited. So again the cluster unit was not sufficiently protected against hydrolysis.

Chemistry of L^6 with $\text{CuCl}_2 \cdot 2\text{H}_2\text{O}$ again was similar to the above discussed cases. If copper(II) chloride was added in excess $(\text{HL}^6)_2[\text{CuCl}_4]$ was obtained. Again increasing the amount of L^6 led to an olive compound which decomposed to a turquoise compound during isolation. IR data of this compound supported the formation of copper hydroxides again. If the amount of L^6 was increased further the complexes $[\text{CuL}^6_2\text{Cl}_2]$ (**6c**, Figure 3.5) and $[\text{CuL}^6_4\text{Cl}_2]$ (**6d**, **6e**, Figure 3.5, see Supporting Information for spectroscopic data) were formed. Again cluster formation under atmospheric conditions was not possible. To find out whether cluster formation was possible at all with the ligands L^3 , L^5 and L^6 , template syntheses were performed under inert conditions. Here the cluster $[\text{Cu}_4\text{OCl}_6(\text{MeOH})_4]$ was prepared and used as a precursor. In a second step the ligand was added to a solution of this cluster. A photograph of the obtained compounds for L^3 - L^6 is shown in Figure 3.11.



Figure 3.11.: Photographs of the obtained copper cluster compounds with the ligands L^2 (a), L^3 (b), L^4 (c), L^5 (d) and L^6 (e).

In all cases except with L^3 a cluster formation was detected via IR spectroscopy. Elemental analyses also confirmed the formation of the following compounds: $[\text{Cu}_4\text{OCl}_6\text{L}^2_4] \cdot [\text{CuL}^2_2\text{Cl}_2] \cdot \text{CH}_3\text{CN}$ (cluster III), $[\text{Cu}_4\text{OCl}_6\text{L}^4_4]$ (cluster IV), $[\text{Cu}_4\text{OCl}_6\text{L}^5_4] \cdot \text{CH}_3\text{CN}$ (cluster V) and $[\text{Cu}_4\text{OCl}_6\text{L}^6_4] \cdot 1.5 [\text{CuL}^6_2\text{Cl}_2]$ (cluster VI). The spectroscopic data of the cluster compounds are presented in the Supporting Information. In addition it was possible to determine the molecular structure of cluster VI, which is shown in Figure 3.12.

3.1. Investigations Concerning $[\text{Cu}_4\text{OCl}_6\text{L}_4]$ -Cluster Formation

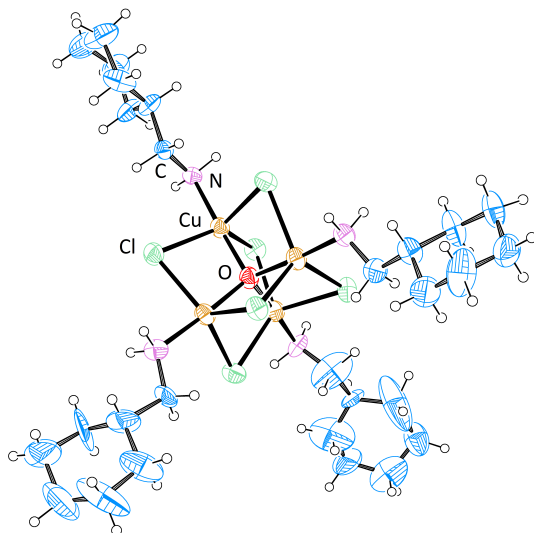


Figure 3.12.: Molecular structure of $[\text{Cu}_4\text{OCl}_6\text{L}^6_4] \cdot 1.5 [\text{CuL}^6_2\text{Cl}_2]$ (cluster VI). The co-crystallized complexes are omitted for clarity. Ellipsoids are drawn at the 40 % probability level.

Again the co-crystallization with the complex $[\text{CuL}^6_2\text{Cl}_2]$ was eye-catching. Cluster VI co-crystallized with 1.5 complexes. The coordination of these complexes to the cluster unit is shown in Figure 3.13. It gives a good impression of how effectively the complexes can shield the cluster unit against water molecules: Once again cluster VI was stable at air and hydrolysis did not occur. A second interesting observation was the formation of the orange colored compound $[\text{Cu}_4\text{OCl}_6\text{L}^4_4]$. Just as the compounds prepared under atmospheric conditions it started soon to decompose if not stored in a closed vessel. For cluster V a similar behavior could be observed. This cluster did not co-crystallize with a shielding complex either. However it seemed to be more stable towards moisture than cluster IV. All other prepared clusters did not need to be protected from air - and their olive color and elemental analyses gave evidence for co-crystallization with a simple copper complex. This was interesting because the fourfold of the ligands $\text{L}^3\text{-L}^6$ was added to the cluster template in order to obtain the pure compound $[\text{Cu}_4\text{OCl}_6\text{L}_4]$.

3. Reactions of CuCl_2 with Derivatives of Benzylamine

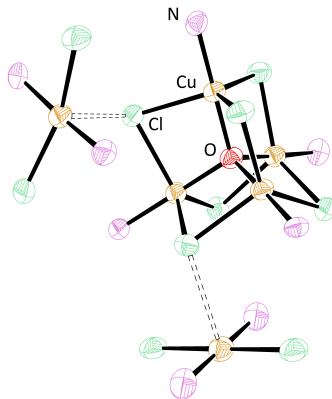


Figure 3.13.: Coordination of the $[\text{CuL}^6_2\text{Cl}_2]$ complexes to the cluster unit. The C atoms are omitted for clarity. Ellipsoids are drawn at the 40% probability level.

The result for L^3 was surprising. In contrast to all other ligands, it was not possible to prepare a cluster with L^3 . IR spectra and elemental analyses clearly showed the formation of the simple copper complex $[\text{CuL}^3_2\text{Cl}_2]$ even if prepared with the "methanol cluster" as precursor. This is astonishing because a cluster formation with the dimethylated ligand L^4 was observed even under atmospheric conditions, as well as cluster formation with the non-methylated ligand benzylamine (L^1). So far there is no clear explanation for this behavior. To sum it up, it remained difficult to predict a cluster formation under atmospheric conditions. While syntheses under inert conditions were successful in most cases syntheses under atmospheric conditions remained difficult. But the experiments allowed several conclusions: Firstly co-crystallization with the simple amine complex $[\text{CuL}_2\text{Cl}_2]$ may enhance the stability towards hydrolysis due to shielding the cluster unit. And secondly steric challenging ligands on the one hand may prohibit co-crystallization and so prevent stable cluster formation under air. But on the other hand they slightly may protect the cluster unit as well. Of course many additional experiments with modified ligands have to be carried out to prove these conclusions and to obtain more insight into the formation of clusters.

An interesting second question was if cluster formation is possible by chang-

3.1. Investigations Concerning $[\text{Cu}_4\text{OCl}_6\text{L}_4]$ -Cluster Formation

ing the halogenide. Because of the easy formation of cluster I benzylamine was kept as ligand and only the copper salts were changed. In case of copper(II) bromide we already reported the molecular structure of a bromide analogue of cluster I.[103] Preparation of a $[\text{Cu}_4\text{OI}_6\text{L}_4]$ compound certainly was not possible because of the redox potentials of iodide and copper. So it was interesting to find out if formation of a $[\text{Cu}_4\text{OF}_6\text{L}_4]$ cluster was possible. Copper(II) fluoride is only slightly soluble in most solvents, which led to synthetic difficulties. Nevertheless it was possible to obtain a bluish compound. However this compound was not stable and a colorless solid was separated after a few hours and the sample began to smell of benzaldehyde. IR measurements were complicated by this behavior because it was difficult to obtain a pure sample. Yet the IR data gave no evidence for a cluster formation. Investigations of the colorless compound suggested a mixture of the protonated ligand (HL^1F) and benzaldehyde. Attempts to synthesize a cluster under inert conditions by heating CuO and dried CuF_2 in methanol under reflux in order to obtain the cluster $[\text{Cu}_4\text{OF}_6(\text{MeOH})_4]$ failed once again because of the poor solubility of CuF_2 .

As a last change towards the Cu_4OCl_6 -unit the central oxide should be replaced by sulfide. Often it is possible to exchange an oxide-ion with a sulfid-ion by simply stirring a solution of the compound with elemental sulfur. Yet this did not work with cluster I, so a stoichiometric amount of NaHS was added to a solution of cluster I. Instead of the suspected formation of CuS green crystals were obtained which could be structurally identified as $[\text{CuL}^1_2\text{Cl}_2]$. This compound is already known in literature.[73] In addition colorless crystals formed. Despite much effort it was not possible to determine their molecular structure. Since simple exchange of the central ion did not lead to success the synthesis of the "methanol cluster" $[\text{Cu}_4\text{OCl}_6(\text{MeOH})_4]$ was modified. It is possible to obtain this cluster by heating CuCl_2 and CuO under inert conditions in methanol.[28] In order to obtain a $[\text{Cu}_4\text{SCl}_6]$ unit CuO was exchanged with CuS . As previously reported instead of a cluster the complex $[\text{Cu}(\text{MeOH})_2\text{Cl}_2]$ was formed in large quantities.[103] This result raised the question if S^{2-} with a radius of 184 pm (O^{2-} : 140 pm) is too large for a Cu_4SCl_6 unit. Crystallographic data showed that the Cu_4OBr_6 unit is minimal bigger than the Cu_4OCl_6 unit. So the experiment was repeated with CuBr_2 instead of CuCl_2 . This however was complicated due to the low heat stability of copper(II) bromide. But heating during the reaction in turn was necessary due to the low solubility of CuS . Despite careful syntheses it was not possible to obtain crystals suitable for x-ray analysis. In all cases a dark purple solid was obtained which with contact to air rapidly turned to orange and then turquoise. How much of the color change was owed to disproportionated copper(II) bromide during

3. Reactions of CuCl_2 with Derivatives of Benzylamine

the reaction is not known. The experiments were repeated in acetonitrile in order to offer a stronger coordinating ligand than methanol and so to stabilize the cluster unit. Dark green, red, orange and colorless crystals were obtained. All types of crystals were sensitive towards air and decomposed to copper(II) bromide. The dark green crystals were obtained in large quantities whereas the other crystals only seemed to be byproducts. The molecular structure of the dark green crystals is shown in Figure 3.16.

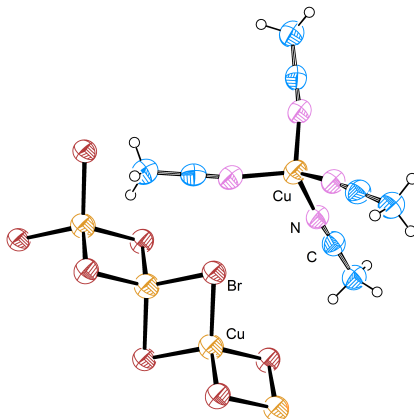


Figure 3.14.: Molecular structure of $[\text{Cu}(\text{acetonitrile})_4][\text{Cu}_2\text{Br}_4]$ (compound **7**). Ellipsoids are drawn at the 50% probability level.

The molecular structure shows the tetrahedral coordinated copper(I) complex $[\text{Cu}(\text{acetonitrile})_4]^+$ and a polymeric anion. The anion is mixed valent concerning the copper ions. Alternating Cu^+ and Cu^{2+} ions are bridged via bromide anions. The tetrahedral coordinated $[\text{Cu}(\text{acetonitrile})_4]^+$ is well known in literature from diverse copper(I) salts, but it seems to be the first time, that this complex co-crystallized with a mixed valent anion.[109]-[112] There are several examples in literature concerning mixed valent copper complexes or polymeric compounds (only few are given in the references).[113]-[119] Here it is interesting to note that the Cu^I and Cu^{II} ions often are bridged via bromide as well. The appearance of both Cu^+ and Cu^{2+} supported the assumption of disproportionation of CuBr_2 during the reaction. The molecular structure of the colorless crystals could also be determined and is shown in Figure 3.16.

3.1. Investigations Concerning $[\text{Cu}_4\text{OCl}_6\text{L}_4]$ -Cluster Formation

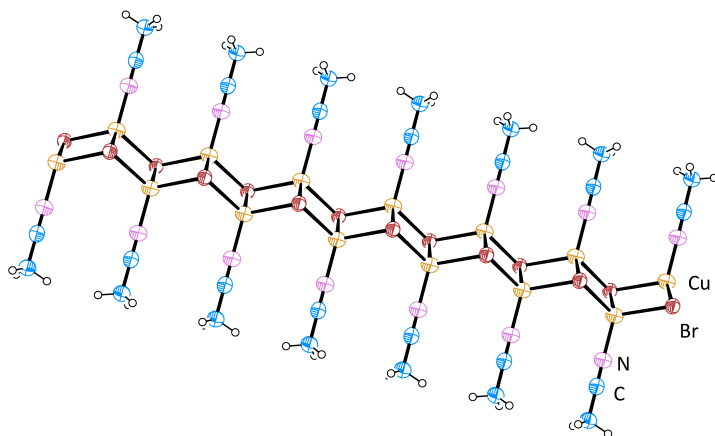


Figure 3.15.: Molecular structure of $[\text{Cu}(\text{acetonitrile})\text{Br}]$ (compound **8**). To give an expression of the polymeric character of this compound a greater part than the elemental cell is shown. Ellipsoids are drawn at the 50% probability level.

Again the formation of a copper(I) compound gave evidence for the disproportionation of CuBr_2 . The crystal structure of the red crystals could be determined as well and is shown in Figure 3.16.

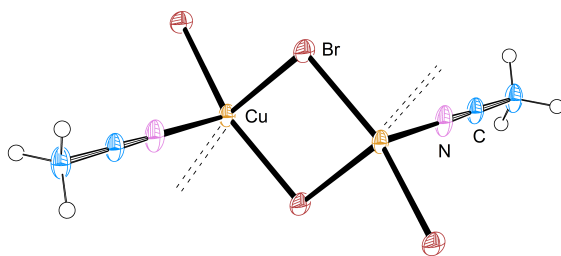


Figure 3.16.: Molecular structure of $[\text{Cu}(\text{acetonitrile})\text{Br}_2]$ (compound **9**). An excerpt of the polymeric structure is given. Ellipsoids are drawn at the 50% probability level.

The formation of compound **9** resembled the formation of $[\text{Cu}(\text{MeOH})_2\text{Cl}_2]$

3. Reactions of CuCl_2 with Derivatives of Benzylamine

and was consequent concerning the formation of the copper(I) equivalent (compound **8**). The crystal structure of the similiar copper(II) complex $[\text{Cu}(\text{acetonitrile})_2\text{Br}_2]$ is already known in literature. [120], [121] The molecular structure of the orange crystals could not be determined. In conclusion despite many attempts it was not possible to synthesize a cluster with a Cu_4SX_6 unit ($\text{X} = \text{Cl}, \text{Br}$). Instead in most cases copper solvent complexes were obtained. This substantiates suspicion that sulfide is too large to form a Cu_4SX_6 unit.

Despite diversifying the $[\text{Cu}_4\text{OCl}_6\text{L}^1_4]$ system we were also interested in the cluster formation of copper(II) chloride with solvent molecules. H. tom Dieck and co-workers already provided an easy synthesis route for $[\text{Cu}_4\text{OCl}_6\text{L}_4]$ clusters with $\text{L} =$ solvent molecules.[28] Pursuing these results we already reported the crystal structures of the "solvent clusters" $[\text{Cu}_4\text{OCl}_6(\text{MeOH})_4]$, $[\text{Cu}_4\text{OCl}_6(\text{acetonitrile})_4]$, $[\text{Cu}_4\text{OCl}_6(\text{dmf})_4]$ and $[\text{Cu}_4\text{OCl}_6(\text{dmsO})_4]$. [103] As mentioned above these clusters could easily be prepared from CuO and CuCl_2 . An interesting question now is if these clusters can also be obtained by simple recrystallization of $\text{CuCl}_2 \cdot 2\text{H}_2\text{O}$ in the according solvent. This is interesting concerning catalyses with simple copper salts as copper(II) chloride. Copper(II) and/or copper(I) chloride are widely used as a good catalyst in organic reactions.[87]-[92], [95]-[100] Mostly the reaction mechanism is not clarified and it remains unknown how a simple copper salt like CuCl_2 with only one copper center can catalyze reactions with more than one electron transfer. Surely CuCl_2 is not "naked" in solution. But the question remains how it looks like and if multinuclear compounds such as clusters for example are formed. To find out if there are formed multinuclear compounds indeed, $\text{CuCl}_2 \cdot 2\text{H}_2\text{O}$ was recrystallized in common solvents. Recrystallization of $\text{CuCl}_2 \cdot 2\text{H}_2\text{O}$ in methanol only led to $\text{CuCl}_2 \cdot 2\text{H}_2\text{O}$ again, but under inert conditions the already described $[\text{Cu}(\text{MeOH})_2\text{Cl}_2]$ complex was formed. Attempts in acetone led to pale orange needles in large quantities. The molecular structure is shown in Figure 3.17. It shows that one crystal water of $\text{CuCl}_2 \cdot 2\text{H}_2\text{O}$ was exchanged with half an acetone molecule. But in contrast to $\text{CuCl}_2 \cdot 2\text{H}_2\text{O}$ the copper-chloride units are not separated by water molecules. Instead large polymeric copper-chloride-chains are formed, which are known from the structure of pure CuCl_2 . The compound was sensitive towards air and decomposed rapidly to a colorless solid. If not isolated from solution the solution turned green and crystalline CuCl was formed within a day.

3.1. Investigations Concerning $[\text{Cu}_4\text{OCl}_6\text{L}_4]$ -Cluster Formation

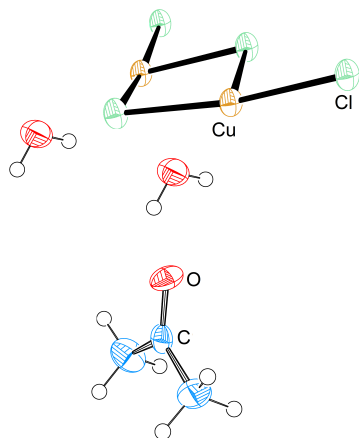


Figure 3.17.: Part of the polymeric structure of $[\text{CuCl}_2] \cdot \text{H}_2\text{O} \cdot 0.5$ acetone (compound **10**). Ellipsoids are drawn at the 50% probability level.

The recrystallization in acetonitrile led to two different compounds. Beside $\text{CuCl}_2 \cdot 2\text{H}_2\text{O}$ red crystals were obtained. The molecular structure is presented in Figure 3.18.

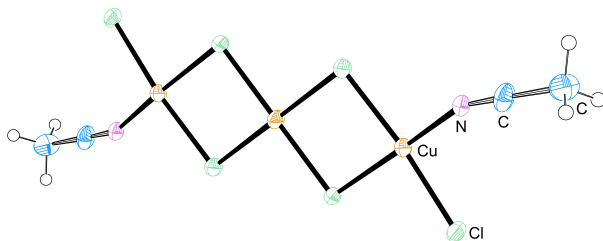


Figure 3.18.: Molecular structure of $[\text{Cu}_3(\text{acetonitrile})_2\text{Cl}_6]$ (compound **11**). Ellipsoids are drawn at the 50% probability level.

Likewise the experiments in acetone a multinuclear copper-chloride chain was formed. But in contrast the chain is limited to three copper ions bridged via chloride. Acetonitrile molecules occupy the empty coordination sites at the

3. Reactions of CuCl_2 with Derivatives of Benzylamine

end of the chain. The red crystals were slightly sensitive towards air and decomposed to yellow crystals. The molecular structure of these crystals is shown in Figure 3.19.

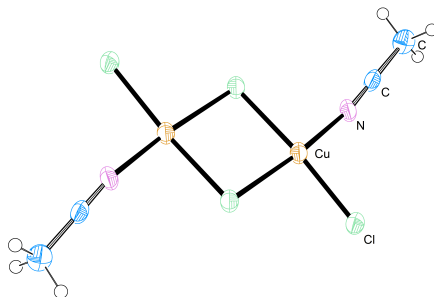


Figure 3.19.: Molecular structure of $[\text{Cu}_2(\text{acetonitrile})_2\text{Cl}_4]$ (compound **12**). Ellipsoids are drawn at the 50 % probability level.

The structure shows a copper chloride dimer with coordinated acetonitrile molecules and has already been reported in literature. [122] It strongly resembles the crystal structure of the red crystals above. The only difference is a missing CuCl_2 -unit. The yellow crystals were also sensitive towards air and decomposed again to a colorless solid which again turned to blue $\text{CuCl}_2 \cdot 2\text{H}_2\text{O}$ after a few days. This suggests the formation of $[\text{Cu}(\text{acetonitrile})_2\text{Cl}_2]$ as colorless compound in between. However it was not possible to determine the molecular structure of this colorless compound.

Recrystallization of $\text{CuCl}_2 \cdot 2\text{H}_2\text{O}$ in dmf led to olive green crystals. The molecular structure is shown in Figure 3.20. The structure shows a trigonal planar coordinated $[\text{CuCl}_3]^{2-}$ anion and two dimethylammonium cations. Obviously $\text{CuCl}_2 \cdot 2\text{H}_2\text{O}$ caused cleavage of dmf during the recrystallization process. It is known that light and heat promote cleavage of dmf into dimethylamine and formaldehyde. A similar process probably occurred with copper(II) chloride. Although temperatures were not very high during recrystallization, $\text{CuCl}_2 \cdot 2\text{H}_2\text{O}$ seemed to promote cleavage. However it remained unclear why Cu^I was formed instead of Cu^{II} . Similar compounds with the copper(II) anion $[\text{CuCl}_4]^{2-}$ have already been reported in literature.[122], [123]

3.1. Investigations Concerning $[\text{Cu}_4\text{OCl}_6\text{L}_4]$ -Cluster Formation

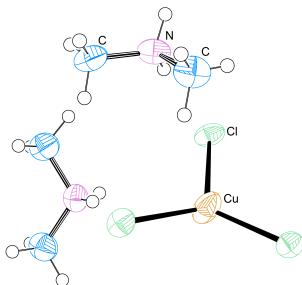


Figure 3.20.: Molecular structure of $(\text{H}_2\text{N}(\text{CH}_3)_2)_2[\text{CuCl}_3]$ (compound **13**). Ellipsoids are drawn at the 50% probability level.

Experiments in dmsO led to slightly green crystals in good yield. The molecular structure was determined as $[\text{Cu}(\text{dmsO})_2\text{Cl}_2]$ (compound **14**), a complex which already has been reported in literature.[86], [124] These recrystallization experiments showed that in all cases not pure $\text{CuCl}_2 \cdot 2\text{H}_2\text{O}$ was obtained, but that multinuclear compounds or at least solvent complexes were formed. However clusters of the type $[\text{Cu}_4\text{OCl}_6(\text{solvent})_4]$ could not be isolated. This was not very surprising since all of these "solvent clusters" are sensitive towards moisture and the dihydrate, $\text{CuCl}_2 \cdot 2\text{H}_2\text{O}$, was used in all experiments. A certain amount of water as oxygen source for the central oxide is indeed necessary. But using the dihydrate meant a huge excess of water, additionally dried solvents were not used either. Experiments in absolute methanol and with dry CuCl_2 and a stoichiometric amount of crystal water did not lead to a cluster formation either. This again is not surprising because there was no appropriate base present in solution. The central oxide of the cluster derives from deprotonated water. If an amine ligand is provided, it acts as base. This is proved by the fact that in nearly all of the described experiments concerning variation of the ligand system above HLCl (L = benzylamine, N -methylbenzylamine, N,N -dimethylbenzylamine, cyclohexylamine) was obtained as side product. Together with unreacted amine a buffer is formed, keeping the pH constant and so prevents the cluster unit Cu_4OCl_6 from acidic decomposition. If no base is added (as in the recrystallization experiments) H_2O reacts amphoteric and per one mole O^{2-} two moles H_3O^+ are formed. Because of the missing buffer, the cluster unit either is decomposed by the acid or prevented to form. Because of this consideration the recrystallization of $\text{CuCl}_2 \cdot 2\text{H}_2\text{O}$ with CuCl_2 in methanol was repeated, but this time NaO^tBu was added as base. The

3. Reactions of CuCl_2 with Derivatives of Benzylamine

solution dyed brown immediately and a yellow solid (compound **15**) was obtained in very good yield. IR data confirmed the formation of the "solvent cluster" $[\text{Cu}_4\text{OCl}_6(\text{MeOH})_4] \cdot \text{MeOH}$. Figure 3.21 shows the IR spectra of crystalline $[\text{Cu}_4\text{OCl}_6(\text{MeOH})_4]$ (obtained via [28]) and compound **15**.

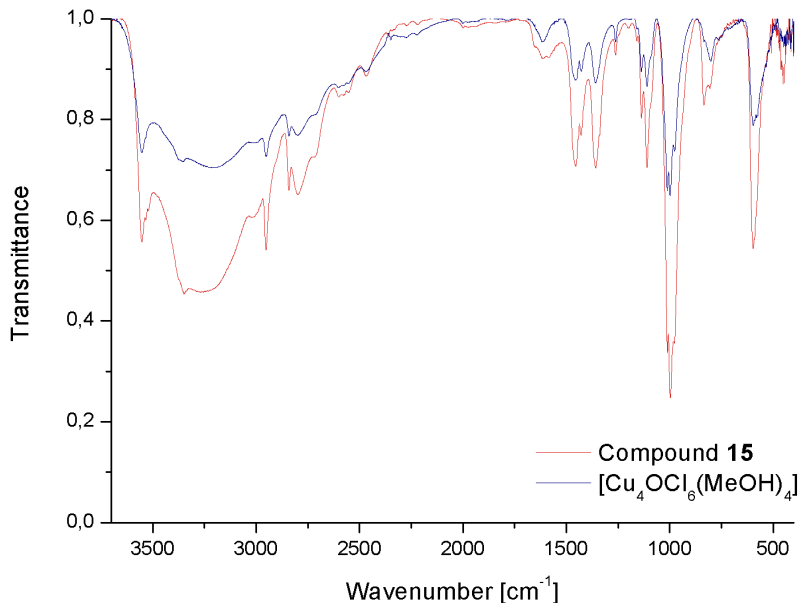


Figure 3.21.: Comparison of the IR spectra of crystalline $[\text{Cu}_4\text{OCl}_6(\text{MeOH})_4]$ and compound **15**. The Cu_4O -vibration is clearly seen at 691 cm^{-1} .

This experiment showed how easy a cluster formation can occur. This is remarkable since the "methanol cluster" is very sensitive towards moisture, but readily formed in the presence of water if a base was added. Interestingly in many cases when copper chloride is used in organic syntheses a base as NaO^tBu is added as well. Traces of water or oxygen are sufficient to form a cluster of the type $[\text{Cu}_4\text{OCl}_6]$. In addition copper(I) chloride (if purchased from a commercial supplier) often is contaminated with copper(II) chloride, which is revealed by the green color of " CuCl ". So in most reactions with CuCl as catalyst there probably is a mixture of copper(I), copper(II) chloride and traces of water. As could be shown under these conditions cluster

formation is fairly easy and there is no "naked" copper chloride in solution. This emphasizes the important role these clusters may take up in catalyses. In addition it might explain why copper chloride itself shows catalytic activity in many oxygenation reactions. Some cases of catalytic activity for $[\text{Cu}_4\text{OCl}_6]$ and similar copper clusters and other multinuclear copper clusters have already been reported.[38]-[40], [53]-[57] However the experiments were conducted with a previously synthesized cluster compound and not a self-organized "solvent cluster". In preliminary experiments the catalytic activity of these "solvent clusters" was investigated. It could be shown that these "solvent clusters" indeed show catalytic activity (see Supporting Information for first results). Remarkably these "solvent clusters" showed a great similarity with copper(II) chloride. This again supports the assumption of cluster formation of copper(II) chloride, which than act as catalyst. Surely further experiments with "solvent clusters" and copper(II) chloride in comparison as catalysts should be carried out.

3.1.4. Conclusion

New insight into cluster formation under atmospheric conditions was provided. Due to reacting $\text{CuCl}_2 \cdot 2\text{H}_2\text{O}$ with simple amine ligands the molecular structures of diverse copper-amine-complexes and copper clusters could be reported. It is eye-catching that most of the obtained copper clusters co-crystallized with a simple copper-amine complex to form the compound $[\text{Cu}_4\text{OCl}_6\text{L}_4] \cdot 1-1.5 [\text{CuL}_2\text{Cl}_2]$. An extraordinary stability towards hydrolysis was observed for these compounds. It is very likely that the co-crystallized complexes shield the cluster unit Cu_4OCl_6 from water molecules and so prevent fast hydrolysis of these compounds under atmospheric conditions. According to the experiments co-crystallization may only occur if the amine donor group is not sterically hindered. Attempts with methylated N donor groups did not lead to co-crystallization of a cluster and a complex. Instead the pure clusters $[\text{Cu}_4\text{OCl}_6\text{L}^4]$ and in the case of L^5 $[\text{Cu}_4\text{OCl}_6\text{L}^5]$ were obtained. However these compounds were slightly stable at air. Probably the aliphatic residues, which on the one hand prevent co-crystallization with a simple complex shield the cluster unit on the other hand little as well themselves. But this shielding is not as efficient as shielding by a complex because hydrolysis of $[\text{Cu}_4\text{OCl}_6\text{L}^4]$ occurred at air within days. However it was not possible to prepare the cluster $[\text{Cu}_4\text{OCl}_6\text{L}^3]$ with the monomethylated ligand L^3 . So far there is no explanation for this observation. Attempts to exchange the central oxide with a sulfide failed. Instead of a Cu_4SX_6 ($\text{X} = \text{Cl}, \text{Br}$) unit the formation of many other products was observed. Especially experiments with CuBr_2 and acetonitrile led to a colorful

3. Reactions of CuCl_2 with Derivatives of Benzylamine

chemistry. Disproportionation of CuBr_2 caused the formation of copper(I) or mixed valent compounds. However $[\text{Cu}_4\text{OBr}_6]$ -cluster formation with CuBr_2 itself was possible. Analogues to copper(II) chloride copper(II) bromide formed the cluster $2[\text{Cu}_4\text{OBr}_6\text{L}^2_4] \cdot [\text{CuL}^2_2\text{Br}_2]$ if treated with L^2 as previously reported. [103] Attempts to obtain a fluorine analogue failed because of the minor solubility of CuF_2 . By recrystallization of $\text{CuCl}_2 \cdot 2\text{H}_2\text{O}$ in diverse organic solvents mostly polymeric $[\text{CuCl}_2]$ -chains with organic solvent molecules as ligands or co-crystallized solvent molecules were obtained. These polymeric chains are known from pure CuCl_2 , so it was surprising that these compounds are obtained from copper(II) chloride dihydrate and under atmospheric conditions. This may hint at the outstanding catalytic activity of simple copper(II) chloride in many organic reactions. Due to the formation of polymeric chains copper chloride is able to accept/provide more than only one electron. This strong tendency towards polymeric chains might explain the qualities as catalyst in many organic redox reactions, which cannot be explained with the structure of single $\text{CuCl}_2 \cdot 2\text{H}_2\text{O}$ alone. In addition it could be shown that cluster formation occurs if copper(II) chloride and a base (NaO^tBu e. g.) are added to a coordinating solvent. This emphasizes the important role such copper clusters may play in catalytic reactions. In most organic reactions with copper chloride as catalyst a base is added in addition. If these experiments are conducted in coordinating solvents (acetonitrile, acetone, methanol, ethanol, dmf, dmsO, thf etc.) a cluster formation is very likely. An interesting question now is if these "solvent clusters" exhibit catalytic activity as well. In preliminary experiments a similar catalytic activity of these clusters as cluster I or copper(II) chloride was observed. It is important to carry out further experiments with "solvent clusters" and copper(II) chloride in comparison as catalysts. This might be important for the future goal to find out more about the "real" active species in catalyses with copper chloride.

3.1.5. Acknowledgements

S. Löw and S. Schindler are thankful to the Stiftung Stipendienfonds der Chemischen Industrie e.V. for providing a Ph.D. scholarship to S. Löw. Furthermore, we appreciate the collaboration with Prof. Dr. U. Behrens and his support in crystal structure determination.

3.2. Selected Supporting Information and Unpublished Material

3.2.1. Investigations Concerning the Catalytic Activity of "Solvent Clusters"

To investigate the reactivity of "solvent clusters" several experiments with them as a catalyst in a hydroxylation reaction of cyclohexane were performed. We already reported the hydroxylation of cyclohexane with cluster I and $\text{CuCl}_2 \cdot 2\text{H}_2\text{O}$ by adding hydrogenperoxide according to Figure 3.22.[103]

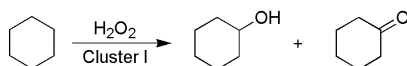


Figure 3.22.: Oxygenation of cyclohexane with cluster I.

This reaction was repeated with the "solvent clusters" as catalysts. Because of the incorporation of solvent molecules in all of these compounds it was necessary to vary the solvent during the oxygenation reaction as well. Control experiments with cluster I and $\text{CuCl}_2 \cdot 2\text{H}_2\text{O}$ were pursued in all of the chosen solvents. Table 3.1 gives an overview of the yields and the reactions performed.

Table 3.1.: Reaction conditions and average yields of the oxygenation of cyclohexane with "solvent clusters".

catalyst	solvent	alcohol [%]	ketone [%]	turn- over
cluster I	acetonitrile	7.8	2.7	42
$\text{CuCl}_2 \cdot 2\text{H}_2\text{O}$	acetonitrile	15.9	8.6	98
$[\text{Cu}_4\text{OCl}_6(\text{acetonitrile})_4]$	acetonitrile	9.5	3.3	52
$[\text{Cu}_4\text{OCl}_6(\text{acetone})_4]$	acetone	1.1	2.5	15
cluster I	methanol	—	—	—

continue next page

3. Reactions of CuCl_2 with Derivatives of Benzylamine

Table 3.1.: Reaction conditions and average yields of the oxygenation of cyclohexane with "solvent clusters". (*continuation*)

$\text{CuCl}_2 \cdot 2 \text{H}_2\text{O}$	methanol	—	—	—
$[\text{Cu}_4\text{OCl}_6(\text{methanol})_4]$	methanol	—	—	—
cluster I	dmf	—	—	—
$\text{CuCl}_2 \cdot 2 \text{H}_2\text{O}$	dmf	—	—	—
$[\text{Cu}_4\text{OCl}_6(\text{dmf})_4]$	dmf	—	—	—
cluster I	dmsO	—	—	—
$\text{CuCl}_2 \cdot 2 \text{H}_2\text{O}$	dmsO	—	—	—
$[\text{Cu}_4\text{OCl}_6(\text{dmsO})_4]$	dmsO	—	—	—
$[\text{Cu}(\text{dmsO})_2\text{Cl}_2]$	dmsO	—	—	—

Some of the "solvent clusters" indeed showed catalytic activity. The yields of cyclohexanol and cyclohexanone are comparable to the yields obtained by cluster I and $\text{CuCl}_2 \cdot 2 \text{H}_2\text{O}$. However in most solvents (dmf, dmsO and methanol) the oxygenation of cyclohexane was not successful. Again the behavior of the "solvent clusters" and $\text{CuCl}_2 \cdot 2 \text{H}_2\text{O}$ was identical since oxygenation with $\text{CuCl}_2 \cdot 2 \text{H}_2\text{O}$ was not successful in the named solvents either. This supports the hypothesis that multinuclear copper compounds are formed by $\text{CuCl}_2 \cdot 2 \text{H}_2\text{O}$ during catalytic reactions. If these active species resemble the "solvent clusters" or the compounds obtained by recrystallization of $\text{CuCl}_2 \cdot 2 \text{H}_2\text{O}$ is unknown. A future goal is to find out more about this active species.

3.2.2. Reactivity of Cluster I

Oxygenation of adamantane

Several copper compounds were tested as catalyst in the oxygenation of adamantane. However the procedure was complicated due to the low solubility of adamantane. The reaction was carried out in acetonitrile and only tiny

3.2. Selected Supporting Information and Unpublished Material

amounts of adamantane were used, but still in some cases the precipitation of adamantane was observed, which may distort the determination of the yield. Adamantane (1 mmol, 136 mg) was dissolved in acetonitrile (20 mL) and the catalyst was added. Aqueous H₂O₂ (30 %, 2 mL, ca. 20 mmol) was added dropwise to the stirred solution. The solution was stirred until gas evolution stopped. Then the catalyst was removed through a chromatography column and the yield of the corresponding alcohol and aldehyde determined via GC-MS. The amounts of copper compounds were chosen to give equal amounts of copper(II) ions in solution. Therefore the amount of substance used is different in most cases. Figure 3.23 shows the reaction scheme for the performed oxygenation. Two products were obtained: adamantane-1-ol (hydroxylated at the tertiary C-atom) and adamantane-1-on. Table 3.2 shows the reaction conditions and average results.

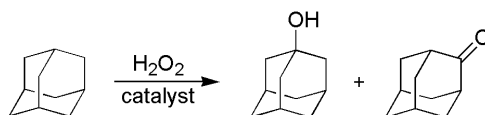


Figure 3.23.: Oxygenation of adamantane.

Table 3.2.: Reaction conditions and average results for the oxygenation of adamantane.

n(catalyst) ([μmol])	copper centers	alcohol [%]	ketone [%]	turn-over
cluster I (25)	9	16	13	12
cluster I, bromide (25)	9	2	2	1.6
cluster II (56)	4	18	14	5.8
[CuL ₂ ¹ Cl ₂] (225)	1	9	8	0.7
[CuL ₄ ¹ Cl ₂] (225)	1	—	—	—
(HL ¹) ₂ [CuCl ₄]	1	14	12	1.2
CuCl ₂ · 2 H ₂ O (225)	1	17	12	1.3

continue next page

3. Reactions of CuCl_2 with Derivatives of Benzylamine

Table 3.2.: Reaction conditions and average results for the oxygenation of adamantane. (*continuation*)

CuBr_2 (225)	1	6	4	0.4
$\text{Cu}(\text{NO}_3)_2 \cdot 3 \text{H}_2\text{O}$ (225)	1	22	14	1.6
$\text{CuSO}_4 \cdot 5 \text{H}_2\text{O}$ (225)	1	3	3	0.3
$\text{Cu}(\text{CH}_3\text{COO})_2 \cdot \text{H}_2\text{O}$ (225)	1	—	—	—
$[\text{Cu}_3\text{Cl}_6(\text{acetonitrile})_2]$ (75)	3	14	9	3.1
$[\text{Cu}_2\text{Cl}_4(\text{acetonitrile})_2]$ (113)	2	11	5	1.4
$[\text{Cu}_4\text{OCl}_6(\text{acetonitrile})_4]$ (56)	4	12	6	3.2
$[\text{ZnL}_2\text{Cl}_2]$ (225)	1	—	—	—
$\text{ZnCl}_2 \cdot 2 \text{H}_2\text{O}$	1	—	—	—

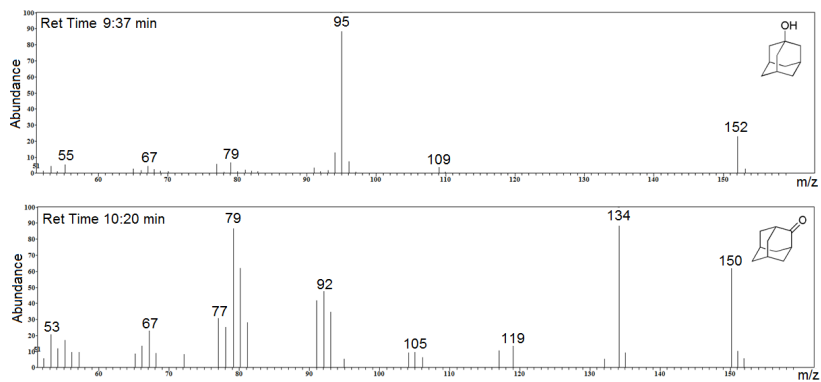


Figure 3.24.: MS spectra of adamantan-1-ol and adamantan-1-one.

3.2. Selected Supporting Information and Unpublished Material

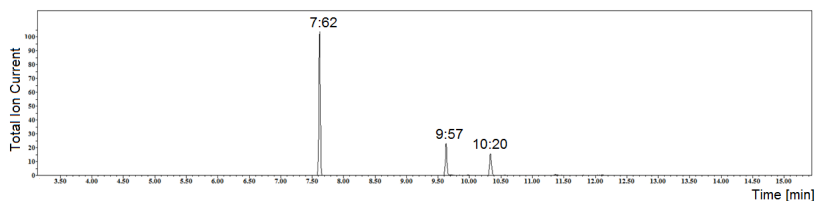


Figure 3.25.: Gas chromatogram of the oxygenation reaction of adamantane with cluster I as catalyst.

Oxidation of solvents

During oxidation reactions with cluster I the oxidation of solvent molecules was observed as a side-reaction. Figure 3.26 gives an overview of the observed reactions. In all cases only traces of the oxidized solvent molecules were observed.

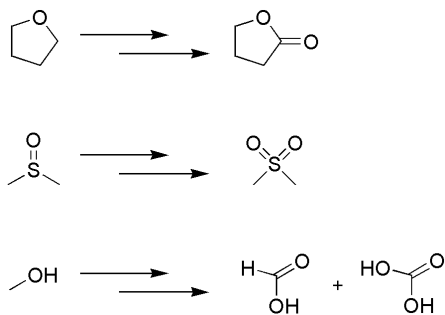


Figure 3.26.: Oxidation of solvent molecules as side-reactions.

3.2.3. Additional Molecular Structures

Protonated ligands

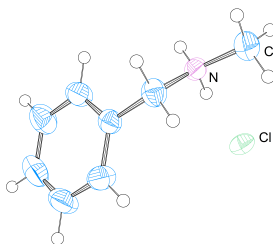


Figure 3.27.: Molecular structure of HL^3Cl , thermal ellipsoids are set at 50 % probability.

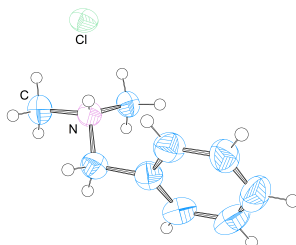


Figure 3.28.: Molecular structure of HL^4Cl , thermal ellipsoids are set at 50 % probability.

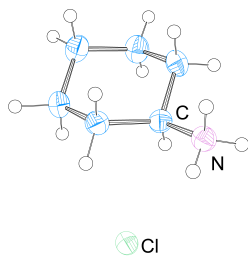


Figure 3.29.: Molecular structure of HL⁵Cl, thermal ellipsoids are set at 50 % probability.

Cluster I recrystallized

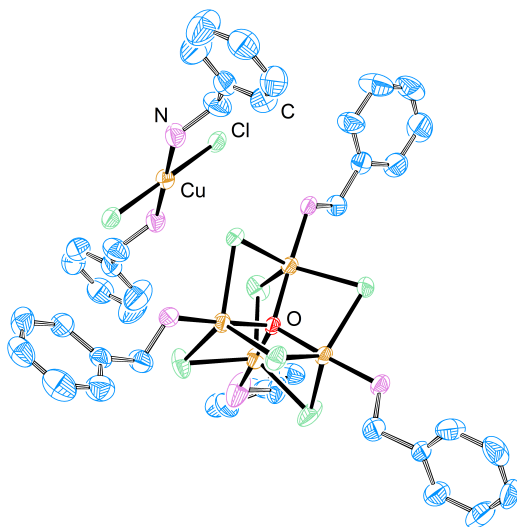


Figure 3.30.: Molecular structure of [Cu₄OCl₆L¹₄] · [CuL¹₂Cl₂], thermal ellipsoids are set at 50 % probability. Hydrogen atoms and solvent molecules are omitted for clarity.

3. Reactions of CuCl_2 with Derivatives of Benzylamine

Cluster I was recrystallized in acetone and acetonitrile. In both cases the composition of the cluster complex changed and the compound $[\text{Cu}_4\text{OCl}_6\text{L}^1_4] \cdot [\text{CuL}^1_2\text{Cl}_2]$ was obtained (see Figure 3.30). However this compound decomposed to $(\text{HL}^1)_2[\text{CuCl}_4]$ if stored in acetonitrile after a few days.

4. Reactions of Copper(I) Chloride with Benzylamine

This chapter includes one manuscript that is going to be submitted to the journal "*Zeitschrift für Allgemeine und Anorganische Chemie*".

Contribution of the co-author:

The co-author solved two of the crystal structures, to detail:

- U. Behrens: **4** and $(HL^1)(C_7H_7NHCOO)$

4.1. Synthesis, Structure and Reactivity of the Compound [Cu(C₇H₇NH₂)Cl]₄

This work is to be submitted to "Zeitschrift für Allgemeine und Anorganische Chemie (ZAAC)".

Sabine Löw, Ulrich Behrens and Siegfried Schindler

The facile synthesis, molecular structure and preliminary investigations concerning the reactivity of [Cu(C₇H₇NH₂)Cl]₄ towards dioxygen and derivatives is reported. The compound could easily be prepared in good yields by mixing CuCl and benzylamine under inert conditions in dichloromethane. Surprisingly this copper(I) compound was formed instead of the expected cubane analogue. It shows Cu^I...Cu^I interactions with Cu-Cu bonds of 2.89 Å. Preliminary experiments concerning the reactivity towards dioxygen and derivatives were performed and now the first UV-vis features of dioxygen activation with a copper(I) compound that exhibits Cu^I...Cu^I interactions are reported. However determination of the exact Cu/O₂ species that are formed was not possible.

4.1.1. Introduction

Copper(I) cubane clusters of the type [Cu₄X₄L₄] (X = Cl, Br, I, see Figure 4.1) are well known in literature and have been investigated intensively because of their optical properties. [125]-[129] In most cases synthesis is easy and conducted through self-assembly of the cubane core.[44], [130]-[134] Therefore, simply mixing a copper(I) halogenide with the ligand system usually lead to the cubane cluster. Especially Davies and El-Sayed investigated copper(I) cubane systems concerning their reactivity towards dioxygen.[44], [94], [130], [131], [135]-[140] In this context they also reported the formation of the μ₄-oxido copper(II) cluster [Cu₄OCl₆L₄] (L = N,N-dimethylaminomethylferrocene, see Figure 3.2) after the reaction of the cubane cluster [Cu₄Cl₄L₄] with dioxygen.[44] This is another popular structure type of copper clusters and again well known in literature since the 1960s.[27]-[41]

4. Reactions of Copper(I) Chloride with Benzylamine

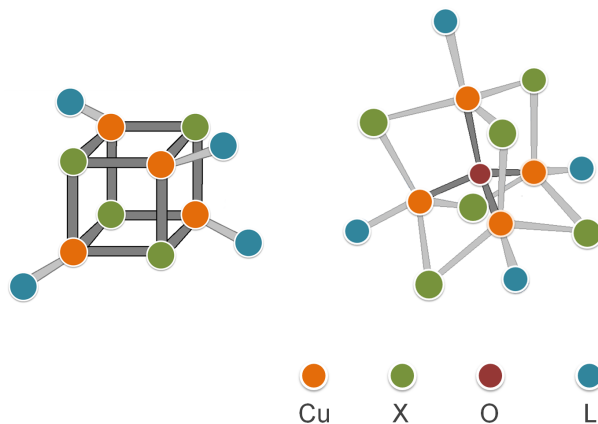


Figure 4.1.: Schematic representation of the structural motif of a copper(I) cubane core (*left*) and a μ_4 -oxido copper(II) cluster (*right*).

We previously reported the copper cluster $2[\text{Cu}_4\text{OCl}_6\text{L}^1_4] \cdot [\text{CuL}^1_2\text{Cl}_2]$ (cluster I, $\text{L}^1 = \text{benzylamine}$).^[103] Storing this cluster I in denatured ethanol led to the formation of various copper(I) compounds and the copper(II) cubane cluster $[\text{Cu}_4(\text{O-L})_4\text{Cl}_4]$ ($\text{L} = \text{C}_{11}\text{NH}_{14}$) as already described in chapter 2. There seemed to be similarities in the reactivity of cluster I with the systems Davies and El-Toukhy presented. Because of that formation of a cubane cluster with CuCl and benzylamine was very interesting. Hence the reaction of CuCl towards benzylamine was investigated. In the following the synthesis, structure and reactivity of the compound $[\text{Cu}(\text{C}_7\text{H}_7\text{NH}_2)\text{Cl}]_4$ are presented.

4.1.2. Results and Discussion

When mixing CuCl and benzylamine the formation of a copper(I) cubane cluster was expected. However, mixing CuCl with benzylamine under inert conditions led to the formation of an unexpected copper(I)-tetramer (compound 1). Stoichiometric variations led to the same result. The molecular structure of the colorless crystals obtained is shown in Figure 4.2.

4.1. Synthesis, Structure and Reactivity of $[\text{Cu}(\text{C}_7\text{H}_7\text{NH}_2)\text{Cl}]_4$

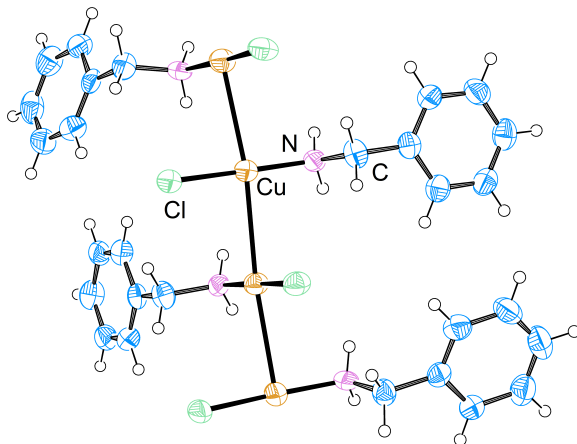


Figure 4.2.: Molecular structure of $[\text{CuL}^1\text{Cl}]_4$ (**1**). Ellipsoids are drawn at the 50 % probability level.

The asymmetric unit of the elemental cell shows half the tetramer with copper-copper bonds of 2.89 Å. $\text{Cu}^I \cdots \text{Cu}^I$ interactions are well known in literature. [77]-[80], [141] But still reasons for these interactions are not quite clear, especially if there is no ligand environment which forces the copper(I) ions in this arrangement as in this case. As already mentioned the formation of this tetramer was unexpected because of the usual formation of a cubane cluster. Only the crystal structure revealed the linear character of compound **1**. The structural similarities between a cubane core and compound **1** probably makes it difficult to distinguish (e. g. IR) spectroscopically between these two compounds. Probably only a crystal structure gives clear evidence for a cubane core. So previously proposed cubane clusters without a molecular structure should be considered carefully because of the mentioned above similarities of structural and spectroscopic properties. An attempt to distinguish between both structural units could be fluorescence analysis. Copper(I) cubane cores often show fluorescence. Because of that compound **1** was tested as well, but no fluorescence was observed. Of course this observation results from only one compound. Hence to confirm this assumption more investigations of compound **1** derivatives have to be carried out. We previously reported the compound $[\text{CuL}^1\text{Cl}]_3$ (Compound

4. Reactions of Copper(I) Chloride with Benzylamine

2).[103] This compound crystallized as trimer in the asymmetric unit. Thus besides the asymmetric units these compounds are chemically identical. This was very interesting because compound **2** was obtained by simply suspending cluster I in denatured ethanol.[103] However many side reactions and a chemical equilibrium between cluster I, compound **2** and other species complicated the aimed synthesis of compound **2**. Additionally the exact reactivity of compound **2** was unknown because of the mentioned above difficulties. Thus with the formation of compound **1** now a way for an aimed synthetic route for compound **2** was finally found. Concerning the previous investigations of the reactivity of cluster I the finding of compound **1** is very interesting. Cluster I underwent many redox reactions at air which led to the selective oxidation of ethanol and the hydroxylation of 2-butanone for example. The formation of an active copper(I) species which enabled the hydroxylation of 2-butanone for example was suggested.[103] Because of the formation of compound **1** now the question arose if this compound was the active copper(I) species which was previously proposed. In order to answer this question a large number of experiments was performed to test the reactivity of compound **1** towards dioxygen and derivatives. Bubbling dioxygen through a solution of compound **1** led to a color change from colorless to green. However even at room temperature this reaction was very slow. Figure 4.4 shows the UV-vis spectra of this reaction over a time range of 20 min. The spectra show the development of absorption bands at 259, 746 and 824 nm. Additionally a shoulder at ca. 357 nm was formed. In contrast the absorption band at 570 nm decreased. The formed species was stable for days at room temperature before it decomposed. It is difficult to relate the absorption maxima to certain Cu/O₂ species, because only little is known about dioxygen activation with tetranuclear copper clusters. The formation of these "oxygen-adduct" complexes follows a more complex mechanism, since the 4 e⁻ provided by the tetranuclear clusters do not correlate with the 2e⁻ reduction of O₂ to peroxide.[5] Reim et al. reported a tetranuclear μ_4 -peroxido complex and provided UV-Vis data of this compound.[142], [143] However these data do not correlate with the data here presented. In addition there are no reports of dioxygen activation with compounds that exhibit Cu^I...Cu^I interactions. So a comparison with spectroscopic features of mononuclear and dinuclear Cu/O₂ species does not indicate a formation of any known Cu/O₂ species. Most equivalent UV-vis features are exposed by $\mu - \eta^2 : \eta^2$ -peroxido complexes.[5] Here absorption maxima are observed at 338-350 nm, 530-550 nm and 730-760 nm (compound **1**: $\lambda_{max} = 259$ nm, 746 nm, 829 nm and a shoulder at 357 nm). However the absorption band at 570 nm decreased during the reaction of compound **1** with dioxygen and did not increase.

4.1. Synthesis, Structure and Reactivity of $[\text{Cu}(\text{C}_7\text{H}_7\text{NH}_2)\text{Cl}]_4$

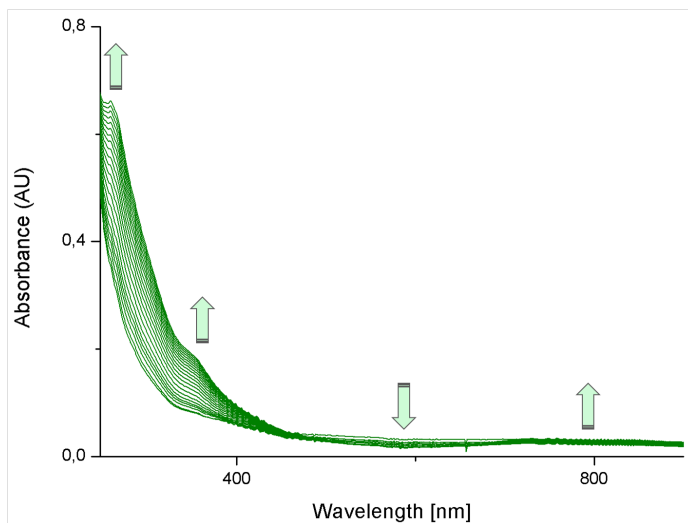


Figure 4.3.: UV-vis spectra of the reaction of compound **1** towards O₂ (solvent: dcm, T = 25 °C, c = 2 · 10⁻⁵ mol/L, t = 20 min). λ_{max} = 259 nm, 746 nm, 829 nm, shoulder at 357 nm.

Interestingly the UV-vis features here reported closely resemble UV-vis data reported by Davies et al. concerning dioxygen activation with copper(I) cubane clusters (see Figure 4.4). They observed maxima at 725 and 812 nm in the reaction of $\text{Cu}_4\text{Cl}_4(\text{pyridine})_4$ towards dioxygen.[130] The formation of a μ_4 -oxido species with one oxygen coordinated in the center of the cubane core and one outlying was proposed. The appearance of two maxima in the infrared range was assigned to the formation of two copper(II) species, whereas one of them (the μ_4 -oxido species) was active in oxygenation reactions.[130], [144] However they did not report crystal structures for all clusters they used. As discussed above the formation of a linear tetramer as **1** instead of a cubane cluster is imaginable as well. This could explain the observed similarities in the UV-vis spectra. Indeed a full comparison of the UV-vis data remained difficult because Davies et al. only provided data in the range of 700-900 nm. Attempts to obtain crystals of the Cu/O₂ species were not successful and resulted in recrystallization of compound **1**. This emphasized the extraordinary stability of compound **1** towards O₂. However crystals after the decomposition of the Cu/O₂ species could be obtained. The molecular structure is shown in Figure 4.5.

4. Reactions of Copper(I) Chloride with Benzylamine

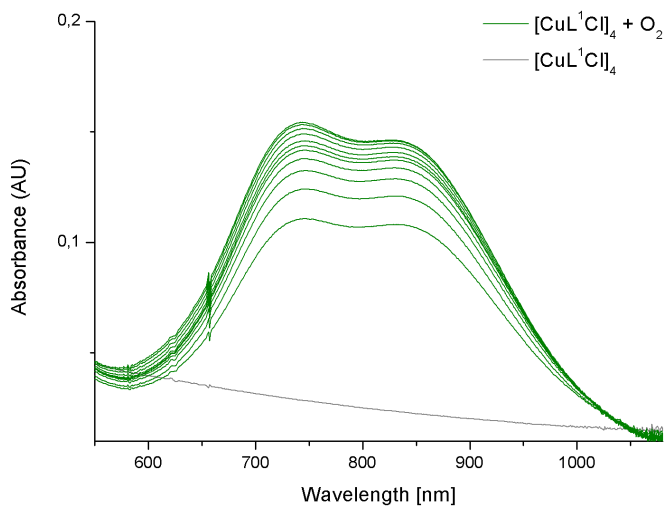


Figure 4.4.: Infrared and near-infrared part of the UV-vis spectra of the reaction of compound **1** towards O_2 (solvent: dcm, $T = 25\text{ }^\circ\text{C}$, $c = 1 \cdot 10^{-4}\text{ mol/L}$). $\lambda_{max} = 746$ and 829 nm .

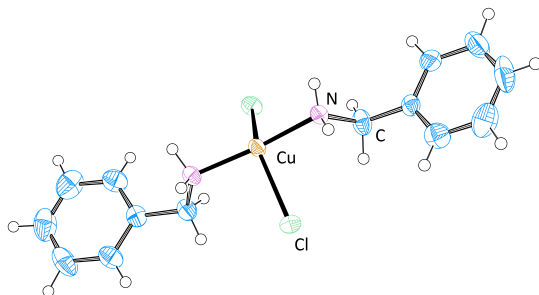


Figure 4.5.: Molecular structure of $[\text{CuL}^1_2\text{Cl}_2]$ (compound **3**). Ellipsoids are drawn at the 50% probability level.

Compound **3** is already known in literature.[73] The UV-vis spectra of the

4.1. Synthesis, Structure and Reactivity of $[\text{Cu}(\text{C}_7\text{H}_7\text{NH}_2)\text{Cl}]_4$

pure compound **1** was compared with these of the "oxygen-adduct", compound **3** and cluster I. The comparison is shown in Figure 4.6.

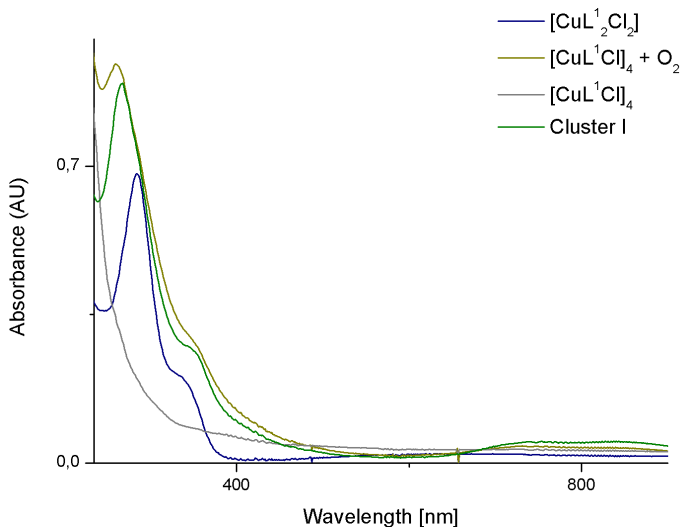


Figure 4.6.: UV-vis spectra of compound **1**, **3**, the "oxygen-adduct" and cluster I (solvent: dcm, $T = 25^\circ\text{C}$, $c(\mathbf{1}) = 2 \cdot 10^{-5}$ mol/L, $c(\mathbf{3})$, cluster I) = $1 \cdot 10^{-4}$ mol/L).

Compound **3** exhibits an intense absorption maximum at 285 nm and a shoulder at 350 nm. The absorption maxima at 285 nm is assigned to $n \rightarrow \sigma^*$ of the coordinated benzylamine group.[145] The shoulder at 350 nm is identified as a LMCT band. Weaker $d \rightarrow d^*$ transfers are observed at 660 nm. The comparison of the UV-vis spectra of the Cu/O_2 species and cluster I shows strong similarities. For cluster I absorption maxima at 286, 754 and 834 nm and a shoulder at 360 nm are observed. These similarities raised suspicion that compound **1** reacted with dioxygen to form cluster I. However as mentioned above the reaction of compound **1** with dioxygen was very slow. Thus the observation of an oxygen intermediate before a thinkable decomposition to cluster I should be possible even at room temperature. But analysis of the UV-vis data is complicated due to the structural similarities between the by Davies et al. proposed oxygen intermediates and cluster I (both contain a μ_4 -oxido motif). Thus without careful further investigations drawing clear conclusions concerning the Cu/O_2 species derived from compound **1** and

4. Reactions of Copper(I) Chloride with Benzylamine

dioxygen is not possible.

As mentioned above the oxygen intermediate described by Davies et al. and Endres et al. was active in catalytic reactions.[130], [144] Since compound **1** showed similar UV-vis data for the reaction with dioxygen, it was obvious to test the ability of it to catalyze oxidation reactions if activated with dioxygen as well. Thus compound **1** was dissolved either in dichloromethane or acetonitrile, cyclohexane was added and dioxygen was bubbled into the solution. However no oxygenation product was observed. So H_2O_2 was added instead of O_2 to the solution. But again no oxygenation occurred. In another attempt H_2O_2 was substituted with the urea adduct $(\text{H}_2\text{N})_2\text{CO} \cdot \text{H}_2\text{O}_2$ in order to avoid water molecules. But once again no oxygenation was observed. In addition the substrate was changed from the aliphatic cyclohexane to aromatic benzene. But again compound **1** proved to be unreactive as oxygenation catalyst. Additionally it was interesting to find out if compound **1** was responsible for the conversion of cluster I into a copper(II) cubane cluster (cluster II) if stored in denatured ethanol (reaction described in chapter 2). Here the ligand benzylamine reacted with the 2-butanone present in solution to give a Schiff base. We proposed the hydroxylation of this Schiff base to give the ligand 3-benzylimino-butan-2-olate and so cluster II.[103] Figure 4.7 shows the proposed mechanism for the ligand formation.

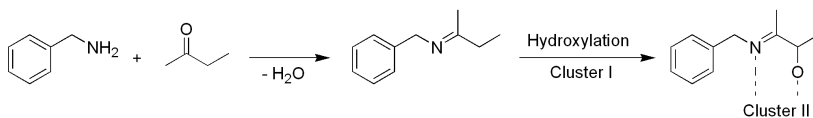


Figure 4.7.: Proposed reaction for the formation of 3-benzylimino-butan-2-olate. [103]

Thus compound **1** was added to a solution of 2-butanone and dioxygen was bubbled into it. However the formation of cluster II could not be observed. In conclusion compound **1** was extraordinary stable concerning reactivity towards dioxygen and derivatives. No oxygenation reaction could be observed. Certainly this stability was very interesting. As already mentioned the nature of $\text{Cu}^I \cdots \text{Cu}^I$ interactions is not fully clarified. It is surprising that these interactions probably are responsible for the great stability at air of compound **1**. This is remarkable because there is no ligand environment which could shield the copper-copper bonds from moisture. Solutions of compound **1** turned green only within hours if stored under atmospheric conditions. Crystals of compound **1** were even more stable and in many

4.1. Synthesis, Structure and Reactivity of $[\text{Cu}(\text{C}_7\text{H}_7\text{NH}_2)\text{Cl}]_4$

cases the pure copper (I) compound recrystallized after treating a solution of it with dioxygen. So far this extraordinary stability towards dioxygen cannot be explained exactly.

In addition the reactivity of CuBr and CuI towards benzylamine was investigated. While mixing either CuBr or CuI with benzylamine under inert conditions no reaction occurred. So the syntheses were repeated under atmospheric conditions. Because of the great stability of both copper salts syntheses of cubane clusters are sometimes carried out under atmospheric conditions as well. [132], [126] However neither formation of a cubane cluster nor formation of the discussed tetramer was observed. When reacting CuI with benzylamine in methanol the solution turned blue and green crystals were obtained. The salt $[\text{CuL}^1_2(\text{OMe})_2][\text{Cu}_{3,5}\text{I}_6](\text{HL}^1)_{0.5} \cdot n \text{H}_2\text{O} \cdot n \text{MeOH}$ (compound **4**) was obtained. The molecular structure of the cation of compound **4** is shown in Figure 4.8.

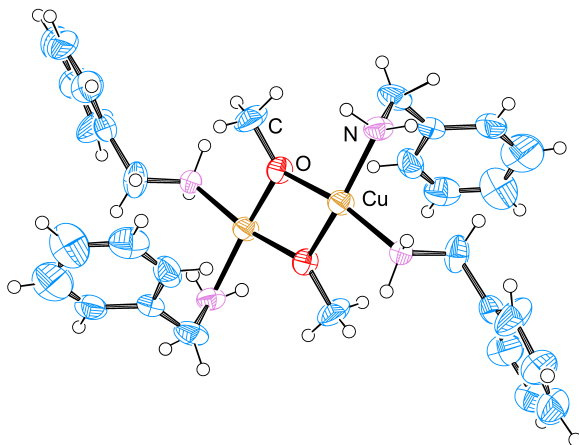


Figure 4.8.: Molecular structure of $[(\text{L}^1)_2(\text{OMe})\text{Cu}(\text{II})]_2^{2+}$, the cation of compound **4**. Ellipsoids are drawn at the 50 % probability level.

For clarity the anion $[\text{Cu}_{3,5}^{\text{I}}\text{I}_6]\text{HL}^1_{0.5}{}^{2-}$ is not shown. The structure of the cation shows the copper(II)-complex $[(\text{L}^1)_2(\text{OMe})\text{Cu}(\text{II})]_2^{2+}$. Here the copper(II) ions have a square-planar geometry. They coordinate two benzylamine groups per ion and are bridged via methoxygroups derived from the solvent. Via methoxygroups bridged copper compounds are well known. Only some examples for such compounds with monodentate N-donor ligands

4. Reactions of Copper(I) Chloride with Benzylamine

are given in the references.[146]-[150]

The question of the origin of the copper(II) ions arose. It was not very likely that the copper(I) ions disproportionated because the precipitation of elemental copper was not observed. Probably a part of the dissolved copper(I) ions had been oxidized by atmospheric oxygen to give copper(II) ions. In addition an acid-base-reaction occurred between methanol and benzylamine. This formed the methoxy complex and the benzylammonium ions, which were incorporated in the complex structure of the anion. The larger part of CuI probably did not react with either benzylamine nor atmospheric dioxxygen and formed long polymeric chains. The voids of these chains were filled with solvent molecules as methanol and water.

The reaction of CuBr with benzylamine led to a dark green solution and colorless crystals were obtained. However no copper complex but the carbamate of benzylamine was obtained. Figure 4.12 shows the molecular structure of the salt $(HL^1)(C_7H_7NHCOO)$, which is already known in literature.[151], [152]

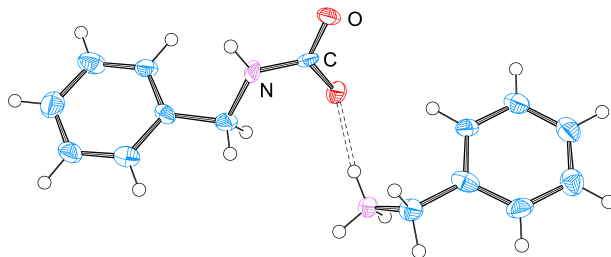


Figure 4.9.: Molecular structure of $(HL^1)(C_7H_7NHCOO)$. Ellipsoids are drawn at the 50% probability level.

Probably benzylamine reacted with the carbon dioxide present in air to give this carbamate. In summary in both cases the synthesis of a cubane cluster or a compound **1** derivative was neither possible under inert nor under atmospheric conditions. Further experiments have to be carried out.

4.1.3. Conclusion

Instead of the formation of a cubane cluster during the reaction of CuCl with benzylamine the tetramer $[\text{CuL}^1\text{Cl}]_4$ was obtained and could be fully characterized. Eye-catching were the unsupported $\text{Cu}^I \cdots \text{Cu}^I$ interactions. We already reported the similar compound $[\text{CuL}^1\text{Cl}]_3$ which was in a complex chemical equilibrium with diverse copper(I) and copper(II) species.[103] As byproducts of this chemical equilibrium oxidation reactions occurred. Thus the question arose if compound **1** played a role in these oxidation reactions. However despite many different experiments no oxidation reaction was supported by compound **1** if treated with O_2 or H_2O_2 . In contrast compound **1** turned out to possess an extraordinary stability towards dioxygen and derivatives. Probably the $\text{Cu}^I \cdots \text{Cu}^I$ interactions were responsible for this stability. At the moment less is known about $\text{Cu}^I \cdots \text{Cu}^I$ interactions and so this extraordinary stability is even more surprising. In addition the UV-vis features of the Cu/O_2 species which arose from the reaction of compound **1** with O_2 were reported. Probably these are the first UV-vis data presented for oxygen activation with a compound that exhibits $\text{Cu}^I \cdots \text{Cu}^I$ interactions. However these UV-vis data could not be assigned to any known Cu/O_2 species because of the complexity of the system.

Attempts to synthesize either a cubane cluster or the compound **1** derivatives with CuBr or CuI failed. However in the case of CuI the interesting salt $[\text{CuL}^1_2(\text{OMe})_2][\text{Cu}_{3,5}\text{I}_6](\text{HL}^1)_{0.5} \cdot n \text{H}_2\text{O} \cdot n \text{MeOH}$ was obtained. In conclusion the formation of cubane clusters derived from copper halogenides is not always as easy as expected. In addition the structural similarities between a cubane cluster and the polymeric compound **1** probably complicates the spectroscopic distinction via standard methods as infrared spectroscopy or elemental analyses. Therefore proposed cubane clusters without a reported crystal structure are to be considered carefully. Since most of the reported cubane cores showed fluorescence and compound **1** did not this might be an appropriate way to distinguish between the two species. However to confirm this idea additional investigations with derivatives of compound **1** have to be carried out. Additionally it would be of great interest to find out more about the unsupported $\text{Cu}^I \cdots \text{Cu}^I$ interactions and how they stabilize a copper(I) compound at air. DFT calculations for example are essential for this purpose.

4. Reactions of Copper(I) Chloride with Benzylamine

4.1.4. Experimental Section

All chemicals used were of p.a. quality and were purchased from either Acros, Aldrich, Fluka or Merck, if not mentioned otherwise. Dry solvents for air sensitive reactions were redistilled under argon. Analytical data (elemental analyses, IR spectra, and crystallographic data [101]) are summarized in the Supporting Information.

Preparation of **1**: [CuL¹Cl]₄

The synthesis was performed under inert conditions in a glove box. CuCl (165 mg, 1.67 mmol) was dissolved in absolute dichloromethane (ca. 10 mL) and benzylamine (358 mg, 3.33 mmol) was added dropwise to the solution under stirring. The mixture was stirred until CuCl was dissolved completely and crystallization occurred. The resulting colorless crystals were filtered off and dried to give compound **1** (260 g, 0.31 mmol, 79 %).

Preparation of compound **4**

CuI (170 mg, 0.892 mmol) was dissolved in methanol (ca. 20 mL) and benzylamine (96 mg, 0.89 mmol) was added to the stirred solution. The solution was allowed to stand until crystallization occurred.

Preparation of (HL¹)(C₇H₇NHCOO)

CuBr (128 mg, 0.892 mmol) was dissolved in methanol (ca. 20 mL) and benzylamine (96 mg, 0.89 mmol) was added to the stirred solution. The solution was allowed to stand until crystallization occurred.

Attempted oxygenation of cyclohexane

With O₂:

Compound **1** (10 mg, 13 μmol) was dissolved in acetonitrile (ca. 3 mL) and cyclohexane (840 mg, 10 mmol) was added. Then dry O₂ was bubbled into the solution for 20 min. The solution was investigated by GC-MS. The reaction was also performed in dichloromethane.

With H₂O₂:

Compound **1** (21 mg, 25 μmol) was dissolved in acetonitrile (ca. 10 mL)

4.1. Synthesis, Structure and Reactivity of $[\text{Cu}(\text{C}_7\text{H}_7\text{NH}_2)\text{Cl}]_4$

and cyclohexane (840 mg, 10 mmol) was added. Then H_2O_2 (aqueous 30 %, 2.0 mL, 20 mmol) was added to the stirred solution. The solution was stirred for ca. 6 h and then investigated by GC-MS. The reaction was also performed in dichloromethane.

With $(\text{NH}_2)_2\text{CO} \cdot \text{H}_2\text{O}_2$:

Compound **1** (21 mg, 25 μmol) was dissolved in dichloromethane (ca. 10 mL) and cyclohexane (840 mg, 10 mmol) was added. Then $(\text{NH}_2)_2\text{CO} \cdot \text{H}_2\text{O}_2$ (1.9 g, 20 mmol) was added to the stirred solution. The solution was stirred for ca. 6 h and then investigated by GC-MS.

Attempted hydroxylation of benzene

Compound **1** (10 mg, 13 μmol) was dissolved in absolute benzene (ca. 3 mL) and dry O_2 was bubbled into the solution for 20 min. Then the solution was separated into three parts. The first was investigated by GC-MS. A small part of H_2O was added to the second part and a small part of HCl to the third part. All samples were investigated by GC-MS.

Attempted hydroxylation of 2-butanone

The reaction was performed under inert conditions in a glove box. Compound **1** (8 mg, 10 μmol) was dissolved in absolute dichloromethane (ca. 20 mL) and 2-butanone (ca. 3 mL) was added. The solution was heated to ca. 30 °C for ca. 15 min and then dry O_2 was bubbled into the solution for 20 min. The solution was investigated by GC-MS. The reaction was also performed in absolute methanol.

4.2. Selected Supporting Information and Unpublished Material



Figure 4.10.: The photographs show a solution of $[\text{CuL}^1\text{Cl}]_4$ ($c = 1 \cdot 10^{-4}$ mol/L, *left*) and the same solution after the reaction with O_2 (*right*). The green "oxygen adduct" is stable for days.



Figure 4.11.: The photographs show a solution of $[\text{CuL}^1_2\text{Cl}_2]$ ($c = 5 \cdot 10^{-4}$ mol/L, *left*) and a solution of cluster I ($c = 1 \cdot 10^{-4}$ mol/L, *right*).

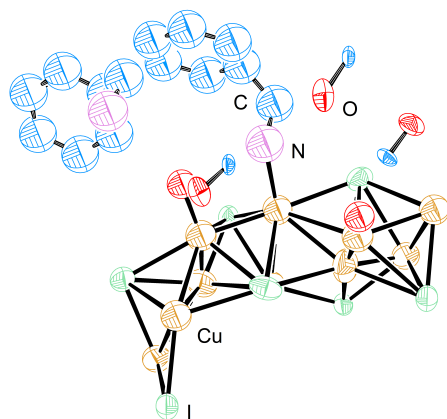


Figure 4.12.: Molecular structure of $[\text{Cu}^{\text{I}}_{3.5}\text{I}_6]\text{HL}^{1.0.5^{2-}}$, the anion of compound **4**. Ellipsoids are drawn at the 50% probability level.

5. Materials, Methods and Spectroscopy

5.1. Materials and Methods

5.1.1. Chemicals and Solvents

All chemicals used were of p.a. quality and were purchased from either Acros, Aldrich, Fluka or Merck, if not mentioned otherwise. Dry solvents for air sensitive reactions were redistilled under argon.

5.1.2. Air Sensitive Compounds

The preparation and handling of air sensitive compounds were performed under an argon atmosphere. For reactions and preparations either glove boxes from MBraun (equipped with water and dioxygen sensors) or standard Schlenk techniques were used.

5.1.3. Crystallography

Single crystals suitable for X-ray diffraction were mounted on the tip of a glass rod using inert perfluoropolyether oil. The X-ray crystallographic data were collected on a STOE IPDS-, a BRUKER APEX 2 QUAZAR-diffractometer or a BRUKER NONIUS KappaCCD equipped with low temperature systems. Mo-K α radiation ($\lambda = 0.71073 \text{ \AA}$) and a graphite monochromator (STOE IPDS) alternatively a quazarTH optic (BRUKER APEX 2 QUAZAR) was used. The structures were solved by direct methods in SHELXS97 and SHELXL 2013 and refined by using full-matrix least squares in SHELXL97. [101]

Crystallographic data for most of the reported structures have been deposited with the Cambridge Crystallographic Data Centre as supplementary publication. For the corresponding numbers please see tables of crystal data and structure refinement for the specific compound. Copies of the data can be obtained, free of charge from the Cambridge Crystallographic Data

5. Materials, Methods and Spectroscopy

Centre via www.ccdc.cam.ac.uk/data_request/cif. The crystallographic data for some compounds were not deposited because the crystals diffracted rather weakly.

5.1.4. Infrared Spectroscopy

All IR measurements were performed on either Bruker IFS48, IFS25, IFS85 or on Jasco FT/IR 4100. If not mentioned otherwise all samples were measured as KBr-pellet.

5.1.5. Elemental Analysis

All measurements concerning elemental analysis were carried out using a Carlo-Erba 1106 CHN.

5.1.6. GC-MS Spectrometry

All GC-MS experiments were performed using a HP GL 6890 chromatograph equipped with HP 5973 mass selective detector. The GC-MS conditions for the product analysis were:

Injector port temperature: 250 °C; solvent delay: 0 min; column temperature: initial temperature: 60 °C (2 min); gradient rate: 13.5 °C/min (14 min); final temperature: 250 °C (5 min); flow rate: 80 mL/min.

5.1.7. UV-vis Spectroscopy

The UV-vis measurements were performed on an HP 8452 A diode array spectrophotometer. Cuvettes of quartz glass were used (d = 10 mm).

5.2. Crystallography

5.2.1. Crystallographic Data for Chapter 2

This chapter contains the crystallographic data of the compounds presented in chapter 2. Most of the data are part of the Supporting Information of the publication of chapter 2 and therefore are available in the online library of the journal " *Chemistry - A European Journal*" (<http://onlinelibrary.wiley.com/journal/10.1002/%28ISSN%291521-3765/issues>). For detailed information concerning the nomenclature and abbreviations please see chapter 2.

Cluster I: 2[Cu₄OCl₆L¹₄] · [CuL¹₂Cl₂] · MeOH (L¹ = benzylamine)

Table 5.1.: Crystal data and structure refinement for cluster I.

Internal identification code	SHIN248s
CCDC-no.	873402
Diffractometer type	STOE IPDS
Empirical formula	C ₇₁ H ₉₄ Cl ₁₄ Cu ₉ N ₁₀ O ₃
Formula weight	2203.72
Temperature	193(2) K
Wavelength	0.71073 Å
Crystal system, space group	Monoclinic, <i>C</i> 2/ <i>c</i>
Unit cell dimensions	a = 21.430(4) Å $\alpha = 90^\circ$ b = 18.135(4) Å $\beta = 99.12(3)^\circ$ c = 23.815(5) Å $\gamma = 90^\circ$
Volume	9138(3) Å ³
Z, Calculated density	4, 1.602 Mg/m ³
Absorption coefficient	2.507 mm ⁻¹
F(000)	4452
Habit, color	Block, green
Crystal size	0.48 x 0.40 x 0.28 mm
Theta range for data collection	2.16 to 25.01 °
Limiting indices	-25 ≤ h ≤ 25, -21 ≤ k ≤ 21, -28 ≤ l ≤ 28
Reflections collected / unique	29508 / 8011 [R(int) = 0.0563]
Completeness to theta = 25.01	99.2 %
Absorption correction	None
Refinement method	Full-matrix least-squares on F ²
Data / restraints / parameters	8011 / 0 / 547
Goodness-of-fit on F ²	1.021
Final R indices [I > 2sigma(I)]	R1 = 0.0350, wR2 = 0.0961
R indices (all data)	R1 = 0.0436, wR2 = 0.1002
Largest diff. peak and hole	0.657 and -0.546 e. Å ⁻³

The refinement shows one cluster, one methanol solvent molecule and half a molecule of the connected [CuL¹₂Cl₂] molecule in the independent unit of the elementary cell. One benzylic-group at the cluster molecule is disordered in two positions (50:50). All C-H and N-H hydrogen atoms were positioned geometrically. The O-H hydrogen atom was found and isotropically refined. All non-hydrogen atoms were refined anisotropically. No absorption corrections were applied.

Symmetry transformations used to generate equivalent atoms:

a: -x+2,-y+2,-z+1 **b:** -x+2,y,-z+3/2

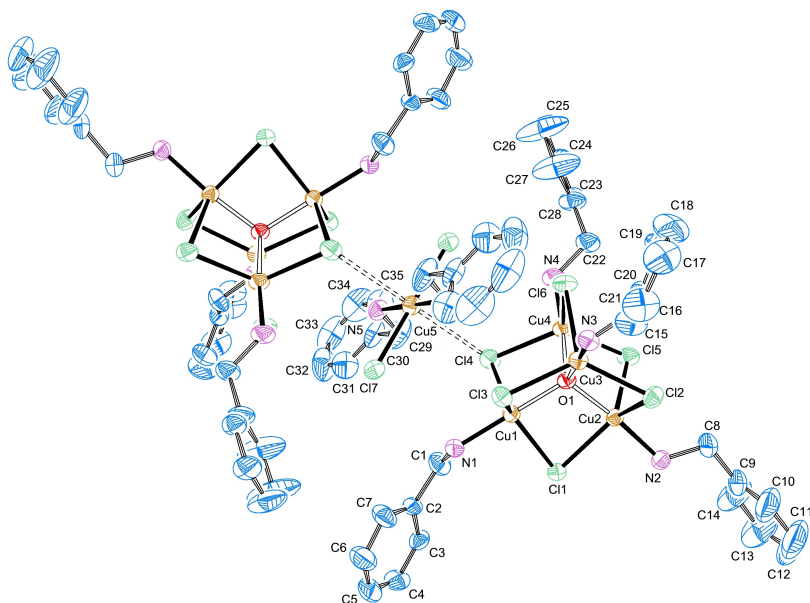


Figure 5.1.: ORTEP plot with thermal ellipsoids set at 50 % probability shows the cluster dimer that is connected through a $[\text{CuL}_2\text{Cl}_2]$ unit. Hydrogen atoms, methanol solvent and the 50 % disorder position of the benzylic group are not shown.

Table 5.2.: Selected bond lengths [\AA] and angles [$^\circ$] for cluster I.

C11-Cu2	2.390	Cl1-Cu1	2.433	Cl2-Cu3	2.410
Cl2-Cu2	2.412	Cl3-Cu3	2.383	Cl3-Cu1	2.443
Cl4-Cu4	2.420	Cl4-Cu1	2.432	Cl5-Cu4	2.402
Cl5-Cu2	2.457	Cl6-Cu4	2.408	Cl6-Cu3	2.446
Cl7-Cu5	2.321	Cu1-O1	1.883	Cu1-N1	1.952
Cu2-O1	1.895	Cu2-N2	1.964	Cu3-O1	1.907
Cu3-N3	1.964	Cu4-O1	1.897	Cu4-N4	1.955
Cu5-N5	2.002	Cu5-N5 _a	2.002	Cu5-Cl7 _a	2.321
Cu2-Cl1-Cu1	79.51	Cu3-Cl2-Cu2	79.43	Cu3-Cl3-Cu1	79.54

continue next page

5. Materials, Methods and Spectroscopy

Table 5.2.: Selected bond lengths [Å] and angles [°] for cluster I. (*continuation*)

Cu4-Cl4-Cu1	79.09	Cu4-Cl5-Cu2	79.74	Cu4-Cl6-Cu3	79.90
O1-Cu1-N1	174.58	O1-Cu1-Cl4	85.48	N1-Cu1-Cl4	89.72
O1-Cu1-Cl1	84.82	N1-Cu1-Cl1	96.58	Cl4-Cu1-Cl1	131.43
O1-Cu1-Cl3	85.00	N1-Cu1-Cl3	99.534	Cl4-Cu1-Cl3	118.66
Cl1-Cu1-Cl3	107.68	O1-Cu2-N2	177.09	O1-Cu2-Cl1	85.79
N2-Cu2-Cl1	95.56	O1-Cu2-Cl2	85.80	N2-Cu2-Cl2	95.73
Cl1-Cu2-Cl2	120.68	O1-Cu2-Cl5	84.11	N2-Cu2-Cl5	93.06
Cl1-Cu2-Cl5	128.57	Cl2-Cu2-Cl5	108.65	O1-Cu3-N3	175.46
O1-Cu3-Cl3	86.18	N3-Cu3-Cl3	97.57	O1-Cu3-Cl2	85.61
N3-Cu3-Cl2	94.49	Cl3-Cu3-Cl2	122.53	O1-Cu3-Cl6	84.31
N3-Cu3-Cl6	91.58	Cl3-Cu3-Cl6	120.04	Cl2-Cu3-Cl6	115.50
O1-Cu4-N4	177.12	O1-Cu4-Cl5	85.61	N4-Cu4-Cl5	91.65
O1-Cu4-Cl6	85.60	N4-Cu4-Cl6	96.51	Cl5-Cu4-Cl6	119.72
O1-Cu4-Cl4	85.51	N4-Cu4-Cl4	95.60	Cl5-Cu4-Cl4	128.27
Cl6-Cu4-Cl4	110.21	N5-Cu5-N5 _a	180.00	N5-Cu5-Cl7	90.15
N5 _a -Cu5-Cl7	89.87	N5-Cu5-Cl7 _a	89.87	Cu4-O1-Cu3	110.02
Cl7-Cu5-Cl7 _a	180.00	C1-N1-Cu1	119.83	C8-N2-Cu2	115.92
C15-N3-Cu3	117.62	C22-N4-Cu4	117.62	C29-N5-Cu5	117.82
Cu1-O1-Cu2	109.46	Cu1-O1-Cu4	109.57	Cu2-O1-Cu4	110.44
Cu1-O1-Cu3	109.06	Cu2-O1-Cu3	108.26		

**Bromide version of cluster I: [Cu₄OBr₆L¹₄] · [CuL¹₂Br₂]
(L¹ = benzylamine)**

Table 5.3.: Crystal data and structure refinement for cluster I (bromide version).

Internal identification code	SHIN273s
CCDC-no.	898380
Diffractometer type	STOE IPDS
Empirical formula	C ₇₀ H ₉₀ Br ₁₄ Cu ₉ N ₁₀ O ₂
Formula weight	2794.12
Temperature	193(2) K
Wavelength	0.71073 Å
Crystal system, space group	Triclinic, P $\bar{1}$
Unit cell dimensions	a = 11.380(2) Å α = 115.67(3) ° b = 15.149(3) Å β = 100.42(3) ° c = 15.577(3) Å γ = 99.82(3) °
Volume	2284.6(8) Å ³
Z, Calculated density	1, 2.031 Mg/m ³
Absorption coefficient	8.218 mm ⁻¹
F(000)	1347
Habitus, color	Block, red
Crystal size	0.36 x 0.08 x 0.04 mm
Theta range for data collection	2.46 to 28.16 °
Limiting indices	-15 ≤ h ≤ 14, -19 ≤ k ≤ 19, -20 ≤ l ≤ 20
Reflections collected / unique	20426 / 10272 [R(int) = 0.1159]
Completeness to theta = 28.16	91.7 %
Absorption correction	None
Refinement method	Full-matrix least-squares on F ²
Data / restraints / parameters	10272 / 0 / 475
Goodness-of-fit on F ²	0.837
Final R indices [I > 2sigma(I)]	R1 = 0.0729, wR2 = 0.1765
R indices (all data)	R1 = 0.1464, wR2 = 0.2097
Largest diff. peak and hole	2.134 and -2.523 e. Å ⁻³

The refinement shows one cluster and half a molecule of the connected [CuL¹₂Br₂] molecule in the independent unit of the elementary cell. All C-H and N-H hydrogen atoms were positioned geometrically and isotropically refined. All non-hydrogen atoms were refined anisotropically. No absorption corrections were applied.

Symmetry transformations used to generate equivalent atoms:

a: -x+1,-y+1,-z

5. Materials, Methods and Spectroscopy

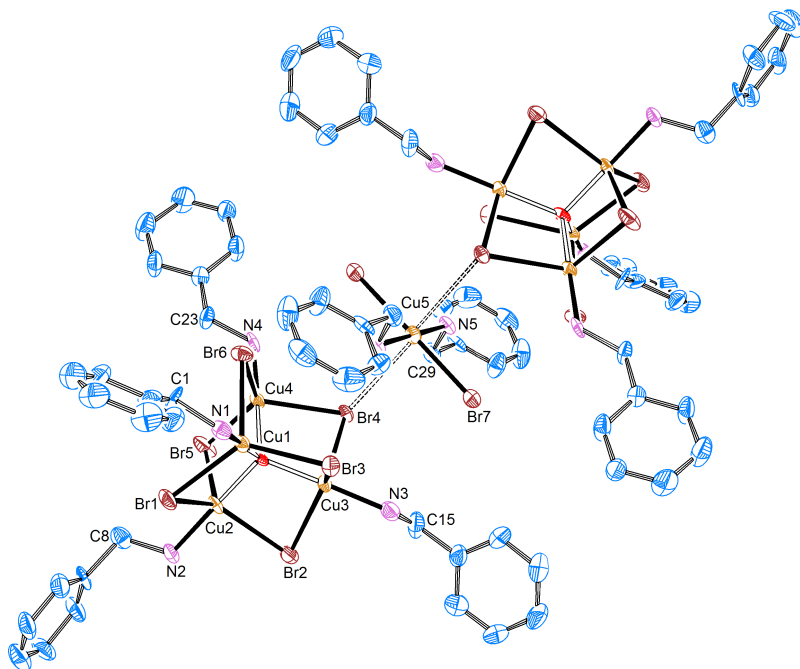


Figure 5.2.: ORTEP plot with thermal ellipsoids set at 50% probability shows the cluster dimer that is connected through a $[\text{CuL}_2\text{Br}_2]$ unit. Hydrogen atoms are not shown.

Table 5.4.: Selected bond lengths [\AA] and angles [$^\circ$] for cluster I (bromide version).

Br1-Cu1	2.502	Br1-Cu2	2.532	Br2-Cu2	2.535
Br2-Cu3	2.548	Br3-Cu3	2.509	Br3-Cu1	2.525
Br4-Cu4	2.541	Br4-Cu3	2.557	Br5-Cu2	2.543
Br5-Cu4	2.548	Br6-Cu1	2.532	Br6-Cu4	2.550
Br7-Cu5	2.495	Cu1-O1	1.914	Cu1-N1	1.961
Cu2-O1	1.911	Cu2-N2	1.962	Cu3-O1	1.919
Cu3-N3	1.967	Cu4-O1	1.916	Cu4-N4	1.967
Cu5-N5 _a	1.968	Cu5-N5	1.968	Cu5-Br7 _a	2.495
Cu1-Br1-Cu2	77.0	Cu2-Br2-Cu3	75.7	Cu3-Br3-Cu1	76.6
Cu4-Br4-Cu3	76.0	Cu2-Br5-Cu4	75.6	Cu1-Br6-Cu4	75.8

continue next page

Table 5.4.: Selected bond lengths [Å] and angles [°] for cluster I (bromide version).
(*continuation*)

O1-Cu1-N1	178.2	O1-Cu1-Br1	86.7	N1-Cu1-Br1	91.9
O1-Cu1-Br3	86.6	N1-Cu1-Br3	95.1	Br1-Cu1-Br3	122.0
O1-Cu1-Br6	87.5	N1-Cu1-Br6	92.5	Br1-Cu1-Br6	129.2
Br3-Cu1-Br6	107.8	O1-Cu2-N2	177.0	O1-Cu2-Br1	85.9
N2-Cu2-Br1	91.7	O1-Cu2-Br2	87.5	N2-Cu2-Br2	95.2
Br1-Cu2-Br2	122.6	O1-Cu2-Br5	87.5	N2-Cu2-Br5	92.7
Br1-Cu2-Br5	129.0	Br2-Cu2-Br5	107.4	O1-Cu3-N3	178.5
O1-Cu3-Br3	87.0	N3-Cu3-Br3	91.9	O1-Cu3-Br2	87.0
N3-Cu3-Br2	93.1	Br3-Cu3-Br2	134.0	O1-Cu3-Br4	86.8
N3-Cu3-Br4	94.6	Br3-Cu3-Br4	113.5	Br2-Cu3-Br4	111.5
O1-Cu4-N4	174.9	O1-Cu4-Br4	87.3	N4-Cu4-Br4	96.6
O1-Cu4-Br5	87.3	N4-Cu4-Br5	94.3	Br4-Cu4-Br5	113.3
O1-Cu4-Br6	87.0	N4-Cu4-Br6	88.3	Br4-Cu4-Br6	114.9
Br5-Cu4-Br6	130.9	N5 _a -Cu5-N5	180.0	N5 _a -Cu5-Br7	89.8
N5-Cu5-Br7	90.2	N5 _a -Cu5-Br7 _a	90.2	N5-Cu5-Br7 _a	89.8
Br7-Cu5-Br7 _a	180.0	C1-N1-Cu1	116.9	C8-N2-Cu2	116.9
C15-N3-Cu3	114.1	C22-N4-Cu4	122.7	C29-N5-Cu5	116.2
Cu2-O1-Cu1	110.2	Cu2-O1-Cu4	109.3	Cu1-O1-Cu4	109.3
Cu2-O1-Cu3	109.1	Cu1-O1-Cu3	109.1	Cu4-O1-Cu3	109.9

Cluster II: [Cu₄O₄Cl₄(C₁₁H₁₄)₄]

Table 5.5.: Crystal data and structure refinement for cluster II.

Internal identification code	SHIN266s
CCDC-no.	873403
Diffractometer type	STOE IPDS
Empirical formula	C ₁₁ H ₁₄ ClCuNO
Formula weight	1100.88
Temperature	193(2) K
Wavelength	0.71073 Å
Crystal system, space group	Tetragonal, $I\bar{4}c2$
Unit cell dimensions	a = 15.336(2) Å $\alpha = 90^\circ$ b = 15.336(2) Å $\beta = 90^\circ$ c = 20.782(3) Å $\gamma = 90^\circ$
Volume	4888.0(11) Å ³
Z, Calculated density	16, 1.496 Mg/m ³
Absorption coefficient	1.979 mm ⁻¹
F(000)	2256
Habitus, color	Block, green
Crystal size	0.36 x 0.28 x 0.28 mm
Theta range for data collection	3.13 to 27.50 °
Limiting indices	-19 ≤ 19, -19 ≤ 19, -25 ≤ 26
Reflections collected / unique	20612 / 2814 [R(int) = 0.0707]
Completeness to theta = 27.50	99.5 %
Absorption correction	None
Refinement method	Full-matrix least-squares on F ²
Data / restraints / parameters	2814 / 0 / 138
Goodness-of-fit on F ²	1.035
Final R indices [I > 2σ(I)]	R1 = 0.0300, wR2 = 0.0764
R indices (all data)	R1 = 0.0384, wR2 = 0.0790
Absolute structure parameter	-0.001(18)
Largest diff. peak and hole	0.436 and -0.374 e.Å ⁻³

The refinement shows the fourth part of the cluster molecule in the independent unit of the elementary cell. All hydrogen atoms were positioned geometrically and refined isotropically. All non-hydrogen atoms were refined anisotropically. No absorption corrections were applied.

Symmetry transformations used to generate equivalent atoms:

a: -x,-y+1,z

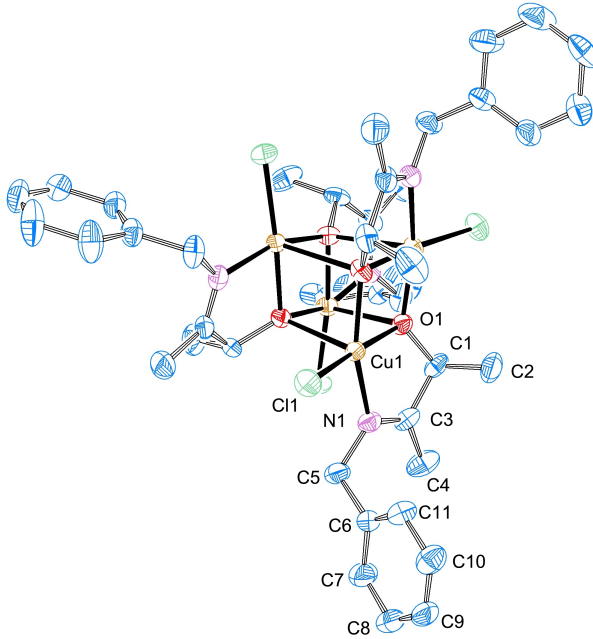


Figure 5.3.: ORTEP plot with thermal ellipsoids set at 50% probability shows the full cluster II. Hydrogen atoms are not shown.

Table 5.6.: Selected bond lengths [\AA] and angles [$^\circ$] for cluster II.

Cu1-O1	1.944	Cu1-O1 _a	1.949	Cu1-N1	1.975
Cu1-Cl1	2.207	Cu1-Cu1 _a	3.008	O1-Cu1 _a	1.949
O1-Cu1-O1 _a	78.58	O1-Cu1-N1	81.21	O1 _a -Cu1-N1	159.56
O1-Cu1-Cl1	173.48	O1 _a -Cu1-Cl1	100.00	N1-Cu1-Cl1	99.73
O1-Cu1-Cu1 _a	39.44	O1 _a -Cu1-Cu1 _a	39.34	N1-Cu1-Cu1 _a	120.25
Cl1-Cu1-Cu1 _a	138.28	C1-O1-Cu1	112.01	C1-O1-Cu1 _a	133.86
Cu1-O1-Cu1 _a	101.21	C3-N1-C5	120.8	C3-N1-Cu1	114.4
C5-N1-Cu1	124.6				

Compound 2: [CuL¹₄Cl₂] (L¹ = benzylamine)

Table 5.7.: Crystal data and structure refinement for compound 2.

Internal identification code	SHIN319s
CCDC-no.	Not submitted.
Diffractometer type	STOE IPDS
Empirical formula	C ₂₈ H ₃₆ Cl ₂ CuN ₄
Formula weight	563.05
Temperature	193(2) K
Wavelength	0.71073 Å
Crystal system, space group	Monoclinic, <i>P</i> 2 ₁ / <i>n</i>
Unit cell dimensions	a = 5.8720(10) Å α = 90° b = 13.140(4) Å β = 90.00(3)° c = 17.649(4) Å γ = 90°
Volume	1361.8(6) Å ³
Z, Calculated density	2, 1.373 Mg/m ³
Absorption coefficient	1.022 mm ⁻¹
F(000)	590
Habitus, color	Plate, blue
Crystal size	0.80 x 0.32 x 0.08 mm ³
Theta range for data collection	2.78 to 21.98°
Limiting indices	-6 ≤ h ≤ 6, -13 ≤ k ≤ 13, -18 ≤ l ≤ 18
Reflections collected / unique	6226 / 1668 [R(int) = 0.1543]
Completeness to theta = 21.98	99.9 %
Absorption correction	None
Refinement method	Full-matrix least-squares on F ²
Data / restraints / parameter	1668 / 0 / 137
Goodness-of-fit on F ²	0.832
Final R indices [I > 2σ(I)]	R1 = 0.0586, wR2 = 0.1223
R indices (all data)	R1 = 0.1353, wR2 = 0.1560
Largest diff. peak and hole	0.563 and -0.425 e. Å ⁻³

The crystal structure was solved in a triclinic crystal system and refined in a monoclinic crystal system (*P*2₁/*n*) as a twin (TWIN -1 0 0 0 -1 0 0 0 1, BASF 0.35544). The refinement shows a half molecule in the independent unit of the elementary cell. All hydrogen atoms were positioned geometrically and refined isotropically. All non-hydrogen atoms were refined anisotropically. No absorption corrections were applied.

Symmetry transformations used to generate equivalent atoms:

a: -x+1,-y+1,-z+1

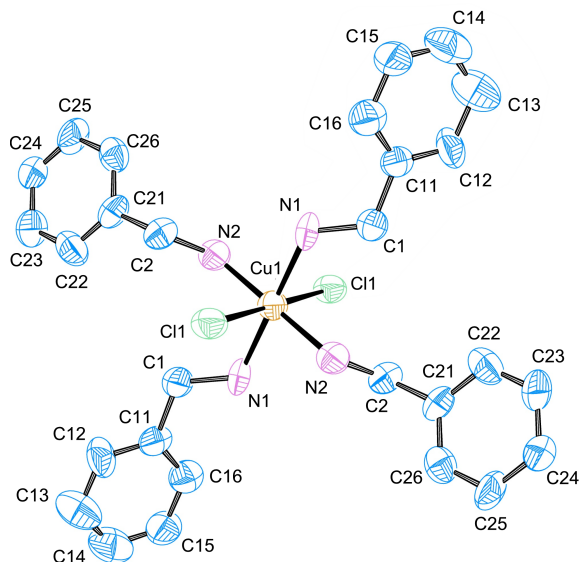


Figure 5.4.: ORTEP plot with thermal ellipsoids set at 50% probability shows the full compound **2**. Hydrogen atoms are not shown.

Table 5.8.: Selected bond lengths [\AA] and angles [$^\circ$] for compound **2**.

Cu1-N1 _a	1.993	Cu1-N1	1.993	Cu1-N2	2.036
Cu1-N2 _a	2.036	Cu1-Cl1 _a	2.745	Cu1-Cl1	2.745
N1 _a -Cu1-N1	180.0	N1 _a -Cu1-N2	91.7	N1-Cu1-N2	88.3
N1 _a -Cu1-N2 _a	88.3	N1-Cu1-N2 _a	91.7	N2-Cu1-N2 _a	180.0
N1 _a -Cu1-Cl1 _a	96.8	N1-Cu1-Cl1 _a	83.2	N2-Cu1-Cl1 _a	93.9
N2 _a -Cu1-Cl1 _a	86.1	N1 _a -Cu1-Cl1	83.2	N1-Cu1-Cl1	96.83
N2-Cu1-Cl1	86.1	N2 _a -Cu1-Cl1	93.9	Cl _a -Cu1-Cl1	180.0
C1-N1-Cu1	122.9	Cu1-N1-H1C	106.6	Cu1-N1-H1D	106.6
C2-N2-Cu1	122.0	Cu1-N2-H2C	106.8	Cu1-N2-H2D	106.8

Compound 3:(HL¹)₂[CuCl₄] (L¹ = benzylamine)Table 5.9.: Crystal data and structure refinement for compound **3**.

CCDC-no.	Not submitted.
Diffractometer type	STOE IPDS
Empirical formula	C ₁₄ H ₂₀ Cl ₄ CuN ₂
Formula weight	421.66
Temperature	293(2) K
Wavelength	0.71073 Å
Crystal system, space group	Triclinic, <i>P</i> 1
Unit cell dimensions	a = 10.444(2) Å α = 98.43(3) ° b = 10.492(2) Å β = 99.49(3) ° c = 15.979(3) Å γ = 90.00(3) °
Volume	1707.8(6) Å ³
Z, Calculated density	4, 1.640 Mg/m ³
Absorption coefficient	1.898 mm ⁻¹
F(000)	860
Habitus, colour	Block, yellow
Crystal size	0.10 x 0.20 x 0.25 mm
Theta range for data collection	2.51 to 27.50 °
Limiting indices	-13 ≤ h ≤ 13, -13 ≤ k ≤ 13, -20 ≤ l ≤ 20
Reflections collected / unique	14828 / 12505 [R(int) = 0.1653]
Completeness to theta = 28.36	92.4 %
Absorption correction	None
Refinement method	Full-matrix least-squares on F ²
Data / restraints / parameters	12505 / 182 / 346
Goodness-of-fit on F ²	0.984
Final R indices [I > 2σ(I)]	R1 = 0.1150, wR2 = 0.2803
R indices (all data)	R1 = 0.2684, wR2 = 0.3332
Absolute structure parameter	0.01(4)
Largest diff. peak and hole	2.689 and -1.970 e. Å ⁻³

The refinement shows four molecules in the independent unit of the elementary cell. The position of the benzylammonium ions in the crystal are completely disordered (50:50). All hydrogen atoms were positioned geometrically. All non-hydrogen atoms were refined partly isotropically and partly anisotropically. No absorption corrections were applied.

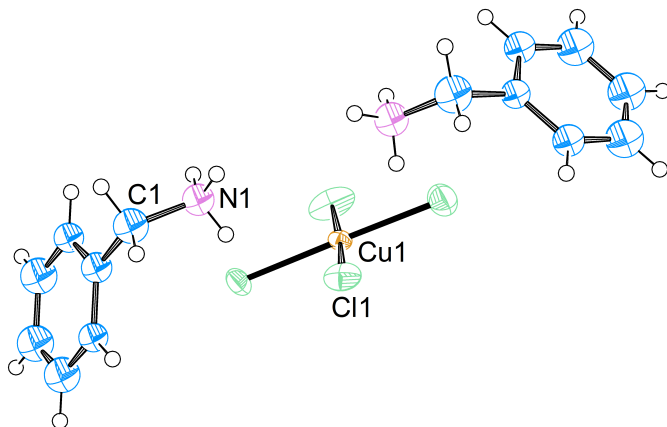


Figure 5.5.: ORTEP plot with thermal ellipsoids set at 50% probability shows the full compound **3**. Disorder of the benzylammonium ions is not shown.

Table 5.10.: Selected bond lengths [\AA] and angles [$^\circ$] for compound **3**.

Cu1-Cl11	2.289	Cu1-Cl12	2.289	Cu1-Cl13	2.293
Cu1-Cl14	2.298	Cu2-Cl21	2.288	Cu2-Cl22	2.288
Cu2-Cl23	2.295	Cu2-Cl24	2.295	Cu3-Cl31	2.288
Cu3-Cl32	2.289	Cu3-Cl34	2.299	Cu3-Cl33	2.299
Cu4-Cl41	2.289	Cu4-Cl42	2.290	Cu4-Cl44	2.293
Cu4-Cl43	2.298				
Cl11-Cu1-Cl12	177.8	Cl11-Cu1-Cl13	90.1	Cl12-Cu1-Cl13	92.1
Cl11-Cu1-Cl14	87.5	Cl12-Cu1-Cl14	90.3	Cl13-Cu1-Cl14	176.3
Cl21-Cu2-Cl22	172.0	Cl21-Cu2-Cl23	89.8	Cl22-Cu2-Cl23	90.1
Cl21-Cu2-Cl24	89.9	Cl22-Cu2-Cl24	91.1	Cl23-Cu2-Cl24	174.0
Cl31-Cu3-Cl32	173.6	Cl31-Cu3-Cl34	90.4	Cl32-Cu3-Cl34	88.5
Cl31-Cu3-Cl33	89.8	Cl32-Cu3-Cl33	92.0	Cl34-Cu3-Cl33	173.3
Cl41-Cu4-Cl42	174.7	Cl41-Cu4-Cl44	93.7	Cl42-Cu4-Cl44	91.7
Cl41-Cu4-Cl43	85.6	Cl42-Cu4-Cl43	89.1	Cl44-Cu4-Cl43	177.1

Compound 4a: $[\text{Cu}(\text{benz}_2\text{mpa})_2]\text{CuCl}_2$ Table 5.11.: Crystal data and structure refinement for compound **4a**.

Internal identification code	schindler12051
CCDC-no.	898385
Diffractometer type	Bruker Nonius FR591 with Kappa CCD
Empirical formula	$\text{C}_{36}\text{H}_{40}\text{Cl}_2\text{Cu}_2\text{N}_4$
Formula weight	726.70
Temperature	190(2) K
Wavelength	0.71073 Å
Crystal system, space group	Triclinic, $P\bar{1}$
Unit cell dimensions	a = 13.341(3) Å $\alpha = 102.25(3)^\circ$ b = 14.293(3) Å $\beta = 104.47(3)^\circ$ c = 19.855(4) Å $\gamma = 98.68(3)^\circ$
Volume	3498.3(12) Å ³
Z, Calculated density	4, 1.380 Mg/m ³
Absorption coefficient	1.399 mm ⁻¹
F(000)	1504
Habitus, colour	Needle, red
Crystal size	0.60 x 0.17 x 0.10 mm
Theta range for data collection	1.95 to 27.45 °
Limiting indices	-17 ≤ h ≤ 17, -18 ≤ k ≤ 18, -25 ≤ l ≤ 25
Reflections collected / unique	61768 / 15985 [R(int) = 0.0656]
Completeness to theta = 27.45	99.8 %
Absorption correction	Semiempirical
Max. and min. transmission	0.57166 and 0.48648
Refinement method	Full-matrix least-squares on F ²
Data / restraints / parameters	15985 / 0 / 1115
Goodness-of-fit on F ²	1.020
Final R indices [I > 2σ(I)]	R1 = 0.0480, wR2 = 0.1134
R indices (all data)	R1 = 0.0792, wR2 = 0.1292
Extinction coefficient	1.45
Largest diff. peak and hole	0.712 and -0.954 e. Å ⁻³

The refinement shows two molecules in the independent unit of the elementary cell. The hydrogen atoms were partly found and partly positioned geometrically, all were refined isotropically. Non-hydrogen atoms were refined anisotropically. Semiempirical absorption corrections were applied.

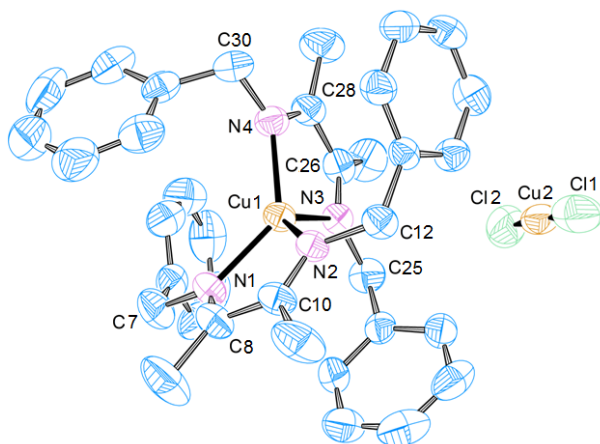


Figure 5.6.: ORTEP plot with thermal ellipsoids set at 50% probability shows one complex molecule of compound **4a** with one anion. Hydrogen atoms are not shown.

Table 5.12.: Selected bond lengths [\AA] and angles [$^\circ$] for compound **4a**.

Cu1-N3	2.002	Cu1-N2	2.004	Cu1-N4	2.021
Cu1-N1	2.023	Cl1-Cu2	2.1062	Cu2-Cl2	2.094
Cu3-N8	2.002	Cu3-N7	2.005	Cu3-N6	2.009
Cu3-N5	2.014	Cl3-Cu4	2.0865	Cu4-Cl4	1.67
Cu4-Cl4	2.092				
N3-Cu1-N2	122.27	N3-Cu1-N4	80.76	N2-Cu1-N4	123.09
N3-Cu1-N1	124.24	N2-Cu1-N1	80.32	N4-Cu1-N1	132.35
C8-N1-Cu1	114.1	C7-N1-Cu1	126.8	Cl2-Cu2-Cl1	178.45
C10-N2-Cu1	114.76	C12-N2-Cu1	125.51	N8-Cu3-N7	80.80
N8-Cu3-N6	121.30	N7-Cu3-N6	129.29	N8-Cu3-N5	127.43
N7-Cu3-N5	124.47	N6-Cu3-N5	80.32	C26-N3-Cu1	113.9
C25-N3-Cu1	125.8	Cl4-Cu4-Cl3	152.0	Cl4-Cu4-Cl4	28.4
Cl3-Cu4-Cl4	179.32	C28-N4-Cu1	113.1	C30-N4-Cu1	125.3
C44-N5-C43	119.7	C44-N5-Cu3	114.3	C43-N5-Cu3	124.84
C46-N6-Cu3	114.2	C48-N6-Cu3	125.8	C62-N7-Cu3	113.4
C61-N7-Cu3	123.66	C64-N8-Cu3	113.5	C66-N8-Cu3	123.5

Compound 7: [CuL¹Cl]₃ (L¹ = benzylamine)Table 5.13.: Crystal data and structure refinement for compound **7**.

Internal identification code	schindler12060
CCDC-no.	Not submitted.
Diffractometer type	Bruker Nonius FR591 with Kappa CCD
Empirical formula	C ₂₁ H ₂₆ Cl ₃ Cu ₃ N ₃
Formula weight	617.42
Temperature	190(2) K
Wavelength	0.71073 Å
Crystal system, space group	Triclinic, $C\bar{1}$
Unit cell dimensions	a = 31.851(6) Å $\alpha = 90^\circ$ b = 4.4080(9) Å $\beta = 107.98(3)^\circ$ c = 17.519(4) Å $\gamma = 90^\circ$
Volume	2339.5(8) Å ³
Z, Calculated density	4, 1.753 Mg/m ³
Absorption coefficient	3.059 mm ⁻¹
F(000)	1244
Habitus, color	Plate, colorless
Crystal size	0.35 x 0.25 x 0.12 mm
Theta range for data collection	2.59 to 25.00 °
Limiting indices	-36 ≤ h ≤ 37, -5 ≤ k ≤ 5, -19 ≤ l ≤ 19
Reflections collected / unique	5195 / 2510 [R(int) = 0.0927]
Completeness to theta = 25.00	60.8 %
Absorption correction	None
Refinement method	Full-matrix least-squares on F ²
Data / restraints / parameters	2510 / 1 / 138
Goodness-of-fit on F ²	1.086
Final R indices [I > 2σ(I)]	R1 = 0.1164, wR2 = 0.2875
R indices (all data)	R1 = 0.1849, wR2 = 0.3758
Largest diff. peak and hole	0.959 and -1.364 e. Å ⁻³

The structure was solved as a twin (TWIN -1 0 0 0 1 0 0 0 -1, BASF 0.51532). The refinement shows a trimer of compound **7** in the independent unit of the elementary cell. The hydrogen atoms were positioned geometrically and refined isotropically. Non-hydrogen atoms were refined anisotropically. No absorption corrections were applied.

Symmetry transformations used to generate equivalent atoms:

a: x,y,-1,z **b:** -x+1/2,-y+1/2,-z **c:** x,y+1,z

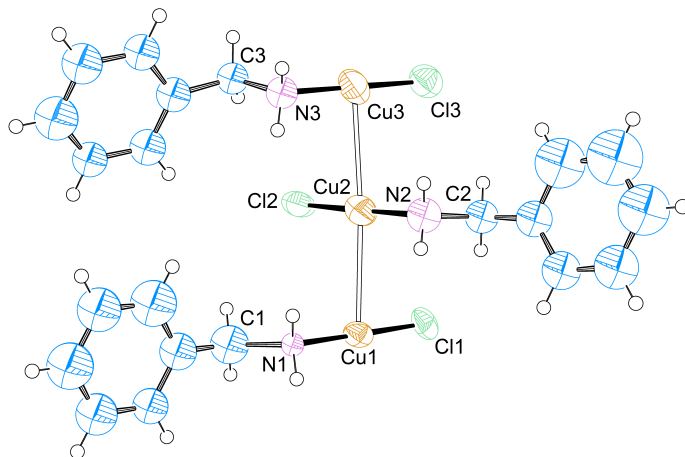


Figure 5.7.: ORTEP plot with thermal ellipsoids set at 50% probability shows the complex trimer of compound **7**.

Table 5.14.: Selected bond lengths [\AA] and angles [$^\circ$] for compound **7**.

Cu1-N1	1.89	Cu1-Cl1	2.14	Cu1-Cu2	2.88
Cu2-N2	1.92	Cu2-Cl2	2.09	Cu2-Cu3	2.93
Cu3-N3	1.88	Cu3-Cl3	2.10	Cu3A-N3A	1.72
Cu3A-Cl3A _a	2.08	Cu3A-Cu3A _a	3.04	Cl3A-Cu3A _a	2.08
N1-C1	1.47	N2-C2	1.54	N3-C3	1.65
N1-Cu1-Cl1	172.8	N1-Cu1-Cu2	90.4	Cl1-Cu1-Cu2	89.5
N2-Cu2-Cl2	177.4	N2-Cu2-Cu1	91.4	Cl2-Cu2-Cu1	88.2
N2-Cu2-Cu3	91.2	Cl2-Cu2-Cu3	89.4	Cu1-Cu2-Cu3	175.8
N3A-Cu3A-Cu3A _a	88.7	N3-Cu3-Cu2	91.8	Cl3-Cu3-Cu2	88.0
N3A-Cu3A-Cl3A _a	167.7	N3-Cu3-Cl3	176.9	C1-N1-Cu1	114
Cl3A _a -Cu3A-Cu3A _a	98.5	C2-N2-Cu2	109.1	C3-N3-Cu3	119
N1-C1-C11	113	C21-C2-N2	114	C31-C3-N3	119
C12-C11-C16	120.0	C12-C11-C1	119.5	C16-C11-C1	120.2
C11-C12-C13	120.0	C12-C13-C14	120.0	C15-C14-C13	120.0

HC₁₃H₁₉NOCl (benzyl-(1,1-dimethyl-3-oxo-butyl)-ammoniumchloride)Table 5.15.: Crystal data and structure refinement for HC₁₃H₁₉NOCl.

CCDC-no.	898382
Diffractometer type	Bruker Nonius FR591 with Kappa CCD
Empirical formula	C ₁₃ H ₂₀ ClNO
Formula weight	241.75
Temperature	190(2) K
Wavelength	0.71073 Å
Crystal system, space group	Tetragonal, <i>P</i> 4 ₂ / <i>n</i>
Unit cell dimensions	a = 18.983(3) Å $\alpha = 90^\circ$ b = 18.983(3) Å $\beta = 90^\circ$ c = 7.5320(15) Å $\gamma = 90^\circ$
Volume	2714.2(8) Å ³
Z, Calculated density	8, 1.183 Mg/m ³
Absorption coefficient	0.263 mm ⁻¹
F(000)	1040
Habitus, colour	Plate, colourless
Crystal size	0.36 x 0.30 x 0.13 mm
Theta range for data collection	2.15 to 30.07 °
Limiting indices	-21 ≤ h ≤ 25, -26 ≤ k ≤ 20, -6 ≤ l ≤ 10
Reflections collected / unique	19771 / 3969 [R(int) = 0.0635]
Completeness to theta = 28.36	99.4 %
Absorption correction	Semiempirical
Max. and min. transmission	1.00306 and 0.91437
Refinement method	Full-matrix least-squares on F ²
Data / restraints / parameters	3969 / 0 / 225
Goodness-of-fit on F ²	1.028
Final R indices [I > 2σ(I)]	R1 = 0.0473, wR2 = 0.1027
R indices (all data)	R1 = 0.0985, wR2 = 0.1191
Largest diff. peak and hole	0.195 and -0.208 e. Å ⁻³

The refinement shows one molecule in the independent unit of the elementary cell. The hydrogen atoms were found and refined isotropically. Non-hydrogen atoms were refined anisotropically. Semiempirical absorption corrections were applied.

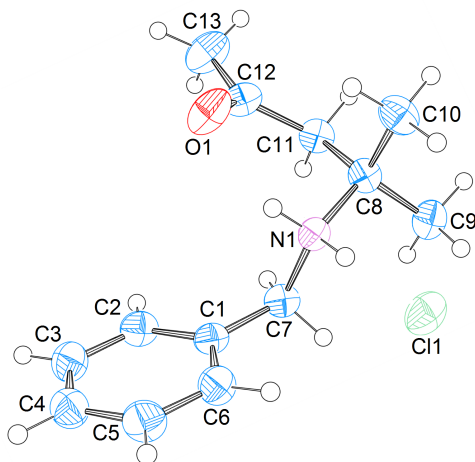


Figure 5.8.: ORTEP plot with thermal ellipsoids set at 50% probability shows the full compound $\text{HC}_{13}\text{H}_{19}\text{NOCl}$.

Table 5.16.: Selected bond lengths [\AA] and angles [$^\circ$] for $\text{HC}_{13}\text{H}_{19}\text{NOCl}$.

O1-C12	1.215	N1-C7	1.503	N1-C8	1.525
C1-C6	1.385	C1-C2	1.388	C2-C3	1.379
C3-C4	1.380	C4-C5	1.387	C5-C6	1.388
C6-C7	1.508	C8-C11	1.531	C8-C10	1.533
C8-C9	1.533	C11-C12	1.516	C12-C13	1.492
C7-N1-C8	117.26	N1-C7-C6	110.34	N1-C8-C11	110.43
N1-C8-C10	105.47	N1-C8-C9	108.63	O1-C12-C13	120.88
O1-C12-C11	121.81	C6-C1-C2	120.82	C3-C2-C1	119.65
C2-C3-C4	120.01	C3-C4-C5	120.33	C4-C5-C6	120.13
C1-C6-C5	119.05	C1-C6-C7	120.10	C5-C6-C7	120.84
C11-C8-C10	111.24	C11-C8-C9	110.23	C10-C8-C9	110.71
C12-C11-C8	117.29	C13-C12-C11	117.24		

[Zn(benz₂dba)Cl₂]
(benz₂dba = benzyl-(3-benzylimino-1,1-dimethyl-butyl)-amine)

Table 5.17.: Crystal data and structure refinement for [Zn(benz₂dba)Cl₂].

Internal identification code	SS60
CCDC-no.	898379
Diffractometer type	BRUKER APEX 2 QUAZAR
Empirical formula	C ₂₀ H ₂₆ Cl ₂ N ₂ Zn
Formula weight	430.70
Temperature	193(2) K
Wavelength	0.71073 Å
Crystal system, space group	Monoclinic, <i>P</i> 2 ₁ / <i>c</i>
Unit cell dimensions	a = 9.675(3) Å α = 90° b = 25.070(8) Å β = 115.181(4)° c = 9.408(3) Å γ = 90°
Volume	2065.2(11) Å ³
Z, Calculated density	4, 1.385 Mg/m ³
Absorption coefficient	1.453 mm ⁻¹
F(000)	896
Habitus, colour	Plate, colourless
Crystal size	0.15 x 0.12 x 0.08 mm
Theta range for data collection	1.62 to 28.32°
Limiting indices	-12 ≤ h ≤ 12, -33 ≤ k ≤ 32, -12 ≤ l ≤ 12
Reflections collected / unique	27612 / 5036 [R(int) = 0.0379]
Completeness to theta = 28.36	97.8 %
Absorption correction	Semiempirical
Max. and min. transmission	0.6814 and 0.5301
Refinement method	Full-matrix least-squares on F ²
Data / restraints / parameters	5036 / 0 / 330
Goodness-of-fit on F ²	0.972
Final R indices [I > 2σ(I)]	R1 = 0.0291, wR2 = 0.0673
R indices (all data)	R1 = 0.0464, wR2 = 0.0712
Largest diff. peak and hole	0.349 and -0.221 e. Å ⁻³

The refinement shows one molecule in the independent unit of the elementary cell. The hydrogen atoms were found. The hydrogen atoms were positioned geometrically and refined isotropically. Non-hydrogen atoms were refined anisotropically. Semiempirical absorption corrections were applied.

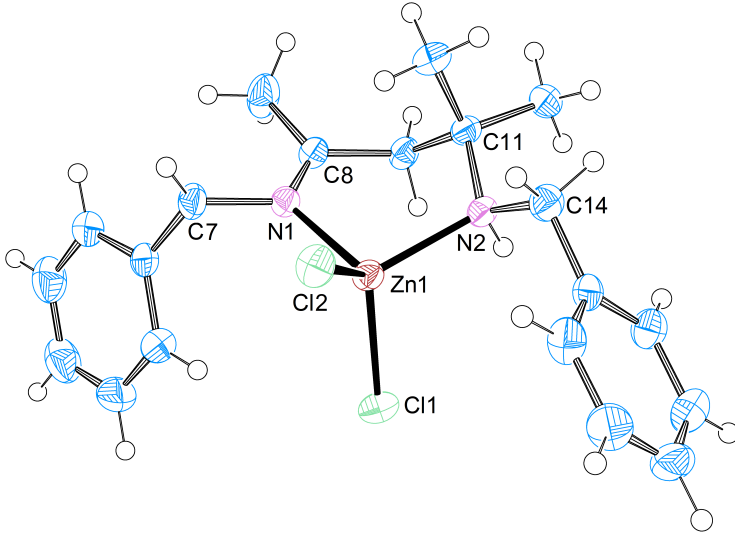


Figure 5.9.: ORTEP plot with thermal ellipsoids set at 50 % probability shows the full complex molecule of $[\text{Zn}(\text{benz}_2\text{dba})\text{Cl}_2]$.

Table 5.18.: Selected bond lengths [\AA] and angles [$^\circ$] for $[\text{Zn}(\text{benz}_2\text{dba})\text{Cl}_2]$.

Zn1-N1	2.042	Zn1-N2	2.057	Zn1-Cl1	2.219
Zn1-Cl2	2.237	N1-C8	1.280	N1-C7	1.492
C1-C6	1.375	C1-C2	1.378	N2-C14	1.494
N2-C11	1.507				
<hr/>					
N1-Zn1-N2	100.30	N1-Zn1-Cl1	112.96	N2-Zn1-Cl1	108.47
N1-Zn1-Cl2	103.85	N2-Zn1-Cl2	115.66	Cl1-Zn1-Cl2	114.69
C8-N1-C7	120.52	C8-N1-Zn1	120.97	C7-N1-Zn1	118.08
C6-C1-C2	121.3	C14-N2-C11	114.71	C14-N2-Zn1	113.32
C11-N2-Zn1	112.26	C8-N1-C7	120.52	C8-N1-Zn1	120.97
C7-N1-Zn1	118.08	C6-C1-C2	121.32	C14-N2-C11	114.71

[Cu(aniline)₂Cl₂]Table 5.19.: Crystal data and structure refinement for [Cu(aniline)₂Cl₂].

Internal identification code	SSIT6
CCDC-no.	873404
Diffractometer type	BRUKER APEX 2 QUAZAR
Empirical formula	C ₁₂ H ₁₄ Cl ₂ CuN ₂
Formula weight	320.69
Temperature	200(2) K
Wavelength	0.71073 Å
Crystal system, space group	Monoclinic, <i>P</i> 2 ₁ / <i>c</i>
Unit cell dimensions	a = 6.145(2) Å α = 90 ° b = 4.5530(17) Å β = 94.339(7) ° c = 23.200(10) Å γ = 90 °
Volume	647.2(4) Å ³
Z, Calculated density	2, 1.646 Mg/m ³
Absorption coefficient	2.077 mm ⁻¹
F(000)	326
Habitus, colour	Block, green
Crystal size	0.35 x 0.25 x 0.20 mm
Theta range for data collection	1.76 to 28.36 °
Limiting indices	-8 ≤ h ≤ 8, -5 ≤ k ≤ 6, -30 ≤ l ≤ 29
Reflections collected / unique	9252 / 1531 [R(int) = 0.0662]
Completeness to theta = 26.45	94.6 %
Absorption correction	Semiempirical
Max. and min. transmission	0.6814 and 0.5301
Refinement method	Full-matrix least-squares on F ²
Data / restraints / parameters	1531 / 0 / 87
Goodness-of-fit on F ²	0.899
Final R indices [I > 2σ(I)]	R1 = 0.0292, wR2 = 0.0453
R indices (all data)	R1 = 0.0574, wR2 = 0.0491
Largest diff. peak and hole	0.354 and -0.313 e. Å ⁻³

The refinement shows a half molecule in the independent unit of the elementary cell. All C-H hydrogen atoms were positioned geometrically, the N-H hydrogen atoms were found and isotropically refined. Non-hydrogen atoms were refined anisotropically. Semiempirical absorption corrections were applied.

Symmetry transformations used to generate equivalent atoms:

a: -x+1,-y+1,-z+1

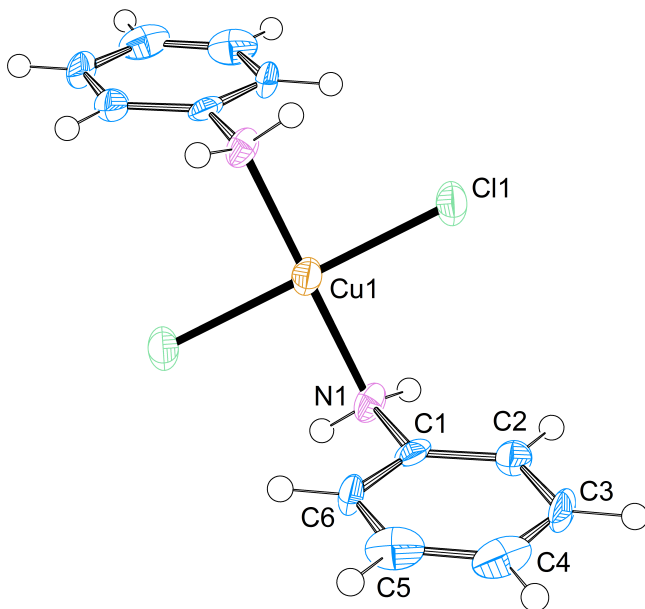


Figure 5.10.: ORTEP plot with thermal ellipsoids set at 60% probability shows the full complex molecule of $[\text{Cu}(\text{aniline})_2\text{Cl}_2]$.

Table 5.20.: Selected bond lengths [\AA] and angles [$^\circ$] for $[\text{Cu}(\text{aniline})_2\text{Cl}_2]$.

Cl1-Cu1	2.261	Cu1-N1	2.018	Cu1-N1 _a	2.018
Cu1-Cl1 _a	2.261	C1-C2	1.381	C1-C6	1.390
C1-N1	1.437	C2-C3	1.382	C3-C4	1.384
C4-C5	1.377	C5-C6	1.384		
N1-Cu1-N1 _a	180.00	N1-Cu1-Cl1	90.54	N1 _a -Cu1-Cl1	89.46
N1-Cu1-Cl1 _a	89.46	N1 _a -Cu1-Cl1 _a	90.54	Cl1-Cu1-Cl1 _a	180.0
C1-N1-Cu1	114.82	C2-C1-C6	120.22	C2-C1-N1	119.82
C6-C1-N1	120.02	C1-C2-C3	119.62	C2-C3-C4	120.72
C5-C4-C3	119.42	C4-C5-C6	120.62	C5-C6-C1	119.52

[Cu₄OCl₆(MeOH)₄] · MeOHTable 5.21.: Crystal data and structure refinement for [Cu₄OCl₆(MeOH)₄] · MeOH.

Internal identification code	schindler12002
CCDC-no.	898381
Diffractometer type	BRUKER Nonius FR591 with Kappa CCD
Empirical formula	C ₆ H ₂₄ Cl ₆ Cu ₄ O ₇
Formula weight	675.11
Temperature	170(2) K
Wavelength	0.71073 Å
Crystal system, space group	Monoclinic, <i>C</i> 2/ <i>c</i>
Unit cell dimensions	a = 17.338(4) Å $\alpha = 90^\circ$ b = 10.519(2) Å $\beta = 104.33(3)^\circ$ c = 12.753(3) Å $\gamma = 90^\circ$
Volume	2253.5(8) Å ³
Z, Calculated density	4, 1.990 Mg/m ³
Absorption coefficient	4.455 mm ⁻¹
F(000)	1336
Habitus, color	Block, yellow
Crystal size	0.20 x 0.17 x 0.07 mm
Theta range for data collection	2.28 to 30.06 °
Limiting indices	-21 ≤ 2θ, -14 ≤ 13, -17 ≤ 16
Reflections collected / unique	7553 / 3286 [R(int) = 0.0690]
Completeness to theta = 26.45	99.3 %
Absorption correction	Semiempirical
Max. and min. transmission	0.7456 and 0.4694
Refinement method	Full-matrix least-squares on F ²
Data / restraints / parameters	3286 / 0 / 118
Goodness-of-fit on F ²	1.022
Final R indices [I > 2σ(I)]	R1 = 0.0421, wR2 = 0.1048
R indices (all data)	R1 = 0.0567, wR2 = 0.1117
Extinction coefficient	1.14
Largest diff. peak and hole	0.465 and -1.321 e.Å ⁻³

The refinement shows the half part of the cluster molecule together with one methanol molecule in the independent unit of the elementary cell. All hydrogen atoms were positioned geometrically and refined isotropically. All non-hydrogen atoms were refined anisotropically, semiempirical absorption corrections were applied.

Symmetry transformations used to generate equivalent atoms:

a: $-x+1, y, -z+1/2$

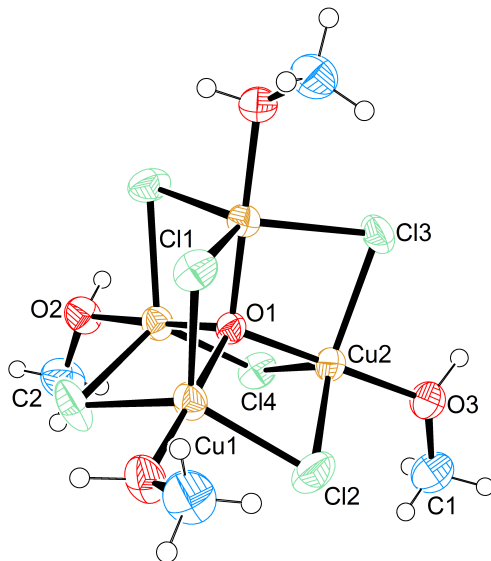


Figure 5.11.: ORTEP plot with thermal ellipsoids set at 50% probability shows the full "methanol cluster". Solvent molecules are not shown.

Table 5.22.: Selected bond lengths [\AA] and angles [$^\circ$] for $[\text{Cu}_4\text{OCl}_6(\text{MeOH})_4] \cdot \text{MeOH}$.

Cu1-Cl1 _a	2.351	Cu1-Cl1	2.351	Cu2-Cl2	2.390
Cu1-O2	1.932	Cu1-Cl3 _a	2.374	Cu2-Cl3	2.382
Cu2-O3	1.956	Cu1-Cl4	2.393	Cu1-O1	1.886
O1-Cu2 _a	1.893	Cu2-Cl2 _a	3.041	Cu2-O1	1.893
Cu2-Cu2 _a	3.04	O1-Cu1 _a	1.88	O1-Cu1 _a	1.886
Cu1 _a -Cl1-Cu1	81.56	Cu2-Cl2-Cu1	79.34	O1-Cu2 _a	1.89
Cu2-Cl4-Cu2 _a	78.89	O1-Cu1-O2	178.78	Cu1 _a -Cl3-Cu2	80.14
				O1-Cu1-Cl1	84.72

continue next page

5. Materials, Methods and Spectroscopy

Table 5.22.: Selected bond lengths [Å] and angles [°] for [Cu₄OCl₆(MeOH)₄] · MeOH. (*continuation*)

O2-Cu1-Cl1	95.93	O1-Cu1-Cl3 _a	85.87	O2-Cu1-Cl3 _a	94.55
Cl1-Cu1-Cl3 _a	126.59	O1-Cu1-Cl2	82.33	O2-Cu1-Cl2	96.46
Cl1-Cu1-Cl2	117.64	Cl3 _a -Cu1-Cl2	112.90	O1-Cu2-O3	177.13
O1-Cu2-Cl3	85.47	O3-Cu2-Cl3	93.46	O1-Cu2-Cl2	85.99
O3-Cu2-Cl2	96.81	Cl3-Cu2-Cl2	123.59	O1-Cu2-Cl4	87.13
O3-Cu2-Cl4	90.95	Cl3-Cu2-Cl4	115.85	Cl2-Cu2-Cl4	119.23
O1-Cu2-Cu2 _a	36.58	O3-Cu2-Cu2	141.46	Cl3-Cu2-Cu2 _a	101.48
Cl2-Cu2-Cu2 _a	103.73	Cl4-Cu2-Cu2	50.55	Cu1 _a -O1-Cu1	108.99
Cu1 _a -O1-Cu2 _a	112.33	Cu1-O1-Cu2 _a	108.19	Cu1 _a -O1-Cu2	108.19
Cu1-O1-Cu2	112.33	Cu2 _a -O1-Cu2	106.85	C1-O2-Cu1	121.52
C2-O3-Cu2	121.62				

[Cu₄OCl₆(CH₃CN)₄] · 2 CH₃CN

Table 5.23.: Crystal data and structure refinement for [Cu₄OCl₆(CH₃CN)₄] · 2 CH₃CN.

Internal identification code	schindler12033
CCDC-no.	898383
Diffractometer type	BRUKER Nonius FR591 with Kappa CCD
Empirical formula	C ₁₂ H ₁₈ Cl ₆ Cu ₄ N ₆ O
Formula weight	729.18
Temperature	190(2) K
Wavelength	0.71073 Å
Crystal system, space group	Monoclinic, <i>C</i> 2/ <i>c</i>
Unit cell dimensions	a = 8.7960(18) Å α = 90° b = 24.447(5) Å β = 95.15(3)° c = 12.442(3) Å γ = 90°
Volume	2664.7(9) Å ³
Z, Calculated density	4, 1.818 Mg/m ³
Absorption coefficient	3.766 mm ⁻¹
F(000)	1432
Habitus, color	Block, red
Crystal size	0.17 x 0.17 x 0.13 mm
Theta range for data collection	1.67 to 27.47°
Limiting indices	-11 ≤ 11, -27 ≤ 31, -16 ≤ 15
Reflections collected / unique	10249 / 3030 [R(int) = 0.0766]
Completeness to theta = 27.47	99.1 %

continue next page

Table 5.23.: Crystal data and structure refinement for $[\text{Cu}_4\text{OCl}_6(\text{CH}_3\text{CN})_4] \cdot 2\text{CH}_3\text{CN}$. (*continuation*)

Absorption correction	Semiempirical
Max. and min. transmission	0.22637 and 0.19056
Refinement method	Full-matrix least-squares on F^2
Data / restraints / parameters	3030 / 0 / 147
Goodness-of-fit on F^2	0.954
Final R indices [$I > 2\sigma(I)$]	$R1 = 0.0427$, $wR2 = 0.0880$
R indices (all data)	$R1 = 0.0931$, $wR2 = 0.1028$
Extinction coefficient	3.88
Largest diff. peak and hole	0.585 and $-0.565 \text{ e.}\text{\AA}^{-3}$

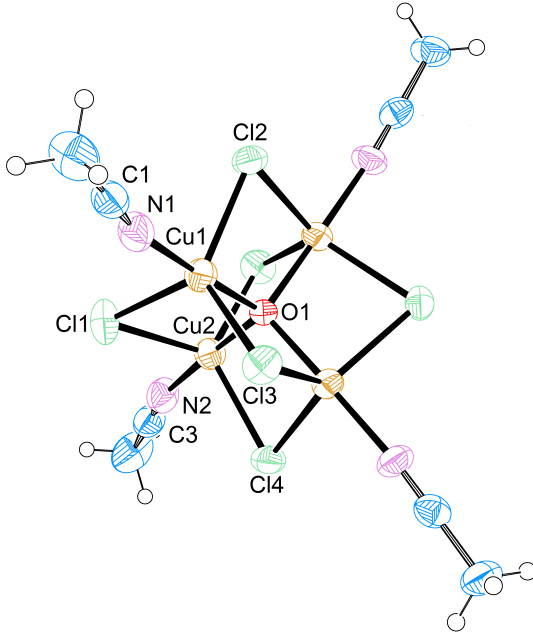


Figure 5.12.: ORTEP plot with thermal ellipsoids set at 50% probability shows the "acetonitrile cluster". Solvent molecules are not shown.

5. Materials, Methods and Spectroscopy

The refinement shows the half part of the cluster molecule together with two acetonitrile molecules in the independent unit of the elementary cell. All hydrogen atoms were positioned geometrically and refined isotropically. All non-hydrogen atoms were refined anisotropically, semiempirical absorption corrections were applied.

Symmetry transformations used to generate equivalent atoms:

a: $-x+2, y, -z+3/2$

Table 5.24.: Selected bond lengths [Å] and angles [°] for $[\text{Cu}_4\text{OCl}_6(\text{CH}_3\text{CN})_4] \cdot 2\text{CH}_3\text{CN}$.

Cu1-O1	1.904	Cu1-N1	1.936	Cu1-Cl3	2.386
Cu1-Cl2	2.386	Cu1-Cl1	2.404	O1-Cu2 _a	1.898
O1-Cu2	1.898	O1-Cu1 _a	1.904	Cl1-Cu2	2.389
Cu2-N2	1.964	Cu2-Cl3 _a	2.362	Cu2-Cl4	2.443
Cl2-Cu1	2.386	Cl3-Cu2 _a	2.362	Cl4-Cu2 _a	2.443
C1-N1	1.122	C1-C4	1.469	C2-N3	1.140
C2-C6	1.420	C3-N2	1.128		
O1-Cu1-N1	177.87	O1-Cu1-Cl3	84.30	N1-Cu1-Cl3	93.77
O1-Cu1-Cl2	84.42	N1-Cu1-Cl2	95.84	Cl3-Cu1-Cl2	121.34
O1-Cu1-Cl1	84.91	N1-Cu1-Cl1	96.74	Cl3-Cu1-Cl1	114.88
Cl2-Cu1-Cl1	121.09	Cu2 _a -O1-Cu2	110.82	Cu2 _a -O1-Cu1	109.08
Cu2-O1-Cu1	109.07	Cu2 _a -O1-Cu1 _a	109.07	Cu2-O1-Cu1 _a	109.08
Cu1-O1-Cu1 _a	109.70	C1-N1-Cu1	173.24	Cu2-Cl1-Cu1	80.48
O1-Cu2-N2	177.01	O1-Cu2-Cl3 _a	85.09	N2-Cu2-Cl3 _a	93.33
O1-Cu2-Cl1	85.46	N2-Cu2-Cl1	93.38	Cl3 _a -Cu2-Cl1	124.57
O1-Cu2-Cl4	84.83	N2-Cu2-Cl4	98.16	Cl3 _a -Cu2-Cl4	116.42
Cl1-Cu2-Cl4	116.86	C3-N2-Cu2	166.64	Cu1 _a -Cl2-Cu1	81.46
Cu2 _a -Cl3-Cu1	81.42	Cu2-Cl4-Cu2 _a	79.53	N1-C1-C4	179.36
N3-C2-C6	178.19	N2-C3-C5	179.56		

[Cu₄OCl₆(dms_o)₄] · dms_oTable 5.25.: Crystal data and structure refinement for [Cu₄OCl₆(dms_o)₄] · dms_o.

Internal identification code	schindler12036
CCDC-no.	898384
Diffractometer type	BRUKER Nonius FR591 with Kappa CCD
Empirical formula	C ₁₀ H ₃₀ Cl ₆ Cu ₄ O ₆ S ₅
Formula weight	873.50
Temperature	190(2) K
Wavelength	0.71073 Å
Crystal system, space group	Orthorhombic, <i>P</i> 2 ₁ 2 ₁ 2 ₁
Unit cell dimensions	a = 10.450(2) Å α = 90° b = 10.574(2) Å β = 90° c = 28.111(6) Å γ = 90°
Volume	3106.2(11) Å ³
Z, Calculated density	4, 1.868 Mg/m ³
Absorption coefficient	3.577 mm ⁻¹
F(000)	1744
Habitus, color	Block, yellow
Crystal size	0.26 x 0.23 x 0.03 mm ³
Theta range for data collection	2.06 to 27.47°
Limiting indices	-13 ≤ h ≤ 11, -13 ≤ k ≤ 12, -27 ≤ l ≤ 36
Reflections collected / unique	14371 / 6983 [R(int) = 0.0577]
Completeness to theta = 27.47	99.8 %
Absorption correction	Semiempirical
Max. and min. transmission	0.74264 and 0.55688
Refinement method	Full-matrix least-squares on F ²
Data / restraints / parameter	6983 / 0 / 321
Goodness-of-fit on F ²	0.914
Final R indices [I > 2σ(I)]	R1 = 0.0430, wR2 = 0.0984
R indices (all data)	R1 = 0.0619, wR2 = 0.1071
Absolute structure parameter	-0.027(14)
Extinction coefficient	0.91
Largest diff. peak and hole	0.717 and -0.630 e. Å ⁻³

The refinement shows one cluster and one dms_o solvent molecule in the independent unit of the elementary cell. The dms_o solvent molecule is disordered in two positions (50:50). The C-H hydrogen atoms were partly found and partly positioned geometrically, all were isotropically refined. All non-hydrogen atoms were refined anisotropically, semiempirical absorption corrections were applied.

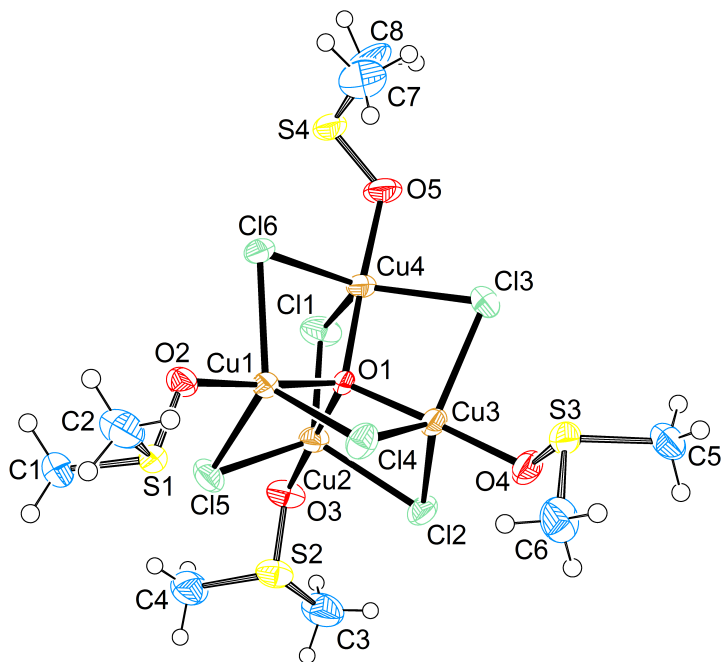


Figure 5.13.: ORTEP plot with thermal ellipsoids set at 50% probability shows the "dmsO cluster". Solvent molecules and disorder are not shown.

Table 5.26.: Selected bond lengths [Å] and angles [°] for $[\text{Cu}_4\text{OCl}_6(\text{dmsO})_4] \cdot \text{dmsO}$.

Cu1-O1	1.886	Cu1-O2	1.911	Cu1-Cl5	2.378
Cu1-Cl4	2.409	Cu1-Cl6	2.480	Cl1-Cu4	2.417
Cl1-Cu2	2.425	O1-Cu3	1.895	O1-Cu2	1.902
O1-Cu4	1.906	Cu2-O3	1.923	Cu2-Cl5	2.375
Cu2-Cl2	2.430	Cl2-Cu3	2.413	Cu3-O4	1.934
Cu3-Cl4	2.381	Cu3-Cl3	2.442	Cl3-Cu4	2.433
Cu4-O5	1.919	Cu4-Cl6	2.395	C1-S1	1.732
S1-O2	1.538	S1-C2	1.848	S2-O3	1.549
S2-C3	1.753	S2-C4	1.785	S3-O4	1.533
S3-C5	1.770	S3-C6	1.787	S4-O5	1.532

continue next page

Table 5.26.: Selected bond lengths [Å] and angles [°] for $[\text{Cu}_4\text{OCl}_6(\text{dmsO})_4] \cdot \text{dmsO}$.
(*continuation*)

S4-C8	1.773	S4-C7	1.774	O6-S5	1.364
O6-S5	1.571	C9-S5	1.734	C9-S5	1.872
S5-C10	1.232	S5-C10	1.460		
O1-Cu1-O2	177.73	O1-Cu1-Cl5	84.52	O2-Cu1-Cl5	96.38
O1-Cu1-Cl4	85.27	O2-Cu1-Cl4	92.51	Cl5-Cu1-Cl4	125.27
O1-Cu1-Cl6	83.88	O2-Cu1-Cl6	97.61	Cl5-Cu1-Cl6	114.50
Cl4-Cu1-Cl6	117.57	Cu4-Cl1-Cu2	79.17	Cu1-O1-Cu3	108.86
Cu1-O1-Cu2	109.75	Cu3-O1-Cu2	109.88	Cu1-O1-Cu4	110.72
Cu3-O1-Cu4	109.32	Cu2-O1-Cu4	108.29	O1-Cu2-O3	179.65
O1-Cu2-Cl5	84.26	O3-Cu2-Cl5	95.79	O1-Cu2-Cl1	85.91
O3-Cu2-Cl1	94.35	Cl5-Cu2-Cl1	123.48	O1-Cu2-Cl2	84.83
O3-Cu2-Cl2	94.84	Cl5-Cu2-Cl2	120.75	Cl-Cu-Cl	113.49
Cu3-Cl2-Cu2	79.81	S1-O2-Cu1	122.03	O1-Cu3-O4	177.73
O1-Cu3-Cl4	85.89	O4-Cu3-Cl4	95.98	O1-Cu3-Cl2	85.46
O4-Cu3-Cl2	92.46	Cl4-Cu3-Cl2	121.13	O1-Cu3-Cl3	85.84
O4-Cu3-Cl3	94.41	Cl4-Cu3-Cl3	117.43	Cl2-Cu3-Cl3	119.79
Cu4-Cl3-Cu3	78.98	S2-O3-Cu2	116.42	O1-Cu4-O5	177.09
O1-Cu4-Cl6	85.87	O5-Cu4-Cl6	91.22	O1-Cu4-Cl1	86.07
O5-Cu4-Cl1	95.60	Cl6-Cu4-Cl1	125.41	O1-Cu4-Cl3	85.86
O5-Cu4-Cl3	95.64	Cl6-Cu4-Cl3	119.89	Cl1-Cu4-Cl3	113.20
Cu3-Cl4-Cu1	79.88	O5-S4-C8	102.33	O5-S4-C7	103.53
C8-S4-C7	97.94	S3-O4-Cu3	118.52	Cu2-Cl5-Cu1	81.33
S4-O5-Cu4	119.62	Cu4-Cl6-Cu1	79.52	O2-S1-C1	102.83
O2-S1-C2	102.34	C1-S1-C2	95.26	O3-S2-C3	103.83
O3-S2-C4	104.33	C3-S2-C4	99.54	O4-S3-C5	104.33
O4-S3-C6	103.43	C5-S3-C6	99.53	O5-S4-C8	102.33
O5-S4-C7	103.53	C8-S4-C7	97.94	S5-O6-S5	30.73
S5-C9-S5	25.32				

[Cu₄OCl₆(dmf)₄]Table 5.27.: Crystal data and structure refinement for [Cu₄OCl₆(dmf)₄].

Internal identification code	schindler12045
CCDC-no.	Not submitted.
Diffractometer type	BRUKER Nonius FR591 with Kappa CCD
Empirical formula	C ₁₂ H ₂₈ Cl ₆ Cu ₄ N ₄ O ₅
Formula weight	775.24
Temperature	190(2) K
Wavelength	0.71073 Å
Crystal system, space group	Monoclinic, <i>I</i> 2/ <i>a</i>
Unit cell dimensions	a = 15.800(3) Å α = 90 ° b = 8.6060(17) Å β = 100.71(3) ° c = 40.796(8) Å γ = 90 °
Volume	5450.5(19) Å ³
Z, Calculated density	8, 1.889 Mg/m ³
Absorption coefficient	3.696 mm ⁻¹
F(000)	3088
Habitus, colour	Plate, yellow
Crystal size	0.26 x 0.13 x 0.02 mm
Theta range for data collection	2.62 to 27.53 °
Limiting indices	-20 ≤ h ≤ 20, -11 ≤ k ≤ 11, -52 ≤ l ≤ 52
Reflections collected / unique	46282 / 6262 [R(int) = 0.1141]
Completeness to theta = 27.53	99.5 %
Absorption correction	Semiempirical
Max. and min. transmission	0.08072 and 0.05117
Refinement method	Full-matrix least-squares on F ²
Data / restraints / parameters	6262 / 0 / 288
Goodness-of-fit on F ²	1.064
Final R indices [I > 2σ(I)]	R1 = 0.0973, wR2 = 0.2376
R indices (all data)	R1 = 0.1410, wR2 = 0.2716
Extinction coefficient	7.61
Largest diff. peak and hole	4.925 and -0.790 e. Å ⁻³

The refinement shows one cluster molecule in the independent unit of the elementary cell. The C-H hydrogen atoms were positioned geometrically and refined isotropically. All non-hydrogen atoms were refined anisotropically, semiempirical absorption corrections were applied.

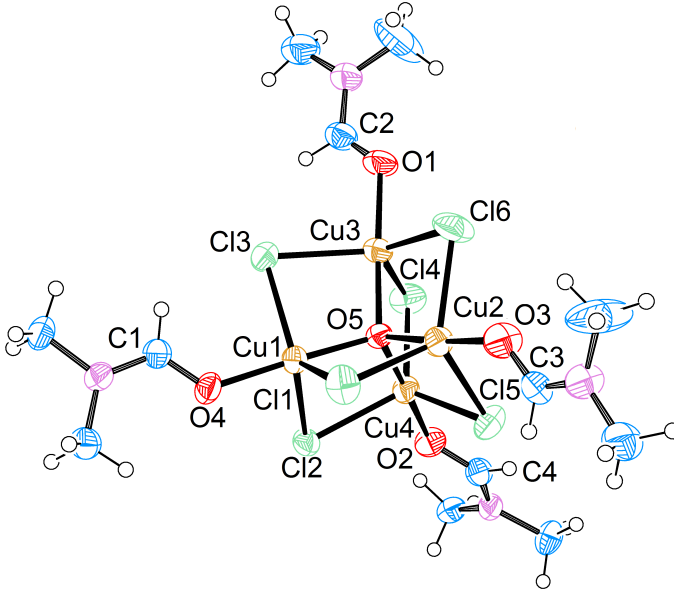


Figure 5.14.: ORTEP plot with thermal ellipsoids set at 50 % probability shows the "dmf cluster".

Table 5.28.: Selected bond lengths [Å] and angles [°] for $[\text{Cu}_4\text{OCl}_6(\text{dmf})_4]$.

Cu1-O5	1.903	Cu1-O4	1.939	Cu1-Cl2	2.375
Cu1-Cl3	2.405	Cu1-Cl1	2.410	Cl1-Cu2	2.367
O1-Cu3	1.936	Cl2-Cu4	2.381	Cu2-O5	1.888
Cu2-O3	1.942	Cu2-Cl6	2.418	Cu2-Cl5	2.421
O2-Cu4	1.927	Cu3-O5	1.906	Cu3-Cl4	2.367
Cu3-Cl3	2.407	Cu3-Cl6	2.436	Cl4-Cu4	2.417
Cu4-O5	1.910	Cu4-Cl5	2.398		
O5-Cu1-O4	175.5	O5-Cu1-Cl2	85.6	O4-Cu1-Cl2	89.9
O5-Cu1-Cl3	85.0	O4-Cu1-Cl3	96.9	Cl2-Cu1-Cl3	123.3
O5-Cu1-Cl1	83.4	O4-Cu1-Cl1	99.6	Cl2-Cu1-Cl1	122.4
Cl3-Cu1-Cl1	111.7	Cu2-Cl1-Cu1	81.2	C2-O1-Cu3	125.8
Cu1-Cl2-Cu4	80.9	O5-Cu2-O3	178.5	O5-Cu2-Cl1	84.9

continue next page

5. Materials, Methods and Spectroscopy

Table 5.28.: Selected bond lengths [Å] and angles [°] for [Cu₄OCl₆(dmf)₄]. (*continuation*)

O3-Cu2-Cl1	94.5	O5-Cu2-Cl6	85.7	O3-Cu2-Cl6	93.3
Cl1-Cu2-Cl6	117.9	O5-Cu2-Cl5	84.8	O3-Cu2-Cl5	96.6
Cl1-Cu2-Cl5	124.6	Cl6-Cu2-Cl5	115.2	C4-O2-Cu4	128.9
O5-Cu3-O1	177.7	O5-Cu3-Cl4	85.3	O1-Cu3-Cl4	94.6
O5-Cu3-Cl3	84.9	O1-Cu3-Cl3	96.9	Cl4-Cu3-Cl3	127.0
O5-Cu3-Cl6	84.8	O1-Cu3-Cl6	93.2	Cl4-Cu3-Cl6	114.7
Cl3-Cu3-Cl6	115.9	Cu1-Cl3-Cu3	80.4	C3-O3-Cu2	126.1
Cu3-Cl4-Cu4	81.26	C1-O4-Cu1	127.3	O5-Cu4-O2	175.8
O5-Cu4-Cl2	85.2	O2-Cu4-Cl2	90.6	O5-Cu4-Cl5	85.0
O2-Cu4-Cl5	97.1	Cl2-Cu4-Cl5	123.6	O5-Cu4-Cl4	83.8
O2-Cu4-Cl4	98.7	Cl2-Cu4-Cl4	121.6	Cl5-Cu4-Cl4	112.1
Cu4-Cl5-Cu2	80.2	Cu2-O5-Cu1	110.3	Cu2-O5-Cu3	109.9
Cu1-O5-Cu3	109.3	Cu2-O5-Cu4	109.7	Cu1-O5-Cu4	108.2
Cu3-O5-Cu4	109.4	Cu2-Cl6-Cu3	79.5		

[Cu(MeOH)₂Cl₂]

Table 5.29.: Crystal data and structure refinement for [Cu(MeOH)₂Cl₂].

Internal identification code	schindler12040
CCDC-no.	Not submitted.
Diffractometer type	BRUKER Nonius FR591 with Kappa CCD
Empirical formula	C ₂ H ₈ Cl ₂ CuO ₂
Formula weight	198.52
Temperature	190(2) K
Wavelength	0.71073 Å
Crystal system, space group	Triclinic, $P\bar{1}$
Unit cell dimensions	a = 3.8310(10) Å α = 85.41(3) ° b = 5.5280(10) Å β = 77.89(3) ° c = 7.813(2) Å γ = 81.31(3) °
Volume	159.72(7) Å ³
Z, Calculated density	1, 2.064 Mg/m ³
Absorption coefficient	4.150 mm ⁻¹
F(000)	99
Habitus	Plate
Crystal size	0.30 x 0.20 x 0.10 mm
Theta range for data collection	2.67 to 27.47 °
Limiting indices	-4 ≤ h ≤ 4, -7 ≤ k ≤ 7, -10 ≤ l ≤ 9

continue next page

Table 5.29.: Crystal data and structure refinement for $[\text{Cu}(\text{MeOH})_2\text{Cl}_2]$. (*continuation*)

Reflections collected / unique	1576 / 644 [R(int) = 0.0640]
Completeness to $\theta = 27.47$	88.8 %
Absorption correction	Semiempirical
Max. and min. transmission	0.22633 and 0.13965
Refinement method	Full-matrix least-squares on F^2
Data / restraints / parameters	644 / 1 / 39
Goodness-of-fit on F^2	1.144
Final R indices [$I > 2\sigma(I)$]	R1 = 0.0638, wR2 = 0.1925
R indices (all data)	R1 = 0.0673, wR2 = 0.1969
Extinction coefficient	4.26
Largest diff. peak and hole	2.369 and -0.948 e. \AA^{-3}

The refinement shows one molecule in the independent unit of the elementary cell. All C-H hydrogen atoms were positioned geometrically. The N-H hydrogen atoms were found, all were isotropically refined. All non-hydrogen atoms were refined anisotropically, semiempirical absorption corrections were applied.

Symmetry transformations used to generate equivalent atoms:

a: $-x+1, -y+1, -z+1$

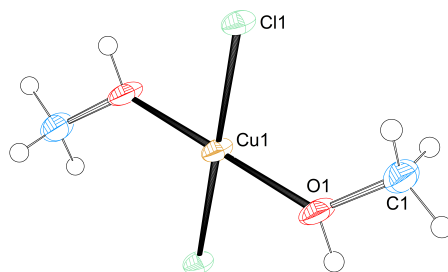


Figure 5.15.: ORTEP plot with thermal ellipsoids set at 50% probability shows the full complex $[\text{Cu}(\text{MeOH})_2\text{Cl}_2]$.

5. *Materials, Methods and Spectroscopy*

Table 5.30.: Selected bond lengths [\AA] and angles [$^\circ$] for $[\text{Cu}(\text{MeOH})_2\text{Cl}_2]$.

Cu1-O1 _a	1.976	Cu1-O1	1.976	Cu1-Cl1	2.277
Cu1-Cl1 ₁	2.277				
O1 _a -Cu1-O1	179.99	O1 _a -Cu1-Cl1	92.07	O1-Cu1-Cl1	87.93
O1 _a -Cu1-Cl1 _a	87.93	O1-Cu1-Cl1 _a	92.07	Cl1-Cu1-Cl1 _a	180.0
Cl1-O1-Cu1	129.54				

5.2.2. Crystallographic Data for Chapter 3

This chapter contains the crystallographic data of the compounds presented in chapter 3. Most of the data are part of the Supporting Information of the manuscript in chapter 3. For detailed information concerning the nomenclature and abbreviations please see chapter 3.

Cluster III: [Cu₄OCl₆L²₄] · [CuL²₂Cl₂] (L² = phenethylamine)

Table 5.31.: Crystal data and structure refinement for cluster III.

Internal identification code	schindler13127
CCDC-no.	982987
Diffractometer type	BRUKER Nonius FR591 with Kappa CCD
Empirical formula	C ₅₀ H ₆₉ Cl ₈ Cu ₅ N ₇ O
Formula weight	1385.42
Temperature	190(2) K
Wavelength	0.71073 Å
Crystal system, space group	Triclinic, <i>P</i> $\bar{1}$
Unit cell dimensions	a = 13.072(3) Å α = 102.56(3) ° b = 14.729(3) Å β = 100.11(3) ° c = 16.854(3) Å γ = 102.06(3) °
Volume	3013.3(12) Å ³
Z, Calculated density	2, 1.527 Mg/m ³
Absorption coefficient	2.131 mm ⁻¹
F(000)	1414
Habitus, color	Block, green
Crystal size	0.400 x 0.250 x 0.250 mm
Theta range for data collection	1.668 to 27.544 °
Limiting indices	-16 ≤ h ≤ 16, -18 ≤ k ≤ 19, -21 ≤ l ≤ 21
Reflections collected / unique	53381 / 13795 [R(int) = 0.1212]
Completeness to theta = 25.24	99.9%
Absorption correction	Semiempirical
Max. and min. transmission	0.49912 and 0.34105
Refinement method	Full-matrix least-squares on F ²
Data / restraints / parameters	13795 / 0 / 644
Goodness-of-fit on F ²	0.946
Final R indices [I > 2σ(I)]	R1 = 0.0448, wR2 = 0.0960
R indices (all data)	R1 = 0.0870, wR2 = 0.1121
Extinction coefficient	2.20
Largest diff. peak and hole	0.663 and -0.603 e. Å ⁻³

The refinement shows one cluster, one acetonitrile solvent molecule and one molecule of the connected [CuL²₂Cl₂] complex in the independent unit of the elementary cell. The C-H hydrogen atoms were positioned geometrically and refined isotropically. All non-hydrogen atoms were refined anisotropically, semiempirical absorption corrections were applied.

Symmetry transformations used to generate equivalent atoms:

a: -x,-y+1,-z **b:** -x+1,-y+1,-z+1

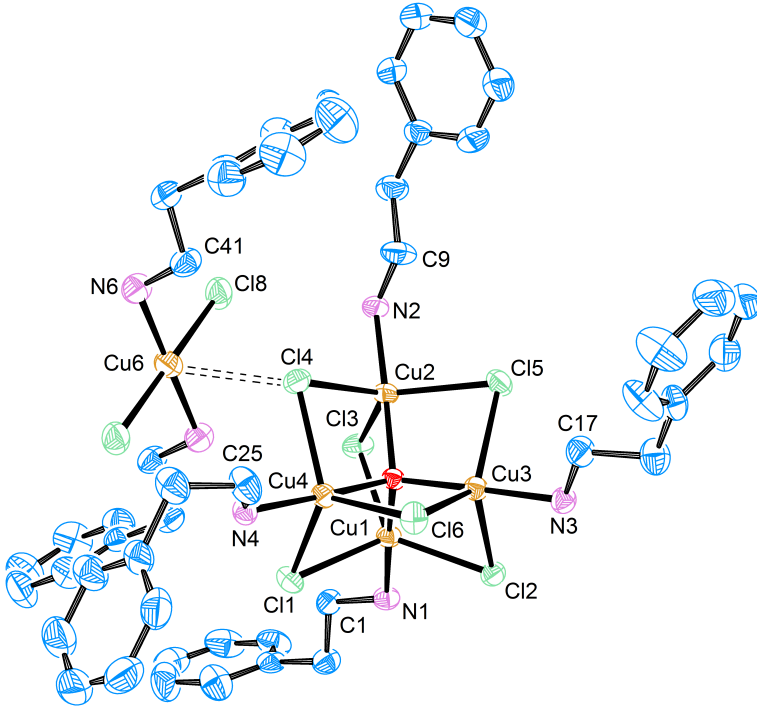


Figure 5.16.: ORTEP plot with thermal ellipsoids set at 50% probability shows the cluster molecule and the bridging complex of cluster III. H atoms are not shown.

Table 5.32.: Selected bond lengths [\AA] and angles [$^\circ$] for cluster III.

Cu1-O1	1.879	Cu1-N1	1.944	Cu1-Cl1	2.390
Cu1-Cl3	2.405	Cu1-Cl2	2.441	C1-N1	1.479
C1-C2	1.507	Cl1-Cu4	2.432	O1-Cu3	1.892
O1-Cu4	1.898	O1-Cu2	1.903	Cu2-N2	1.951
Cu2-Cl5	2.391	Cu2-Cl3	2.415	Cu2-Cl4	2.418
C2-C3	1.489	N2-C9	1.479	Cl2-Cu3	2.384
Cu3-N3	1.946	Cu3-Cl5	2.390	Cu3-Cl6	2.518

continue next page

5. Materials, Methods and Spectroscopy

Table 5.32.: Selected bond lengths [Å] and angles [°] for cluster III. (*continuation*)

C3-C8	1.371	C3-C4	1.376	N3-C17	1.478
Cu4-N4	1.958	Cu4-Cl6	2.382	Cu4-Cl4	2.385
C4-C5	1.370	N4-C25	1.474	C5-C6	1.353
N5-C33	1.468	N5-Cu5	1.980	Cu5-N5 _a	1.980
Cu5-Cl7 _a	2.307	Cu5-Cl7	2.307	Cu6-N6	1.992
Cu6-N6 _b	1.992	Cu6-Cl8 _b	2.298	Cu6-Cl8	2.298
Cu6-Cl4	2.984				
O1-Cu1-N1	179.20	O1-Cu1-Cl1	86.05	N1-Cu1-Cl1	93.62
O1-Cu1-Cl3	85.26	N1-Cu1-Cl3	95.51	Cl1-Cu1-Cl3	129.58
O1-Cu1-Cl2	84.88	N1-Cu1-Cl2	94.63	Cl1-Cu1-Cl2	117.61
Cl3-Cu1-Cl2	110.90	N1-C1-C2	113.73	C1-N1-Cu1	115.42
Cu1-Cl1-Cu4	79.69	Cu1-O1-Cu3	109.50	Cu1-O1-Cu4	109.78
Cu3-O1-Cu4	110.64	Cu1-O1-Cu2	109.60	Cu3-O1-Cu2	107.56
Cu4-O1-Cu2	109.72	O1-Cu2-N2	178.02	O1-Cu2-Cl5	85.59
N2-Cu2-Cl5	95.36	O1-Cu2-Cl3	84.47	N2-Cu2-Cl3	96.54
Cl5-Cu2-Cl3	119.91	O1-Cu2-Cl4	84.05	N2-Cu2-Cl4	93.97
Cl5-Cu2-Cl4	115.79	Cl3-Cu2-Cl4	121.75	C3-C2-C1	113.04
C9-N2-Cu2	115.32	Cu3-Cl2-Cu1	79.31	O1-Cu3-N3	175.37
O1-Cu3-Cl2	86.24	N3-Cu3-Cl2	90.61	O1-Cu3-Cl5	85.84
N3-Cu3-Cl5	98.79	Cl2-Cu3-Cl5	130.90	O1-Cu3-Cl6	83.33
N3-Cu3-Cl6	95.24	Cl2-Cu3-Cl6	118.54	Cl5-Cu3-Cl6	108.47
C17-N3-Cu3	117.82	Cu1-Cl3-Cu2	79.73	O1-Cu4-N4	176.74
O1-Cu4-Cl6	87.09	N4-Cu4-Cl6	92.00	O1-Cu4-Cl4	85.08
N4-Cu4-Cl4	92.85	Cl6-Cu4-Cl4	123.88	O1-Cu4-Cl1	84.46
N4-Cu4-Cl1	98.70	Cl6-Cu4-Cl1	119.79	Cl4-Cu4-Cl1	114.55
Cu4-Cl4-Cu2	80.63	Cu3-Cl5-Cu2	79.62	C33-N5-Cu5	117.62
N5 _a -Cu5-N5	180.0	N5 _a -Cu5-Cl7 _a	89.90	N5-Cu5-Cl7 _a	90.10
N5 _a -Cu5-Cl7	90.10	N5-Cu5-Cl7	89.90	Cl7 _a -Cu5-Cl7	180.0
N6-Cu6-N6 _a	180.00	N6-Cu6-Cl8 _b	90.88	N6 _b -Cu6-Cl8 _b	89.12
N6-Cu6-Cl8	89.12	N6 _b -Cu6-Cl8	90.88	Cl8 _b -Cu6-Cl8	180.00
C41-N6-Cu6	114.32	Cu4-Cl6-Cu3	78.94		

Compound 3c: [CuL³₂Cl₂] (L³ = N-methylbenzylamine)Table 5.33.: Crystal data and structure refinement for compound **3c**.

Internal identification code	schindler13113
CCDC-no.	982984
Diffractometer type	BRUKER Nonius FR591 with Kappa CCD
Empirical formula	C ₁₆ H ₂₂ Cl ₂ CuN ₂
Formula weight	376.79
Temperature	190(2) K
Wavelength	0.71073 Å
Crystal system, space group	Monoclinic, <i>P</i> 2 ₁
Unit cell dimensions	a = 6.3210(13) Å α = 90 ° b = 15.207(3) Å β = 107.88(3) ° c = 9.4290(19) Å γ = 90 °
Volume	862.6(3) Å ³
Z, Calculated density	2, 1.451 Mg/m ³
Absorption coefficient	1.570 mm ⁻¹
F(000)	390
Habitus, color	Plate, violet
Crystal size	0.400 x 0.300 x 0.200 mm
Theta range for data collection	2.270 to 27.522 °
Limiting indices	-8 ≤ h ≤ 7, -18 ≤ k ≤ 19, -10 ≤ l ≤ 12
Reflections collected / unique	6142 / 3367 [R(int) = 0.0784]
Completeness to theta = 25.24	100.0%
Absorption correction	Semiempirical
Max. and min. transmission	0.80071 and 0.37429
Refinement method	Full-matrix least-squares on F ²
Data / restraints / parameters	3367 / 1 / 193
Goodness-of-fit on F ²	1.093
Final R indices [I > 2σ(I)]	R1 = 0.0480, wR2 = 0.1370
R indices (all data)	R1 = 0.0548, wR2 = 0.1423
Absolute structure parameter	0.72(3)
Extinction coefficient	1.62
Largest diff. peak and hole	1.135 and -0.807 e. Å ⁻³

The refinement shows one molecule in the independent unit of the elementary cell. All hydrogen atoms were positioned geometrically and were isotropically refined. All non-hydrogen atoms were refined anisotropically, semiempirical absorption corrections were applied.

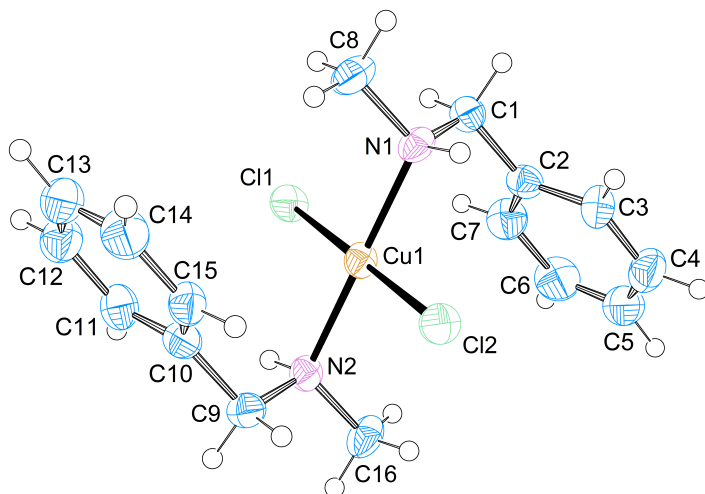


Figure 5.17.: ORTEP plot with thermal ellipsoids set at 50% probability shows the full compound **3c**.

Table 5.34.: Selected bond lengths [\AA] and angles [$^\circ$] for compound **3c**.

Cu1-N1	1.996	Cu1-N2	2.006	Cu1-Cl3	2.263
Cu1-Cl2	2.264	C1-N1	1.482	C1-C2	1.496
N1-C8	1.472	C2-C7	1.373	C2-C3	1.401
N2-C16	1.457	N2-C9	1.473	C3-C4	1.381
C5-C6	1.355	C5-C4	1.385	C7-C6	1.407
C7-C10	1.501	C10-C15	1.376	C10-C11	1.385
C14-C13	1.373	C14-C15	1.374	C11-C12	1.376
N1-Cu1-N2	179.93	N1-Cu1-Cl3	89.08	N2-Cu1-Cl3	90.95
N1-Cu1-Cl2	90.94	N2-Cu1-Cl2	89.03	Cl3-Cu1-Cl2	179.66
C8-N1-Cu1	113.15	C1-N1-Cu1	114.25	C16-N2-Cu1	114.55
C9-N2-Cu1	113.15	N1-C1-C2	110.66	C8-N1-C1	110.17
C7-C2-C3	119.47	C7-C2-C1	120.77	C3-C2-C1	119.97
C16-N2-C9	111.76	C4-C3-C2	119.68	C6-C5-C4	119.88
C2-C7-C6	120.08	C5-C6-C7	120.49	N2-C9-C10	111.66

Compound 3d: [CuL³₂Cl₂] (L³ = N-methylbenzylamine)Table 5.35.: Crystal data and structure refinement for compound **3d**.

Internal identification code	schindler13120
CCDC-no.	Not submitted.
Diffractometer type	BRUKER Nonius FR591 with Kappa CCD
Empirical formula	C ₁₆ H ₂₂ Cl ₂ CuN ₂
Formula weight	376.79
Temperature	190(2) K
Wavelength	0.71073 Å
Crystal system, space group	Orthorhombic, <i>C m c m</i>
Unit cell dimensions	a = 17.328(4) Å $\alpha = 90^\circ$ b = 10.455(2) Å $\beta = 90^\circ$ c = 9.4880(19) Å $\gamma = 90^\circ$
Volume	1718.9(6) Å ³
Z, Calculated density	4, 1.456 Mg/m ³
Absorption coefficient	1.576 mm ⁻¹
F(000)	780
Habitus, color	Plate, blue
Crystal size	0.370 x 0.350 x 0.050 mm
Theta range for data collection	2.351 to 26.986 °
Limiting indices	-22 ≤ h ≤ 19, -13 ≤ k ≤ 12, -11 ≤ l ≤ 12
Reflections collected / unique	5350 / 1027 [R(int) = 0.1318]
Completeness to theta = 25.24	99.8%
Absorption correction	None
Refinement method	Full-matrix least-squares on F ²
Data / restraints / parameters	1027 / 2 / 77
Goodness-of-fit on F ²	1.037
Final R indices [I > 2σ(I)]	R1 = 0.0485, wR2 = 0.1215
R indices (all data)	R1 = 0.0629, wR2 = 0.1287
Largest diff. peak and hole	0.971 and -1.017 e. Å ⁻³

The refinement shows the half part of the molecule in the independent unit of the elementary cell. The benzylic residue is disordered in four positions (25:25:25:25). All hydrogen atoms were positioned geometrically and isotropically refined. All non-hydrogen atoms were refined anisotropically. No absorption corrections were applied.

Symmetry transformations used to generate equivalent atoms:

a: x,y,-z+1/2

5. Materials, Methods and Spectroscopy

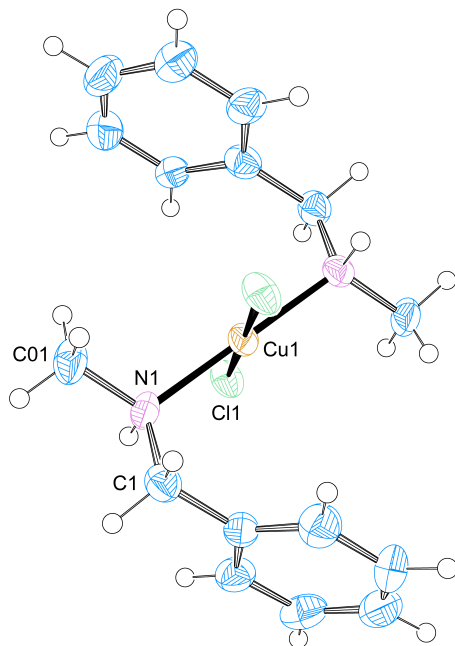


Figure 5.18.: ORTEP plot with thermal ellipsoids set at 50% probability shows the full compound **3d**. Disorder of the benzylic residue is not shown.

Table 5.36.: Selected bond lengths [\AA] and angles [$^\circ$] for compound **3d**.

Cu1-N1	2.004	Cu1-N1 _a	2.004	Cu1-Cl1	2.263
Cu1-Cl2	2.287				
N1-Cu1-N1 _a	176.65	N1-Cu1-Cl1	91.67	N1 _a -Cu1-Cl1	91.67
N1-Cu1-Cl2	88.33	N1 _a -Cu1-Cl2	88.33	Cl1-Cu1-Cl2	180.00
Cl1-N1-Cu1	111.91	C01-N1-Cu1	115.01	Cu1-N1-H1	105.50

Cluster IV: [Cu₄OCl₆L⁴₄] (L⁴ = N,N-dimethylbenzylamine)

Table 5.37.: Crystal data and structure refinement for cluster IV.

Internal identification code	schindler13132
CCDC-no.	Not submitted.
Diffractometer type	BRUKER Nonius FR591 with Kappa CCD
Empirical formula	C ₃₆ H ₅₂ Cl ₆ Cu ₄ N ₄ O
Formula weight	1023.67
Temperature	190(2) K
Wavelength	0.71073 Å
Crystal system, space group	Monoclinic, <i>C</i> 2/ <i>c</i>
Unit cell dimensions	a = 52.733(11) Å $\alpha = 90^\circ$ b = 9.3290(19) Å $\beta = 97.50(3)^\circ$ c = 26.701(5) Å $\gamma = 90^\circ$
Volume	13023(5) Å ³
Z, Calculated density	12, 1.566 Mg/m ³
Absorption coefficient	2.335 mm ⁻¹
F(000)	6264
Habitus, color	Needle, orange
Crystal size	0.40 x 0.04 x 0.01 mm
Theta range for data collection	1.813 to 16.999°
Limiting indices	-43 ≤ h ≤ 42, -7 ≤ k ≤ 7, -6 ≤ l ≤ 21
Reflections collected / unique	3784 / 3784
Completeness to theta = 25.24	32.1%
Absorption correction	None
Refinement method	Full-matrix least-squares on F ²
Data / restraints / parameters	3784 / 0 / 632
Goodness-of-fit on F ²	1.081
Final R indices [I > 2σ(I)]	R1 = 0.0924, wR2 = 0.2167
R indices (all data)	R1 = 0.1677, wR2 = 0.2545
Largest diff. peak and hole	1.066 and -0.769 e. Å ⁻³

The refinement shows one and a half cluster molecule in the independent unit of the elementary cell. The C-H hydrogen atoms were positioned geometrically and refined isotropically. All non-hydrogen atoms were refined anisotropically, no absorption corrections were applied.

Symmetry transformations used to generate equivalent atoms:

a: -x,y,-z+1/2

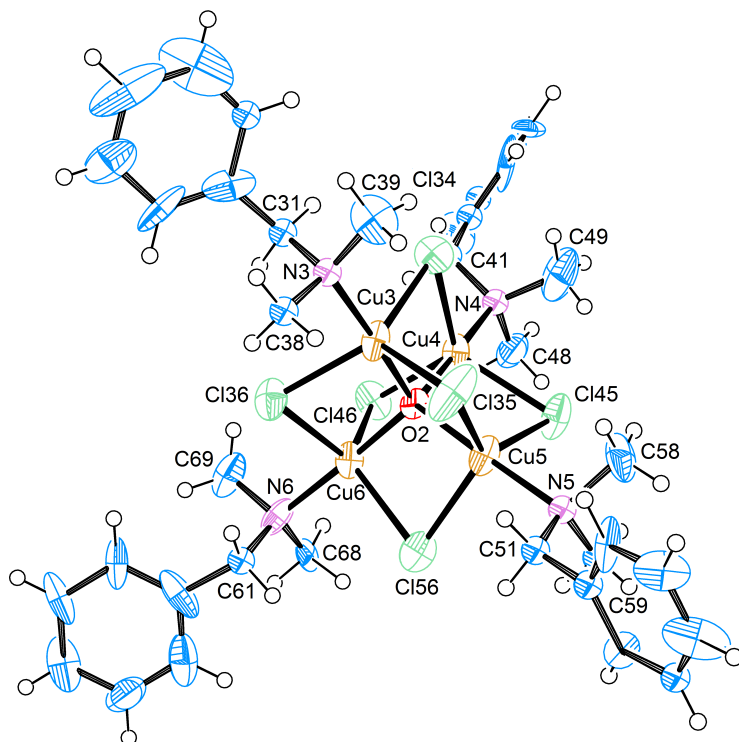


Figure 5.19.: ORTEP plot with thermal ellipsoids set at 50% probability shows the full cluster IV.

Table 5.38.: Selected bond lengths [\AA] and angles [$^\circ$] for cluster IV.

Cu3-O2	1.942	Cu3-N3	2.022	Cu3-Cl36	2.393
Cu3-Cl35	2.406	Cu3-Cl34	2.415	Cu4-O2	1.909
Cu4-N4	2.043	Cu4-Cl45	2.358	Cu4-Cl34	2.424
Cu4-Cl46	2.432	Cu5-O2	1.862	Cu5-N5	2.003
Cu5-Cl45	2.385	Cu5-Cl56	2.412	Cu5-Cl35	2.422
Cu6-O2	1.941	Cu6-N6	2.023	Cu6-Cl36	2.381

continue next page

Table 5.38.: Selected bond lengths [Å] and angles [°] for cluster IV. (*continuation*)

Cu6-Cl46	2.424	Cu6-Cl56	2.442	Cl11-Cu1 _a	2.382
Cl21-Cu2 _a	2.419	Cl22-Cu2 _a	2.383	O1-Cu2 _a	1.899
O1-Cu1 _a	1.920				
O2-Cu3-N3	176.2	O2-Cu3-Cl36	86.1	N3-Cu3-Cl36	97.3
O2-Cu3-Cl35	83.4	N3-Cu3-Cl35	93.5	Cl36-Cu3-Cl35	118.5
O2-Cu3-Cl34	85.2	N3-Cu3-Cl34	95.0	Cl36-Cu3-Cl34	110.5
Cl35-Cu3-Cl34	128.5	O2-Cu4-N4	177.6	O2-Cu4-Cl45	83.1
N4-Cu4-Cl45	94.5	O2-Cu4-Cl34	85.5	N4-Cu4-Cl34	95.9
Cl45-Cu4-Cl34	121.6	O2-Cu4-Cl46	85.2	N4-Cu4-Cl46	95.9
Cl45-Cu4-Cl46	119.7	Cl34-Cu4-Cl46	116.1	O2-Cu5-N5	177.2
O2-Cu5-Cl45	83.3	N5-Cu5-Cl45	97.5	O2-Cu5-Cl56	85.4
N5-Cu5-Cl56	96.4	Cl45-Cu5-Cl56	124.2	O2-Cu5-Cl35	84.5
N5-Cu5-Cl35	92.7	Cl45-Cu5-Cl35	112.1	Cl56-Cu5-Cl35	120.8
O2-Cu6-N6	178.1	O2-Cu6-Cl36	86.4	N6-Cu6-Cl36	94.5
O2-Cu6-Cl46	84.7	N6-Cu6-Cl46	93.4	Cl36-Cu6-Cl46	126.9
O2-Cu6-Cl56	82.9	N6-Cu6-Cl56	98.1	Cl36-Cu6-Cl56	121.4
Cl46-Cu6-Cl56	109.2	Cu3-Cl34-Cu4	80.2	Cu3-Cl35-Cu5	80.9
Cu6-Cl36-Cu3	81.1	Cu4-Cl45-Cu5	81.9	Cu6-Cl46-Cu4	80.3
Cu5-Cl56-Cu6	80.5	Cu5-O2-Cu4	111.0	Cu5-O2-Cu3	111.1
Cu4-O2-Cu3	108.3	Cu5-O2-Cu6	111.1	Cu4-O2-Cu6	108.7
Cu3-O2-Cu6	106.4	C31-N3-Cu3	105	C38-N3-Cu3	110
C39-N3-Cu3	117	C41-N4-Cu4	110	C49-N4-Cu4	107
C48-N4-Cu4	109	C58-N5-Cu5	110	C59-N5-Cu5	108
C51-N5-Cu5	114				

[CuL⁵₄]Cl₂ (L⁵ = cyclohexylamine)Table 5.39.: Crystal data and structure refinement for [CuL⁵₄]Cl₂.

Internal identification code	schindler13131
CCDC-no.	982989
Diffractometer type	BRUKER Nonius FR591 with Kappa CCD
Empirical formula	C ₂₄ H ₅₂ Cl ₂ CuN ₄
Formula weight	531.13
Temperature	190(2) K
Wavelength	0.71073 Å
Crystal system, space group	Tetragonal, $I\bar{4}$
Unit cell dimensions	a = 13.5360(19) Å $\alpha = 90^\circ$ b = 13.5360(19) Å $\beta = 90^\circ$ c = 15.966(3) Å $\gamma = 90^\circ$
Volume	2925.3(10) Å ³
Z, Calculated density	4, 1.206 Mg/m ³
Absorption coefficient	0.947 mm ⁻¹
F(000)	1148
Habitus, color	Block, blue
Crystal size	0.240 x 0.170 x 0.140 mm
Theta range for data collection	2.551 to 26.997°
Limiting indices	-17 ≤ h ≤ 12, -17 ≤ k ≤ 15, -17 ≤ l ≤ 20
Reflections collected / unique	10385 / 3181 [R(int) = 0.0665]
Completeness to theta = 25.24	99.9%
Absorption correction	Semiempirical
Max. and min. transmission	0.74922 and 0.59199
Refinement method	Full-matrix least-squares on F ²
Data / restraints / parameters	3181 / 0 / 141
Goodness-of-fit on F ²	0.992
Final R indices [I > 2σ(I)]	R1 = 0.0340, wR2 = 0.0645
R indices (all data)	R1 = 0.0443, wR2 = 0.0674
Absolute structure parameter	0.014(12)
Extinction coefficient	0.98
Largest diff. peak and hole	0.303 and -0.210 e. Å ⁻³

The structure was solved as twin (TWIN -1 0 0 0 1 0 0 0 -1, BASF 0.50008). The refinement shows one and a half of the molecule in the independent unit of the elementary cell. All hydrogen atoms were positioned geometrically and isotropically refined. All non-hydrogen atoms were refined anisotropically. Semiempirical absorption corrections were applied.

Symmetry transformations used to generate equivalent atoms:

a: $-x+1,-y,z$
 d: $-y+1,x-1,-z$

b: $-y+1/2,x-1/2,-z+1/2$
 e: $y+1,-x+1,-z$

c: $y+1/2,-x+1/2,-z+1/2$
 f: $-x+2,-y,z$

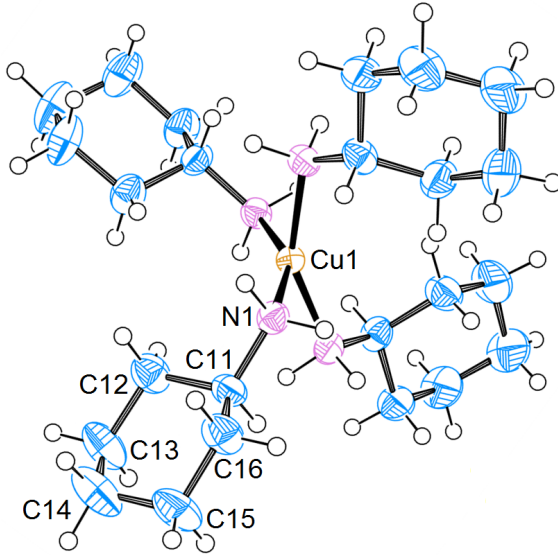


Figure 5.20.: ORTEP plot with thermal ellipsoids set at 50% probability shows $[\text{CuL}_5^4]\text{Cl}_2$. The chloride anions are not shown.

Table 5.40.: Selected bond lengths [\AA] and angles [$^\circ$] for $[\text{CuL}_5^4]\text{Cl}_2$.

Cu1-N1 _a	1.996	Cu1-N1 _b	1.996	Cu1-N1 _c	1.996
Cu1-N1	1.996	N1-C11	1.481	N1-H1A	0.990
N1 _a -Cu1-N1 _b	93.20	N1 _a -Cu1-N1 _c	93.20	N1 _b -Cu1-N1 _c	152.72
N1 _a -Cu1-N1	152.72	N1 _b -Cu1-N1	93.20	N1 _c -Cu1-N1	93.20
C11-N1-Cu1	117.13	Cu1-N1-H1A	108.00	Cu1-N1-H1B	108.00

Cluster VI: [Cu₄OCl₆L⁶₄] · 1.5 [CuL⁶₂Cl₂] (L⁶ = cyclohexanemethylamine)

Table 5.41.: Crystal data and structure refinement for cluster VI.

Internal identification code	schindler13130
CCDC-no.	982988
Diffractionmeter type	BRUKER Nonius FR591 with Kappa CCD
Empirical formula	C ₁₀₂ H ₂₁₆ Cl ₁₈ Cu ₁₁ N ₁₆ O ₂
Formula weight	3035.94
Temperature	190(2) K
Wavelength	0.71073 Å
Crystal system, space group	Triclinic, <i>P</i> $\bar{1}$
Unit cell dimensions	a = 14.304(3) Å α = 99.01(3) ° b = 14.622(3) Å β = 107.56(3) ° c = 17.938(4) Å γ = 95.63(3) °
Volume	3490.4(14) Å ³
Z, Calculated density	1, 1.444 Mg/m ³
Absorption coefficient	2.030 mm ⁻¹
F(000)	1581
Habitus, color	Block, green
Crystal size	0.120 x 0.100 x 0.050 mm
Theta range for data collection	1.511 to 25.407 °
Limiting indices	-17 ≤ h ≤ 17, -17 ≤ k ≤ 17, -21 ≤ l ≤ 21
Reflections collected / unique	52719 / 12632 [R(int) = 0.3066]
Completeness to theta = 25.24	99.0%
Absorption correction	Semiempirical
Max. and min. transmission	0.51804 and 0.37246
Refinement method	Full-matrix least-squares on F ²
Data / restraints / parameters	12632 / 0 / 675
Goodness-of-fit on F ²	1.014
Final R indices [I > 2σ(I)]	R1 = 0.0954, wR2 = 0.2253
R indices (all data)	R1 = 0.2388, wR2 = 0.2956
Extinction coefficient	2.09
Largest diff. peak and hole	0.734 and -0.780 e. Å ⁻³

The refinement shows one cluster, one acetonitrile solvent molecule and one and a half molecules of the connected [CuL⁶₂Cl₂] complex in the independent unit of the elementary cell. The C-H hydrogen atoms were positioned geometrically and refined isotropically. All non-hydrogen atoms were refined anisotropically, semiempirical absorption corrections were applied.

Symmetry transformations used to generate equivalent atoms:

a: -x+1,-y+1,-z

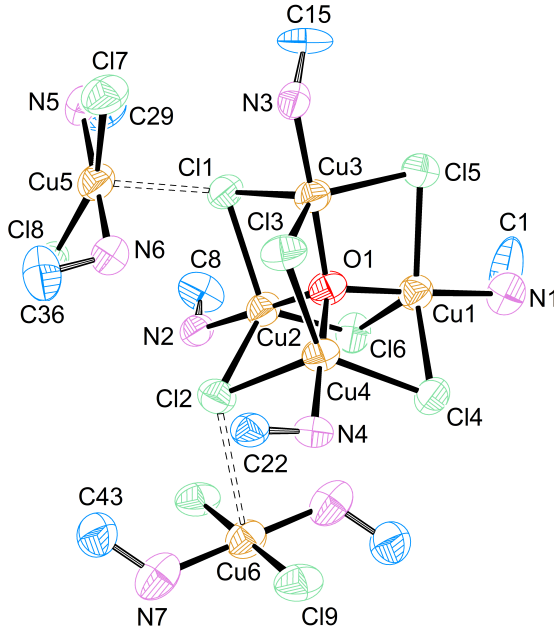


Figure 5.21.: ORTEP plot with thermal ellipsoids set at 50% probability shows the cluster molecule and two bridging complexes of cluster VI. Benzylic residues and H atoms are not shown for clarity.

Table 5.42.: Selected bond lengths [\AA] and angles [$^\circ$] for cluster VI.

Cu1-O1	1.903	Cu1-N1	1.950	Cu1-Cl5	2.379
Cu1-Cl4	2.397	Cu1-Cl1	2.446	Cl1-Cu2	2.456
Cl1-Cu5	2.645	O1-Cu4	1.884	O1-Cu3	1.887
O1-Cu2	1.896	Cu2-N2	1.957	Cu2-Cl6	2.344
Cu2-Cl2	2.442	Cl2-Cu3	2.470	Cu3-N3	1.971
Cu3-Cl3	2.387	Cu3-Cl5	2.399	Cl3-Cu4	2.419
Cu4-N4	1.964	Cu4-Cl4	2.394	Cu4-Cl6	2.481
Cu5-N6	1.955	Cu5-N5	1.972	Cu5-Cl8	2.290
Cu5-Cl7	2.327	Cu6-N7	1.952	Cu6-N7 _a	1.952
Cu6-Cl9	2.329	Cu6-Cl9 _a	2.329	Cu6-Cl2	3.020
Cu5-Cl1	2.645				

continue next page

5. Materials, Methods and Spectroscopy

Table 5.42.: Selected bond lengths [Å] and angles [°] for cluster VI. (*continuation*)

O1-Cu1-N1	176.7	O1-Cu1-Cl5	85.6	N1-Cu1-Cl5	91.2
O1-Cu1-Cl4	84.8	N1-Cu1-Cl4	97.9	Cl5-Cu1-Cl4	131.9
O1-Cu1-Cl1	84.6	N1-Cu1-Cl1	96.2	Cl5-Cu1-Cl1	118.8
Cl4-Cu1-Cl1	106.9	C1-N1-Cu1	119.3	Cu1-Cl1-Cu2	79.50
Cu1-Cl1-Cu5	113.6	Cu2-Cl1-Cu5	112.6	Cu4-O1-Cu3	109.6
Cu4-O1-Cu2	108.5	Cu3-O1-Cu2	110.0	Cu4-O1-Cu1	109.0
Cu3-O1-Cu1	108.4	Cu2-O1-Cu1	111.2	O1-Cu2-N2	176.2
O1-Cu2-Cl6	87.9	N2-Cu2-Cl6	95.7	O1-Cu2-Cl2	85.8
N2-Cu2-Cl2	91.2	Cl6-Cu2-Cl2	121.03	O1-Cu2-Cl1	84.4
N2-Cu2-Cl1	94.8	Cl6-Cu2-Cl1	120.8	Cl2-Cu2-Cl1	116.6
C8-N2-Cu2	114.9	Cu2-Cl2-Cu3	78.2	O1-Cu3-N3	178.0
O1-Cu3-Cl3	85.2	N3-Cu3-Cl3	93.8	O1-Cu3-Cl5	85.4
N3-Cu3-Cl5	96.6	Cl3-Cu3-Cl5	133.6	O1-Cu3-Cl2	85.2
N3-Cu3-Cl2	93.8	Cl3-Cu3-Cl2	116.3	Cl5-Cu3-Cl2	107.8
C15-N3-Cu3	116.4	Cu3-Cl3-Cu4	79.7	O1-Cu4-N4	177.6
O1-Cu4-Cl4	85.3	N4-Cu4-Cl4	92.8	O1-Cu4-Cl3	84.3
N4-Cu4-Cl3	96.1	Cl4-Cu4-Cl3	134.3	O1-Cu4-Cl6	84.2
N4-Cu4-Cl6	97.9	Cl4-Cu4-Cl6	118.7	Cl3-Cu4-Cl6	104.2
C22-N4-Cu4	114.8	Cu4-Cl4-Cu1	80.1	N6-Cu5-N5	174.1
N6-Cu5-Cl8	89.8	N5-Cu5-Cl8	94.9	N6-Cu5-Cl7	88.7
N5-Cu5-Cl7	85.7	Cl8-Cu5-Cl7	160.6	N6-Cu5-Cl1	90.9
N5-Cu5-Cl1	91.8	Cl8-Cu5-Cl1	99.1	Cl7-Cu5-Cl1	100.1
C29-N5-Cu5	119.7	Cu1-Cl5-Cu3	80.1	N7-Cu6-N7 _a	180.0
N7-Cu6-Cl9	87.8	N7 _a -Cu6-Cl9	92.2	N7-Cu6-Cl9 _a	92.2
N7 _a -Cu6-Cl9 _a	87.8	Cl9-Cu6-Cl9 _a	180.0	C36-N6-Cu5	111.6
Cu2-Cl6-Cu4	78.9	C43-N7-Cu6	122.0	Cl2-Cu6-Cu1	21.79
Cu5-Cl1-Cl2	85.40				

HL³Cl (L³ = N-methylbenzylamine)Table 5.43.: Crystal data and structure refinement for HL³Cl.

Internal identification code	schindler13119
CCDC-no.	Not submitted.
Diffractometer type	BRUKER Nonius FR591 with Kappa CCD
Empirical formula	C ₈ H ₁₂ ClN
Formula weight	157.64
Temperature	190(2) K
Wavelength	0.71073 Å
Crystal system, space group	Orthorhombic, <i>P c a</i> 2 ₁
Unit cell dimensions	a = 17.480(4) Å $\alpha = 90^\circ$ b = 4.9820(10) Å $\beta = 90^\circ$ c = 10.197(2) Å $\gamma = 90^\circ$
Volume	888.0(3) Å ³
Z, Calculated density	4, 1.179 Mg/m ³
Absorption coefficient	0.359 mm ⁻¹
F(000)	336
Habitus, color	Needle, colorless
Crystal size	1.300 x 0.200 x 0.070 mm
Theta range for data collection	3.070 to 27.503°
Limiting indices	-22 ≤ h ≤ 19, -5 ≤ k ≤ 6, -12 ≤ l ≤ 13
Reflections collected / unique	4950 / 1950 [R(int) = 0.0697]
Completeness to theta = 25.24	99.9%
Absorption correction	None
Refinement method	Full-matrix least-squares on F ²
Data / restraints / parameters	1950 / 1 / 100
Goodness-of-fit on F ²	1.025
Final R indices [I > 2σ(I)]	R1 = 0.0444, wR2 = 0.1090
R indices (all data)	R1 = 0.0617, wR2 = 0.1194
Absolute structure parameter	-0.25(11)
Largest diff. peak and hole	0.255 and -0.337 e. Å ⁻³

The refinement shows one molecule in the independent unit of the elementary cell. The N-H hydrogen atoms were found, the C-H hydrogen atoms were positioned geometrically and isotropically refined. All non-hydrogen atoms were refined anisotropically. No absorption corrections were applied.

5. Materials, Methods and Spectroscopy

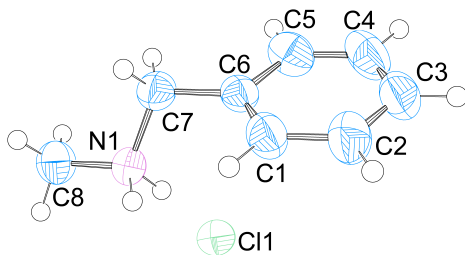


Figure 5.22.: ORTEP plot with thermal ellipsoids set at 50% probability shows the full molecule HL^3Cl .

Table 5.44.: Selected bond lengths [\AA] and angles [$^\circ$] for HL^3Cl .

N1-C7	1.481	N1-C8	1.482	C1-C6	1.364
C7-N1-C8	112.8	C6-C1-C2	121.3	C4-C3-C2	119.2

HL^4Cl ($\text{L}^4 = \text{N,N-dimethylbenzylamine}$)

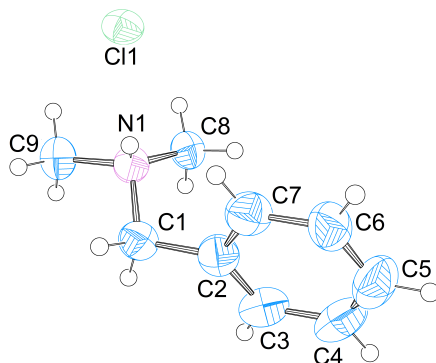
Table 5.45.: Crystal data and structure refinement for HL^4Cl .

Internal identification code	schindler12101
CCDC-no.	Not submitted.
Diffractometer type	BRUKER Nonius FR591 with Kappa CCD
Empirical formula	$\text{C}_9\text{H}_{14}\text{ClN}$
Formula weight	171.66
Temperature	190(2) K
Wavelength	0.71073 \AA
Crystal system, space group	Monoclinic, $P2_1/c$
Unit cell dimensions	$a = 9.941(2) \text{\AA}$ $\alpha = 90^\circ$ $b = 9.941(2) \text{\AA}$ $\beta = 91.23(3)^\circ$ $c = 19.994(4) \text{\AA}$ $\gamma = 90^\circ$
Volume	1975.4(7) \AA^3

continue next page

Table 5.45.: Crystal data and structure refinement for HL⁴Cl. (*continuation*)

Z, Calculated density	8, 1.154 Mg/m ³
Absorption coefficient	0.328 mm ⁻¹
F(000)	736
Habitus, color	Block, colorless
Crystal size	0.38 x 0.43 x 0.25 mm
Theta range for data collection	2.038 to 27.669 °
Limiting indices	-12 ≤ h ≤ 12, -12 ≤ k ≤ 12, 0 ≤ l ≤ 26
Reflections collected / unique	4509 / 4509 [R(int) = 0.1300]
Completeness to theta = 25.24	99.9%
Absorption correction	Semiempirical
Max. and min. transmission	0.92820 and 0.77384
Refinement method	Full-matrix least-squares on F ²
Data / restraints / parameters	4509 / 0 / 232
Goodness-of-fit on F ²	1.092
Final R indices [I > 2σ(I)]	R1 = 0.1002, wR2 = 0.2651
R indices (all data)	R1 = 0.1274, wR2 = 0.2798
Extinction coefficient	0.023(4)
Largest diff. peak and hole	0.675 and -0.868 e. Å ⁻³

Figure 5.23.: ORTEP plot with thermal ellipsoids set at 50% probability shows the full molecule HL⁴Cl.

The structure was solved as twin (TWIN -1 0 0 0 -1 0 0.086 0 1, BASF 0.33266). The refinement shows two molecules in the independent unit of

5. Materials, Methods and Spectroscopy

the elementary cell. The N-H hydrogen atoms were found, the rest was positioned geometrically and isotropically refined. All non-hydrogen atoms were refined anisotropically. Semiempirical absorption corrections were applied.

Table 5.46.: Selected bond lengths [Å] and angles [°] for HL⁴Cl.

C2-C7	1.384	C2-C3	1.387	C2-C1	1.488
C7-C2-C3	118.4	C2-C1-N1	113.6	C3-C2-C1	121.4

HL⁵Cl (L⁵ = cyclohexylamine)

Table 5.47.: Crystal data and structure refinement for HL⁵Cl.

Internal identification code	schindler12104
CCDC-no.	Not submitted.
Diffractometer type	BRUKER Nonius FR591 with Kappa CCD
Empirical formula	C ₆ H ₁₄ ClN
Formula weight	135.63
Temperature	190(2) K
Wavelength	0.71073 Å
Crystal system, space group	Orthorhombic, <i>P</i> <i>c</i> <i>a</i> 2 ₁
Unit cell dimensions	a = 9.2840(19) Å $\alpha = 90^\circ$ b = 11.302(2) Å $\beta = 90^\circ$ c = 7.4960(15) Å $\gamma = 90^\circ$
Volume	786.5(3) Å ³
Z, Calculated density	4, 1.145 Mg/m ³
Absorption coefficient	0.394 mm ⁻¹
F(000)	296
Habitus, color	Needle, colorless
Crystal size	0.48 x 0.08 x 0.15 mm
Theta range for data collection	2.839 to 27.513 °
Limiting indices	-11 ≤ h ≤ 12, -14 ≤ k ≤ 14, -8 ≤ l ≤ 9
Reflections collected / unique	5168 / 1482 [R(int) = 0.0935]
Completeness to theta = 25.24	99.7%
Absorption correction	None
Refinement method	Full-matrix least-squares on F ²
Data / restraints / parameters	1482 / 1 / 131
Goodness-of-fit on F ²	1.042

continue next page

Table 5.47.: Crystal data and structure refinement for HL⁵Cl. (*continuation*)

Final R indices [$I > 2\sigma(I)$]	R1 = 0.0408, wR2 = 0.0971
R indices (all data)	R1 = 0.0499, wR2 = 0.1026
Absolute structure parameter	0.15(15)
Largest diff. peak and hole	0.247 and -0.297 e. Å ⁻³

The structure was solved as inversion twin. The refinement shows one molecule in the independent unit of the elementary cell. The N-H hydrogen atoms were found, the rest was positioned geometrically and isotropically refined. All non-hydrogen atoms were refined anisotropically. No absorption corrections were applied.

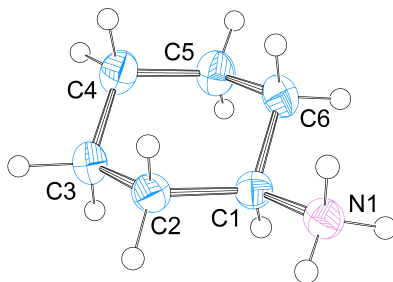


Figure 5.24.: ORTEP plot with thermal ellipsoids set at 50% probability shows the full molecule HL⁵Cl. The chloride anion is not shown.

Table 5.48.: Selected bond lengths [Å] and angles [°] for HL⁵Cl.

C1-N1	1.494	C1-C2	1.509	C1-C6	1.515
N1-C1-C2	110.4	N1-C1-C6	109.5	C2-C1-C6	112.5

Compound 7: [Cu(acetonitrile)₄][Cu₂Br₄]Table 5.49.: Crystal data and structure refinement for compound **7**.

Internal identification code	schindler13098
CCDC-no.	982983
Diffractometer type	BRUKER Nonius FR591 with Kappa CCD
Empirical formula	C ₈ H ₁₂ Br ₄ Cu ₃ N ₄
Formula weight	674.48
Temperature	190(2) K
Wavelength	0.71073 Å
Crystal system, space group	Tetragonal, <i>I</i> 4̄2 <i>m</i>
Unit cell dimensions	a = 12.6342(18) Å α = 90° b = 12.6342(18) Å β = 90° c = 5.5900(11) Å γ = 90°
Volume	892.3(3) Å ³
Z, Calculated density	2, 2.510 Mg/m ³
Absorption coefficient	12.489 mm ⁻¹
F(000)	630
Habitus, color	Block, green
Crystal size	0.450 x 0.100 x 0.070 mm
Theta range for data collection	3.225 to 27.378°
Limiting indices	-16 ≤ h ≤ 13, -16 ≤ k ≤ 15, -5 ≤ l ≤ 7
Reflections collected / unique	3542 / 544 [R(int) = 0.0843]
Completeness to theta = 25.24	99.6%
Absorption correction	Semiempirical
Max. and min. transmission	0.04725 and 0.01165
Refinement method	Full-matrix least-squares on F ²
Data / restraints / parameters	544 / 6 / 35
Goodness-of-fit on F ²	1.101
Final R indices [I > 2σ(I)]	R1 = 0.0307, wR2 = 0.0767
R indices (all data)	R1 = 0.0401, wR2 = 0.0809
Extinction coefficient	12.62
Absolute structure parameter	0.50(5)
Largest diff. peak and hole	0.542 and -0.609 e. Å ⁻³

The refinement shows a quarter of the complex molecule in the independent unit of the elementary cell. All hydrogen atoms were found and isotropically refined. All non-hydrogen atoms were refined anisotropically, semiempirical absorption corrections were applied.

Symmetry transformations used to generate equivalent atoms:

a: $-x+1, y, -z$ **b:** $y+1, -x+1, -z+1$ **c:** $-x+2, -y, z$
d: $-y+1, x-1, -z+1$ **e:** $y+1/2, -x+1/2, -z+1/2$ **f:** $-x+1, -y, z$
g: $-y+1/2, x-1/2, -z+1/2$ **h:** $-x+1, y, -z+1$

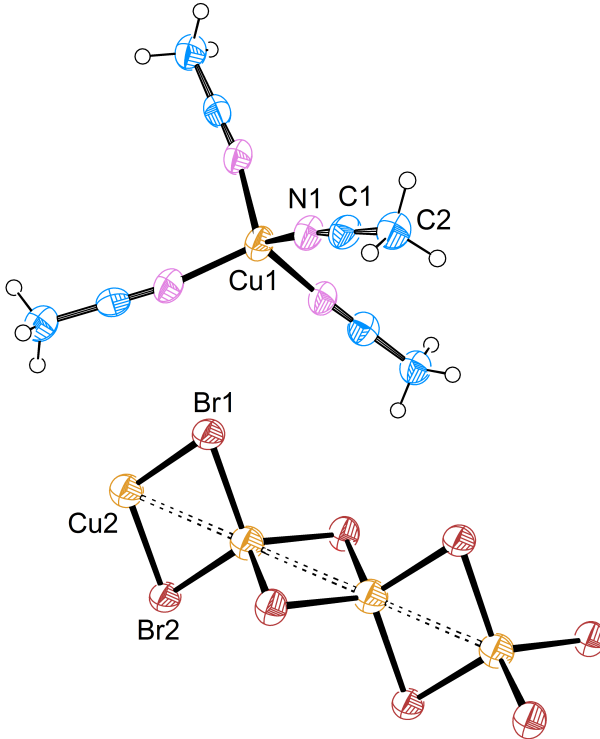


Figure 5.25.: ORTEP plot with thermal ellipsoids set at 50% probability shows a part of the linear $[\text{Cu}_2\text{Br}_4]$ -chain and the complex $[\text{Cu}(\text{acetonitrile})_4]^+$.

5. Materials, Methods and Spectroscopy

Table 5.50.: Selected bond lengths [Å] and angles [°] for compound **7**.

Br1-Cu2 _a	2.4	Br1-Cu2	2.4	Cu1-N1 _b	2.0
Cu1-N1 _c	2.0	Cu1-N1 _d	2.0	Cu1-N1	2.0
Cu2-Cu2 _h	2.8	Cu2-Cu2 _a	2.8		
Cu2 _a -Br1-Cu2	71	N1 _b -Cu1-N1 _c	113	N1 _b -Cu1-N1 _d	102
N1 _c -Cu1-N1 _d	113	N1 _b -Cu1-N1	113	N1 _c -Cu1-N1	102
N1 _d -Cu1-N1	113	Br1 _e -Cu2-Br1 _f	110	Br1 _e -Cu2-Br1 _g	109
Br1 _f -Cu2-Br1 _g	110	Br1 _e -Cu2-Br1	110	Br1 _f -Cu2-Br1	109
Br1 _g -Cu2-Br1	110	Br1 _e -Cu2-Cu2 _h	55	Br1 _f -Cu2-Cu2 _h	125
Br1 _g -Cu2-Cu2 _h	55	Br1-Cu2-Cu2 _h	125	Br1 _e -Cu2-Cu2 _a	125
Br1 _f -Cu2-Cu2 _a	55	Br1 _g -Cu2-Cu2 _a	125	Br1-Cu2-Cu2 _a	55
Cu2 _h -Cu2-Cu2 _a	180	C1-N1-Cu1	171		

Compound 8: [Cu(acetonitrile)Br]

Table 5.51.: Crystal data and structure refinement for compound **8**.

Internal identification code	schindler13124
CCDC-no.	982986
Diffractometer type	BRUKER Nonius FR591 with Kappa CCD
Empirical formula	C ₂ H ₃ BrCuN
Formula weight	184.50
Temperature	190(2) K
Wavelength	0.71073 Å
Crystal system, space group	Orthorhombic, <i>P n m a</i>
Unit cell dimensions	a = 8.6370(17) Å $\alpha = 90^\circ$ b = 4.0160(8) Å $\beta = 90^\circ$ c = 12.897(3) Å $\gamma = 90^\circ$
Volume	447.35(15) Å ³
Z, Calculated density	4, 2.739 Mg/m ³
Absorption coefficient	13.613 mm ⁻¹
F(000)	344
Habitus, color	Block, colorless
Crystal size	0.100 x 0.070 x 0.050 mm
Theta range for data collection	2.838 to 27.515 °
Limiting indices	-10 ≤ h ≤ 11, -5 ≤ k ≤ 4, -16 ≤ l ≤ 15
Reflections collected / unique	3710 / 585 [R(int) = 0.0766]

continue next page

Table 5.51.: Crystal data and structure refinement for compound **8**. (*continuation*)

Completeness to theta = 25.24	100.0%
Absorption correction	Semiempirical
Max. and min. transmission	0.03175 and 0.00914
Refinement method	Full-matrix least-squares on F ²
Data / restraints / parameters	585 / 0 / 32
Goodness-of-fit on F ²	1.075
Final R indices [I > 2σ(I)]	R1 = 0.0264, wR2 = 0.0569
R indices (all data)	R1 = 0.0346, wR2 = 0.0591
Extinction coefficient	13.79
Largest diff. peak and hole	0.384 and -0.466 e. Å ⁻³

The refinement shows one molecule in the independent unit of the elementary cell. All hydrogen atoms were positioned geometrically and isotropically refined. All non-hydrogen atoms were refined anisotropically, semiempirical absorption corrections were applied.

Symmetry transformations used to generate equivalent atoms:

a: $-x, -y, -z + 1$ **b:** $-x, -y + 1, -z + 1$

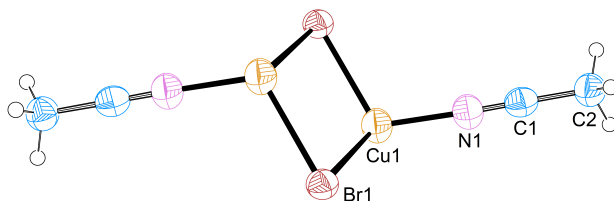


Figure 5.26.: ORTEP plot with thermal ellipsoids set at 50% probability shows a part of the linear chain, compound **8** forms.

5. Materials, Methods and Spectroscopy

Table 5.52.: Selected bond lengths [Å] and angles [°] for compound **8**.

Br1-Cu2	2.499	Br1-Cu2 _a	2.504	Br1-Cu2 _a	2.504
Cu2-Br1 _a	2.504	Cu2-Br1 _b	2.504	Cu2-Cu2 _a	3.055
Cu2-Br1-Cu2 _a	75.28	Cu2-Br1-Cu2 _b	75.28	Cu2 _a -Br1-Cu2 _b	106.59
C1-N1-Cu2	176.24	N1-Cu2-Br1	116.82	N1-Cu2-Br1 _a	111.60

Compound 9: [Cu(acetonitrile)Br₂]

Table 5.53.: Crystal data and structure refinement for compound **9**.

Internal identification code	schindler13122
CCDC-no.	982985
Diffractometer type	BRUKER Nonius FR591 with Kappa CCD
Empirical formula	C ₂ H ₃ Br ₂ CuN
Formula weight	264.41
Temperature	190(2) K
Wavelength	0.71073 Å
Crystal system, space group	Orthorhombic, <i>I m m a</i>
Unit cell dimensions	a = 9.758(2) Å $\alpha = 90^\circ$ b = 6.9750(14) Å $\beta = 90^\circ$ c = 8.2480(16) Å $\gamma = 90^\circ$
Volume	561.38(19) Å ³
Z, Calculated density	4, 3.129 Mg/m ³
Absorption coefficient	17.973 mm ⁻¹
F(000)	484
Habitus, color	Block, red
Crystal size	0.150 x 0.060 x 0.050 mm
Theta range for data collection	3.234 to 27.433 °
Limiting indices	-12 ≤ h ≤ 11, -9 ≤ k ≤ 9, -9 ≤ l ≤ 10
Reflections collected / unique	2256 / 369 [R(int) = 0.1154]
Completeness to theta = 25.24	100.0%
Absorption correction	None
Refinement method	Full-matrix least-squares on F ²
Data / restraints / parameters	369 / 0 / 24
Goodness-of-fit on F ²	1.099
Final R indices [I > 2σ(I)]	R1 = 0.0465, wR2 = 0.1089
R indices (all data)	R1 = 0.0478, wR2 = 0.1097
Largest diff. peak and hole	2.138 and -1.780 e. Å ⁻³

The refinement shows one molecule in the independent unit of the elementary cell. All hydrogen atoms were positioned geometrically and isotropically refined. All non-hydrogen atoms were refined anisotropically. No absorption corrections were applied.

Symmetry transformations used to generate equivalent atoms:

a: $-x,-y+1,-z$ **b:** $-x,-y+1/2,z$ **c:** $3x,y-1/2,-z$

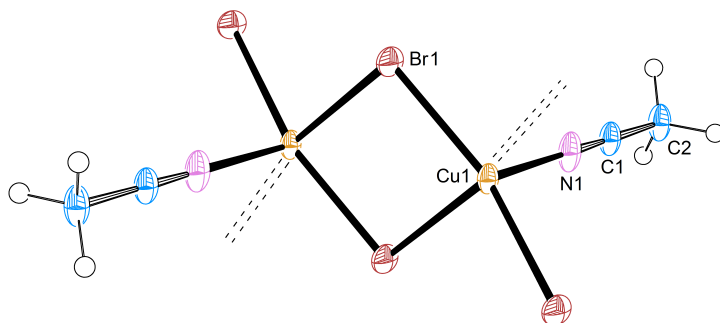


Figure 5.27.: ORTEP plot with thermal ellipsoids set at 50% probability shows a part of the linear chain, compound **9** forms.

Table 5.54.: Selected bond lengths [\AA] and angles [$^\circ$] for compound **9**.

Br1-Cu1	2.433	Br1-Cu1 _a	2.433	Cu1-N1	2.154
Cu1-Br1 _b	2.433	Cu1-Br1 _c	2.433	Cu1-Br1 _a	2.433
Cu1-Br1-Cu1 _a	94.68	N1-Cu1-Br1 _b	99.53	N1-Cu1-Br1 _d	99.53

Compound 10: [CuCl₂] · H₂O · 0.5 acetoneTable 5.55.: Crystal data and structure refinement for compound **10**.

Internal identification code	schindler13114
CCDC-no.	Not submitted.
Diffractometer type	BRUKER Nonius FR591 with Kappa CCD
Empirical formula	C _{1.50} H ₅ Cl ₂ CuO _{1.50}
Formula weight	181.49
Temperature	190(2) K
Wavelength	0.71073 Å
Crystal system, space group	Monoclinic, <i>C2/m</i>
Unit cell dimensions	a = 17.836(4) Å $\alpha = 90^\circ$ b = 3.2840(10) Å $\beta = 93.88(3)^\circ$ c = 9.593(2) Å $\gamma = 90^\circ$
Volume	560.6(2) Å ³
Z, Calculated density	4, 2.150 Mg/m ³
Absorption coefficient	4.713 mm ⁻¹
F(000)	356
Habitus, color	Needle, orange
Crystal size	0.500 x 0.030 x 0.010 mm
Theta range for data collection	2.128 to 24.976°
Limiting indices	-20 ≤ h ≤ 19, -3 ≤ k ≤ 3, -11 ≤ l ≤ 11
Reflections collected / unique	1775 / 580 [R(int) = 0.1467]
Completeness to theta = 25.24	96.8%
Absorption correction	None
Refinement method	Full-matrix least-squares on F ²
Data / restraints / parameters	580 / 4 / 53
Goodness-of-fit on F ²	1.129
Final R indices [I > 2σ(I)]	R1 = 0.0668, wR2 = 0.1599
R indices (all data)	R1 = 0.0819, wR2 = 0.1683
Largest diff. peak and hole	1.312 and -0.828 e. Å ⁻³

The refinement shows half of the complex molecule in the independent unit of the elementary cell. All hydrogen atoms were found and isotropically refined. All non-hydrogen atoms were refined anisotropically, no absorption corrections were applied.

Symmetry transformations used to generate equivalent atoms:

a: x,y-1,z **b:** x,y+1,z **c:** x,-y+1,z

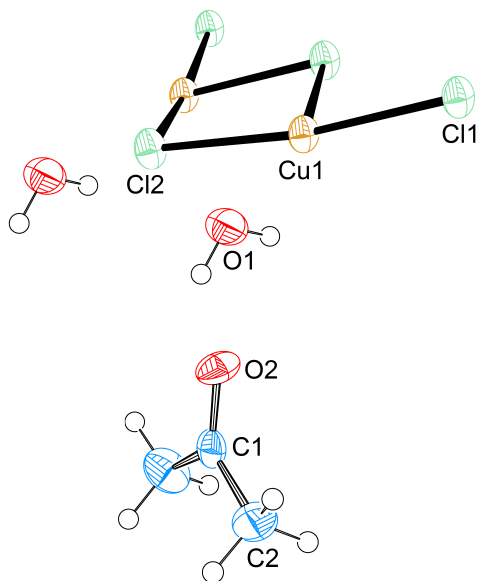


Figure 5.28.: ORTEP plot with thermal ellipsoids set at 50 % probability shows the full compound **10**.

Table 5.56.: Selected bond lengths [\AA] and angles [$^\circ$] for compound **10**.

Cu1-Cl2 _a	2.276	Cu1-Cl2	2.276	Cu1-Cl1	2.282
Cu1-Cl1 _a	2.282	Cu1-O1	2.287	Cl1-Cu1 _b	2.282
Cl2 _a -Cu1-Cl2	92.32	Cl2 _a -Cu1-Cl1	171.93	Cl2-Cu1-Cl1	87.26
Cl2 _a -Cu1-Cl1 _a	87.26	Cl2-Cu1-Cl1 _a	171.93	Cl1-Cu1-Cl1 _a	92.03
Cl2 _a -Cu1-O1	94.68	Cl2-Cu1-O1	94.68	Cl1-Cu1-O1	93.38
Cl1 _a -Cu1-O1	93.38	Cu1-Cl1-Cu1 _b	92.03	Cu1 _b -Cl2-Cu1	92.32
Cu1-O1-H1	127.0	Cu1-O1-H2	128.0		

Compound 11: [Cu₃(acetonitrile)₂Cl₆]

Table 5.57.: Crystal data and structure refinement for compound 11.

Internal identification code	schindler12106
CCDC-no.	982980
Diffractometer type	BRUKER Nonius FR591 with Kappa CCD
Empirical formula	C ₄ H ₆ Cl ₆ Cu ₃ N ₂
Formula weight	485.43
Temperature	190(2) K
Wavelength	0.71073 Å
Crystal system, space group	Monoclinic, <i>P</i> 2 ₁ / <i>c</i>
Unit cell dimensions	a = 6.737(2) Å α = 90° b = 6.1293(15) Å β = 105.91(3)° ° c = 16.438(6) Å γ = 90°
Volume	652.8(4) Å ³
Z, Calculated density	2, 2.470 Mg/m ³
Absorption coefficient	6.035 mm ⁻¹
F(000)	466
Habitus, color	Block, red
Crystal size	0.40 x 0.40 x 0.20 mm
Theta range for data collection	3.144 to 27.594°
Limiting indices	-8 ≤ h ≤ 8, -7 ≤ k ≤ 7, -21 ≤ l ≤ 20
Reflections collected / unique	10874 / 1496 [R(int) = 0.1203]
Completeness to theta = 25.24	99.9%
Absorption correction	None
Refinement method	Full-matrix least-squares on F ²
Data / restraints / parameters	1496 / 0 / 72
Goodness-of-fit on F ²	1.104
Final R indices [I > 2σ(I)]	R1 = 0.0353, wR2 = 0.0879
R indices (all data)	R1 = 0.0395, wR2 = 0.0904
Largest diff. peak and hole	0.858 and -1.306 e. Å ⁻³

The refinement shows half the molecule in the independent unit of the elementary cell. All hydrogen atoms were positioned geometrically and isotropically refined. All non-hydrogen atoms were refined anisotropically. No absorption corrections were applied.

Symmetry transformations used to generate equivalent atoms:

a: -x,-y+2,-z **b:** -x+1,-y+3,-z

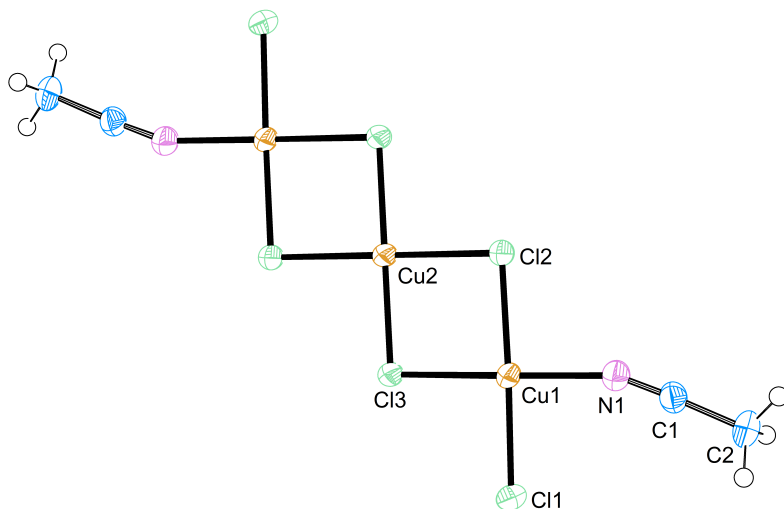


Figure 5.29.: ORTEP plot with thermal ellipsoids set at 50% probability shows the full compound **11**.

Table 5.58.: Selected bond lengths [\AA] and angles [$^\circ$] for compound **11**.

Cu1-N1	1.993	Cu1-Cl1	2.262	Cu1-Cl3	2.299
Cu1-Cl2	2.300	Cu1-Cl1 _a	2.699	Cu2-Cl3	2.265
Cu2-Cl3 _b	2.265	Cu2-Cl2 _b	2.282	Cu2-Cl2	2.282
Cl1-Cu1 _a	2.699				
<hr/>					
N1-Cu1-Cl1	89.06	N1-Cu1-Cl3	170.84	Cl1-Cu1-Cl3	91.14
N1-Cu1-Cl2	93.46	Cl1-Cu1-Cl2	173.67	Cl3-Cu1-Cl2	85.45
N1-Cu1-Cl1 _a	89.03	Cl1-Cu1-Cl1 _a	92.17	Cl3-Cu1-Cl1 _a	100.12
Cl2-Cu1-Cl1 _a	93.68	Cl3-Cu2-Cl3 _b	180.00	Cl3-Cu2-Cl2 _b	93.35
Cl3 _b -Cu2-Cl2 _b	86.65	Cl3-Cu2-Cl2	86.65	Cl3 _b -Cu2-Cl2	93.35
Cl2 _b -Cu2-Cl2	180.00	Cu1-Cl1-Cu1 _a	87.83	Cu2-Cl2-Cu1	93.70
Cu2-Cl3-Cu1	94.19	C1-N1-Cu1	159.03		

Compound 12: [Cu₂(acetonitrile)₂Cl₄]Table 5.59.: Crystal data and structure refinement for compound **12**.

Internal identification code	schindler12109
CCDC-no.	Not submitted.
Diffractionmeter type	BRUKER Nonius FR591 with Kappa CCD
Empirical formula	C ₄ H ₆ Cl ₄ Cu ₂ N ₂
Formula weight	350.99
Temperature	190(2) K
Wavelength	0.71073 Å
Crystal system, space group	Monoclinic, <i>P</i> 2 ₁ / <i>c</i>
Unit cell dimensions	a = 3.7990(8) Å α = 90° b = 7.9080(16) Å β = 89.94(3)° c = 18.075(4) Å γ = 90°
Volume	543.02(19) Å ³
Z, Calculated density	2, 2.147 Mg/m ³
Absorption coefficient	4.847 mm ⁻¹
F(000)	340
Habitus, color	Needle, yellow
Crystal size	0.750 x 0.050 x 0.020 mm
Theta range for data collection	2.576 to 27.574°
Limiting indices	-4 ≤ h ≤ 4, -10 ≤ k ≤ 7, -22 ≤ l ≤ 23
Reflections collected / unique	3334 / 1213 [R(int) = 0.1491]
Completeness to theta = 25.24	99.5%
Absorption correction	Semiempirical
Max. and min. transmission	0.49496 and 0.11067
Refinement method	Full-matrix least-squares on F ²
Data / restraints / parameters	1213 / 0 / 57
Goodness-of-fit on F ²	1.041
Final R indices [I > 2σ(I)]	R1 = 0.0747, wR2 = 0.1936
R indices (all data)	R1 = 0.0959, wR2 = 0.2093
Extinction coefficient	4.98
Largest diff. peak and hole	1.877 and -1.361 e. Å ⁻³

The structure was solved as twin (TWIN 1 0 0 0 -1 0 0 0 1, BASF 0.45521). The refinement shows half of the complex molecule in the independent unit of the elementary cell. All hydrogen atoms were positioned geometrically and isotropically refined. All non-hydrogen atoms were refined anisotropically, semiempirical absorption corrections were applied.

Symmetry transformations used to generate equivalent atoms:

a: -x+1,-y+1,-z+1

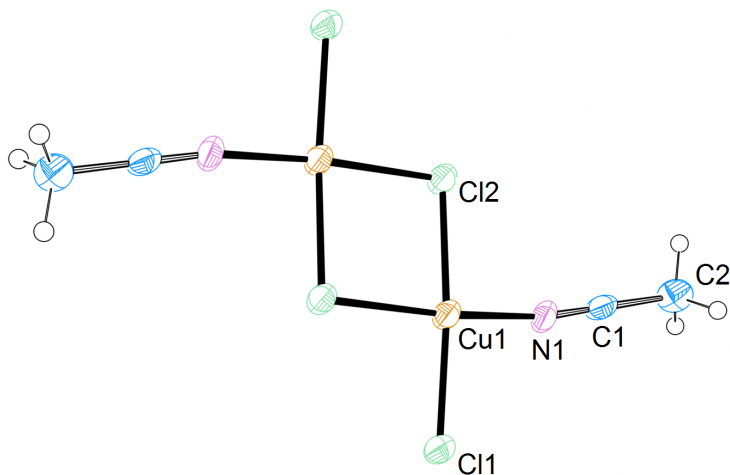


Figure 5.30.: ORTEP plot with thermal ellipsoids set at 50% probability shows the full compound **12**.

Table 5.60.: Selected bond lengths [Å] and angles [°] for compound **12**.

Cu1-N1	1.967	Cu1-Cl2	2.236	Cu1-Cl1	2.293
Cu1-Cl1 _a	2.310	Cl1-Cu1 _a	2.310	N1-C1	1.133
C1-C2	1.467	C2-H2A	0.980	C2-H2B	0.980
C2-H2C	0.980				
<hr/>					
N1-Cu1-Cl2	93.1	N1-Cu1-Cl1	172.6	Cl2-Cu1-Cl1	92.4
N1-Cu1-Cl1 _a	88.3	Cl2-Cu1-Cl1 _a	172.8	Cl1-Cu1-Cl1 _a	85.5
Cu1-Cl1-Cu1 _a	94.4	C1-N1-Cu1	168.0	N1-C1-C2	178.8
C1-C2-H2A	109.5	C1-C2-H2B	109.5	H2A-C2-H2B	109.5
C1-C2-H2C	109.5	H2A-C2-H2C	109.5	H2B-C2-H2C	109.5

Compound 13: (H₂N(CH₃)₂)₂[CuCl₃]Table 5.61.: Crystal data and structure refinement for compound **13**.

Internal identification code	schindler12113
CCDC-no.	982981
Diffractometer type	BRUKER Nonius FR591 with Kappa CCD
Empirical formula	C ₄ H ₁₆ Cl ₃ CuN ₂
Formula weight	262.08
Temperature	190(2) K
Wavelength	0.71073 Å
Crystal system, space group	Triclinic, <i>P</i> $\bar{1}$
Unit cell dimensions	a = 7.2930(15) Å α = 113.14(3) ° b = 9.0060(18) Å β = 100.38(3) ° c = 9.6850(19) Å γ = 100.33(3) °
Volume	552.97(19) Å ³
Z, Calculated density	2, 1.574 Mg/m ³
Absorption coefficient	2.644 mm ⁻¹
F(000)	268
Habitus, color	Block, green
Crystal size	0.70 x 0.45 x 0.25 mm
Theta range for data collection	2.38 to 27.48 °
Limiting indices	-9 ≤ h ≤ 9, -10 ≤ k ≤ 11, -12 ≤ l ≤ 12
Reflections collected / unique	8233 / 2526 [R(int) = 0.1702]
Completeness to theta = 27.48	99.2%
Absorption correction	None
Refinement method	Full-matrix least-squares on F ²
Data / restraints / parameters	2526 / 0 / 155
Goodness-of-fit on F ²	1.052
Final R indices [I > 2σ(I)]	R1 = 0.0494, wR2 = 0.1294
R indices (all data)	R1 = 0.0555, wR2 = 0.1350
Largest diff. peak and hole	0.818 and -1.368 e. Å ⁻³

The refinement shows one molecule in the independent unit of the elementary cell. All hydrogen atoms were found and isotropically refined. All non-hydrogen atoms were refined anisotropically. No absorption corrections were applied.

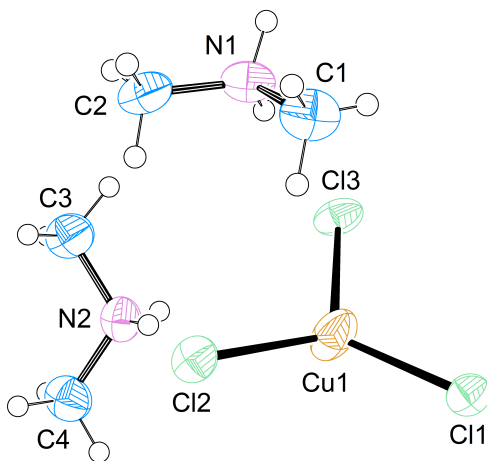


Figure 5.31.: ORTEP plot with thermal ellipsoids set at 50% probability shows the full compound **13**.

Table 5.62.: Selected bond lengths [\AA] and angles [$^\circ$] for compound **13**.

Cl1-Cu1	2.273	Cl2-Cu1	2.281	Cl3-Cu1	2.266
C1-N1	1.466	C2-N1	1.480	C3-N2	1.462
C4-N2	1.471				
Cl3-Cu1-Cl1	115.37	Cl3-Cu1-Cl2	117.39	Cl1-Cu1-Cl2	122.11
C1-N1-C2	114.23	C3-N2-C4	112.93		

Compound 14: [Cu(dmsO)₂Cl₂]

Table 5.63.: Crystal data and structure refinement for compound 14.

Internal identification code	schindler13080
CCDC-no.	Not submitted.
Diffractometer type	BRUKER Nonius FR591 with Kappa CCD
Empirical formula	C ₄ H ₁₂ Cl ₂ CuO ₂ S ₂
Formula weight	290.70
Temperature	190(2) K
Wavelength	0.71073 Å
Crystal system, space group	Orthorhombic, <i>P n m a</i>
Unit cell dimensions	a = 7.9620(16) Å $\alpha = 90^\circ$ b = 11.483(2) Å $\beta = 90^\circ$ c = 11.325(2) Å $\gamma = 90^\circ$
Volume	1035.4(4) Å ³
Z, Calculated density	4, 1.865 Mg/m ³
Absorption coefficient	2.982 mm ⁻¹
F(000)	588
Habitus, color	Plate, green
Crystal size	0.700 x 0.300 x 0.080 mm
Theta range for data collection	2.526 to 27.516 °
Limiting indices	-8 ≤ h ≤ 10, -12 ≤ k ≤ 14, -12 ≤ l ≤ 14
Reflections collected / unique	4783 / 1249 [R(int) = 0.0868]
Completeness to theta = 25.24	99.9%
Absorption correction	None
Refinement method	Full-matrix least-squares on F ²
Data / restraints / parameters	1249 / 0 / 57
Goodness-of-fit on F ²	1.054
Final R indices [I > 2σ(I)]	R1 = 0.0451, wR2 = 0.1162
R indices (all data)	R1 = 0.0508, wR2 = 0.1205
Largest diff. peak and hole	0.992 and -1.459 e. Å ⁻³

The refinement shows half the molecule in the independent unit of the elementary cell. All hydrogen atoms were positioned geometrically and isotropically refined. All non-hydrogen atoms were refined anisotropically, no absorption corrections were applied.

Symmetry transformations used to generate equivalent atoms:

a: x,-y+3/2,z **b:** x+1/2,y,-z+1/2 **c:** x-1/2,y,-z+1/2

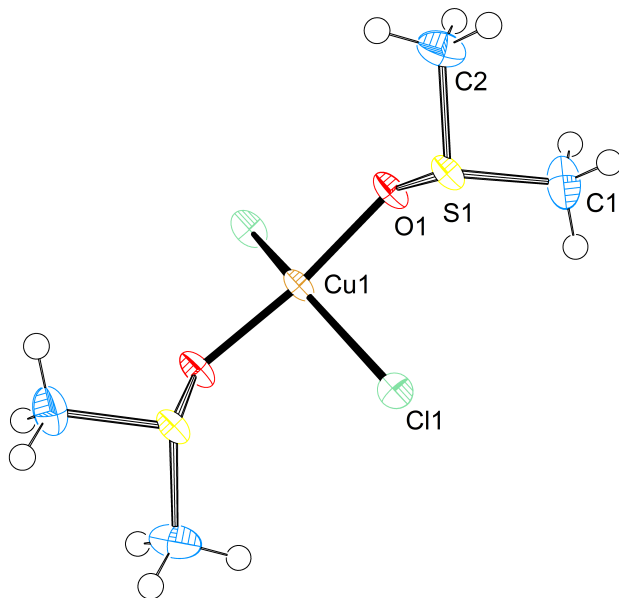


Figure 5.32.: ORTEP plot with thermal ellipsoids set at 65% probability shows the full compound **14**.

Table 5.64.: Selected bond lengths [Å] and angles [°] for compound **14**.

Cu1-O1	1.956	Cu1-O1 _a	1.956	Cu1-Cl1	2.281
Cu1-Cl2	2.286	Cu1-Cl2 _b	2.666	Cl2-Cu1 _{I''}	2.666
O1-Cu1-O1 _a	173.63	O1-Cu1-Cl1	92.76	O1 _a -Cu1-Cl1	92.75
O1-Cu1-Cl2	88.59	O1 _a -Cu1-Cl2	88.60	Cl1-Cu1-Cl2	146.26
O1-Cu1-Cl2 _b	87.90	O1 _a -Cu1-Cl2 _c	87.90	Cl1-Cu1-Cl2 _b	101.27
Cl2-Cu1-Cl2 _b	112.47	Cu1-Cl2-Cu1 _c	143.99		

Cluster I recrystallized

Table 5.65.: Crystal data and structure refinement for cluster I recrystallized.

Internal identification code	schindler13081
CCDC-no.	982982
Diffractometer type	BRUKER Nonius FR591 with Kappa CCD
Empirical formula	C ₄₂ H ₅₄ Cl ₈ Cu ₅ N ₆ O
Formula weight	1260.21
Temperature	190(2) K
Wavelength	0.71073 Å
Crystal system, space group	Triclinic, <i>P</i> $\bar{1}$
Unit cell dimensions	a = 13.546(3) Å α = 71.53(3)° b = 13.911(3) Å β = 75.00(3)° c = 16.018(3) Å γ = 66.21(3)°
Volume	2589.6(12) Å ³
Z, Calculated density	2, 1.616 Mg/m ³
Absorption coefficient	2.471 mm ⁻¹
F(000)	1274
Habitus, color	Needle, green
Crystal size	1.00 x 0.13 x 0.10 mm
Theta range for data collection	1.356 to 27.543°
Limiting indices	-17 ≤ h ≤ 17, -18 ≤ k ≤ 16, -20 ≤ l ≤ 20
Reflections collected / unique	48215 / 11891 [R(int) = 0.1427]
Completeness to theta = 25.24	99.9%
Absorption correction	None
Refinement method	Full-matrix least-squares on F ²
Data / restraints / parameters	11891 / 0 / 663
Goodness-of-fit on F ²	0.929
Final R indices [I > 2σ(I)]	R1 = 0.0478, wR2 = 0.1244
R indices (all data)	R1 = 0.0861, wR2 = 0.1454
Largest diff. peak and hole	1.376 and -0.785 e. Å ⁻³

The refinement shows one cluster and one complex molecule in the independent unit of the elementary cell. One benzylic residue at the cluster is disordered in two positions (50:50). The N-H hydrogen atoms were found and all C-H hydrogen atoms were positioned geometrically and refined isotropically. All non-hydrogen atoms were refined anisotropically, semiempirical absorption corrections were applied.

Symmetry transformations used to generate equivalent atoms:

a: -x,-y+2,-z+1 **b:** -x,-y+1,-z+1

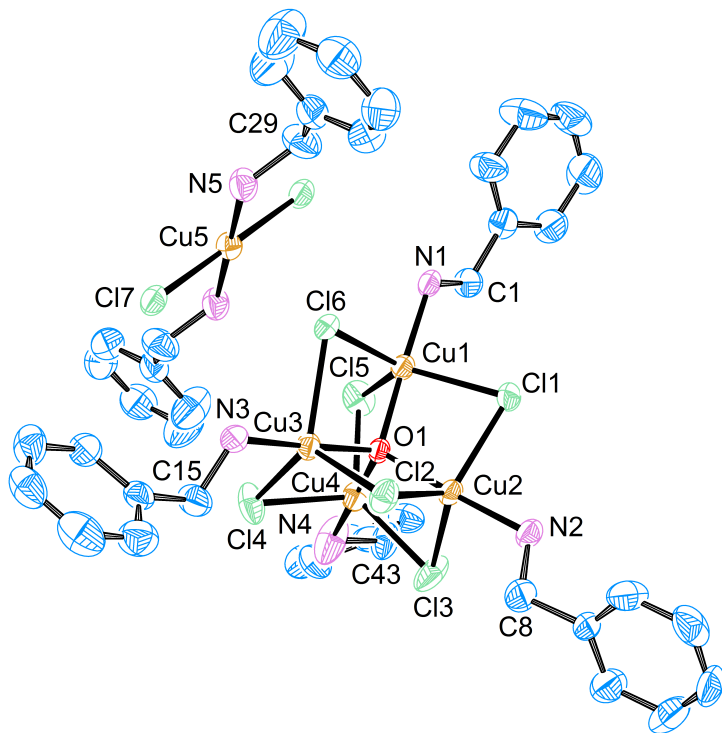


Figure 5.33.: ORTEP plot with thermal ellipsoids set at 50% probability shows the cluster molecule and the bridging complex of cluster I recrystallized. H atoms and disorder are not shown.

Table 5.66.: Selected bond lengths [\AA] and angles [$^\circ$] for cluster I recrystallized.

Cu1-O1	1.896	Cu1-N1	1.960	Cu1-Cl1	2.382
Cu1-Cl6	2.395	Cu1-Cl5	2.407	Cl1-Cu2	2.414
Cu2-O1	1.893	Cu2-N2	1.959	Cu2-Cl3	2.357
Cu2-Cl2	2.467	Cl2-Cu3	2.419	Cu3-O1	1.901
Cu3-N3	1.945	Cu3-Cl4	2.372	Cu3-Cl6	2.414

continue next page

5. Materials, Methods and Spectroscopy

Table 5.66.: Selected bond lengths [Å] and angles [°] for cluster I recrystallized.
(*continuation*)

C13-Cu4	2.448	Cu4-O1	1.890	Cu4-N4	1.966
Cu4-Cl4	2.387	Cu4-Cl5	2.388	Cu4-H4D	2.1
N5-Cu5	1.984	Cu5-N5 _a	1.984	Cu5-Cl7	2.306
Cu5-Cl7 _a	2.306	Cu6-N6	2.000	Cu6-N6 _b	2.000
Cu6-Cl8	2.343	Cu6-Cl8 _b	2.343		
O1-Cu1-N1	177.36	O1-Cu1-Cl1	85.84	N1-Cu1-Cl1	95.59
O1-Cu1-Cl6	84.86	N1-Cu1-Cl6	92.49	Cl1-Cu1-Cl6	120.86
O1-Cu1-Cl5	84.50	N1-Cu1-Cl5	96.78	Cl1-Cu1-Cl5	117.12
Cl6-Cu1-Cl5	119.83	C1-N1-Cu1	117.53	Cu1-N1-H61	109
Cu1-N1-H60	98	Cu1-Cl1-Cu2	80.02	O1-Cu2-N2	177.18
O1-Cu2-Cl3	86.13	N2-Cu2-Cl3	96.64	O1-Cu2-Cl1	84.99
N2-Cu2-Cl1	93.80	Cl3-Cu2-Cl1	125.11	O1-Cu2-Cl2	84.37
N2-Cu2-Cl2	93.64	Cl3-Cu2-Cl2	123.42	Cl1-Cu2-Cl2	109.38
C8-N2-Cu2	115.83	Cu2-N2-H1	108	Cu2-N2-H2	104
Cu3-Cl2-Cu2	79.13	O1-Cu3-N3	177.45	O1-Cu3-Cl4	85.16
N3-Cu3-Cl4	97.13	O1-Cu3-Cl6	84.22	N3-Cu3-Cl6	93.52
Cl4-Cu3-Cl6	125.39	O1-Cu3-Cl2	85.54	N3-Cu3-Cl2	94.44
Cl4-Cu3-Cl2	115.89	Cl6-Cu3-Cl2	116.41	C15-N3-Cu3	115.73
Cu3-N3-H57	108	Cu3-N3-H566	104	Cu2-Cl3-Cu4	80.23
O1-Cu4-N4	178.73	O1-Cu4-Cl4	84.97	N4-Cu4-Cl4	93.83
O1-Cu4-Cl5	85.18	N4-Cu4-Cl5	95.82	Cl4-Cu4-Cl5	136.05
O1-Cu4-Cl3	83.61	N4-Cu4-Cl3	96.72	Cl4-Cu4-Cl3	106.76
Cl5-Cu4-Cl3	114.51	O1-Cu4-H4D	157	N4-Cu4-H4D	22
Cl4-Cu4-H4D	80	Cl5-Cu4-H4D	118	Cl3-Cu4-H4D	84
C43-N4-Cu4	146.91	C22-N4-Cu4	110.35	Cu4-N4-H4A	109.3
Cu3-Cl4-Cu4	80.24	Cu4-O1-Cu2	109.97	Cu4-O1-Cu1	109.53
Cu2-O1-Cu1	108.97	Cu4-O1-Cu3	108.02	Cu2-O1-Cu3	110.28
Cu1-O1-Cu3	110.06	C29-N5-Cu5	117.93	Cu5-N5-H59	110
Cu5-N5-H58	109	N5 _a -Cu5-N5	180.0	N5 _a -Cu5-Cl7	90.71
N5-Cu5-Cl7	89.29	N5 _a -Cu5-Cl7 _a	89.29	N5-Cu5-Cl7 _a	90.71
Cl7-Cu5-Cl7 _a	180.0	Cu4-Cl5-Cu1	80.27	Cu1-Cl6-Cu3	80.63
N6-Cu6-N6 _a	180.0	N6-Cu6-Cl8	94.20	N6 _b -Cu6-Cl8	85.80
N6-Cu6-Cl8 _b	85.80	N6 _b -Cu6-Cl8 _b	94.20	Cl8-Cu6-Cl8 _b	180.0
C36-N6-Cu6	123.24	Cu6-N6-H55	108	Cu6-N6-H54	112

5.2.3. Crystallographic Data for Chapter 4

This chapter contains the crystallographic data of the compounds presented in chapter 4. Most of the data are part of the Supporting Information of the manuscript in chapter 4. For detailed information concerning the nomenclature and abbreviations please see chapter 3.

Compound 1: [CuL¹Cl]₄ (L¹ = benzylamine)

Table 5.67.: Crystal data and structure refinement for compound 1.

Internal identification code	schindler13036
CCDC-no.	982979
Diffractometer type	BRUKER Nonius FR591 with Kappa CCD
Empirical formula	C ₁₄ H ₁₈ Cl ₂ Cu ₂ N ₂
Formula weight	412.28
Temperature	193(2) K
Wavelength	0.71073 Å
Crystal system, space group	Monoclinic, <i>C</i> 2/ <i>c</i>
Unit cell dimensions	a = 37.796(8) Å α = 90° b = 4.4340(9) Å β = 125.88(3)° c = 23.423(5) Å γ = 90°
Volume	3180.6(15) Å ³
Z, Calculated density	8, 1.722 Mg/m ³
Absorption coefficient	3.000 mm ⁻¹
F(000)	1664
Habitus, color	Needle, colorless
Crystal size	0.400 x 0.170 x 0.020 mm
Theta range for data collection	2.660 to 27.569°
Limiting indices	-46 ≤ h ≤ 48, -5 ≤ k ≤ 5, -30 ≤ l ≤ 28
Reflections collected / unique	11388 / 3594 [R(int) = 0.0842]
Completeness to theta = 25.24	99.0 %
Absorption correction	Semiempirical
Max. and min. transmission	0.31509 and 0.24648
Refinement method	Full-matrix least-squares on F ²
Data / restraints / parameters	3594 / 6 / 198
Goodness-of-fit on F ²	1.085
Final R indices [I > 2sigma(I)]	R1 = 0.0630, wR2 = 0.1681
R indices (all data)	R1 = 0.0873, wR2 = 0.1874
Extinction coefficient	3.10
Largest diff. peak and hole	1.385 and -1.261 e. Å ⁻³

The crystal structure was solved as twin (TWIN 1 0 1.891 0 -1 0 0 0 -1, BASF 0.38286). The refinement shows a half molecule in the independent unit of the elementary cell. All hydrogen atoms were positioned geometrically. All non-hydrogen atoms were refined anisotropically. Semiempirical absorption corrections were applied.

Symmetry transformations used to generate equivalent atoms:

a: -x,y,-z+1/2

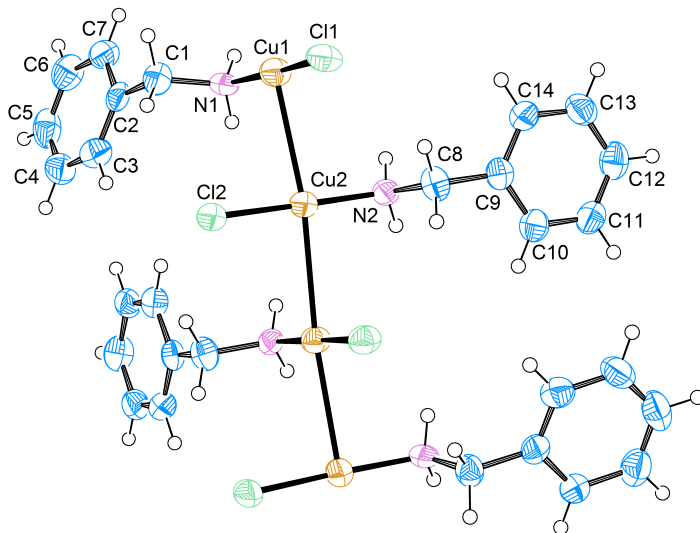


Figure 5.34.: ORTEP plot with thermal ellipsoids set at 50% probability shows the full compound **1**.

Table 5.68.: Selected bond lengths [\AA] and angles [$^\circ$] for compound **1**.

C11-Cu1	2.117	C1-N1	1.494	N1-Cu1	1.924
Cu1-Cu2	2.889	Cl2-Cu2	2.122	N2-Cu2	1.923
Cu2-Cu2 _a	2.927				
C1-N1-Cu1	111.94	N1-Cu1-Cl1	173.22	N1-Cu1-Cu2	90.02
Cl1-Cu1-Cu2	91.56	C8-N2-Cu2	114.34	N2-Cu2-Cl2	177.12
N2-Cu2-Cu1	93.84	Cl2-Cu2-Cu1	85.09	N2-Cu2-Cu2 _a	93.10
Cl2-Cu2-Cu2 _a	88.07	Cu1-Cu2-Cu2 _a	172.80		

Compound 3: [CuL¹₂Cl₂]Table 5.69.: Crystal data and structure refinement for compound **3**.

Internal identification code	schindler13004
CCDC-no.	Not submitted.
Diffractionmeter type	BRUKER Nonius FR591 with Kappa CCD
Empirical formula	C ₁₄ H ₁₈ Cl ₂ CuN ₂
Formula weight	348.74
Temperature	193(2) K
Wavelength	0.71073 Å
Crystal system, space group	Orthorhombic, <i>P b c a</i>
Unit cell dimensions	a = 8.1580(16) Å $\alpha = 90^\circ$ b = 12.418(3) Å $\beta = 90^\circ$ c = 30.903(6) Å $\gamma = 90^\circ$
Volume	3130.7(11) Å ³
Z, Calculated density	8, 1.480 Mg/m ³
Absorption coefficient	1.724 mm ⁻¹
F(000)	1432
Habitus, color	Plate, green
Crystal size	0.25 x 0.20 x 0.03 mm
Theta range for data collection	1.32 to 27.48 °
Limiting indices	-8 ≤ h ≤ 10, -15 ≤ k ≤ 16, -39 ≤ l ≤ 40
Reflections collected / unique	23391 / 3596 [R(int) = 0.0593]
Completeness to theta = 27.48	99.9 %
Absorption correction	Semiempirical
Max. and min. transmission	0.49165 and 0.44408
Refinement method	Full-matrix least-squares on F ²
Data / restraints / parameters	3596 / 0 / 244
Goodness-of-fit on F ²	1.032
Final R indices [I > 2sigma(I)]	R1 = 0.0315, wR2 = 0.0689
R indices (all data)	R1 = 0.0652, wR2 = 0.0917
Extinction coefficient	1.77
Largest diff. peak and hole	0.412 and -0.556 e. Å ⁻³

The refinement shows one molecule in the independent unit of the elementary cell. The hydrogen atoms were partly found and partly positioned geometrically. The N-H hydrogen atoms were found and the C-H hydrogen atoms positioned geometrically and refined isotropically. Non-hydrogen atoms were refined anisotropically. Semiempirical absorption corrections were applied.

Symmetry transformations used to generate equivalent atoms:

a: x+1/2,-y+1/2,-z **b:** x-1/2,-y+1/2,-z

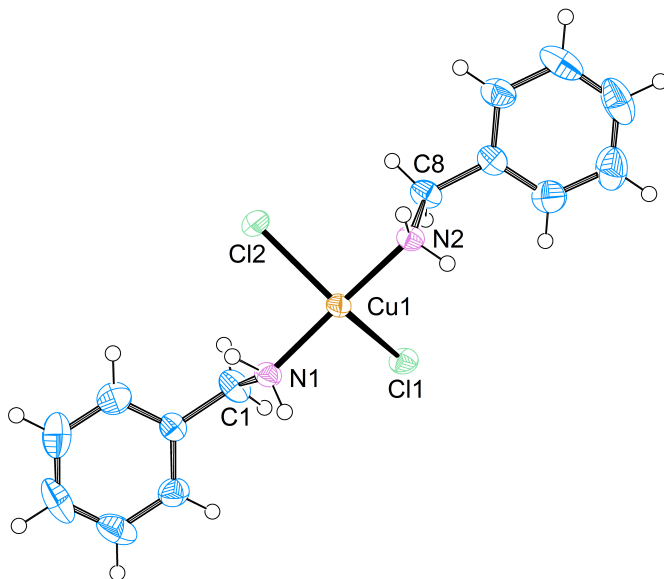


Figure 5.35.: ORTEP plot with thermal ellipsoids set at 50% probability shows the full compound **3**.

Table 5.70.: Selected bond lengths [\AA] and angles [$^\circ$] for compound **3**.

Cu1-Cu1	2.345	Cu1-Cu1 _a	2.583	Cu1-Cu1	2.299
Cu1-N2	1.976	Cu1-N1	1.979	Cu1-Cl1 _a	2.583
Cu1-Cl1-Cu1 _a	172.06	N2-Cu1-N1	170.46	N2-Cu1-Cl2	94.43
N1-Cu1-Cl2	90.64	N2-Cu1-Cl1	89.08	N1-Cu1-Cl1	92.67
Cl2-Cu1-Cl1	137.31	N2-Cu1-Cl1 _a	85.79	N1-Cu1-Cl1 _a	84.87
Cl2-Cu1-Cl1 _a	110.54	Cl1-Cu1-Cl1 _a	112.15	C15-N1-Cu1	119.06
C13-N2-Cu1	117.70				

Compound 4: $[\text{CuL}^1_2(\text{OMe})]_2[\text{Cu}_{3,5}\text{I}_6](\text{HL}^1)_{0.5} \cdot n \text{H}_2\text{O} \cdot n \text{MeOH}$

Table 5.71.: Crystal data and structure refinement for compound 4.

Internal identification code	schindler13095
CCDC-no.	Not submitted.
Diffractometer type	BRUKER Nonius FR591 with Kappa CCD
Empirical formula	$\text{C}_{37}\text{H}_{50}\text{Cu}_{5.50}\text{I}_6\text{N}_{4.50}\text{O}_5$
Formula weight	1748.68
Temperature	193(2) K
Wavelength	0.71073 Å
Crystal system, space group	Orthorhombic, $P c c n$
Unit cell dimensions	$a = 24.441(5) \text{ \AA}$ $\alpha = 90^\circ$ $b = 27.504(6) \text{ \AA}$ $\beta = 90^\circ$ $c = 8.1450(16) \text{ \AA}$ $\gamma = 90^\circ$
Volume	$5475.3(19) \text{ \AA}^3$
Z, Calculated density	4, 2.121 Mg/m ³
Absorption coefficient	5.521 mm^{-1}
F(000)	3284
Habitus, color	Plate, green
Crystal size	0.08 x 0.10 x 0.04 mm
Theta range for data collection	2.738 to 24.997°
Limiting indices	$-28 \leq h \leq 29$, $-32 \leq k \leq 32$, $-9 \leq l \leq 9$
Reflections collected / unique	39007 / 4742 [R(int) = 0.1097]
Completeness to theta = 25.24	95.9 %
Absorption correction	None
Refinement method	Full-matrix least-squares on F ²
Data / restraints / parameters	4742 / 2 / 385
Goodness-of-fit on F ²	1.084
Final R indices [I > 2sigma(I)]	R1 = 0.0568, wR2 = 0.1160
R indices (all data)	R1 = 0.0900, wR2 = 0.1265
Largest diff. peak and hole	0.920 and -0.849 e. Å ⁻³

The refinement shows half a molecule in the independent unit of the elementary cell. The hydrogen atoms were positioned geometrically and refined isotropically. Non-hydrogen atoms were refined anisotropically. No absorption corrections were applied.

Symmetry transformations used to generate equivalent atoms:

$$\begin{array}{lll}
 \mathbf{a}: & -x+1/2, y, z+1/2 & \mathbf{b}: & -x+1/2, y, z-1/2 & \mathbf{c}: & x, y, z+1 \\
 \mathbf{d}: & x, -y+1/2, z+1/2 & \mathbf{e}: & -x+1, -y+1, -z+1 & \mathbf{f}: & -x+1/2, -y+1/2, z \\
 \mathbf{g}: & x, y, z-1 & \mathbf{h}: & x, -y+1/2, z-1/2 & &
 \end{array}$$

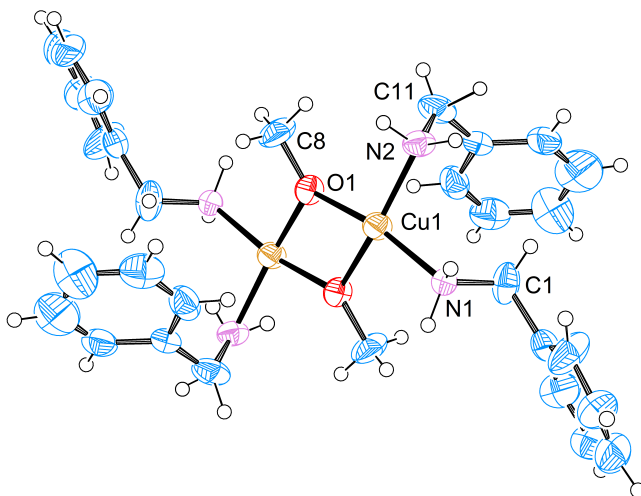


Figure 5.36.: ORTEP plot with thermal ellipsoids set at 50% probability shows the full complex molecule of compound **4**. The polymeric anion and solvent molecules are not shown for clarity.

Table 5.72.: Selected bond lengths [\AA] and angles [$^\circ$] for compound **4**.

Cu1-O1	1.923	Cu1-O1 _e	1.931	Cu1-N2	1.992
Cu1-N1	2.008	O1-Cu1 _e	1.931		
O1-Cu1-O1 _e	76.43	O1-Cu1-N2	94.93	O1 _e -Cu1-N2	164.43
O1-Cu1-N1	169.83	O1 _e -Cu1-N1	93.83	N2-Cu1-N1	95.33
O1-Cu1-Cu1 _e	38.29	O1 _e -Cu1-Cu1 _e	38.11	N2-Cu1-Cu1 _e	131.92
N1-Cu1-Cu1 _e	131.82	C1-N1-Cu1	118.66	Cu1-N2-H2A	108.2
C11-N2-H2B	108.20	Cu1-N2-H2B	108.20	C8-O1-Cu1	125.36
C8-O1-Cu1 _e	124.86	Cu1-O1-Cu1 _e	103.63		

(HL¹)(C₇H₇NHCOO)Table 5.73.: Crystal data and structure refinement for (HL¹)(C₇H₇NHCOO).

Internal identification code	schindler13101
CCDC-no.	Not submitted.
Diffractometer type	BRUKER Nonius FR591 with Kappa CCD
Empirical formula	C ₃₀ H ₃₆ N ₄ O ₄
Formula weight	516.63
Temperature	190(2) K
Wavelength	0.71073 Å
Crystal system, space group	Monoclinic, <i>C</i> $\bar{1}$
Unit cell dimensions	a = 48.769(10) Å α = 90° b = 9.3980(19) Å β = 90.86(3)° c = 5.7740(12) Å γ = 90°
Volume	2646.1(9) Å ³
Z, Calculated density	4, 1.297 Mg/m ³
Absorption coefficient	0.087 mm ⁻¹
F(000)	1104
Habitus, color	Block, colorless
Crystal size	0.900 x 0.300 x 0.100 mm
Theta range for data collection	3.010 to 24.994°
Limiting indices	-54 ≤ h ≤ 57, -11 ≤ k ≤ 9, -6 ≤ l ≤ 6
Reflections collected / unique	9389 / 4387 [R(int) = 0.1141]
Completeness to theta = 25.24	95.7 %
Absorption correction	None
Refinement method	Full-matrix least-squares on F ²
Data / restraints / parameters	4387 / 0 / 347
Goodness-of-fit on F ²	1.064
Final R indices [I > 2sigma(I)]	R1 = 0.0817, wR2 = 0.2047
R indices (all data)	R1 = 0.0971, wR2 = 0.2178
Largest diff. peak and hole	0.612 and -0.343 e. Å ⁻³

The structure was solved as twin (TWIN -1 0 0 0 1 0 0 0 -1, BASF 0.48657). The refinement shows two molecules in the independent unit of the elementary cell. The hydrogen atoms were positioned geometrically and refined isotropically. Non-hydrogen atoms were refined anisotropically. No absorption corrections were applied.

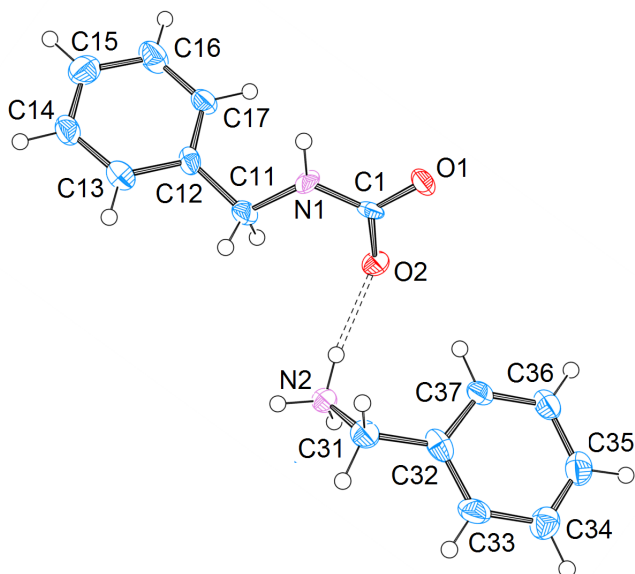


Figure 5.37.: ORTEP plot with thermal ellipsoids set at 50% probability shows the full compound $(HL^1)(C_7H_7NHCOO)$.

Table 5.74.: Selected bond lengths [\AA] and angles [$^\circ$] for $(HL^1)(C_7H_7NHCOO)$.

O1-C1	1.262	O2-C1	1.283	N1-C1	1.339
N1-C11	1.445	N1-H1	0.880	N3-C31	1.485
N3-H3A	0.910	N3-H3B	0.910	N3-H3C	0.910
C1-N1-C11	123.6	C1-N1-H1	118.2	C11-N1-H1	118.2
O1-C1-O2	122.8	O1-C1-N1	118.7	O2-C1-N1	118.5
N1-C11-C12	113.2	N1-C11-H11A	108.9	N1-C11-H11B	108.9
C12-C11-H11B	108.9	H11A-C11-H11B	107.8	C31-N3-H3A	109.5
C31-N3-H3B	109.5	H3A-N3-H3B	109.5	C31-N3-H3C	109.5
H3A-N3-H3C	109.5	H3B-N3-H3C	109.5	N3-C31-H31A	108.9
N3-C31-H31B	108.9				

5.3. Infrared Spectroscopy and Elemental Analyses

5.3.1. Data for Chapter 2

This chapter contains the elemental analyses and infrared data of the compounds presented in chapter 2. Most of the data are part of the Supporting Information of the publication of chapter 2 and therefore are available in the online library of the journal "*Chemistry - A European Journal*" (<http://onlinelibrary.wiley.com/journal/10.1002/%28ISSN%291521-3765/issue>s). For detailed information concerning the nomenclature and abbreviations please see chapter 2.

Cluster I: $2[\text{Cu}_4\text{OCl}_6\text{L}^1_4] \cdot [\text{CuL}^1_2\text{Cl}_2]$ ($\text{L}^1 = \text{benzylamine}$)**Elemental analysis:**

C: 38.5 % H: 4.3 % N: 6.5 % (Experimental)

C: 38.7 % H: 4.2 % N: 6.5 % (Theoretical)

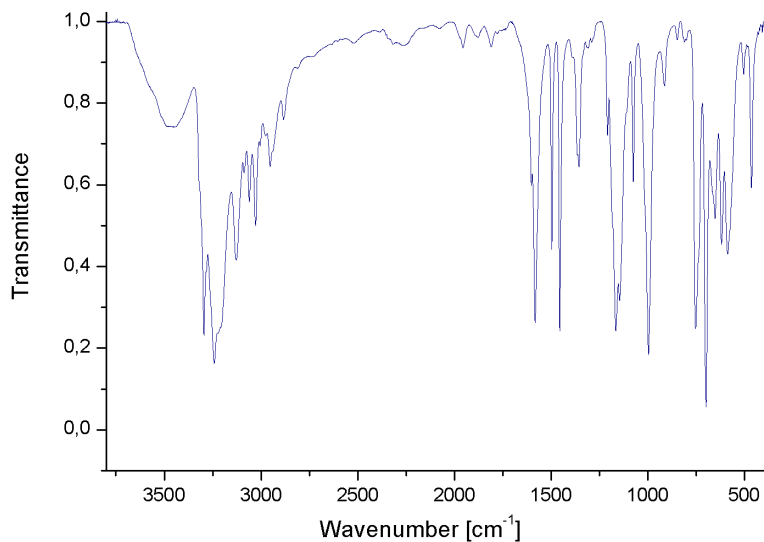


Figure 5.38.: Infrared spectrum of cluster I.

Table 5.75.: Infrared data of cluster I.

3296-3243 cm^{-1}	$\nu(\text{NH}_2)$	3061-3028 cm^{-1}	$\nu(\text{Ar-H})$
2953-2884 cm^{-1}	$\nu(\text{CH}_2)$	1601 cm^{-1}	$\nu(\text{C=C})_{ar}$
1582 cm^{-1}	$\delta(\text{NH}_2)$	1496 cm^{-1}	$\nu(\text{C=C})_{ar}$
1454 cm^{-1}	$\delta(\text{CH}_2)$	752 cm^{-1}	$\delta(\text{Ar-H})$
698 cm^{-1}	$\delta(\text{C=C})_{ar}$	586 cm^{-1}	$\nu(\text{Cu}_4\text{O})$
464 cm^{-1}	$\nu(\text{Cu-N})$		

Cluster I (with bromide): $2[\text{Cu}_4\text{OBr}_6\text{L}^1_4] \cdot [\text{CuL}^1_2\text{Br}_2]$ ($\text{L}^1 = \text{benzylamine}$)**Elemental analysis:**

C: 29.5 % H: 3.1 % N: 4.8 % (Experimental)

C: 30.1 % H: 3.3 % N: 5.0 % (Theoretical)

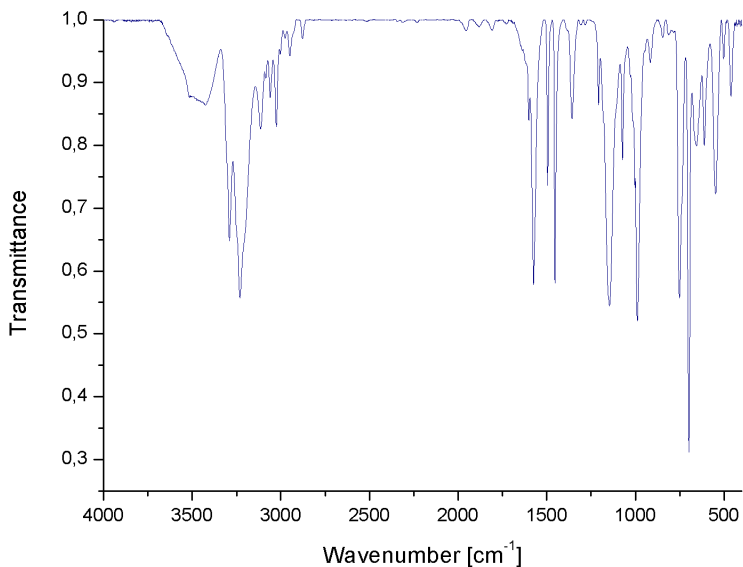


Figure 5.39.: Infrared spectrum of the bromide version of cluster I.

Table 5.76.: Infrared data of the bromide version of cluster I.

3290-3231 cm^{-1}	$\nu(\text{NH}_2)$	3114-3026 cm^{-1}	$\nu(\text{Ar-H})$
2950 cm^{-1}	$\nu(\text{CH}_2)$	1575 cm^{-1}	$\delta(\text{NH}_2)$
1496 cm^{-1}	$\nu(\text{C}=\text{C})_{ar}$	1358 cm^{-1}	$\delta(\text{CH}_2)_{wagg}$
1495 cm^{-1}	$\delta_s(\text{CH}_2)$	751 cm^{-1}	$\delta(\text{Ar-H})$
698 cm^{-1}	$\delta(\text{C}=\text{C})_{ar}$	546 cm^{-1}	$\nu(\text{Cu}_4\text{O})$
460 cm^{-1}	$\nu(\text{Cu-N})$		

Cluster II: [Cu₄O₄Cl₄(C₁₁H₁₄)₄]**Elemental analysis:**

C: 47.9% H: 5.2% N: 4.9% (Experimental)

C: 48.0% H: 5.1% N: 5.1% (Theoretical)

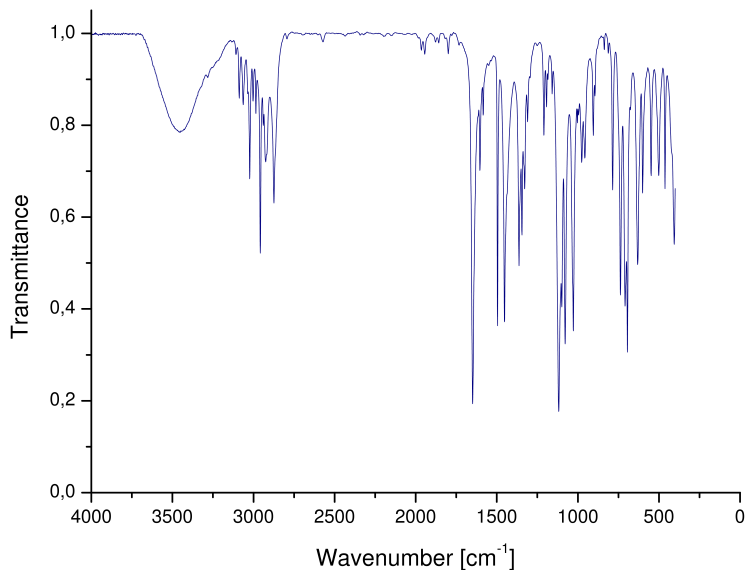


Figure 5.40.: Infrared spectrum of cluster II.

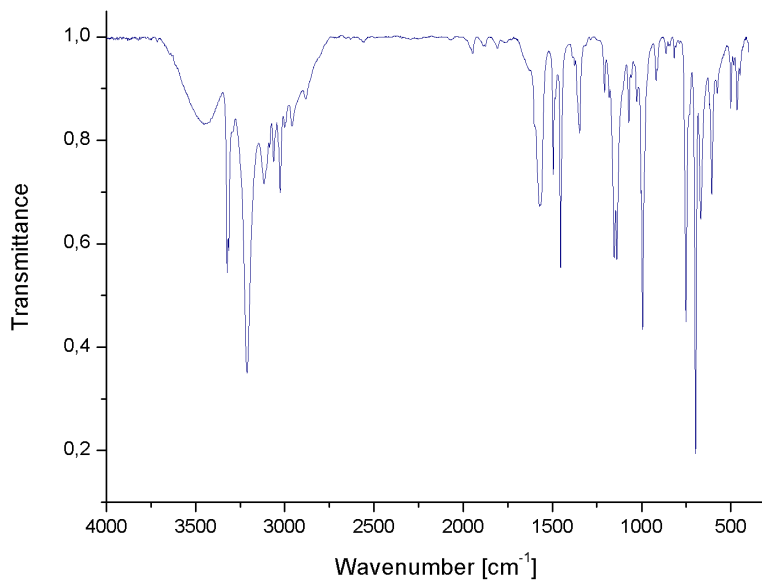
Table 5.77.: Infrared data of cluster II.

3089-3003 cm ⁻¹	$\nu(\text{Ar-H})$	2986-2875 cm ⁻¹	$\nu(\text{CH}_2)$
1649 cm ⁻¹	$\nu(\text{C=N})$	1604 cm ⁻¹	$\nu(\text{C=C})_{ar}$
1496 cm ⁻¹	$\nu(\text{C=C})_{ar}$	1453 cm ⁻¹	$\delta(\text{CH}_2)$
1118 cm ⁻¹	$\nu(\text{C-O})$	709 cm ⁻¹	$\delta(\text{Ar-H})$
695 cm ⁻¹	$\delta(\text{C=C})_{ar}$		

Compound 1: $[\text{CuL}^1_2\text{Cl}_2]$ ($\text{L}^1 = \text{benzylamine}$)**Elemental analysis:**

C: 46.6% H: 5.1% N: 7.7% (Experimental)

C: 48.2% H: 5.2% N: 8.0% (Theoretical)

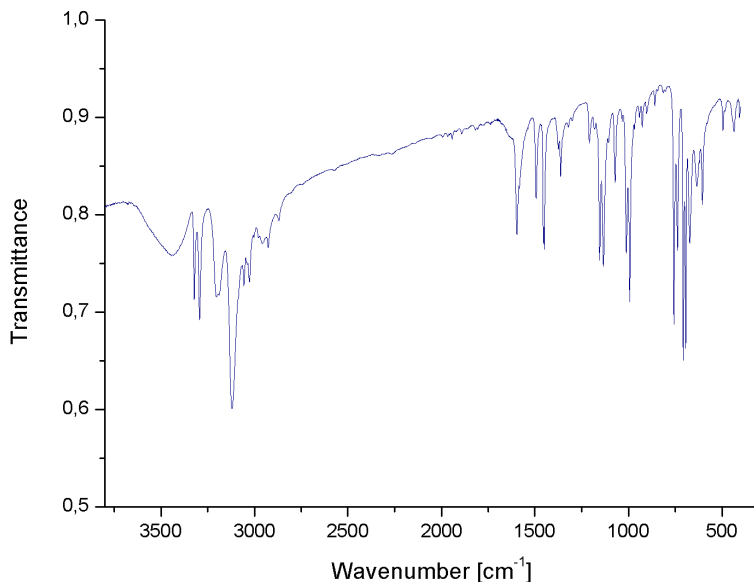
Figure 5.41.: Infrared spectrum of compound **1**.Table 5.78.: Infrared data of compound **1**.

3323 cm^{-1}	$\nu(\text{NH}_2)$	3024 cm^{-1}	$\nu(\text{Ar-H})$
1562 cm^{-1}	$\delta(\text{NH}_2)$	1494 cm^{-1}	$\nu(\text{C}=\text{C})_{ar}$
1454 cm^{-1}	$\delta(\text{CH}_2)$	752 cm^{-1}	$\delta(\text{Ar-H})$
697 cm^{-1}	$\delta(\text{C}=\text{C})_{ar}$	466 cm^{-1}	$\nu(\text{Cu-N})$

Compound 2: [CuL₄Cl₂] (L¹ = benzylamine)**Elemental analysis:**

C: 59.6 % H: 6.4 % N: 9.8 % (Experimental)

C: 59.7 % H: 6.4 % N: 10.0 % (Theoretical)

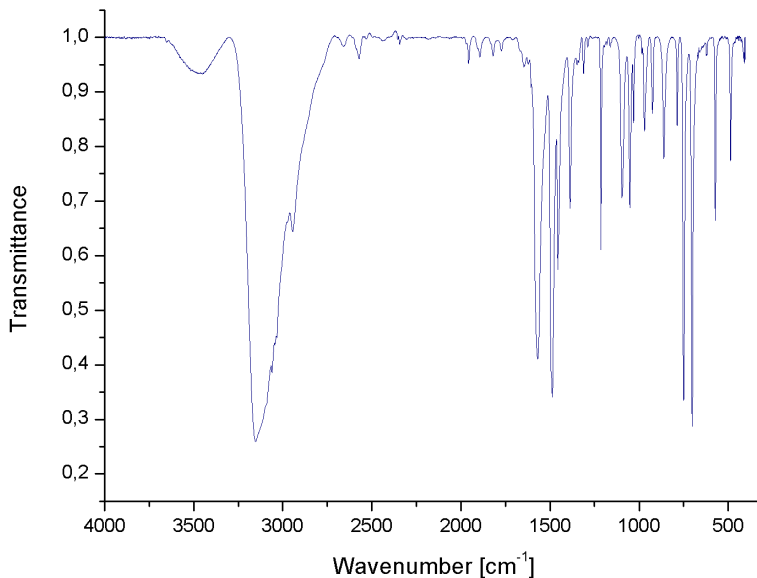
Figure 5.42.: Infrared spectrum of compound **2**.Table 5.79.: Infrared data of compound **2**..

3322-3293 cm ⁻¹	$\nu(\text{NH}_2)$	3119-3026 cm ⁻¹	$\nu(\text{Ar-H})$
2926 cm ⁻¹	$\nu(\text{CH}_2)$	1596 cm ⁻¹	$\delta(\text{NH}_2)$
1493 cm ⁻¹	$\nu(\text{C=C})_{ar}$	1449 cm ⁻¹	$\delta(\text{CH}_2)$
757 cm ⁻¹	$\delta(\text{Ar-H})$	693 cm ⁻¹	$\delta(\text{C=C})_{ar}$
434 cm ⁻¹	$\nu(\text{Cu-N})$		

Compound 3: $(\text{HL}^1)_2[\text{CuCl}_4]$ ($\text{L}^1 = \text{benzylamine}$)**Elemental analysis:**

C: 38.8 % H: 4.8 % N: 6.2 % (Experimental)

C: 39.9 % H: 4.8 % N: 6.6 % (Theoretical)

Figure 5.43.: Infrared spectrum of compound **3**.Table 5.80.: Infrared data of compound **3**.

3152 cm^{-1}	$\nu(\text{NH}_3^+)$	2946 cm^{-1}	$\nu(\text{CH}_2)$
1569 cm^{-1}	$\delta(\text{NH}_2)$	1488 cm^{-1}	$\nu(\text{C}=\text{C})_{ar}$
1456 cm^{-1}	$\delta(\text{CH}_2)$	749 cm^{-1}	$\delta(\text{Ar-H})$
703 cm^{-1}	$\delta(\text{C}=\text{C})_{ar}$		

Compound 4

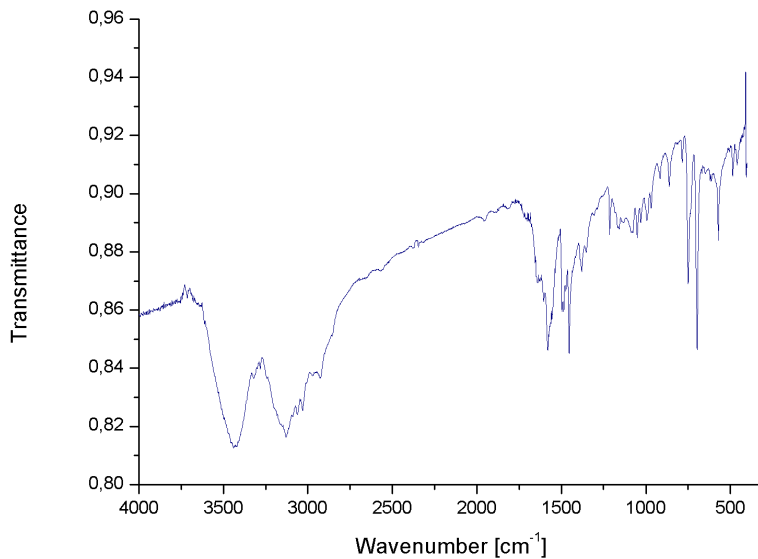


Figure 5.44.: Infrared spectrum of compound 4.

Table 5.81.: Infrared data of compound 4.

3440 cm ⁻¹	$\nu(\text{OH})$	3129-3031 cm ⁻¹	$\nu(\text{Ar-H})$
2929 cm ⁻¹	$\nu(\text{CH}_2)$	1487 cm ⁻¹	$\nu(\text{C=C})_{ar}$
1455 cm ⁻¹	$\delta(\text{CH}_2)$	750 cm ⁻¹	$\delta(\text{Ar-H})$
696 cm ⁻¹	$\delta(\text{C=C})_{ar}$		

Compound 5**Elemental analysis:**

C: 57.0% H: 5.2% N: 6.4% (Experimental)

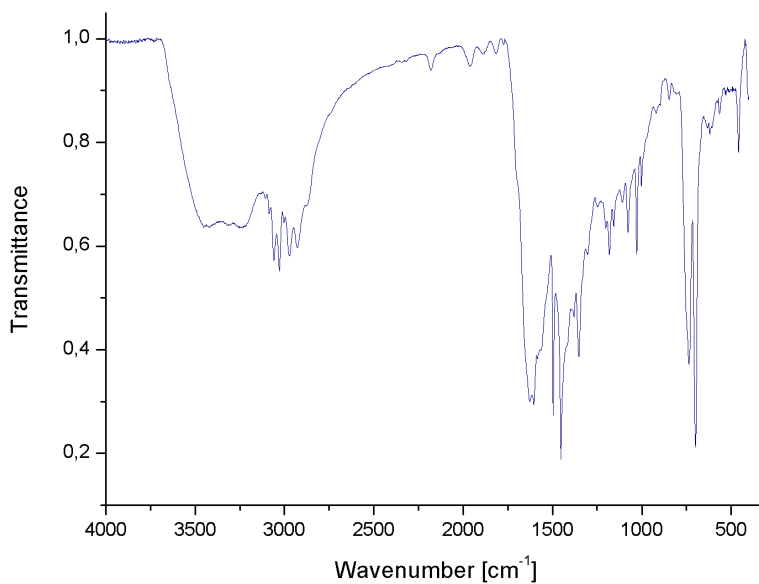


Figure 5.45.: Infrared spectrum of compound 5.

Table 5.82.: Infrared data of compound 5.

3060-3025 cm ⁻¹	$\nu(\text{Ar-H})$	2973-2929 cm ⁻¹	$\nu(\text{CH}_2)$
1499 cm ⁻¹	$\nu(\text{C=C})_{ar}$	1452 cm ⁻¹	$\delta(\text{CH}_2)$
735 cm ⁻¹	$\delta(\text{Ar-H})$	701 cm ⁻¹	$\delta(\text{C=C})_{ar}$
486 cm ⁻¹	$\nu(\text{Cu-N})$		

Compound 6

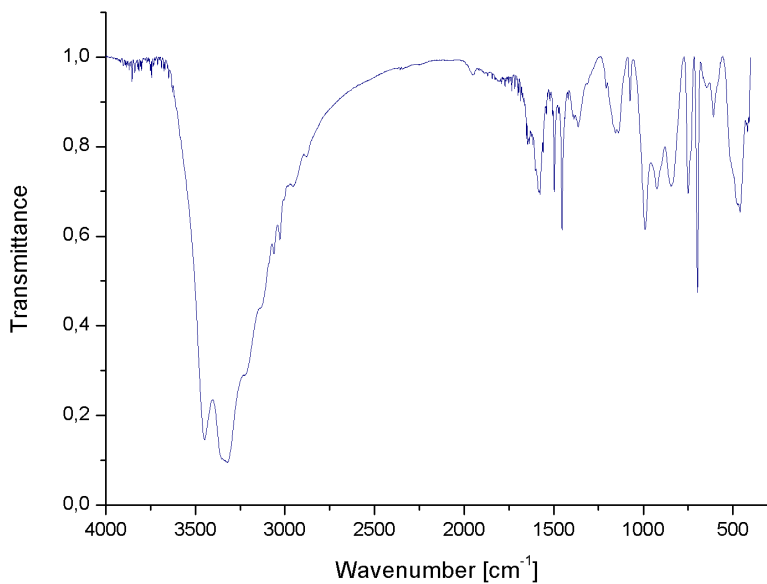


Figure 5.46.: Infrared spectrum of compound 6.

Table 5.83.: Infrared data of compound 6.

3449-3322 cm^{-1}	$\nu(\text{NH}_2)$	3028 cm^{-1}	$\nu(\text{Ar-H})$
1576 cm^{-1}	$\delta(\text{NH}_2)$	1496 cm^{-1}	$\nu(\text{C}=\text{C})_{ar}$
1454 cm^{-1}	$\delta(\text{CH}_2)$	750 cm^{-1}	$\delta(\text{Ar-H})$
697 cm^{-1}	$\delta(\text{C}=\text{C})_{ar}$	461 cm^{-1}	$\nu(\text{Cu-N})$

Compound 7: [CuL¹Cl]₃ (L¹ = benzylamine)

Elemental analysis:

C: 41.1% H: 4.4% N: 7.0% (Experimental)

C: 40.8% H: 4.4% N: 6.8% (Theoretical)

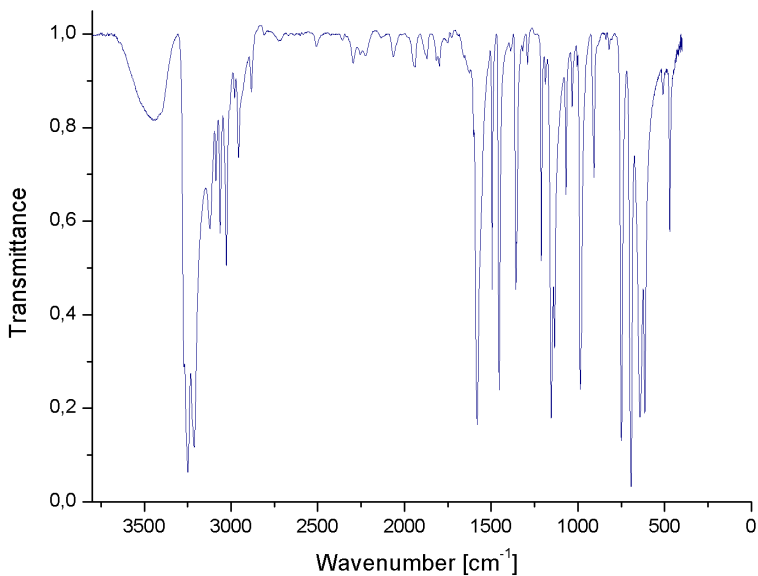


Figure 5.47.: Infrared spectrum of compound **7**.

Table 5.84.: Infrared data of compound **7**.

3249-3212 cm ⁻¹	$\nu(\text{NH}_2)$	3160-3017 cm ⁻¹	$\nu(\text{Ar-H})$
1566 cm ⁻¹	$\delta(\text{NH}_2)$	1495 cm ⁻¹	$\nu(\text{C=C})_{ar}$
1454 cm ⁻¹	$\delta(\text{CH}_2)$	749 cm ⁻¹	$\delta(\text{Ar-H})$
693 cm ⁻¹	$\delta(\text{C=C})_{ar}$	471 cm ⁻¹	$\nu(\text{Cu-N})$

Aniline Complex: [Cu(aniline)₂Cl₂]**Elemental analysis:**

C: 44.4 % H: 4.3 % N: 8.3 % (Experimental)

C: 44.9 % H: 4.4 % N: 8.7 % (Theoretical)

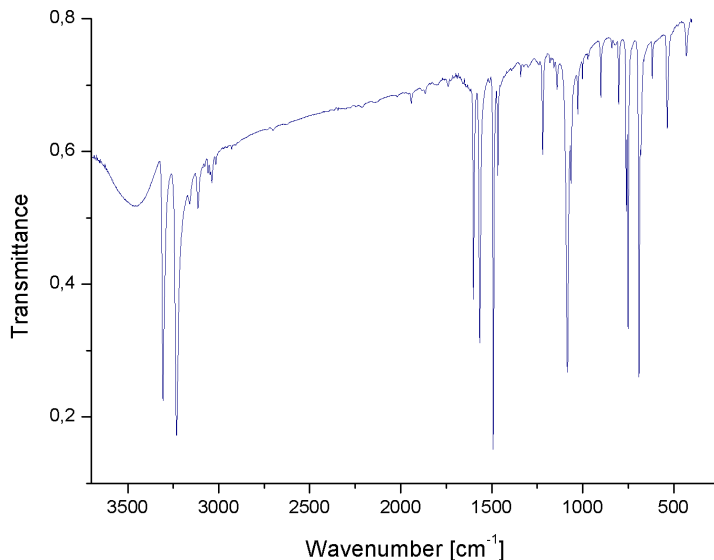


Figure 5.48.: Infrared spectrum of the aniline complex.

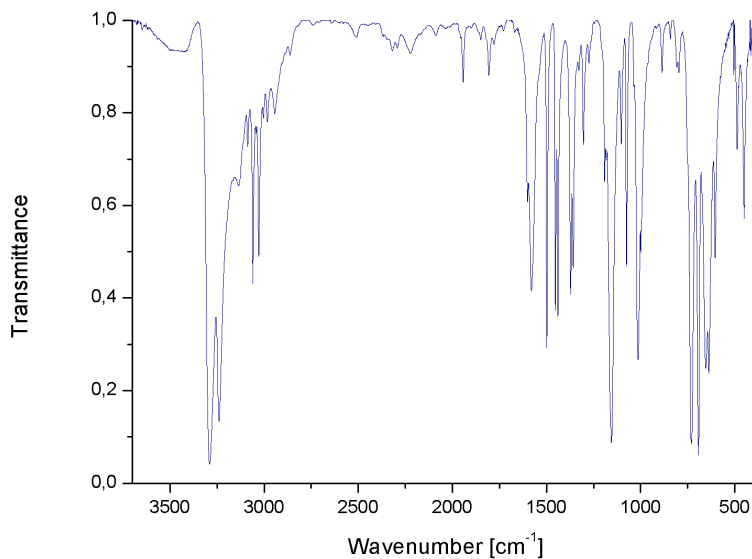
Table 5.85.: Infrared data of the aniline complex.

3307-3232 cm ⁻¹	$\nu(\text{NH}_2)$	3122-3027 cm ⁻¹	$\nu(\text{Ar-H})$
2980-2882 cm ⁻¹	$\nu(\text{CH}_2)$	1581 cm ⁻¹	$\delta(\text{NH}_2)$
1492 cm ⁻¹	$\nu(\text{C=C})_{ar}$	751 cm ⁻¹	$\delta(\text{Ar-H})$
691 cm ⁻¹	$\delta(\text{C=C})_{ar}$		

[ZnL¹₂Cl₂] (L¹ = benzylamine)**Elemental analysis:**

C: 47.9% H: 5.1% N: 7.6% (Experimental)

C: 48.0% H: 5.2% N: 8.0% (Theoretical)

Figure 5.49.: Infrared spectrum of [ZnL¹₂Cl₂].Table 5.86.: Infrared data of [ZnL¹₂Cl₂].

3290-3241 cm ⁻¹	$\nu(\text{NH}_2)$	3057-3025 cm ⁻¹	$\nu(\text{Ar-H})$
1578 cm ⁻¹	$\delta(\text{NH}_2)$	1498 cm ⁻¹	$\nu(\text{C=C})_{ar}$
1452 cm ⁻¹	$\delta(\text{CH}_2)$	727 cm ⁻¹	$\delta(\text{Ar-H})$
690 cm ⁻¹	$\delta(\text{C=C})_{ar}$	471 cm ⁻¹	

5.3.2. Data for Chapter 3

This chapter contains the elemental analyses and infrared data of the compounds presented in chapter 3. Most of the data are part of the Supporting Information of the manuscript in chapter 3. For detailed information concerning the nomenclature and abbreviations please see chapter 3.

Compound 2a: $(HL^2)_2[CuCl_4]$ ($L^2 = \text{phenethylamine}$)

Elemental analysis:

C: 38.5 % H: 5.0 % N: 5.6 % (Experimental)

C: 42.7 % H: 5.3 % N: 6.2 % (Theoretical)

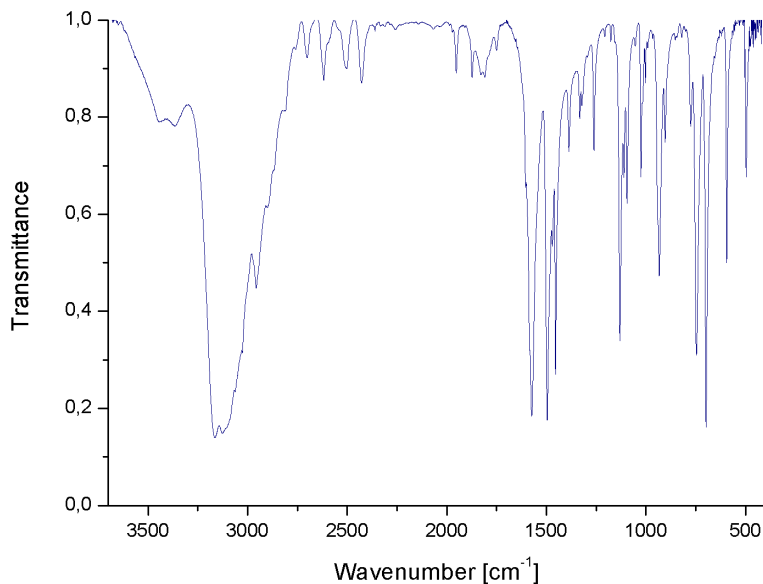


Figure 5.50.: Infrared spectrum of compound **2a**.

Table 5.87.: Infrared data of compound **2a**.

3127 cm^{-1}	$\nu(\text{NH}_3^+)$	2957 cm^{-1}	$\nu(\text{CH}_2)$
1574 cm^{-1}	$\delta(\text{NH}_2)$	1496 cm^{-1}	$\nu(\text{C}=\text{C})_{ar}$
1454 cm^{-1}	$\delta(\text{CH}_2)$	747 cm^{-1}	$\delta(\text{Ar-H})$
698 cm^{-1}	$\delta(\text{C}=\text{C})_{ar}$		

Cluster III: $[\text{Cu}_4\text{OCl}_6\text{L}^2_4] \cdot [\text{CuL}^2_2\text{Cl}_2]$ ($\text{L}^2 = \text{phenethylamine}$)**Elemental analysis:**

C: 41.1 % H: 4.8 % N: 5.8 % (Experimental)

C: 42.9 % H: 4.9 % N: 6.2 % (Theoretical)

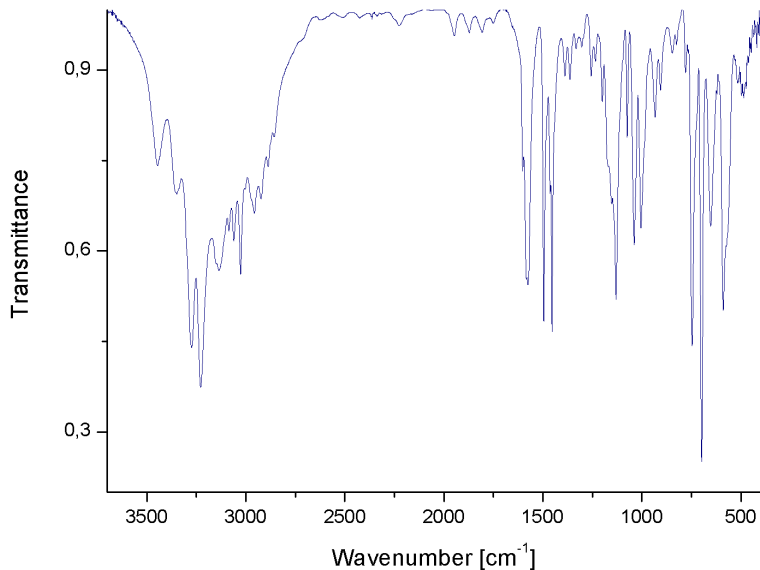


Figure 5.51.: Infrared spectrum of cluster III.

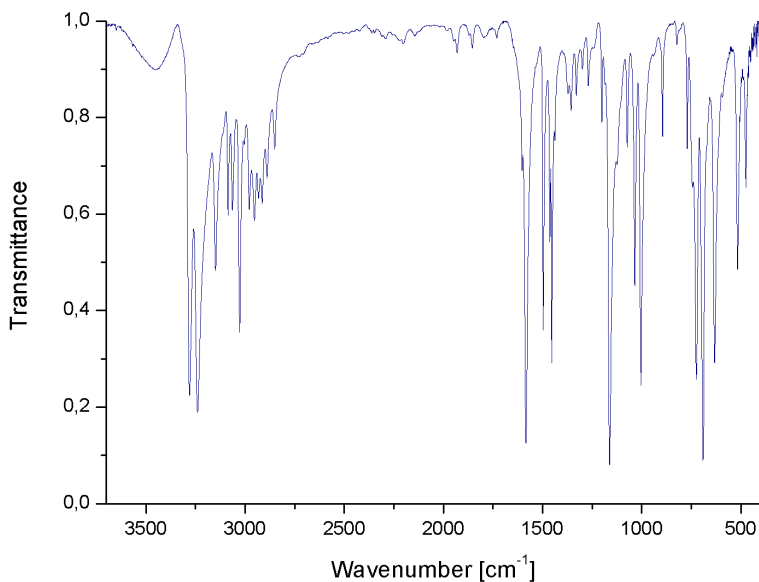
Table 5.88.: Infrared data of cluster III.

3274-3228 cm^{-1}	$\nu(\text{NH}_2)$	3137-3026 cm^{-1}	$\nu(\text{Ar-H})$
2957-2857 cm^{-1}	$\nu(\text{CH}_2)$	1583 cm^{-1}	$\delta(\text{NH}_2)$
1496 cm^{-1}	$\nu(\text{C=C})_{ar}$	1463 cm^{-1}	$\delta(\text{CH}_2)$
747 cm^{-1}	$\delta(\text{Ar-H})$	698 cm^{-1}	$\delta(\text{C=C})_{ar}$
590 cm^{-1}	$\nu(\text{Cu}_4\text{O})$		

Compound 2d: $[\text{CuL}^2_2\text{Cl}_2]$ ($\text{L}^2 = \text{phenethylamine}$)**Elemental analysis:**

C: 59.6 % H: 5.8 % N: 7.0 % (Experimental)

C: 51.0 % H: 5.9 % N: 7.4 % (Theoretical)

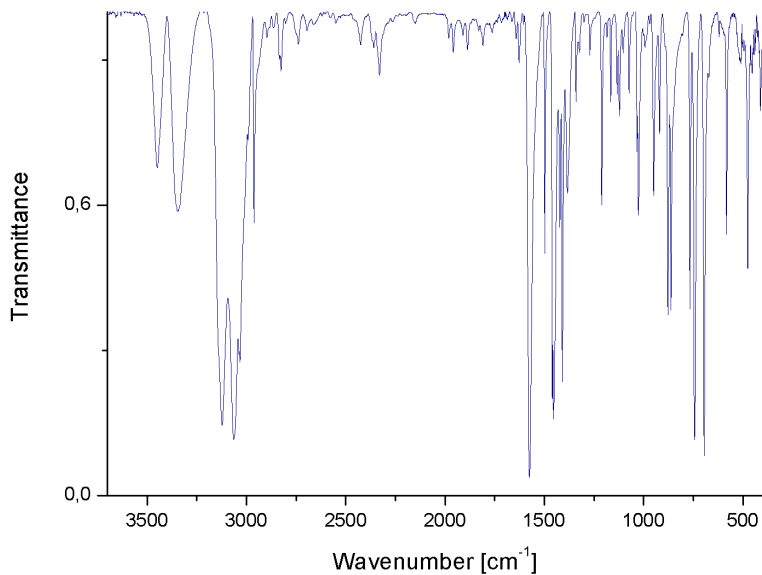
Figure 5.52.: Infrared spectrum of compound **2d**.Table 5.89.: Infrared data of compound **2d**.

3279-3239 cm^{-1}	$\nu(\text{NH}_2)$	3147-3027 cm^{-1}	$\nu(\text{Ar-H})$
2979-2850 cm^{-1}	$\nu(\text{CH}_2)$	1583 cm^{-1}	$\delta(\text{NH}_2)$
1497 cm^{-1}	$\nu(\text{C=C})_{ar}$	1463 cm^{-1}	$\delta(\text{CH}_2)$
724 cm^{-1}	$\delta(\text{Ar-H})$	690 cm^{-1}	$\delta(\text{C=C})_{ar}$
474 cm^{-1}	$\nu(\text{Cu-N})$		

Compound 3a: (HL³)₂[CuCl₄] · 1.5 CuCl₂ (L³ = N-methylbenzylamine)**Elemental analysis:**

C: 29.6 % H: 3.8 % N: 4.1 % (Experimental)

C: 29.5 % H: 3.8 % N: 4.3 % (Theoretical)

Figure 5.53.: Infrared spectrum of compound **3a**.Table 5.90.: Infrared data of compound **3a**.

3122-3063 cm ⁻¹	$\nu(\text{NMeH}_2^+)$	2961 cm ⁻¹	$\nu(\text{CH}_2)$
1575 cm ⁻¹	$\delta(\text{NH}_2)$	1497 cm ⁻¹	$\nu(\text{C}=\text{C})_{ar}$
1459 cm ⁻¹	$\delta(\text{CH}_2)$	744 cm ⁻¹	$\delta(\text{Ar-H})$
695 cm ⁻¹	$\delta(\text{C}=\text{C})_{ar}$		

Compound 3b

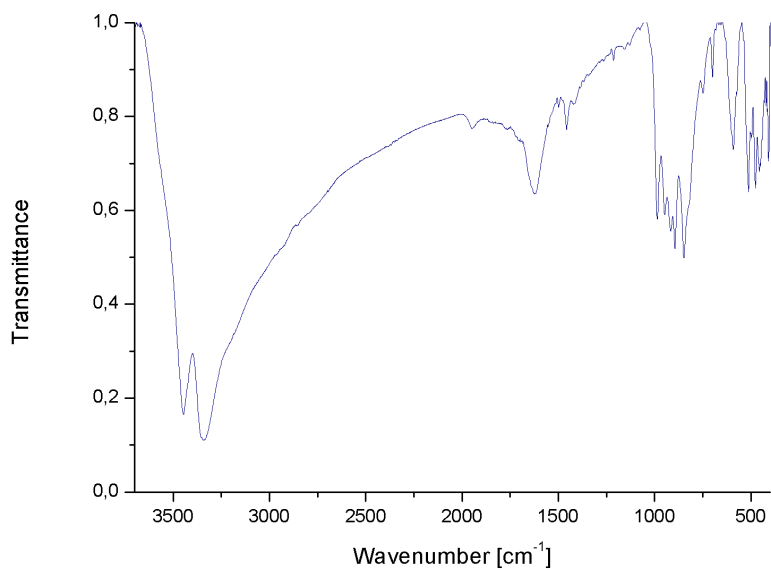


Figure 5.54.: Infrared spectrum of compound **3b**.

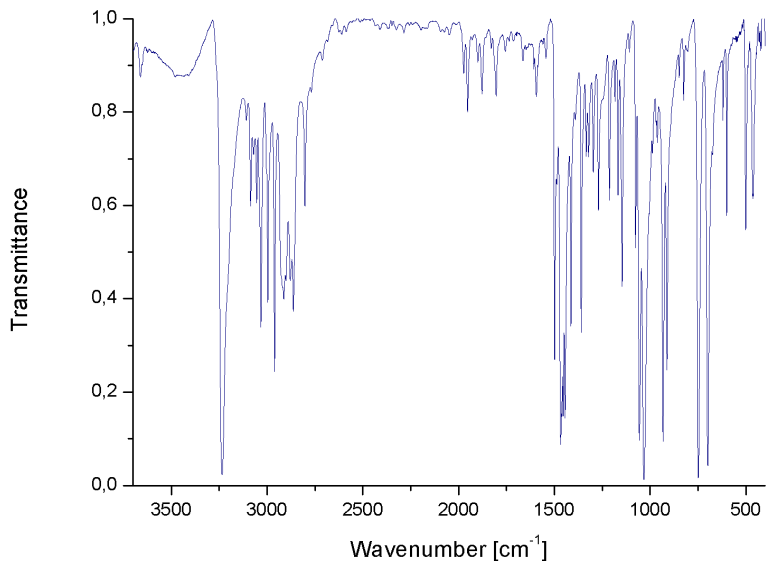
Table 5.91.: Infrared data of compound **3b**.

3446-3341 cm^{-1}	$\nu(\text{NMeH}_2^+)$	1456 cm^{-1}	$\delta(\text{CH}_2)$
----------------------------	------------------------	-----------------------	-----------------------

Compound 3c: [CuL³₂Cl₂] (L³ = N-methylbenzylamine)**Elemental analysis:**

C: 51.0% H: 5.8% N: 7.2% (Experimental)

C: 51.0% H: 5.9% N: 7.4% (Theoretical)

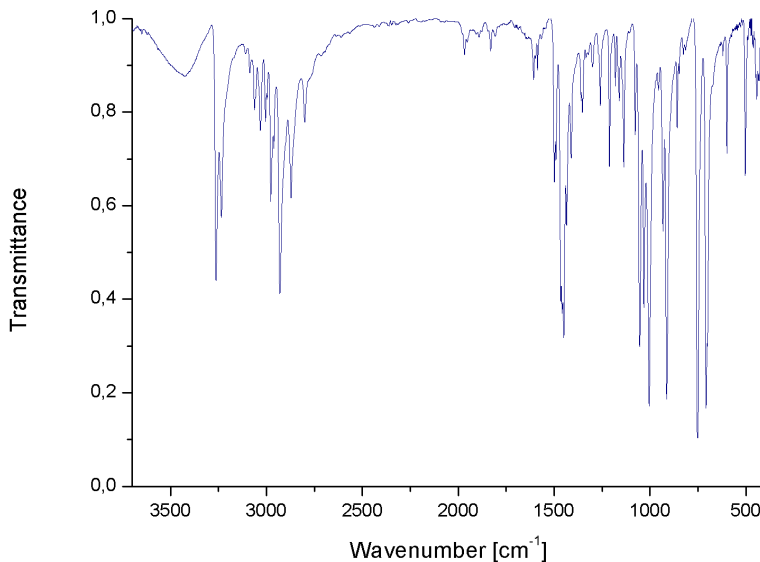
Figure 5.55.: Infrared spectrum of compound **3c**.Table 5.92.: Infrared data of compound **3c**.

3234 cm ⁻¹	$\nu(\text{NH})$	3086-2995 cm ⁻¹	$\nu(\text{Ar-H})$
2960-2802 cm ⁻¹	$\delta(\text{CH}_2)$	1498 cm ⁻¹	$\nu(\text{C=C})_{ar}$
1467 cm ⁻¹	$\delta(\text{CH}_2)$	749 cm ⁻¹	$\delta(\text{Ar-H})$
699 cm ⁻¹	$\delta(\text{C=C})_{ar}$	462 cm ⁻¹	$\nu(\text{Cu-N})$

Compound 3d: $[\text{CuL}^3_2\text{Cl}_2]$ ($\text{L}^3 = \text{N-methylbenzylamine}$)**Elemental analysis:**

C: 50.8 % H: 5.9 % N: 7.1 % (Experimental)

C: 51.0 % H: 5.9 % N: 7.4 % (Theoretical)

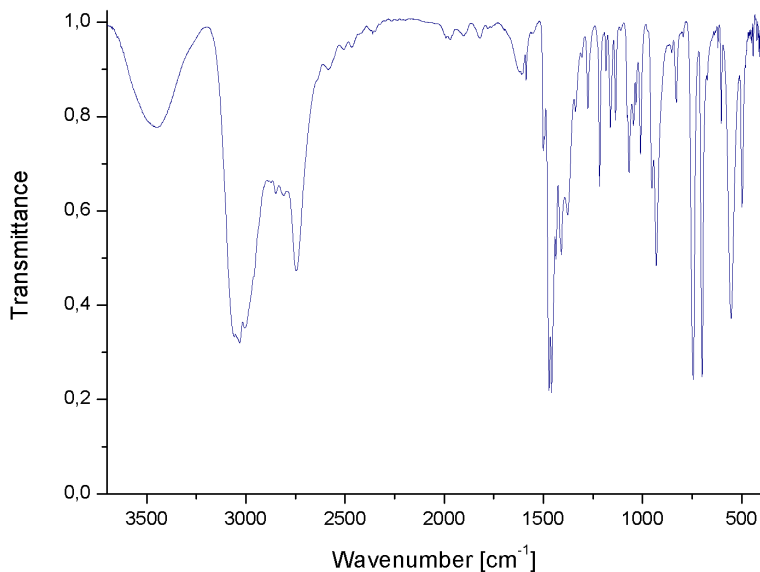
Figure 5.56.: Infrared spectrum of compound **3d**.Table 5.93.: Infrared data of compound **3d**.

3263 cm^{-1}	$\nu(\text{NH})$	3086-3032 cm^{-1}	$\nu(\text{Ar-H})$
2977-2800 cm^{-1}	$\delta(\text{CH}_2)$	1498 cm^{-1}	$\nu(\text{C=C})_{ar}$
1458 cm^{-1}	$\delta(\text{CH}_2)$	751 cm^{-1}	$\delta(\text{Ar-H})$
707 cm^{-1}	$\delta(\text{C=C})_{ar}$	443 cm^{-1}	$\nu(\text{Cu-N})$

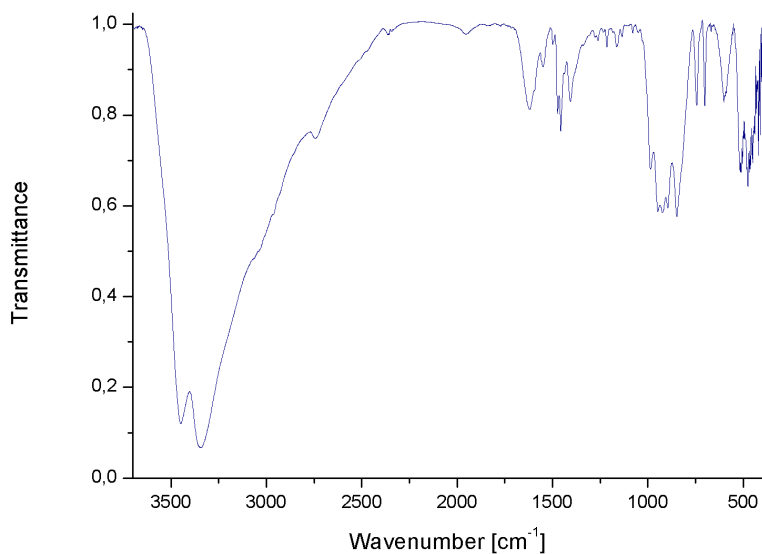
Compound 4a: $(HL^4)_2[CuCl_4] \cdot CuCl_2$ ($L^4 = N,N$ -dimethylbenzylamine)**Elemental analysis:**

C: 35.9 % H: 4.8 % N: 4.3 % (Experimental)

C: 35.3 % H: 4.8 % N: 4.6 % (Theoretical)

Figure 5.57.: Infrared spectrum of compound **4a**.Table 5.94.: Infrared data of compound **4a**.

3032 cm^{-1}	$\nu(\text{NHMe}_2^+)$	2746 cm^{-1}	$\nu(\text{CH}_2)$
1472 cm^{-1}	$\nu(\text{C}=\text{C})_{ar}$	1458 cm^{-1}	$\delta(\text{CH}_2)$
745 cm^{-1}	$\delta(\text{Ar-H})$	700 cm^{-1}	$\delta(\text{C}=\text{C})_{ar}$

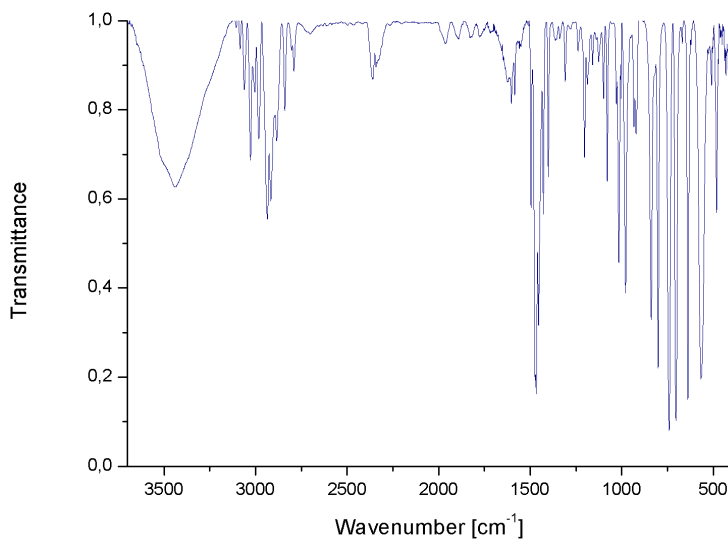
Compound 4bFigure 5.58.: Infrared spectrum of compound **4b**.Table 5.95.: Infrared data of compound **4b**.

3417-3337 cm^{-1}	$\nu(\text{NHMe}_2^+ + \text{OH})$	1478 cm^{-1}	$\nu(\text{C}=\text{C})_{ar}$
1458 cm^{-1}	$\delta(\text{CH}_2)$	743 cm^{-1}	$\delta(\text{Ar-H})$
703 cm^{-1}	$\delta(\text{C}=\text{C})_{ar}$		

Compound 4c/cluster IV: $[\text{Cu}_4\text{OCl}_6\text{L}^4_4]$ ($\text{L}^4 = \text{N,N-dimethylbenzylamine}$)**Elemental analysis:**

C: 40.0 % H: 4.9 % N: 4.5 % (Experimental)

C: 42.2 % H: 5.1 % N: 5.5 % (Theoretical)

Figure 5.59.: Infrared spectrum of compound **4c**.Table 5.96.: Infrared data of compound **4c**.

3127 cm^{-1}	$\nu(\text{NH}_3^+)$	2957 cm^{-1}	$\nu(\text{CH}_2)$
1574 cm^{-1}	$\delta(\text{NH}_2)$	1496 cm^{-1}	$\nu(\text{C}=\text{C})_{ar}$
1454 cm^{-1}	$\delta(\text{CH}_2)$	747 cm^{-1}	$\delta(\text{Ar-H})$
698 cm^{-1}	$\delta(\text{C}=\text{C})_{ar}$		

Compound 5a: $(HL^5)_2[CuCl_4] \cdot 1.5 CuCl_2$ ($L^5 = \text{cyclohexylamine}$)

Elemental analysis:

C: 24.2% H: 5.1% N: 4.5% (Experimental)

C: 23.7% H: 4.6% N: 4.6% (Theoretical)

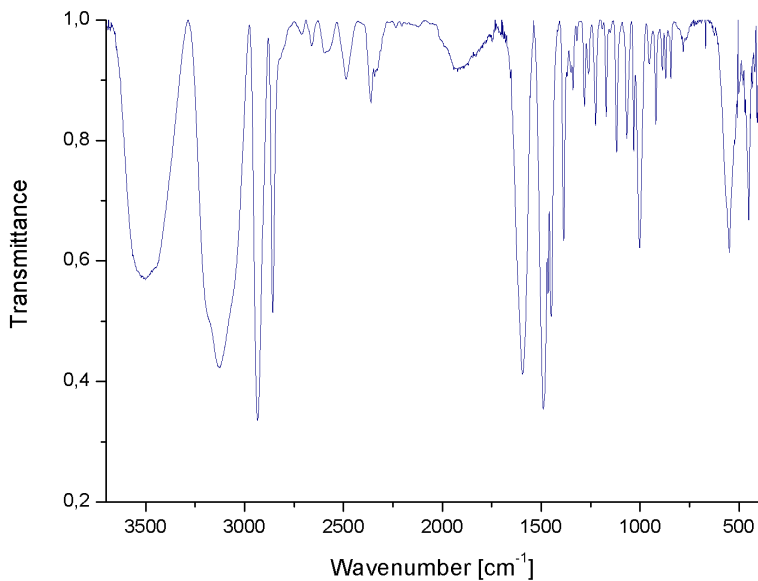
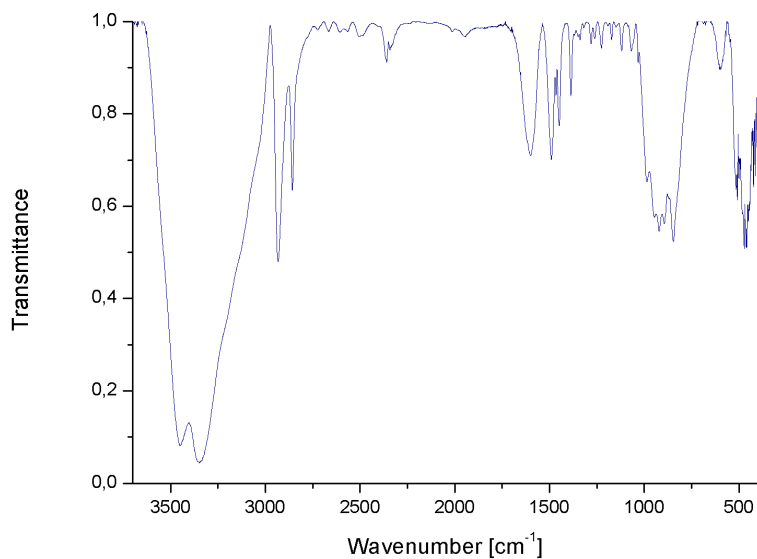


Figure 5.60.: Infrared spectrum of compound **5a**.

Table 5.97.: Infrared data of compound **5a**.

3132 cm^{-1}	$\nu(\text{NH}_3^+)$	2934-2858 cm^{-1}	$\nu(\text{CH}_2)$
1594 cm^{-1}	$\delta(\text{NH}_2)$	1489 cm^{-1}	$\delta(\text{CH}_2)$
451 cm^{-1}	$\nu(\text{Cu}_4\text{O})$		

Compound 5b

Figure 5.61.: Infrared spectrum of compound **5b**.Table 5.98.: Infrared data of compound **5b**.

3451-3356 cm ⁻¹	$\nu(\text{NH}_2+\text{OH})$	2933-2858 cm ⁻¹	$\nu(\text{CH}_2)$
1601 cm ⁻¹	$\delta(\text{NH}_2)$	1490 cm ⁻¹	$\delta(\text{CH}_2)$

5. Materials, Methods and Spectroscopy

Compound 5e: $[\text{CuL}^5_2\text{Cl}_2]$ ($\text{L}^5 = \text{cyclohexylamine}$)

Elemental analysis:

C: 43.0% H: 8.0% N: 8.1% (Experimental)

C: 43.8% H: 6.7% N: 8.5% (Theoretical)

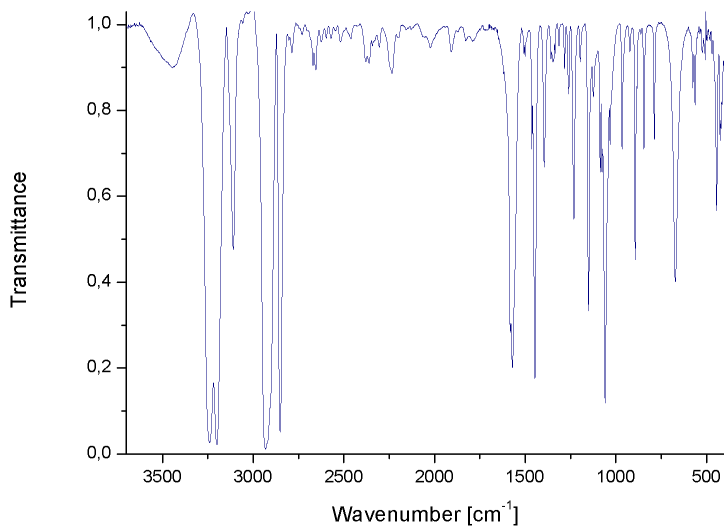


Figure 5.62.: Infrared spectrum of compound 5e.

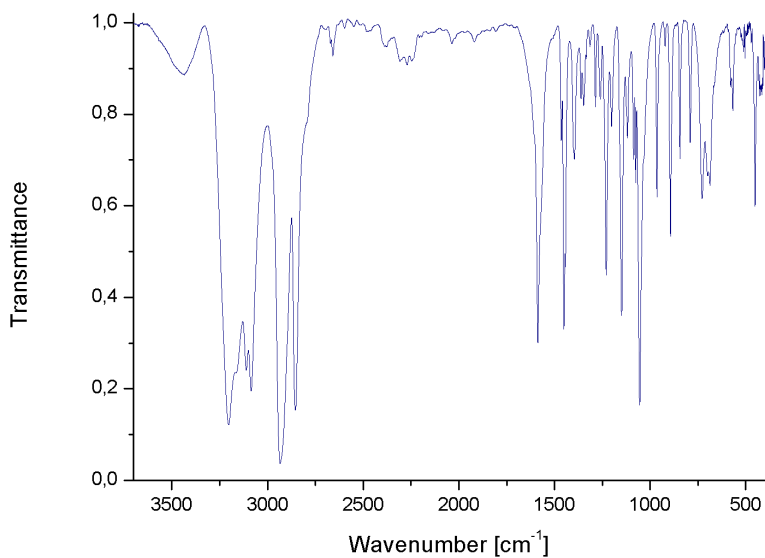
Table 5.99.: Infrared data of compound 5e.

3240-3201 cm^{-1}	$\nu(\text{NH}_2)$	2933-2851 cm^{-1}	$\nu(\text{CH}_2)$
1570 cm^{-1}	$\delta(\text{NH}_2)$	1447 cm^{-1}	$\delta(\text{CH}_2)$
1232 cm^{-1}	$\delta(\text{CH})$	445 cm^{-1}	$\nu(\text{Cu-N})$

Compound $[\text{CuL}^5_4]\text{Cl}_2$ ($\text{L}^5 = \text{cyclohexylamine}$)**Elemental analysis:**

C: 49.9 % H: 9.0 % N: 9.8 % (Experimental)

C: 53.4 % H: 11.2 % N: 10.4 % (Theoretical)

Figure 5.63.: Infrared spectrum of $[\text{CuL}^5_4]\text{Cl}_2$.Table 5.100.: Infrared data of $[\text{CuL}^5_4]\text{Cl}_2$.

3206-3282 cm^{-1}	$\nu(\text{NH}_2)$	2940-2852 cm^{-1}	$\nu(\text{CH}_2)$
1588 cm^{-1}	$\delta(\text{NH}_2)$	1451 cm^{-1}	$\delta(\text{CH}_2)$
1230 cm^{-1}	$\delta(\text{CH})$	453 cm^{-1}	$\nu(\text{Cu-N})$

Cluster V: $[\text{Cu}_4\text{OCl}_6\text{L}^5_4] \cdot \text{CH}_3\text{CN}$ ($\text{L}^5 = \text{cyclohexylamine}$)

Elemental analysis:

C: 33.2 % H: 5.9 % N: 7.3 % (Experimental)

C: 33.9 % H: 6.0 % N: 7.6 % (Theoretical)

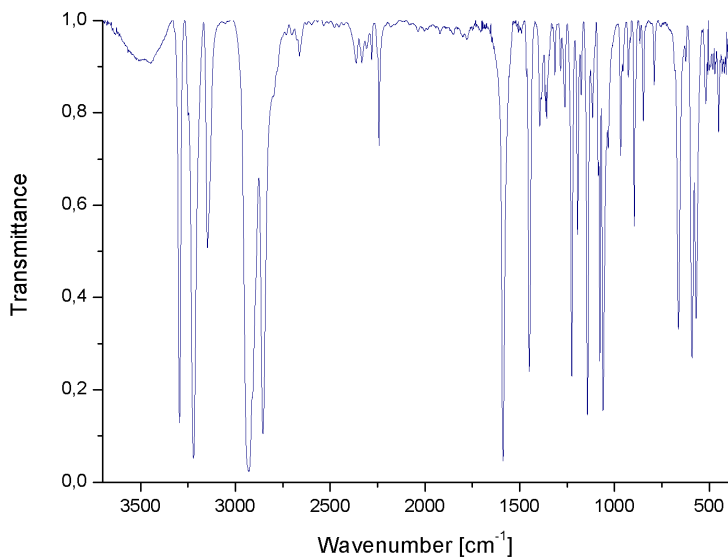


Figure 5.64.: Infrared spectrum of cluster V.

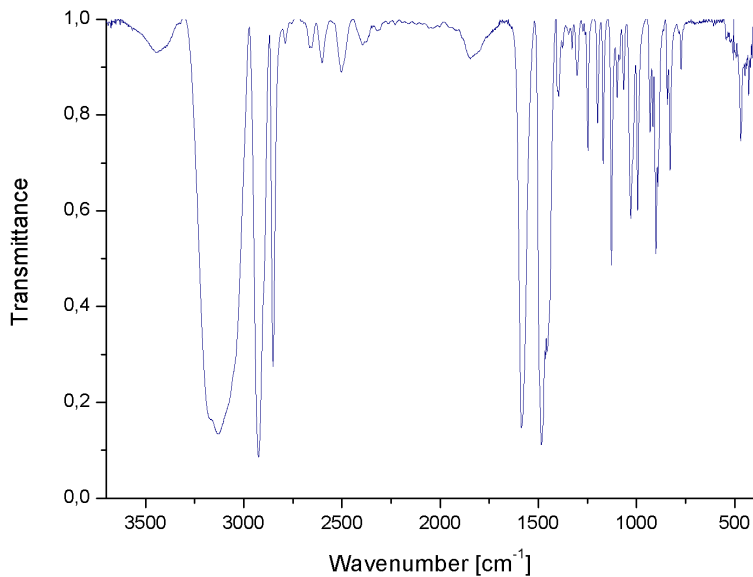
Table 5.101.: Infrared data of cluster V.

3295^{-1}	$\nu(\equiv\text{C}-\text{H})$	$3221\text{-}3147\text{ cm}^{-1}$	$\nu(\text{NH}_2)$
$2982\text{-}2854\text{ cm}^{-1}$	$\nu(\text{CH}_2)$	2242 cm^{-1}	$\nu(\text{C}\equiv\text{N})$
1588 cm^{-1}	$\delta(\text{NH}_2)$	1450 cm^{-1}	$\delta(\text{CH}_2)$
1225 cm^{-1}	$\delta(\text{CH})$	569 cm^{-1}	$\nu(\text{Cu}_4\text{O})$

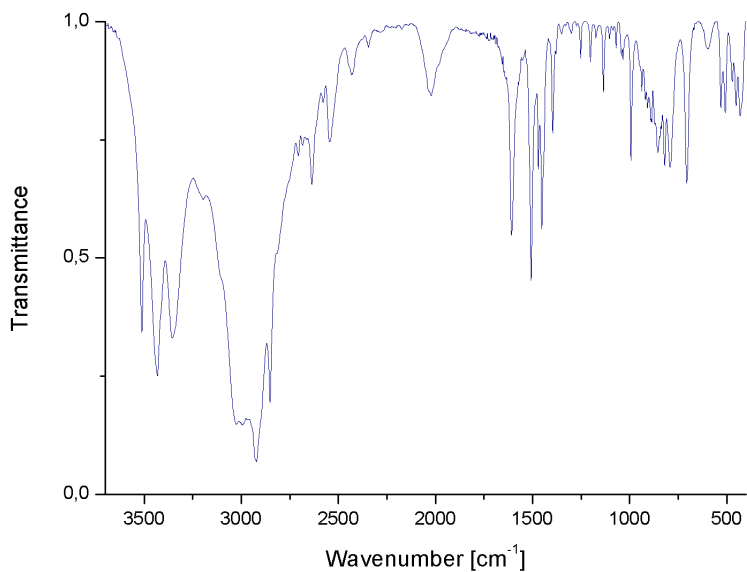
Compound 6a: (HL⁶)₂[CuCl₄] (L⁶ = cyclohexanemethylamine)**Elemental analysis:**

C: 38.6 % H: 7.4 % N: 6.3 % (Experimental)

C: 38.8 % H: 7.4 % N: 6.5 % (Theoretical)

Figure 5.65.: Infrared spectrum of compound **6a**.Table 5.102.: Infrared data of compound **6a**.

3127 cm ⁻¹	$\nu(\text{NH}_3^+)$	2924-2850 cm ⁻¹	$\nu(\text{CH}_2)$
1586 cm ⁻¹	$\delta(\text{NH}_2)$	1484 cm ⁻¹	$\delta(\text{CH}_2)$
1247 cm ⁻¹	$\delta(\text{CH})$		

Compound 6bFigure 5.66.: Infrared spectrum of compound **6b**.Table 5.103.: Infrared data of compound **6b**.

3432-3355 cm ⁻¹	$\nu(\text{NH}_2)$	2922-2706 cm ⁻¹	$\nu(\text{CH}_2)$
1608 cm ⁻¹	$\delta(\text{NH}_2)$	1452 cm ⁻¹	$\delta(\text{CH}_2)$
431 cm ⁻¹	$\nu(\text{Cu-N})$		

Compound 6c: $[\text{CuL}^6_2\text{Cl}_2] \cdot 0.5 (\text{CuCl}_2 \cdot 2 \text{H}_2\text{O})$
 ($\text{L}^6 = \text{cyclohexanemethylamine}$)

Elemental analysis:

C: 37.3 % H: 6.8 % N: 5.9 % (Experimental)

C: 37.7 % H: 7.2 % N: 6.3 % (Theoretical)

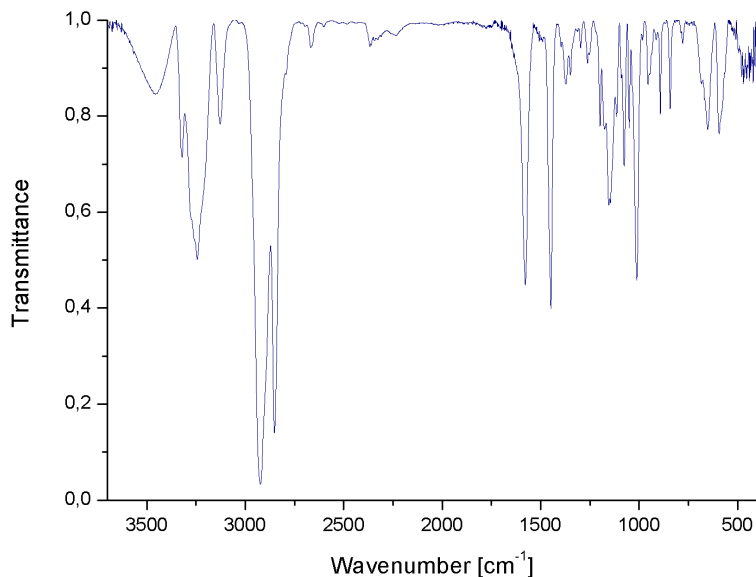


Figure 5.67.: Infrared spectrum of compound **6c**.

Table 5.104.: Infrared data of compound **6c**.

3244 cm^{-1}	$\nu(\text{NH}_2)$	$2923\text{-}2852 \text{ cm}^{-1}$	$\nu(\text{CH}_2)$
1577 cm^{-1}	$\delta(\text{NH}_2)$	1448 cm^{-1}	$\delta(\text{CH}_2)$

Compound 6d: $[\text{CuL}^6_4\text{Cl}_2]$ ($\text{L}^6 = \text{cyclohexanemethylamine}$)

Elemental analysis:

C: 56.3% H: 8.5% N: 7.6% (Experimental)

C: 57.3% H: 10.3% N: 9.5% (Theoretical)

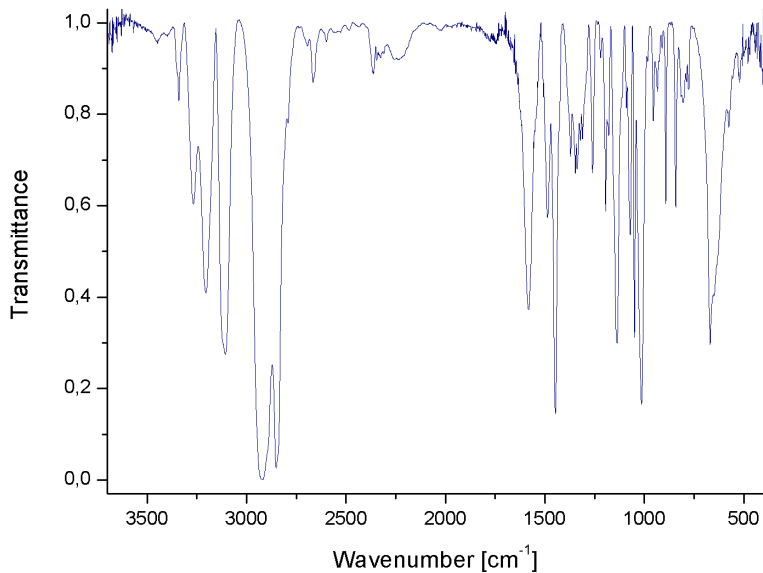


Figure 5.68.: Infrared spectrum of compound **6d**.

Table 5.105.: Infrared data of compound **6d**.

3268-3204 cm^{-1}	$\nu(\text{NH}_2)$	2920-2850 cm^{-1}	$\nu(\text{CH}_2)$
1582 cm^{-1}	$\delta(\text{NH}_2)$	1447 cm^{-1}	$\delta(\text{CH}_2)$
1260 cm^{-1}	$\delta(\text{CH})$		

Cluster VI: $[\text{Cu}_4\text{OCl}_6\text{L}^6_4] \cdot 1.5 [\text{CuL}^6_2\text{Cl}_2]$ ($\text{L}^6 = \text{cyclohexanemethylamine}$)**Elemental analysis:**

C: 39.4 % H: 7.2 % N: 6.5 % (Experimental)

C: 39.5 % H: 7.0 % N: 7.3 % (Theoretical)

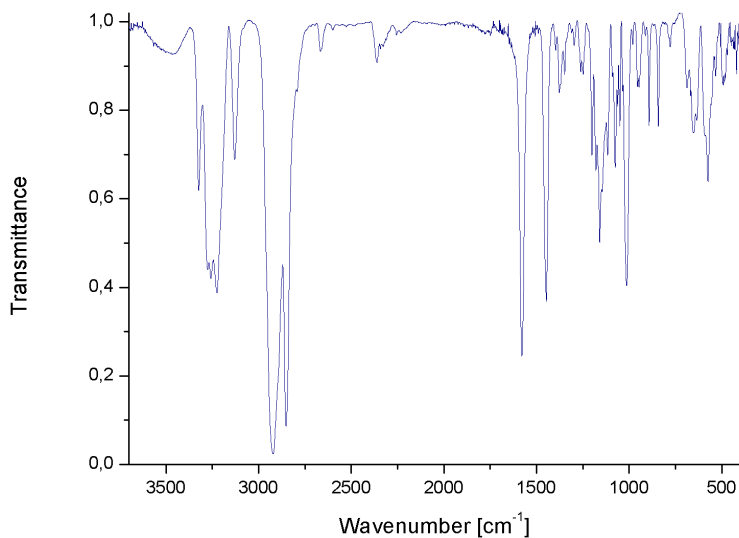


Figure 5.69.: Infrared spectrum of cluster VI.

Table 5.106.: Infrared data of cluster VI.

3323-3224 cm^{-1}	$\nu(\text{NH}_2)$	2921-2852 cm^{-1}	$\nu(\text{CH}_2)$
1580 cm^{-1}	$\delta(\text{NH}_2)$	1447 cm^{-1}	$\delta(\text{CH}_2)$
574 cm^{-1}	$\nu(\text{Cu}_4\text{O})$		

Compound 11: $[\text{Cu}_3\text{Cl}_6(\text{acetonitrile})_2] \cdot \text{CuCl}_2$

Elemental analysis:

C: 8.8 % H: 1.2 % N: 4.6 % (Experimental)

C: 7.8 % H: 1.0 % N: 4.5 % (Theoretical)

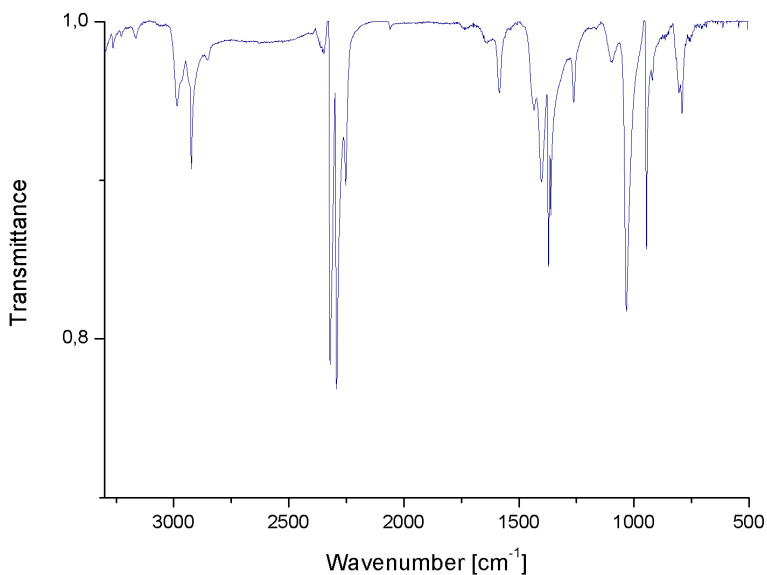


Figure 5.70.: Infrared spectrum of compound **11**.

Table 5.107.: Infrared data of compound **11**.

2982-2921 cm^{-1}	$\nu(\text{CH}_2)$	2316-2285 cm^{-1}	$\nu(\text{CN})$
1399-1368 cm^{-1}	$\delta(\text{CH})$		

Compound 14: [Cu(dmsO)₂Cl₂]**Elemental analysis:**

C: 16.5 % H: 4.1 % N: 0.0 % (Experimental)

C: 16.5 % H: 4.2 % N: 0.0 % (Theoretical)

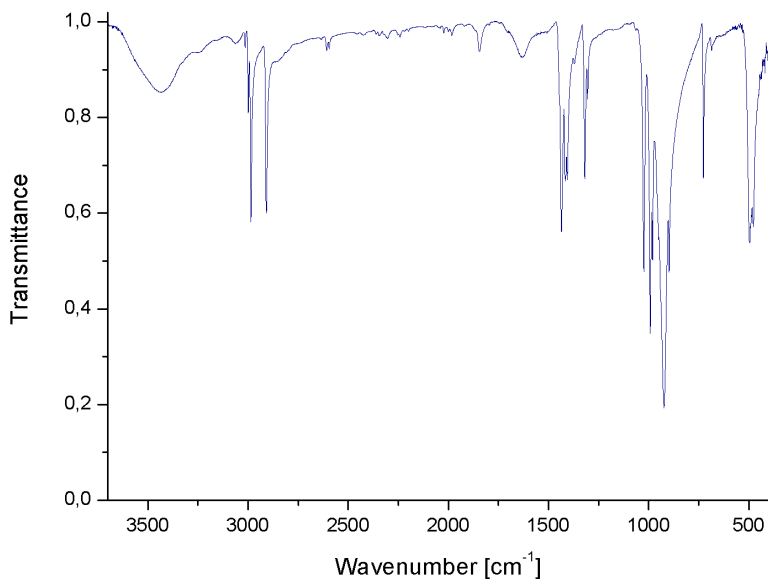


Figure 5.71.: Infrared spectrum of compound 14.

Table 5.108.: Infrared data of compound 14.

2985-2908 cm ⁻¹	$\nu(\text{CH}_2)$	1435 cm ⁻¹	$\delta(\text{CH}_2)$
991 cm ⁻¹	$\nu(\text{S}=\text{O})$		

Compound 15: $[\text{Cu}_4\text{OCl}_6(\text{MeOH})_4]$

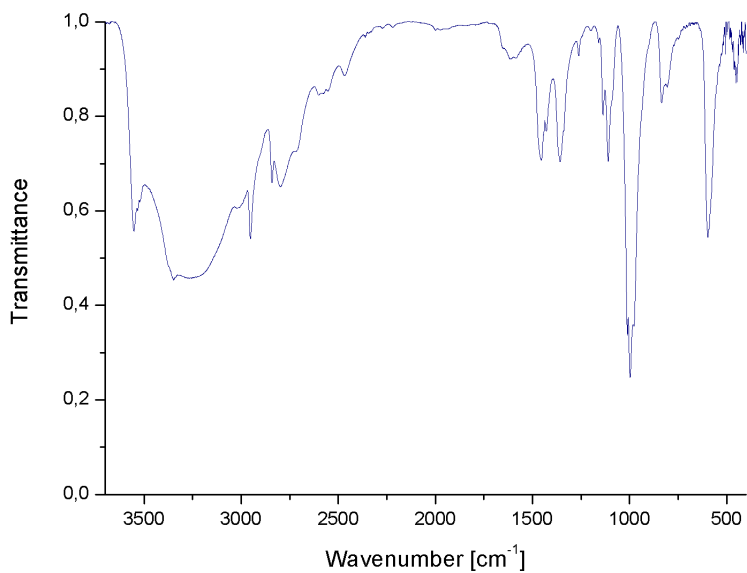


Figure 5.72.: Infrared spectrum of compound **15**.

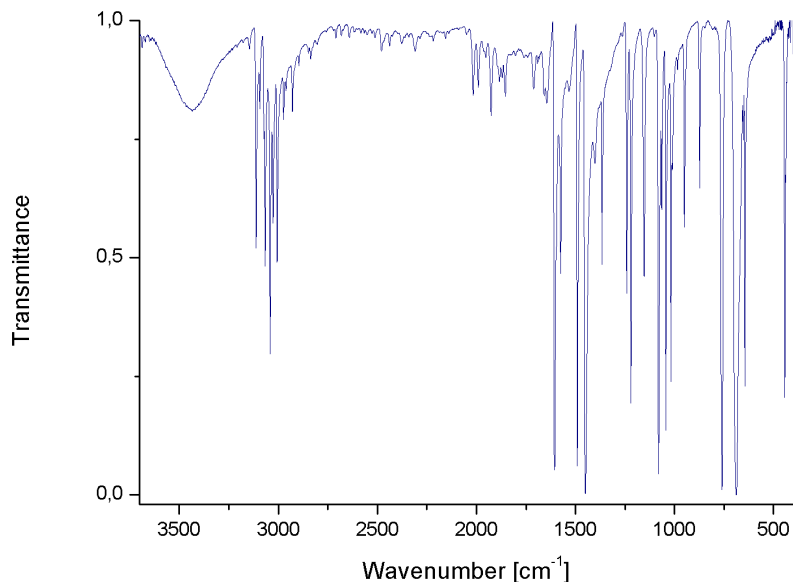
Table 5.109.: Infrared data of compound **15**.

3549-2951 cm^{-1}	$\nu(\text{OH})$	2803 cm^{-1}	$\nu(\text{CH}_2)$
1455 cm^{-1}	$\delta(\text{CH})$	1109 cm^{-1}	$\nu(\text{C-O})$
597 cm^{-1}	$\nu(\text{Cu}_4\text{O})$		

[Cu(pyridine)₂Cl₂]**Elemental analysis:**

C: 41.0% H: 3.4% N: 9.1% (Experimental)

C: 40.3% H: 3.4% N: 9.6% (Theoretical)

Figure 5.73.: Infrared spectrum of [Cu(pyridine)₂Cl₂].Table 5.110.: Infrared data of [Cu(pyridine)₂Cl₂].

3115-2976 cm ⁻¹	$\nu(\text{Ar-H})$	1606 cm ⁻¹	$\nu(\text{C=C})_{ar}$
1492 cm ⁻¹	$\nu(\text{C=C})_{ar}$	761 cm ⁻¹	$\delta(\text{Ar-H})$
687 cm ⁻¹	$\delta(\text{C=C})_{ar}$		

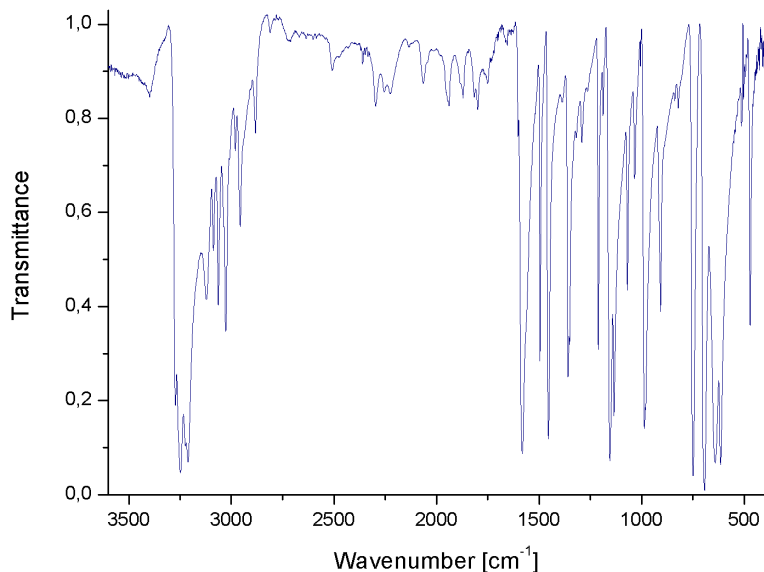
5.3.3. Data for Chapter 4

This chapter contains the elemental analyses and infrared data of the compounds presented in chapter 4. Most of the data are part of the Supporting Information of the manuscript in chapter 4. For detailed information concerning the nomenclature and abbreviations please see chapter 4.

[CuL¹Cl]₄ (L¹ = benzylamine)**Elemental analysis:**

C: 40.8 % H: 4.3 % N: 6.5 % (Experimental)

C: 40.8 % H: 4.4 % N: 6.8 % (Theoretical)

Figure 5.74.: Infrared spectrum of [CuL¹Cl]₄.Table 5.111.: Infrared data of [CuL¹Cl]₄.

3250-3211 cm ⁻¹	$\nu(\text{NH}_2)$	3121-3027 cm ⁻¹	$\nu(\text{Ar-H})$
1581 cm ⁻¹	$\delta(\text{NH}_2)$	1495 cm ⁻¹	$\nu(\text{C=C})_{ar}$
1454 cm ⁻¹	$\delta(\text{CH}_2)$	749 cm ⁻¹	$\delta(\text{Ar-H})$
692 cm ⁻¹	$\delta(\text{C=C})_{ar}$	471 cm ⁻¹	$\nu(\text{Cu-N})$

6. Summary/Zusammenfassung

6.1. Summary

Copper catalysts are very useful in industrial processes as well as in organic synthesis. They can be used as chlorination reagent, coupling reagent or as catalyst in oxygenation reactions. The enormous catalytic activity of copper is resembled in nature, too. Copper is incorporated in many active sites of enzymes and so part of many essential reactions of life on earth. So it is not very surprising that even simple copper salts such as copper chloride for example possesses catalytic activity in the named reactions. There is an increasing interest in the development of "green" catalysts, i. e. catalysts which are highly selective, without poisonous side-products, working under mild conditions - and in the ideal case are cost-efficient. Copper is an interesting candidate since it is not as expensive as the noble metals palladium or platinum, e. g. and shows catalytic potential in many reactions. Here multinuclear copper compounds could be of great interest, because they are able to store/provide more than one redox equivalent due to the higher number of copper centers. Two popular structure types of tetranuclear copper clusters are the cubane core $[\text{Cu}_4(\text{O-L})_4\text{Cl}_4]$ and the μ_4 -oxido cluster $[\text{Cu}_4\text{OX}_6\text{L}_4]$ (with $\text{X} = \text{Cl}, \text{Br}$, $\text{L} = \text{ligand}$). The goal of this work was to find out in more detail how such copper clusters as well as simple copper salts (copper(II) chloride e. g.) act as catalyst in organic redox reactions. The detailed understanding of this reactivity is important for the design and development of new copper catalysts. This work could answer important questions concerning the reaction mechanisms and so clearly contributes to the comprehension of the reactivity of copper compounds that are used as catalysts. The results are summarized in the following sections. For clarity they are presented in two parts, whereas the results of chapter 2 and 3 are summarized in one section and the results of chapter 4 are summarized separately.

6.1.1. Reaction of copper(II) chloride with benzylamine, its derivatives and solvent molecules

The catalytic activity of the μ_4 -oxido cluster $2[\text{Cu}_4\text{OCl}_6\text{L}^1_4] \cdot [\text{CuL}^1_2\text{Cl}_2]$ (cluster I, $\text{L}^1 = \text{benzylamine}$, see Figure 6.1) was tested in oxidation reactions and compared to the catalytic activity of copper(II) chloride. Cluster I can be easily prepared from inexpensive educts and possesses a high stability in air towards hydrolyses which enables an easy handling. This made cluster I a good candidate for investigations concerning its catalytic activity in oxidation reactions. However cluster I underwent many redox processes if stored in solution itself. Especially the reactions in denatured ethanol were interesting and led to a huge color gradient (see Figure 6.1).

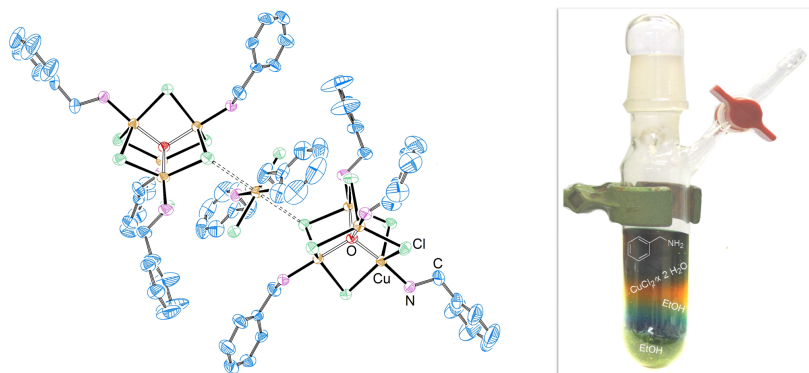


Figure 6.1.: Molecular structure of cluster I (ellipsoids set at the 50 % probability level, *left*) and a photograph of a suspension of cluster I in denatured ethanol (*right*).

In a large number of experiments it was finally possible to elucidate most of the compounds involved in the astonishing color gradient. An aimed synthetic route was established for most of these compounds and so they could be structurally characterized. Among them were the typical copper complexes $(\text{HL}^1)_2[\text{CuCl}_4]$, $[\text{CuL}^1_2\text{Cl}_2]$ and $[\text{CuL}^1_4\text{Cl}_2]$ shown in Figure 6.2.



Figure 6.2.: Structurally characterized copper(II) complexes that derived from cluster I.

These findings were not too surprising. But in addition some copper compounds could be isolated that are formed through redox reactions of cluster I. These copper compounds (see Figure 6.3) were closely related to each other and hence were always found together in samples of cluster I in denatured ethanol.



Figure 6.3.: Cluster II and copper(I) complexes that derived from cluster I.

Among them the formation of the cubane cluster II was most interesting. The ligand of cluster II was obviously formed by condensation between benzylamine and 2-butanone (which is added to ethanol to avoid its usage as drinking alcohol) and selective hydroxylation of this compound by cluster I (see Figure 6.4).

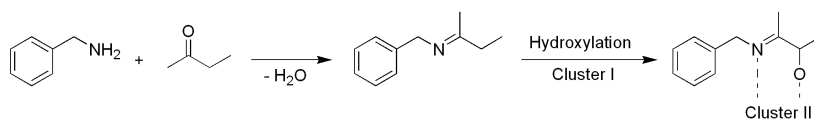


Figure 6.4.: Proposed formation of the ligand of cluster II.

Cluster II was obtained in good yields. In addition two copper(I) complexes were obtained as byproducts: $[Cu(benz_2mpa)_2]CuCl_2$ ($benz_2mpa = benzyl-(2-benzylimino-1-methyl-propylidene)-amine$) and $[CuL^1Cl]_3$ (Figure 6.3).

6. Summary/Zusammenfassung

The red colored complex $[\text{Cu}(\text{benz}_2\text{mpa})_2]\text{CuCl}_2$ converted to an orange colored compound under air (Figure 6.5). Despite many efforts this compound could not be characterized. In addition a pale bluish compound could be isolated, if cluster I was treated with water. But again despite much effort this compound could not be characterized. However infrared data suggested the formation of basic copper hydroxides.



Figure 6.5.: Isolated compounds that could not be structurally characterized.

The formation of copper(I) species rose the question of the reducing agent. In the case of ethanol acetaldehyde was formed as a byproduct of this redox equilibrium, which might explain the formation of copper(I) species. However a redox equilibrium could be observed in other solvents, too. Here the reducing agent could not be determined. Despite this problem the reactivity of cluster I in solution could be virtually elucidated so that cluster I could be tested in oxidation reactions as a catalyst as well.

Cluster I supported the oxidation of catechol and 2-aminophenol to the corresponding quinones. In addition it supported the oxygenation of aliphatic CH-bonds if H_2O_2 was added. In the case of cyclohexane a yield of 100% cyclohexanol could be reached. However benzaldehyde (deriving from benzylamine) occurred massively as byproduct. Cluster I was an active catalyst in the oxygenation of adamantane, too. Again, good yields could be obtained. Additionally the selective oxidation of *p*-chlorobenzylalcohol to *p*-chlorobenzaldehyde with *tert*-butylhydroperoxide was supported by cluster I. In all these reactions the choice of the solvent was important. Choosing acetone for example led to aldol condensation of acetone and followed Michael addition. $\text{CuCl}_2 \cdot 2\text{H}_2\text{O}$ exhibited a similar catalytic activity as cluster I in some of these reactions, e. g. the oxygenation of cyclohexane. This is consistent with the already mentioned catalytic activity of simple copper salts in many reactions. However again the reaction mechanism is not clarified. Complex reactions with more than one electron transfer require catalysts that can store/provide more than one electron at once. So it is very likely that there is no "naked" Cu^{2+} present in solution. Instead the formation of multinuclear cluster compounds with coordinating solvent molecules as ligands, that act as active species/catalyst is more likely. μ_4 -oxido "solvent clusters" are already known and their existence could be proven in this

work by the corresponding molecular structures as shown in Figure 6.6.

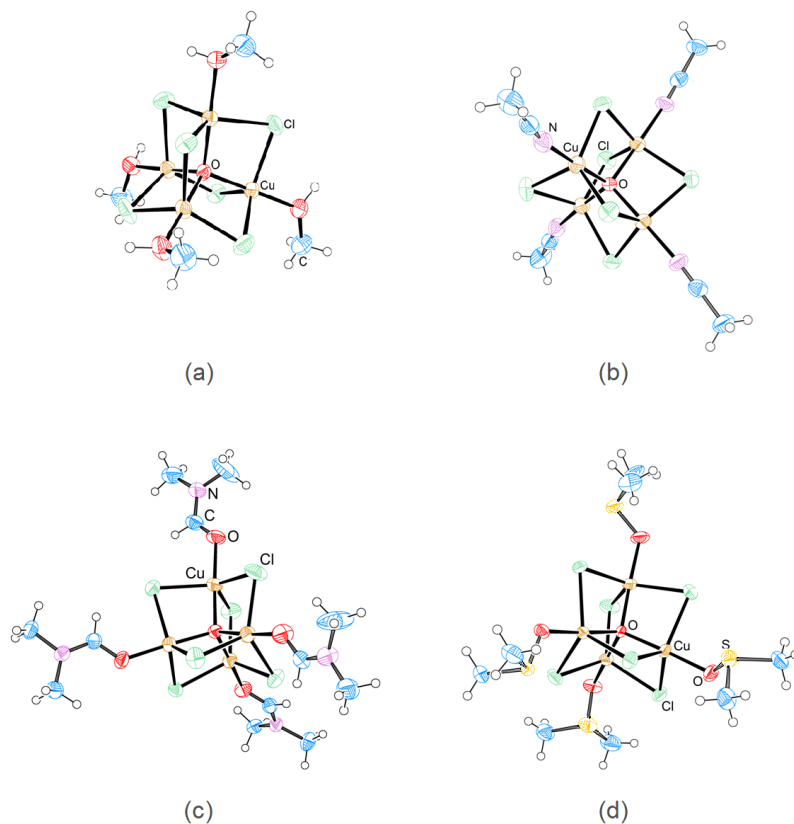


Figure 6.6.: Molecular structures of the "solvent clusters" with (a) methanol, (b) acetonitrile, (c) dmf and (d) dmsu as ligands.

Thus the formation of μ_4 -oxido copper clusters, especially the formation of the "solvent clusters" was of special interest. Hence in chapter 3 the formation of a μ_4 -oxido cluster unit was investigated with variations concerning the bridging halogenide, the central oxide and the ligands themselves. In addition the formation of "solvent clusters" deriving from copper(II) chloride and organic solvents was investigated.

6. Summary/Zusammenfassung

Concerning the variations of the cluster unit several experiments were carried out. Whereas the formation of a $[\text{Cu}_4\text{OBr}_6\text{L}^1]$ unit was possible, neither the formation of $[\text{Cu}_4\text{OF}_6\text{L}^1]$ nor $[\text{Cu}_4\text{SX}_6\text{L}_4]$ ($\text{X} = \text{Cl}, \text{Br}, \text{L} = \text{acetonitrile}, \text{MeOH}$) was observed. Concerning the last example it is suggested that the sulfide ion with a van-der-waals radius of 184 pm (O^{2-} : 140 pm) is too large for the central position. However instead of μ_4 -oxido clusters interesting copper(I) and copper(II) solvent complexes were obtained. The variation of the ligand led to different results. Benzylamine was exchanged with its derivatives phenethylamine (L^2), N-methylbenzylamine (L^3), N,N-dimethylbenzylamine (L^4), cyclohexylamine (L^5) and cyclohexanemethylamine (L^6). Cluster formation was possible with all chosen ligands except N-methylbenzylamine. However the formation did not always occur as spontaneously as in the case of benzylamine: Cluster formation with L^5 and L^6 was only possible under inert conditions. Two conclusions can be drawn from these experiments and especially the crystallization behavior of the obtained clusters. Firstly co-crystallization with the copper complex $[\text{CuL}_2\text{Cl}_2]$ (as observed for L^1 , L^2 and L^6) enhances stability towards hydrolysis due to a shielding effect of the complexes. Secondly sterically hindering residues at the N-donor atom seem to prevent such co-crystallization (as observed for L^4 and L^5) but increases stability towards hydrolysis little as well.

As mentioned above the formation of "solvent clusters" starting from copper(II) chloride and organic solvents was of special interest. For this purpose $\text{CuCl}_2 \cdot 2\text{H}_2\text{O}$ was recrystallized in diverse solvents to investigate a possible cluster formation. Several copper species were obtained and structurally characterized: $[\text{CuCl}_2] \cdot \text{H}_2\text{O} \cdot 0.5$ acetone, $[\text{Cu}_3\text{Cl}_6(\text{acetonitrile})_2]$, $[\text{Cu}_2\text{Cl}_4(\text{acetonitrile})_2]$, $(\text{H}_2\text{N}(\text{CH}_3)_2)_2[\text{CuCl}_3]$ and $[\text{Cu}(\text{dmsO})_2\text{Cl}_2]$. Some of these compounds showed $[\text{CuCl}_2]$ -chains known from dry CuCl_2 although water was present in solution. However μ_4 -oxido copper clusters were not obtained. Using the dihydrate of copper(II) chloride meant that the central oxygen of the μ_4 -oxido core should derive from water. This again made the use of a base in order to deprotonate the water molecules unavoidable. So recrystallization of a mixture of CuCl_2 and $\text{CuCl}_2 \cdot 2\text{H}_2\text{O}$ in methanol was repeated with adding the base NaO^tBu . Here the "solvent cluster" $[\text{Cu}_4\text{OCl}_6(\text{MeOH})_4]$ was obtained in very good yields. This clearly showed how easy cluster formation occurred even in the presence of water molecules. Thus similar cluster formation is very likely if copper(II) chloride in addition with a base is used as a catalyst for organic syntheses. Regarding the conditions of a cluster formation it is very likely that in most cases when copper(II) chloride is used as a catalyst a μ_4 -oxido copper cluster will be formed from copper(II) chloride and solvent molecules: In most cases coordinating solvents are used. If that is not the case often small donor

molecules as pyridine e. g. are added which increase the yield dramatically. In addition commonly bases as NaO^tBu are added as a co-reagent. These reaction conditions are ideal for a cluster formation of copper(II) chloride with solvent molecules so that probably in most cases, copper(II) chloride is used as a catalyst a "solvent cluster" of the μ_4 -oxido or similar type will be formed. Similar conclusions can be drawn for catalysis with copper(I) chloride, because commercial available CuCl is contaminated mostly with traces of copper(II) chloride and water. In addition (as shown for cluster I) copper clusters may be in a chemical equilibrium with copper(I) species. In order to find out if "solvent clusters" are catalytically active, they were tested in the oxygenation of cyclohexane and compared to cluster I and copper(II) chloride. Here the catalytic activity of these "solvent clusters" could be shown for the first time. Interestingly the reaction behavior of the "solvent clusters" and copper(II) chloride was nearly identical. This observation - namely the nearly identical reaction behavior of copper(II) chloride and the "solvent clusters" - clearly shows that cluster formation is an essential part during the reaction mechanism starting from simple copper salts as copper(II) chloride. It could be shown for the first time in this work that the formation of such "solvent clusters" is not limited to aimed synthetic routes, but is under appropriate conditions an ubiquitous phenomenon. In addition it could be shown for the first time that "solvent clusters" are catalytically active indeed. Thus the formation of multinuclear compounds as "solvent clusters" can explain the discrepancy between the capability of storing/providing electrons by simple copper salts as copper(II) chloride and the in the reaction involved electrons. So apparently these "solvent clusters" are very important for the understanding of stoichiometric or catalytic reactions with copper(II) chloride. This does not only answer the important question of how copper(II) chloride can act as a catalyst in complex organic reactions but does in consequence mean that the proposed mechanisms of catalytic reactions with copper(II) chloride have to be reviewed for many known syntheses.

Although not all questions concerning the reaction behavior of copper chloride and copper cluster complexes could be answered in this work the correlation between these compounds clearly could be demonstrated. Thus further investigations concerning the cluster formation are very important because they can provide more insight into the complex reactivity of the CuCl_2 /ligand system. This in turn is important for the development of new potential catalysts based on copper.

6.1.2. Reaction of copper(I) chloride with benzylamine

As shown in chapter 2 there was a complex chemical equilibrium between copper(II) and copper(I) species. Many of the copper(I) species could be characterized and have already been discussed in the first section of the summary. Because of this participation of copper(I) species, the reactivity of copper(I) chloride towards benzylamine was investigated in chapter 4. It turned out that the reactivity of copper(I) chloride in solution was quite complex as well. While not all reactions could be elucidated so far it was possible to isolate and structurally characterize some of the species formed. For example mixing CuCl and benzylamine led to the formation of the linear compound $[\text{CuCIL}^1]_4$ (see Figure 6.7). This was unexpected because usually when adding a (monodentate) ligand to a solution of CuCl the cubane cluster $[\text{Cu}_4\text{Cl}_4\text{L}_4]$ is obtained.

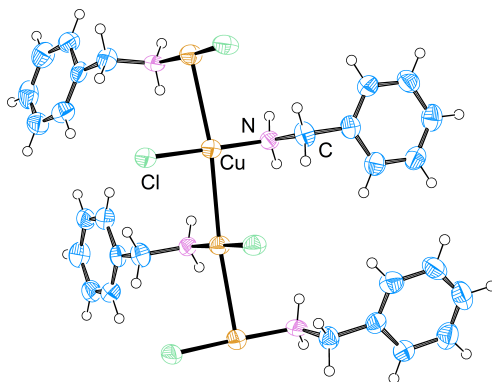


Figure 6.7.: Molecular structure of $[\text{CuCIL}^1]_4$. Ellipsoids are set at the 50 % probability level.

This structure exhibited $\text{Cu}^I \cdots \text{Cu}^I$ interactions with a distance of 2.89 Å. The same compound (only crystallized as trimer in the asymmetric unit) was already found as byproduct of the redox reactions cluster I supported. So the reactivity of $[\text{CuCIL}^1]_4$ towards dioxygen and derivatives was tested in order to find out if this copper(I) compound played an important role in dioxygen activation during the redox reactions of cluster I. However $[\text{CuCIL}^1]_4$ was extraordinary stable under air and only slowly reacted with

dioxygen to give a green colored solution, which was investigated via UV-vis spectroscopy. However since the reaction of dioxygen with multinuclear copper species is very complex, neither the mechanism nor the Cu/O_2 species could be elucidated. There are only little reports in literature about activating dioxygen with multinuclear copper compounds and none for activation with compounds that exhibits $\text{Cu}^I \cdots \text{Cu}^I$ interactions. In addition experiments concerning the ability as oxygenation catalyst were performed. But no oxygenation reaction could be observed. The extraordinary stability of $[\text{CuCIL}^1]_4$ was astonishing. The weak $\text{Cu}^I \cdots \text{Cu}^I$ interactions might be responsible for this stability. However only little is known about $\text{Cu}^I \cdots \text{Cu}^I$ interactions, so it would be of great interest to investigate compounds such as $[\text{CuCIL}^1]_4$ in more detail. For this purpose DFT calculations are probably essential.

6.2. Zusammenfassung

Kupferkatalysatoren sind sowohl in industriellen Prozessen als auch in der organischen Synthese weit verbreitet. Sie können als Chlorierungsmittel, Kupplungsreagenz oder als Katalysator in Oxygenierungsreaktionen verwendet werden. Die enorme katalytische Aktivität von Kupferverbindungen zeigt sich auch in der Natur. Kupfer ist in vielen aktiven Zentren von Enzymen eingebaut und somit Bestandteil vieler essentieller Reaktionen des Lebens auf der Erde. So ist es auch nicht verwunderlich, dass sogar einfache Kupfersalze wie beispielsweise Kupferchlorid ebenfalls katalytische Reaktivität in den genannten Reaktionen aufweisen. Es besteht wachsendes Interesse an der Entwicklung von „grünen“ Katalysatoren, d. h. Katalysatoren, die hochselektiv sind, unter milden Bedingungen und ohne giftige Nebenprodukte zu erzeugen arbeiten - und im Idealfall auch kostengünstig sind. Kupfer ist hierbei ein interessanter Kandidat, da es nicht so teuer wie Edelmetalle (z. B. Palladium oder Platin) ist und in vielen Reaktionen katalytisches Potential zeigt. Hier könnten vor allem mehrkernige Kupferverbindungen von großem Interesse sein, da sie durch die erhöhte Anzahl an Kupferzentren dazu in der Lage sind mehr als ein Redoxäquivalent zu speichern/zur Verfügung zu stellen. Zwei weit verbreitete Struktur motive vierkerniger Kupfercluster sind der Kubankern $[\text{Cu}_4(\text{O-L})_4\text{Cl}_4]$ und der μ_4 -oxido-Cluster $[\text{Cu}_4\text{OX}_6\text{L}_4]$ (mit $\text{X} = \text{Cl}, \text{Br}, \text{L} = \text{Ligand}$). Das Ziel dieser Arbeit war herauszufinden, wie sich solche Kupfercluster als auch einfache Kupfersalze (z. B. Kupfer(II)-Chlorid) im Detail als Katalysator in organischen Redoxreaktionen verhalten. Das detaillierte Verständnis dieser Reaktivität ist für das Design und die Entwicklung von neuen Kupferkatalysatoren wichtig. Diese Arbeit konnte wichtige

6. Summary/Zusammenfassung

Fragen hinsichtlich der Reaktionsmechanismen beantworten und trägt so eindeutig zum Verständnis der Reaktivität von Kupferverbindungen, die als Katalysator benutzt werden, bei. Die Ergebnisse werden in den nachfolgenden Abschnitten zusammengefasst. Zum besseren Verständnis werden sie in zwei Teilen präsentiert, wobei die Ergebnisse von den Kapiteln 2 und 3 in einem Abschnitt zusammengefasst werden und die Ergebnisse von Kapitel 4 separat behandelt werden.

6.2.1. Reaktionen von Kupfer(II)-Chlorid mit Benzylamin

Die katalytische Aktivität des μ_4 -oxido-Clusters $2[\text{Cu}_4\text{OCl}_6\text{L}^1_4] \cdot [\text{CuL}^1_2\text{Cl}_2]$ (Cluster I, $\text{L}^1 = \text{Benzylamin}$, siehe Abbildung 6.8) wurde in Oxidationsreaktionen getestet und mit der katalytischen Aktivität von Kupfer(II)-Chlorid verglichen. Cluster I kann einfach aus kostengünstigen Edukten hergestellt werden und zeigt eine hohe Stabilität an Luft gegenüber Hydrolyse, welches eine einfache Handhabung gewährleistet. Durch diese Eigenschaften war Cluster I ein geeigneter Kandidat für Untersuchungen bezüglich der katalytischen Aktivität in Oxidationsreaktionen. Allerdings zeigte dieser Cluster viele Redoxreaktionen in Lösung. Insbesondere die in vergälltem Ethanol beobachteten Reaktionen waren interessant und führten zu einer großen Farbvielfalt (vgl. Abbildung 6.8).

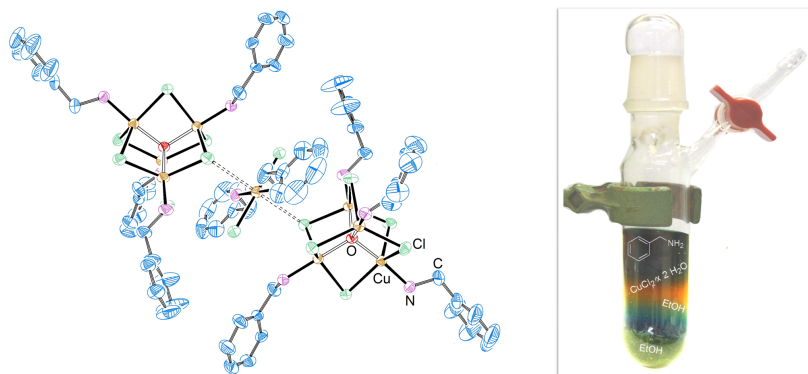


Abbildung 6.8.: Molekülstruktur von Cluster I (Ellipsoide mit 50% Aufenthaltswahrscheinlichkeit, *links*) und eine Fotografie einer Suspension von Cluster I in vergälltem Ethanol (*rechts*).

Durch eine Vielzahl von Experimenten war es letztendlich möglich, einen Großteil dieses Farbverlaufes aufzuklären. Für die meisten Verbindungen konnten gezielte Synthesewege gefunden werden, so dass die Charakterisierung möglich war. Darunter befanden sich typische Kupferkomplexe wie $(HL^1)_2[CuCl_4]$, $[CuL^1_2Cl_2]$ und $[CuL^1_4Cl_2]$ wie in Abbildung 6.9 gezeigt.



Abbildung 6.9.: Vollständig charakterisierte Kupfer(II)-Komplexe, die aus Cluster I entstanden.

Diese Ergebnisse waren nicht allzu überraschend. Allerdings konnten außerdem einige Kupferverbindungen isoliert werden, die durch Redoxreaktionen mit Cluster I entstanden waren. Diese Verbindungen (vgl. Abbildung 6.10) waren eng miteinander verwandt und wurden dementsprechend immer zusammen in Ansätzen von Cluster I in vergälltem Ethanol gefunden.



Abbildung 6.10.: Cluster II und Kupfer(I)-Komplexe, die ausgehend von Cluster I gebildet wurden.

Unter diesen war die Bildung von Cluster II am interessantesten. Der Ligand von Cluster II wurde offensichtlich durch eine Kondensation von Benzylamin und 2-Butanon (Vergällungsmittel) mit anschließender, selektiver Hydroxylierung durch Cluster I gebildet (vgl. Abbildung 6.11).

6. Summary/Zusammenfassung

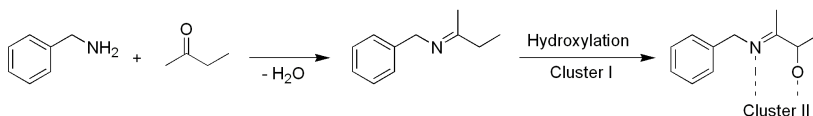


Abbildung 6.11.: Vorgeschlagene Bildung des Liganden von Cluster II.

Cluster II wurde in guten Ausbeuten erhalten. Zusätzlich wurden zwei Kupfer(I)-Komplexe als Nebenprodukte erhalten: $[\text{Cu}(\text{benz}_2\text{mpa})_2]\text{CuCl}_2$ ($\text{benz}_2\text{-mpa}$ = benzyl-(2-benzylimino-1-methyl-propyliden)-amin) und $[\text{CuL}^1\text{Cl}]_3$ (vgl. Abbildung 6.10). Der rote Komplex $[\text{Cu}(\text{benz}_2\text{mpa})_2]\text{CuCl}_2$ wandelte sich an Luft in einen orange gefärbten Feststoff um (vgl. Abbildung 6.12). Trotz vieler Bemühungen konnte diese Verbindung nicht charakterisiert werden. Zusätzlich konnte eine hellblaue Verbindung isoliert werden, die aus der Reaktion von Cluster I mit Wasser hervorging. Aber auch diese konnte trotz starker Bemühungen nicht charakterisiert werden. IR-Daten lassen jedoch die Bildung basischer Kupferhydroxide vermuten.



Abbildung 6.12.: Isolierte Verbindungen, die nicht vollständig charakterisiert werden konnten.

Durch die Bildung von Kupfer(I)-Verbindungen stellte sich die Frage nach dem Reduktionsmittel. Im Falle von Ethanol wurde Acetaldehyd als Nebenprodukt gebildet, welches die Bildung von Kupfer(I)-Verbindungen erklären könnte. Allerdings konnte auch in anderen Lösungsmitteln ein Redoxgleichgewicht beobachtet werden. Hier konnte das Reduktionsmittel jedoch nicht bestimmt werden. Abgesehen von diesem Problem konnte die Reaktivität von Cluster I in Lösung nahezu vollständig aufgeklärt werden, so dass Cluster I auch als Katalysator in Redoxreaktionen getestet werden konnte.

Cluster I katalysierte die Oxidation von Catechol und 2-Aminophenol zu den entsprechenden Chinonen. Zusätzlich katalysierte er die Oxygenierung von aliphatischen CH -Bindungen wenn H_2O_2 zugesetzt wurde. Im Falle von Cyclohexan konnte eine Ausbeute von 100% Cyclohexanol erreicht werden. Allerdings entstand hierbei Benzaldehyd (welches aus Benzylamin gebildet wurde) massiv als Nebenprodukt. Cluster I war außerdem ein aktiver Kata-

lyikator in der Oxygenierung von Adamantan. Auch hier konnten gute Ausbeuten erhalten werden. Des Weiteren wurde die selektive Oxidation von *p*-Chlorbenzylalkohol zu *p*-Chlorbenzaldehyd mit *tert*-Butylhydroperoxid durch Cluster I katalysiert. In all diesen Reaktion war die Wahl des Lösungsmittels entscheidend. Wenn Aceton anstelle von Acetonitril benutzt wurde, führte dies zu einer Aldolkondensation und nachfolgender Michael Addition. $\text{CuCl}_2 \cdot 2 \text{H}_2\text{O}$ zeigte bei einigen der genannten Reaktionen eine ähnliche katalytische Aktivität wie Cluster I, hierunter beispielsweise die Oxygenierung von Cyclohexan. Dieses ist konsistent mit der bereits erwähnten katalytischen Aktivität einfacher Kupfersalze in vielen Reaktionen. Allerdings ist hierbei der Reaktionsmechanismus ungeklärt. Komplexe Reaktionen mit mehr als einem Elektronentransfer benötigen Katalysatoren, die in der Lage sind mehr als ein Elektron zu speichern/zur Verfügung zu stellen. Dadurch ist es sehr wahrscheinlich, dass keine „nackten“ Cu^{2+} -Ionen in der Lösung vorliegen. Stattdessen ist die Bildung mehrkerniger Clusterverbindungen mit koordinierenden Lösungsmittelmolekülen als Liganden, die dann als aktive Spezies fungieren, wahrscheinlicher. μ_4 -oxido-„Lösungsmittelcluster“ sind bereits bekannt und ihre Existenz konnte in dieser Arbeit durch die entsprechenden Molekülstrukturen (wie in Abbildung 6.13 gezeigt) bewiesen werden.

Dadurch war die Bildung dieser μ_4 -oxido-Kupfercluster, insbesondere die Bildung der „Lösungsmittelcluster“ von besonderem Interesse. Deswegen wurde in Kapitel 3 die Bildung der μ_4 -Oxido-Einheit mit Veränderungen hinsichtlich des verbrückenden Halogenids, des zentralen Oxids und der Liganden selber untersucht. Zusätzlich wurde die Bildung von „Lösungsmittelclustern“ ausgehend von Kupfer(II)-Chlorid und organischen Lösungsmitteln untersucht.

Hinsichtlich der Variationen der Clustereinheit wurden mehrere Experimente durchgeführt. Während die Bildung einer $[\text{Cu}_4\text{OBr}_6\text{L}^1_4]$ -Einheit möglich war, konnte hingegen weder die Bildung von $[\text{Cu}_4\text{OF}_6\text{L}^1_4]$ oder $[\text{Cu}_4\text{SX}_6\text{L}_4]$ ($\text{X} = \text{Cl}, \text{Br}, \text{L} = \text{Acetonitril}, \text{MeOH}$) beobachtet werden. Bezüglich des letztgenannten Beispiels wird angenommen, dass das Sulfidion mit einem Van-der-Waals-Radius von 184 pm ($\text{O}^{2-} = 140 \text{ pm}$) zu groß für die zentrale Position ist. Allerdings konnten anstelle von μ_4 -oxido-Clustern interessante Kupfer(I)- und Kupfer(II)-Lösungsmittelkomplexe erhalten werden. Die Variation des Ligandensystems führte zu unterschiedlichen Ergebnissen. Benzylamin wurde mit dessen Derivaten Phenethylamin (L^1), N-Methylbenzylamin (L^3), N,N-Dimethylbenzylamin (L^4), Cyclohexylamin (L^5) und Cyclohexanmethylanilin (L^6) ausgetauscht.

6. Summary/Zusammenfassung

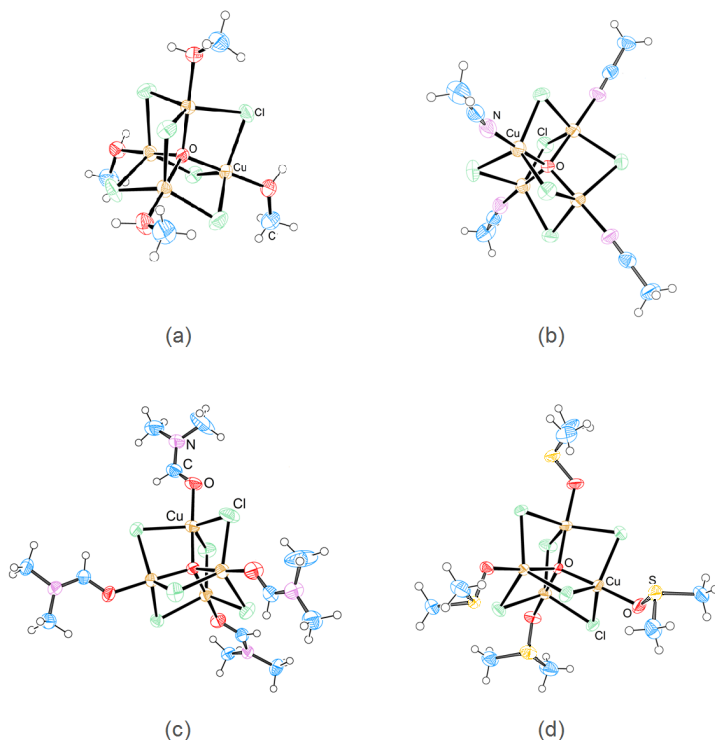


Abbildung 6.13.: Strukturen der „Lösungsmittelcluster“ mit (a) Methanol, (b) Acetonitril, (c) DMF and (d) DMSO.

Eine Clusterbildung war mit allen Liganden außer N-Methylbenzylamin möglich. Allerdings trat die Clusterbildung nicht immer so spontan wie im Falle von Benzylamin auf: Eine Clusterbildung mit L^5 und L^6 war nur unter inerten Bedingungen möglich. Zwei Rückschlüsse können aus diesen Experimenten und insbesondere dem Kristallisationsverhalten der erhaltenen Cluster gezogen werden: Erstens erhöht eine Co-Kristallisation mit dem Komplex $[\text{CuL}_2\text{Cl}_2]$ die Stabilität gegenüber Hydrolyse (wie für L^1 , L^2 und L^6 beobachtet). Und zweitens verhindern sterisch anspruchsvolle Reste am N-Donor-Atom offenbar eine Co-Kristallisation, erhöhen jedoch ebenfalls die Stabilität gegenüber Hydrolyse geringfügig.

Wie bereits beschrieben war die Bildung von „Lösungsmittelclustern“ ausge-

hend von Kupfer(II)-Chlorid und organischen Lösungsmitteln von besonderem Interesse. Hierzu wurde $\text{CuCl}_2 \cdot 2\text{H}_2\text{O}$ in diversen Lösungsmitteln umkristallisiert um eine mögliche Clusterbildung zu untersuchen. Verschiedenste Kupferspezies wurden hierbei erhalten und charakterisiert: $[\text{CuCl}_2] \cdot \text{H}_2\text{O} \cdot 0.5 \text{ Aceton}$, $[\text{Cu}_3\text{Cl}_6(\text{Acetonitril})_2]$, $[\text{Cu}_2\text{Cl}_4(\text{Acetonitril})_2]$, $(\text{H}_2\text{N}(\text{CH}_3)_2)_2\text{-}[\text{CuCl}_3]$ und $[\text{Cu}(\text{DMSO})_2\text{Cl}_2]$. Einige dieser Verbindungen wiesen $[\text{CuCl}_2]$ -Ketten auf, die man von trockenem CuCl_2 her kennt, obwohl Wasser in der Lösung vorhanden war. Allerdings wurden keine μ_4 -oxido-Cluster erhalten. Beim Einsatz des Dihydrats von Kupfer(II)-Chlorid sollte die Bildung des μ_4 -oxido-Kerns aus dem Kristallwasser ermöglichen. Dieses wiederum machte den Einsatz einer Base um das Wasser zu deprotonieren unumgänglich. Deswegen wurde die Umkristallisation einer Mischung aus $\text{CuCl}_2 \cdot 2\text{H}_2\text{O}$ und trockenem CuCl_2 mit Zugabe der Base NaO^tBu wiederholt. Hierbei wurde der „Lösungsmittelcluster“ $[\text{Cu}_4\text{OCl}_6(\text{MeOH})_4]$ in sehr guten Ausbeuten erhalten. Dieses zeigt, wie einfach sich Cluster sogar in Anwesenheit von Wassermolekülen bilden können. Dadurch ist eine ähnliche Clusterbildung sehr wahrscheinlich wenn Kupfer(II)-Chlorid zusammen mit einer Base als Katalysator in der organischen Synthese verwendet wird. Wenn man die Bedingungen für eine Clusterbildung betrachtet ist es sehr wahrscheinlich, dass in den meisten Fällen, wenn Kupfer(II)-Chlorid als Katalysator benutzt wird, μ_4 -oxido-Cluster ausgehend von Kupfer(II)-Chlorid und organischen Lösungsmittelmolekülen gebildet werden: In den meisten Fällen werden koordinierende Lösungsmittel verwendet. Falls dies nicht der Fall ist, werden oft kleine Donormoleküle wie beispielsweise Pyridin zugegeben, die dann die Ausbeute dramatisch erhöhen. Zusätzlich werden üblicherweise Basen wie NaO^tBu als Co-Reagenz verwendet. Diese Reaktionsbedingungen sind ideal für die Clusterbildung von Kupfer(II)-Chlorid mit Lösungsmittelmolekülen, so dass vermutlich in den meisten Fällen, wenn Kupfer(II)-Chlorid als Katalysator verwendet wird, „Lösungsmittelcluster“ des μ_4 -oxido-Typs oder ähnlicher Typen gebildet werden. Ähnliche Rückschlüsse können für katalytische Reaktionen mit Kupfer(I)-Chlorid gezogen werden, da kommerziell erhältliches CuCl meistens mit Spuren von Kupfer(II)-Chlorid und Wasser verunreinigt ist. Außerdem können Kupfercluster (wie für Cluster I gezeigt) im chemischen Gleichgewicht mit Kupfer(I)-Spezies stehen. Um herauszufinden, ob diese „Lösungsmittelcluster“ katalytisch aktiv sind, wurden sie in der Oxygenierung von Cyclohexan getestet und mit Cluster I und Kupfer(II)-Chlorid verglichen. Hier konnte erstmals die katalytische Aktivität dieser „Lösungsmittelcluster“ gezeigt werden. Interessanterweise war das Verhalten der „Lösungsmittelcluster“ nahezu identisch mit dem von Kupfer(II)-Chlorid. Diese Beobachtung - nämlich das nahezu identische Reaktionsverhalten von Kupfer(II)-Chlorid und den Lösungsmittelclustern -

6. Summary/Zusammenfassung

zeigt deutlich, dass die Clusterbildung einen essentiellen Teil im Reaktionsmechanismus ausgehend von einfachen Kupfersalzen wie Kupfer(II)-Chlorid darstellt. In dieser Arbeit konnte erstmals gezeigt werden, dass die Bildung solcher „Lösungsmittelcluster“ nicht auf gezielte Synthesewege limitiert ist, sondern unter geeigneten Reaktionsbedingungen ein allgemein auftretendes Phänomen ist. Zusätzlich konnte erstmals gezeigt werden, dass diese „Lösungsmittelcluster“ tatsächlich katalytisch aktiv sind. Dadurch kann die Bildung mehrkerniger Verbindungen wie „Lösungsmittelcluster“ die Diskrepanz zwischen der Kapazität Elektronen zu speichern/bereit zu stellen und der Anzahl der in der Reaktion involvierten Elektronen für einfache Kupfersalze wie Kupfer(II)-Chlorid erklären. Dementsprechend sind diese „Lösungsmittelcluster“ sehr wichtig für das Verständnis von stöchiometrischen oder katalytischen Reaktionen mit Kupfer(II)-Chlorid. Dieses beantwortet nicht nur die wichtige Frage, wie Kupfer(II)-Chlorid als Katalysator in komplexen organischen Reaktionen wirken kann, sondern hat auch zur Folge, dass die vorgeschlagenen Mechanismen katalytischer Reaktionen mit Kupfer(II)-Chlorid für viele bekannte Synthesen überdacht werden müssen.

Obwohl in dieser Arbeit nicht alle Fragen hinsichtlich des Reaktionsverhaltens von Kupferchlorid und Kupfer-Cluster-Komplexen beantwortet werden konnten, konnte der Zusammenhang zwischen diesen Verbindungen klar demonstriert werden. Dadurch sind zukünftige Untersuchungen bezüglich der Clusterbildung sehr wichtig, da diese mehr Einsicht in die komplexe Reaktivität des CuCl_2 /Liganden-Systems versprechen. Dieses ist wiederum für die Entwicklung neuer, potenter auf Kupfer basierender Katalysatoren notwendig.

6.2.2. Reaktionen von Kupfer(I)-Chlorid mit Benzylamin

Wie in Kapitel 2 gezeigt bestand ein komplexes chemisches Gleichgewicht zwischen Kupfer(II)- und Kupfer(I)-Spezies. Viele dieser Kupfer(I)-Spezies konnten charakterisiert werden und wurden bereits im ersten Abschnitt der Zusammenfassung erläutert. Durch die Beteiligung von Kupfer(I)-Spezies wurde in Kapitel 4 die Reaktivität von Kupfer(I)-Chlorid gegenüber Benzylamin untersucht. Es zeigte sich, dass auch die Reaktivität von Kupfer(I)-Chlorid in Lösung sehr komplex war. Während nicht alle Reaktionen aufgeklärt werden konnten, war es dennoch möglich einige dieser Verbindungen zu isolieren und strukturell zu charakterisieren. Zum Beispiel führte das Vermischen von CuCl und Benzylamin zur Bildung der linearen Verbindung $[\text{CuClL}^1]_4$ (vgl. Abbildung 6.14). Dieses war unerwartet, da für gewöhnlich, wenn ein (einzähniger) Ligand zu einer Lösung von CuCl zugegeben wird,

der Kubancluster $[\text{Cu}_4\text{Cl}_4\text{L}_4]$ erhalten wird.

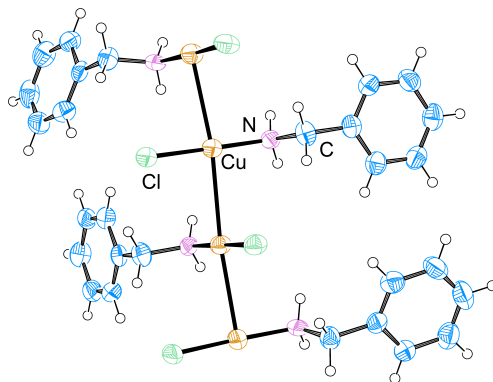


Abbildung 6.14.: Molekülstruktur von $[\text{CuCIL}^1]_4$. (Temperaturrellipsoide mit 50 % Aufenthaltswahrscheinlichkeit).

Diese Struktur zeigt $\text{Cu}^I \cdots \text{Cu}^I$ -Wechselwirkungen mit einem Abstand von 2.89 Å. Die gleiche Verbindung (nur als Trimer in der asymmetrischen Einheit kristallisiert) wurde bereits als Nebenprodukt bei denen durch Cluster I verursachten Redoxreaktionen gefunden. Deswegen wurde die Reaktivität von $[\text{CuL}^1\text{Cl}]_4$ gegenüber Sauerstoff(-derivaten) getestet, um herauszufinden, ob diese Kupfer(I)-Verbindung eine wichtige Rolle in der Sauerstoffaktivierung während der Redoxreaktionen von Cluster I spielte. Allerdings erwies sich $[\text{CuL}^1\text{Cl}]_4$ als außerordentlich stabil an Luft und reagierte nur langsam mit Sauerstoff um eine grüne Lösung zu bilden, welche mit UV-Vis-Spektroskopie untersucht wurde. Da allerdings die Reaktion von Sauerstoff mit mehrkernigen Kupferspezies sehr komplex ist, konnte weder der Mechanismus noch die Cu/O_2 -Spezies aufgeklärt werden. Es gibt nur wenige Berichte in der Literatur über Sauerstoffaktivierung mittels mehrkerniger Kupferverbindungen und keine über Sauerstoffaktivierung mit Verbindungen, die $\text{Cu}^I \cdots \text{Cu}^I$ -Wechselwirkungen aufweisen. Es wurden weiterhin Experimente zur Fähigkeit als Katalysator in Oxygenierungsreaktionen durchgeführt. Allerdings konnten keine Oxygenierungsreaktionen beobachtet werden. Die außerordentliche Stabilität von $[\text{CuL}^1\text{Cl}]_4$ war erstaunlich. Die schwachen $\text{Cu}^I \cdots \text{Cu}^I$ -Wechselwirkungen könnten dafür verantwortlich sein. Nur wenig ist bisher über $\text{Cu}^I \cdots \text{Cu}^I$ -Wechselwirkungen bekannt, deswegen ist es von

6. *Summary/Zusammenfassung*

großem Interesse Verbindungen wie $[\text{CuL}^1\text{Cl}]_4$ nähergehend zu untersuchen. Hierbei sind DFT-Berechnungen vermutlich unerlässlich.

7. List of Figures

1.1.	Overview of the most common copper ores.	1
1.2.	General reaction equation for the Sandmeyer reaction.	3
1.3.	General reaction equation for the Glaser reaction.	3
1.4.	Proposed mechanism for the Wacker-Hoechst-Process.	5
1.5.	Equation for the oxidation of benzene according to [22].	6
1.6.	Equation for the oxidation of phenol according to [23].	6
1.7.	Equation for the oxygenation of alkanes according to [24], [25].	7
1.8.	Schematic presentation of the cubane unit $\text{Cu}_4\text{O}_4\text{L}_4\text{X}_4$ and $\text{Cu}_4\text{OX}_6\text{L}_4$	8
1.9.	Crystalline pomarevite and the volcano Tolbachik in Kamchatka, where pomarevite was found.	9
2.1.	Schematic presentation of the $\text{Cu}_4\text{OX}_6\text{L}_4$ and cubane unit $\text{Cu}_4\text{O}_4\text{L}_4\text{X}_4$	18
2.2.	Molecular structure of cluster I.	19
2.3.	Overview of the color range of cluster I and related compounds.	20
2.4.	Detailed view of a section in a flask containing a mixture of benzylamine and copper(II) chloride in denatured ethanol.	21
2.5.	Molecular structure of 2	22
2.6.	Molecular structure of 3	23
2.7.	Molecular structure of cluster II.	24
2.8.	Molecular structure of compound 7	25
2.9.	Molecular structure of compound 4a	26
2.10.	Hydroxylation of cyclohexane and n-hexane by cluster I.	28
2.11.	Molecular structure of $\text{HC}_{13}\text{H}_{19}\text{NOCl}$	29
2.12.	Proposed (a) aldol condensation and (b) Michael addition for the formation of $\text{HC}_{13}\text{H}_{19}\text{NOCl}$	30
2.13.	Molecular structure of $[\text{Cu}(\text{aniline})_2\text{Cl}_2]$	31
2.14.	Molecular structure of the "methanol cluster".	32
2.15.	Molecular structure of the complex $[\text{Cu}(\text{MeOH})_2\text{Cl}_2]$	33
2.16.	Color change of cluster I in denatured ethanol.	40
2.17.	Comparison of cluster I in denatured ethanol before and after color change.	40
2.18.	Chlorination of 2-butanone supported by cluster I.	41

7. List of Figures

2.19.	Gas chromatogram of the oxygenation of cyclohexane.	42
2.20.	MS spectra of cyclohexanol and cyclohexanone.	42
2.21.	Photograph of the reaction solutions after the oxygenation reactions.	44
2.22.	UV-vis spectrum of the oxidation of 2-aminophenol.	46
2.23.	Oxidation products of allyl alcohol and norbornene.	47
2.24.	Molecular structure of $[\text{Zn}(\text{benz}_2\text{dba})\text{Cl}_2]$	47
2.25.	Proposed mechanism of the formation of benz ₂ dba.	48
2.26.	Photographs of the crystals obtained from the "methanol cluster" and the "acetonitrile cluster".	49
2.27.	Molecular structure of the "acetonitrile cluster".	49
2.28.	Molecular structure of the "dmsc cluster".	50
2.29.	Molecular structure of the "dmf cluster".	50
3.1.	Molecular structure of the mineral ponomarevite.	54
3.2.	Some ligands that were found by chance to form a cluster with copper(II) chloride.	55
3.3.	Schematic illustration of $[\text{Cu}_4\text{OCl}_6\text{L}_4]$ with highlighted positions to diversify the system.	62
3.4.	Overview of the ligands which were used to modify cluster I.	63
3.5.	Overview of the products that were obtained by adding L^2 - L^6 to $\text{CuCl}_2 \cdot 2\text{H}_2\text{O}$ in different stoichiometric amounts.	64
3.6.	Molecular structure of cluster III.	65
3.7.	Molecular structure of $[\text{CuL}_2^3\text{Cl}_2]$	66
3.8.	Molecular structure of cluster IV.	67
3.9.	Color change caused by hydrolysis of cluster IV if it is stored under atmospheric conditions.	68
3.10.	Molecular structure of $[\text{CuL}_4^5]\text{Cl}_2$	69
3.11.	Photographs of the obtained copper cluster compounds with the ligands L^2 , L^3 , L^4 , L^5 and L^6	70
3.12.	Molecular structure of cluster VI.	71
3.13.	Coordination of the complexes to the cluster unit.	72
3.14.	Molecular structure of $[\text{Cu}(\text{acetonitrile})_4][\text{Cu}_2\text{Br}_4]$ compound 7	74
3.15.	Molecular structure of $[\text{Cu}(\text{acetonitrile})\text{Br}]$	75
3.16.	Molecular structure of $[\text{Cu}(\text{acetonitrile})\text{Br}_2]$ (compound 9).	75
3.17.	Part of the polymeric structure of compound 10	77
3.18.	Molecular structure of $[\text{Cu}_3(\text{acetonitrile})_2\text{Cl}_6]$ (compound 11).	77
3.19.	Molecular structure of $[\text{Cu}_2(\text{acetonitrile})_2\text{Cl}_4]$ (compound 12).	78
3.20.	Molecular structure of $(\text{H}_2\text{N}(\text{CH}_3)_2)_2[\text{CuCl}_3]$ (compound 13).	79
3.21.	Comparison of the IR spectra of the crystalline "methanol cluster" and compound 15	80

3.22.	Oxygenation of cyclohexane with cluster I.	83
3.23.	Oxygenation of adamantane.	85
3.24.	MS spectra of adamantan-1-ol and adamantan-1-one.	86
3.25.	Gas chromatogram of the oxygenation reaction of adamantane with cluster I as catalyst.	87
3.26.	Oxidation of solvent molecules as side-reactions.	87
3.27.	Molecular structure of HL^3Cl	88
3.28.	Molecular structure of HL^4Cl	88
3.29.	Molecular structure of HL^5Cl	89
3.30.	Molecular structure of cluster I recrystallized.	89
4.1.	Schematic representation of the structural motif of a copper(I) cubane core and a μ_4 -oxido copper(II) cluster.	94
4.2.	Molecular structure of $[\text{CuL}^1\text{Cl}]_4$ (1).	95
4.3.	UV-vis spectra of the reaction of compound 1 towards dioxygen.	97
4.4.	Infrared and near-infrared part of the UV-vis spectra of the reaction of compound 1 towards dioxygen.	98
4.5.	Molecular structure of $[\text{CuL}_2^1\text{Cl}_2]$ (compound 3).	98
4.6.	UV-vis spectra of compound 1 , 3 , the "oxygen-adduct" and cluster I.	99
4.7.	Proposed reaction for the formation of 3-benzylimino-butan-2-olate.	100
4.8.	Molecular structure of the cation of compound 4	101
4.9.	Molecular structure of $(\text{HL}^1)(\text{C}_7\text{H}_7\text{NHCOO})$	102
4.10.	Photographs of a solution of $[\text{CuL}^1\text{Cl}]_4$ before and after the reaction with O_2	106
4.11.	Photographs of a solution of $[\text{CuL}_2^1\text{Cl}_2]$ and cluster I.	106
4.12.	Molecular structure of the anion of compound 4	107
5.1.	ORTEP plot of cluster I.	113
5.2.	ORTEP plot of the bromide version of cluster I.	116
5.3.	ORTEP plot of cluster II.	119
5.4.	ORTEP plot of compound 2	121
5.5.	ORTEP plot of compound 3	123
5.6.	ORTEP plot of compound 4a	125
5.7.	ORTEP plot of compound 7	127
5.8.	ORTEP plot of $\text{HC}_{13}\text{H}_{19}\text{NOCl}$	129
5.9.	ORTEP plot of $[\text{Zn}(\text{benz}_2\text{dba})\text{Cl}_2]$	131
5.10.	ORTEP plot of $[\text{Cu}(\text{aniline})_2\text{Cl}_2]$	133
5.11.	ORTEP plot of the "methanol cluster".	135
5.12.	ORTEP plot of the "acetonitrile cluster".	137

7. List of Figures

5.13.	ORTEP plot of the "dmsO cluster".	140
5.14.	ORTEP plot of the "dmf cluster".	143
5.15.	ORTEP plot of $[\text{Cu}(\text{MeOH})_2\text{Cl}_2]$	145
5.16.	ORTEP plot of cluster III.	149
5.17.	ORTEP plot of compound 3c	152
5.18.	ORTEP plot of compound 3d	154
5.19.	ORTEP plot of cluster IV.	156
5.20.	ORTEP plot of $[\text{CuL}_4^5]\text{Cl}_2$	159
5.21.	ORTEP plot of cluster VI.	161
5.22.	ORTEP plot of HL^3Cl	164
5.23.	ORTEP plot of HL^4Cl	165
5.24.	ORTEP plot of HL^5Cl	167
5.25.	ORTEP plot of compound 7	169
5.26.	ORTEP plot of compound 8	171
5.27.	ORTEP plot of compound 9	173
5.28.	ORTEP plot of compound 10	175
5.29.	ORTEP plot of compound 11	177
5.30.	ORTEP plot of compound 12	179
5.31.	ORTEP plot of compound 13	181
5.32.	ORTEP plot of compound 14	183
5.33.	ORTEP plot of cluster I recrystallized.	185
5.34.	ORTEP plot of compound 1	189
5.35.	ORTEP plot of compound 3	191
5.36.	ORTEP plot of compound 4	193
5.37.	ORTEP plot of $(\text{HL}^1)(\text{C}_7\text{H}_7\text{NHCOO})$	195
5.38.	Infrared spectrum of cluster I.	197
5.39.	Infrared spectrum of the bromide version of cluster I.	198
5.40.	Infrared spectrum of cluster II.	199
5.41.	Infrared spectrum of compound 1	200
5.42.	Infrared spectrum of compound 2	201
5.43.	Infrared spectrum of compound 3	202
5.44.	Infrared spectrum of compound 4	203
5.45.	Infrared spectrum of compound 5	204
5.46.	Infrared spectrum of compound 6	205
5.47.	Infrared spectrum of compound 7	206
5.48.	Infrared spectrum of the aniline complex.	207
5.49.	Infrared spectrum of $[\text{ZnL}^1_2\text{Cl}_2]$	208
5.50.	Infrared spectrum of compound 2a	210
5.51.	Infrared spectrum of cluster III.	211
5.52.	Infrared spectrum of compound 2d	212
5.53.	Infrared spectrum of compound 3a	213
5.54.	Infrared spectrum of compound 3b	214

5.55. Infrared spectrum of compound 3c	215
5.56. Infrared spectrum of compound 3d	216
5.57. Infrared spectrum of compound 4a	217
5.58. Infrared spectrum of compound 4b	218
5.59. Infrared spectrum of compound 4c	219
5.60. Infrared spectrum of compound 5a	220
5.61. Infrared spectrum of compound 5b	221
5.62. Infrared spectrum of compound 5e	222
5.63. Infrared spectrum of $[\text{CuL}^5_4]\text{Cl}_2$	223
5.64. Infrared spectrum of cluster V.	224
5.65. Infrared spectrum of compound 6a	225
5.66. Infrared spectrum of compound 6b	226
5.67. Infrared spectrum of compound 6c	227
5.68. Infrared spectrum of compound 6d	228
5.69. Infrared spectrum of cluster VI.	229
5.70. Infrared spectrum of compound 11	230
5.71. Infrared spectrum of compound 14	231
5.72. Infrared spectrum of compound 15	232
5.73. Infrared spectrum of $[\text{Cu}(\text{pyridine})_2\text{Cl}_2]$	233
5.74. Infrared spectrum of $[\text{CuL}^1\text{Cl}]_4$	235
6.1. Molecular structure of cluster I (ellipsoids set at the 50% probability level, <i>left</i>) and a photograph of a suspension of cluster I in denatured ethanol (<i>right</i>).	238
6.2. Structurally characterized copper(II) complexes that derived from cluster I.	239
6.3. Cluster II and copper(I) complexes that derived from cluster I.	239
6.4. Proposed formation of the ligand of cluster II.	239
6.5. Isolated compounds that could not be structurally characterized.	240
6.6. Molecular structures of the "solvent clusters" with methanol, acetonitrile, dmf and dmso as ligands.	241
6.7. Molecular structure of $[\text{CuClL}^1]_4$	244
6.8. Molekülstruktur von Cluster I.	246
6.9. Vollständig charakterisierte Kupfer(II)-Komplexe, die aus Cluster I entstanden.	247
6.10. Cluster II und Kupfer(I)-Komplexe, die ausgehend von Cluster I gebildet wurden.	247
6.11. Vorgeschlagene Bildung des Liganden von Cluster II.	248
6.12. Isolierte Verbindungen, die nicht vollständig charakterisiert werden konnten.	248

7. List of Figures

6.13. Strukturen der „Lösungsmittelcluster“ mit Methanol, Acetonitril, DMF and DMSO.	250
6.14. Molekülstruktur von 1	253

8. List of Tables

2.1.	Hydroxylation of cyclohexane with H ₂ O ₂ and cluster I. . . .	28
2.2.	Results of the oxygenation of cyclohexane with increasing amounts of cluster I as catalyst.	43
2.3.	Average results of selective oxidation of p-chlorbenzylic alcohol with tert-butylhydroperoxide to the corresponding aldehyde.	45
3.1.	Reaction conditions and average yields of the oxygenation of cyclohexane with "solvent clusters".	83
3.2.	Reaction conditions and average results for the oxygenation of adamantane.	85
5.1.	Crystal data and structure refinement for cluster I.	112
5.2.	Selected bond lengths [Å] and angles [°] for cluster I.	113
5.3.	Crystal data and structure refinement for cluster I (bromide version).	115
5.4.	Selected bond lengths [Å] and angles [°] for cluster I (bromide version).	116
5.5.	Crystal data and structure refinement for cluster II.	118
5.6.	Selected bond lengths [Å] and angles [°] for cluster II.	119
5.7.	Crystal data and structure refinement for compound 2	120
5.8.	Selected bond lengths [Å] and angles [°] for compound 2 . . .	121
5.9.	Crystal data and structure refinement for compound 3	122
5.10.	Selected bond lengths [Å] and angles [°] for compound 3 . . .	123
5.11.	Crystal data and structure refinement for compound 4a	124
5.12.	Selected bond lengths [Å] and angles [°] for compound 4a . . .	125
5.13.	Crystal data and structure refinement for compound 7	126
5.14.	Selected bond lengths [Å] and angles [°] for compound 7 . . .	127
5.15.	Crystal data and structure refinement for HC ₁₃ H ₁₉ NOCl. . .	128
5.16.	Selected bond lengths [Å] and angles [°] for HC ₁₃ H ₁₉ NOCl. .	129
5.17.	Crystal data and structure refinement for [Zn(benz ₂ dba)Cl ₂].	130
5.18.	Selected bond lengths [Å] and angles [°] for [Zn(benz ₂ dba)Cl ₂].	131
5.19.	Crystal data and structure refinement for [Cu(aniline) ₂ Cl ₂].	132
5.20.	Selected bond lengths [Å] and angles [°] for [Cu(aniline) ₂ Cl ₂].	133

8. List of Tables

5.21.	Crystal data and structure refinement for $[\text{Cu}_4\text{OCl}_6(\text{MeOH})_4] \cdot \text{MeOH}$.	134
5.22.	Selected bond lengths [\AA] and angles [$^\circ$] for $[\text{Cu}_4\text{OCl}_6(\text{MeOH})_4] \cdot \text{MeOH}$.	135
5.23.	Crystal data and structure refinement for $[\text{Cu}_4\text{OCl}_6(\text{CH}_3\text{CN})_4] \cdot 2\text{CH}_3\text{CN}$.	136
5.24.	Selected bond lengths [\AA] and angles [$^\circ$] for $[\text{Cu}_4\text{OCl}_6(\text{CH}_3\text{CN})_4] \cdot 2\text{CH}_3\text{CN}$.	138
5.25.	Crystal data and structure refinement for $[\text{Cu}_4\text{OCl}_6(\text{dmsO})_4] \cdot \text{dmsO}$.	139
5.26.	Selected bond lengths [\AA] and angles [$^\circ$] for $[\text{Cu}_4\text{OCl}_6(\text{dmsO})_4] \cdot \text{dmsO}$.	140
5.27.	Crystal data and structure refinement for $[\text{Cu}_4\text{OCl}_6(\text{dmf})_4]$.	142
5.28.	Selected bond lengths [\AA] and angles [$^\circ$] for $[\text{Cu}_4\text{OCl}_6(\text{dmf})_4]$.	143
5.29.	Crystal data and structure refinement for $[\text{Cu}(\text{MeOH})_2\text{Cl}_2]$.	144
5.30.	Selected bond lengths [\AA] and angles [$^\circ$] for $[\text{Cu}(\text{MeOH})_2\text{Cl}_2]$.	146
5.31.	Crystal data and structure refinement for cluster III.	148
5.32.	Selected bond lengths [\AA] and angles [$^\circ$] for cluster III.	149
5.33.	Crystal data and structure refinement for compound 3c .	151
5.34.	Selected bond lengths [\AA] and angles [$^\circ$] for compound 3c .	152
5.35.	Crystal data and structure refinement for compound 3d .	153
5.36.	Selected bond lengths [\AA] and angles [$^\circ$] for compound 3d .	154
5.37.	Crystal data and structure refinement for cluster IV.	155
5.38.	Selected bond lengths [\AA] and angles [$^\circ$] for cluster IV.	156
5.39.	Crystal data and structure refinement for $[\text{CuL}^5_4]\text{Cl}_2$.	158
5.40.	Selected bond lengths [\AA] and angles [$^\circ$] for $[\text{CuL}^5_4]\text{Cl}_2$.	159
5.41.	Crystal data and structure refinement for cluster VI.	160
5.42.	Selected bond lengths [\AA] and angles [$^\circ$] for cluster VI.	161
5.43.	Crystal data and structure refinement for HL^3Cl .	163
5.44.	Selected bond lengths [\AA] and angles [$^\circ$] for HL^3Cl .	164
5.45.	Crystal data and structure refinement for HL^4Cl .	164
5.46.	Selected bond lengths [\AA] and angles [$^\circ$] for HL^4Cl .	166
5.47.	Crystal data and structure refinement for HL^5Cl .	166
5.48.	Selected bond lengths [\AA] and angles [$^\circ$] for HL^5Cl .	167
5.49.	Crystal data and structure refinement for compound 7 .	168
5.50.	Selected bond lengths [\AA] and angles [$^\circ$] for compound 7 .	170
5.51.	Crystal data and structure refinement for compound 8 .	170
5.52.	Selected bond lengths [\AA] and angles [$^\circ$] for compound 8 .	172
5.53.	Crystal data and structure refinement for compound 9 .	172
5.54.	Selected bond lengths [\AA] and angles [$^\circ$] for compound 9 .	173
5.55.	Crystal data and structure refinement for compound 10 .	174
5.56.	Selected bond lengths [\AA] and angles [$^\circ$] for compound 10 .	175

5.57.	Crystal data and structure refinement for compound 11 .	176
5.58.	Selected bond lengths [Å] and angles [°] for compound 11 .	177
5.59.	Crystal data and structure refinement for compound 12 .	178
5.60.	Selected bond lengths [Å] and angles [°] for compound 12 .	179
5.61.	Crystal data and structure refinement for compound 13 .	180
5.62.	Selected bond lengths [Å] and angles [°] for compound 13 .	181
5.63.	Crystal data and structure refinement for compound 14 .	182
5.64.	Selected bond lengths [Å] and angles [°] for compound 14 .	183
5.65.	Crystal data and structure refinement for cluster I recrystallized.	184
5.66.	Selected bond lengths [Å] and angles [°] for cluster I recrystallized.	185
5.67.	Crystal data and structure refinement for compound 1 .	188
5.68.	Selected bond lengths [Å] and angles [°] for compound 1 .	189
5.69.	Crystal data and structure refinement for compound 3 .	190
5.70.	Selected bond lengths [Å] and angles [°] for compound 3 .	191
5.71.	Crystal data and structure refinement for compound 4 .	192
5.72.	Selected bond lengths [Å] and angles [°] for compound 4 .	193
5.73.	Crystal data and structure refinement for (HL ¹)-(C ₇ H ₇ NHCOO).	194
5.74.	Crystal data and structure refinement for (HL ¹)-(C ₇ H ₇ NHCOO).	195
5.75.	Infrared data of cluster I.	197
5.76.	Infrared data of the bromide version of cluster I.	198
5.77.	Infrared data of cluster II.	199
5.78.	Infrared data of compound 1 .	200
5.79.	Infrared data of compound 2 .	201
5.80.	Infrared data of compound 3 .	202
5.81.	Infrared data of compound 4 .	203
5.82.	Infrared data of compound 5 .	204
5.83.	Infrared data of compound 6 .	205
5.84.	Infrared data of compound 7 .	206
5.85.	Infrared data of the aniline complex.	207
5.86.	Infrared data of [ZnL ¹ ₂ Cl ₂].	208
5.87.	Infrared data of compound 2a .	210
5.88.	Infrared data of cluster III.	211
5.89.	Infrared data of compound 2d .	212
5.90.	Infrared data of compound 3a .	213
5.91.	Infrared data of compound 3b .	214
5.92.	Infrared data of compound 3c .	215
5.93.	Infrared data of compound 3d .	216
5.94.	Infrared data of compound 4a .	217

8. List of Tables

5.95. Infrared data of compound 4b	218
5.96. Infrared data of compound 4c	219
5.97. Infrared data of compound 5a	220
5.98. Infrared data of compound 5b	221
5.99. Infrared data of compound 5e	222
5.100. Infrared data of $[\text{CuL}^5_4]\text{Cl}_2$	223
5.101. Infrared data of cluster V.	224
5.102. Infrared data of compound 6a	225
5.103. Infrared data of compound 6b	226
5.104. Infrared data of compound 6c	227
5.105. Infrared data of compound 6d	228
5.106. Infrared data of cluster VI.	229
5.107. Infrared data of compound 11	230
5.108. Infrared data of compound 14	231
5.109. Infrared data of compound 15	232
5.110. Infrared data of $[\text{Cu}(\text{pyridine})_2\text{Cl}_2]$	233
5.111. Infrared data of $[\text{CuL}^1\text{Cl}]_4$	235

9. Bibliography

- [1] A. F. Holleman and N. Wiberg. *Lehrbuch der Anorganischen Chemie*. 102nd ed. Berlin, New York: de Gruyter, **2007**, pp. 1434–1452.
- [2] J. Sobolewski, R. Lavinsky, D. Weinrich, B. Scheller, M. Roarke, and J. Freilich. <http://www.mineralienatlas.de/>. **2010**.
- [3] W. Kaim and B. Schwederski. *Bioanorganische Chemie*. 4th ed. Marburg: Teubner, **2005**.
- [4] W. Kaim and J. Rall. *Angew. Chem. Int. Ed.* 35.1, **1996**, pp. 43–60.
- [5] L. M. Mirica, X. Ottenwaelder, and T. D. P. Stack. *Chem. Rev.* 104.2, **2004**, pp. 1013–45.
- [6] C. F. Thurston. *Microbiology* 140.1994, **1994**, pp. 19–26.
- [7] H. Decker, T. Schweikardt, and F. Tuzek. *Angew. Chem. Int. Ed.* 45.28, **2006**, pp. 4546–50.
- [8] K. Paraskevopoulos, M. Sundararajan, R. Surendran, M. a. Hough, R. R. Eady, I. H. Hillier, and S. S. Hasnain. *Dalton Trans.* 25, **2006**, pp. 3067–76.
- [9] Y. Matoba, T. Kumagai, A. Yamamoto, H. Yoshitsu, and M. Sugiyama. *J. Biol. Chem.* 281.13, **2006**, pp. 8981–90.
- [10] N. Hakulinen, L.-L. Kiiskinen, K. Kruus, M. Saloheimo, A. Paananen, A. Koivula, and J. Rouvinen. *Nature structural & molecular biology* 9.8, **2002**, pp. 601–5.
- [11] E. I. Solomon, U. M. Sundaram, and T. E. Machonkin. *Chem. Rev.* 96.7, **1996**, pp. 2563–2606.
- [12] F. Xu. *The Encyclopedia of Bioprocessing Technology: Fermentation, Biocatalysis and Bioseparation*. Ed. by M. C. Flickinger and S. W. Drew. New York: John Wiley & Sons, **1999**, pp. 1545–1554.
- [13] T. Sandmeyer. *Ber. Dtsch. Chem. Ges.* 17, **1884**, pp. 1633–1635.
- [14] M. Baerns, A. Behr, A. Brehm, J. Gmehling, H. Hofmann, U. Onken, and A. Renken. *Technische Chemie*. 1st ed. Weinheim: Wiley-VCH Verlag GmbH, **2006**, p. 591.
- [15] P. Siemsen, R. C. Livingston, and F. Diederich. *Angew. Chem. Int. Ed.* 39, **2000**, pp. 2632–2657.
- [16] C. Glaser. *Ber. Dtsch. Chem. Ges.* 2, **1869**, pp. 422–425.

9. Bibliography

- [17] G. Eglington and R. Kocovsky Galbraith. *J. Chem. Soc.* **1959**, pp. 889–896.
- [18] M. C. Kozlowski. *Copper Oxygen Chemistry*. Ed. by K. D. Karlin and S. Itoh. 4th ed. New York: Wiley & Sons Inc., **2011**, pp. 361–429.
- [19] J. Allen. *CHEMICAL CLASSICS Some Founders of the Chemical Industry, Men to be remembered*. London and Manchester: Sherratt & Hughes, **1906**.
- [20] A. P. Amrute, G. O. Larrazábal, C. Mondelli, and J. Pérez-Ramírez. *Angew. Chem. Int. Ed.* **52**, **2013**, pp. 9772–9775.
- [21] M. Baerns, A. Behr, A. Brehm, J. Gmehling, H. Hofmann, U. Onken, and A. Renken. *Technische Chemie*. 1st ed. Weinheim: Wiley-VCH Verlag GmbH, **2006**, p. 573.
- [22] S. Ito, T. Yamasaki, N. Okada, S. Okino, and K. Sasaki. *J. Chem. Soc., Perkin Trans. 2*, **1988**, pp. 285–293.
- [23] K. Takaki, Y. Shimasaki, T. Shishido, and K. Takehira. *Bull. Chem. Soc. Jpn.* **75**, **2002**, pp. 311–317.
- [24] N. Komiya, T. Naota, and S.-I. Murahashi. *Tetrahedron Lett.* **37**, **1996**, pp. 1633–1636.
- [25] S.-I. Murahashi, N. Komiya, Y. Hayashi, and T. Kumano. *Pure Appl. Chem.* **73**, **2001**, pp. 311–314.
- [26] S. J. Firbank, M. S. Rogers, C. M. Wilmot, D. M. Dooley, M. a. Halcrow, P. F. Knowles, M. J. McPherson, and S. E. Phillips. *Proceedings of the National Academy of Sciences of the United States of America* **98.23**, **2001**, pp. 12932–7.
- [27] J. A. Bertrand and J. A. Kelley. *Inorg. Chem.* **879.5**, **1966**, pp. 4746–4747.
- [28] H. tom Dieck and H.-P. Brehm. *Chem. Ber.* **102**, **1969**, pp. 3577–3583.
- [29] H. Bock, H. tom Dieck, H. Pyttlik, and M. Schnöller. *ZAAC* **357**, **1968**, pp. 54–61.
- [30] J. A. Bertrand and J. A. Kelley. *Inorg. Chim. Acta* **4.4**, **1970**, pp. 526–528.
- [31] H Dieck. *Inorg. Chim. Acta* **7.7**, **1973**, pp. 397–403.
- [32] B. T. Kilbourn and J. D. Dunitz. *Inorg. Chim. Acta* **480.I**, **1967**, pp. 209–216.
- [33] J. A. Bertrand. *Inorg. Chem.* **6**, **1967**, pp. 495–498.
- [34] J. J. de Boer, D. Bright, and J. N. Helle. *Acta Crystallogr. Sect. B* **28.11**, **1972**, pp. 3436–3437.
- [35] N. S. Gill and M. Sterns. *Inorg. Chem.* **9.7**, **1970**, pp. 1619–1625.
- [36] F. A. Cotton and G. Wilkinson. *Advanced Inorganic Chemistry*. 5th ed. New York: Wiley & Sons Inc., **1988**.

- [37] J. A. Bertrand, J. A. Kelly, and C. E. Kirkwood. *Chem. Commun.* **1968**, pp. 1329–1330.
- [38] M. Dey, C. P. Rao, P. K. Saarenketo, and K. Rissanen. *Inorg. Chem. Comm.* 5.6, **2002**, pp. 380–383.
- [39] C. Mukherjee, T. Weyhermüller, E. Bothe, E. Rentschler, and P. Chaudhuri. *Inorg. Chem.* 46.23, **2007**, pp. 9895–9905.
- [40] S. Thakurta, P. Roy, R. J. Butcher, M. Salah El Fallah, J. Tercero, E. Garribba, and S. Mitra. *Eur. J. Inorg. Chem.* 2009.29-30, **2009**, pp. 4385–4395.
- [41] R. Wegner, M Gottschaldt, H Görls, E. G. Jäger, and D Klemm. *Chem. Eur. J.* 7.10, **2001**, pp. 2143–57.
- [42] K. Skorda, T. C. Stamatatos, A. P. Vafiadis, A. T. Lithoxidou, A. Terzis, S. P. Perlepes, J. Mrozinski, C. P. Raptopoulou, J. C. Plakatouras, and E. G. Bakalbassis. *Inorg. Chim. Acta* 358.3, **2005**, pp. 565–582.
- [43] S. V. Voitekhovich, P. N. Gaponik, A. S. Lyakhov, J. V. Filipova, A. G. Sukhanova, G. T. Sukhanov, and O. a. Ivashkevich. *Tetrahedron Letts* 50.21, **2009**, pp. 2577–2579.
- [44] A. Ali, G. Davies, S. Larsen, and J. Zubieta. *Inorg. Chim. Acta* 194, **1992**, pp. 139–149.
- [45] G. M. Chiarella, D. Y. Melgarejo, A. V. Prosvirin, K. R. Dunbar, and J. P. Fackler. *J. Clust. Sci.* 21.3, **2010**, pp. 551–565.
- [46] P. F. Kelly, S.-m. Man, A. M. Z. Slawin, and K. W. Waring. *Polyhedron* 18, **1999**, pp. 3173–3179.
- [47] H. Yamada, K., Oguma, E., Nakagawa, H., Kawazura. *Chem. Pharm. Bull.* 42.2, **1994**, pp. 368–370.
- [48] A. K. Mishra and S. Verma. *Inorg. Chem.* 49.8, **2010**, pp. 3691–3.
- [49] T. F. Emenova, I. V. Rozhdestvenskaya, S. K. Filatov, and L. P. Verasova. *Doklady Akademii Nauk SSSR* 304, **1989**, pp. 427–430.
- [50] M. de Graaf.
<http://maurice.strahlen.org/minerals/pics/Ponomarevite.jpg>. **2013**.
- [51] K. Yu. Demyanchuk. IVS FEB RAS.
<http://geoportalkscnet.ru/volcanoes/imgs/1841.jpg>. **2013**.
- [52] H. H. Monfared, J. Sanchiz, Z. Kalantari, and C. Janiak. *Inorg. Chim. Acta* 362.10, **2009**, pp. 3791–3795.
- [53] M. V. Kirillova, Y. N. Kozlov, L. S. Shul'pina, O. Y. Lyakin, A. M. Kirillov, E. P. Talsi, A. J. Pombeiro, and G. B. Shul'pin. *J. Catal.* 268.1, **2009**, pp. 26–38.
- [54] A. M. Kirillov, M. N. Kopylovich, M. V. Kirillova, E. Y. Karabach, M. Haukka, M. F. C. G. da Silva, and A. J. L. Pombeiro. *Adv. Synth. Catal.* 348.1-2, **2006**, pp. 159–174.

9. Bibliography

- [55] S. Jammi and T. Punniyamurthy. *Eur. J. Inorg. Chem.* 2009.17, **2009**, pp. 2508–2511.
- [56] H. Sun, K. Harms, and J. Sundermeyer. *J. Am. Chem. Soc.* 126.31, **2004**, pp. 9550–1.
- [57] A. M. Kirillov, M. N. Kopylovich, M. V. Kirillova, M. Haukka, M. F. C. G. da Silva, and A. J. L. Pombeiro. *Angew. Chem. Int. Ed.* 44.28, **2005**, pp. 4345–9.
- [58] S. Löw. *Masterthesis (Justus-Liebig-Universität Gießen)*, **2010**.
- [59] J. A. Bertrand and J. A. Kelley. *Inorg. Chem.* 8.9, **1969**, pp. 1982–1985.
- [60] M. E. Lines, A. P. Ginsberg, R. I. Martin, and R. C. Sherwood. *J. Chem. Phys.* 57.1, **1972**, pp. 1–19.
- [61] H. Wong, H. tom Dieck, C. J. O'Connor, and E. Sinn. *J. C. S. Dalton* 5, **1980**, p. 786.
- [62] W. J. Jones, S. Gupta, L. J. Theriot, F. T. Helm, and W. A. Baker. *Inorg. Chem.* 17, **1978**, pp. 87–90.
- [63] J. Reim, K. Griesar, W. Haase, and B. Krebs. *Dalton Trans.* **1995**, pp. 2649–2656.
- [64] H. Oshio, Y. Saito, and T. Ito. *Angew. Chem. Int. Ed.* 36, **1997**, pp. 2673–2675.
- [65] J. W. Hall, W. E. Estes, E. D. Estes, R. P. Scaringe, and W. E. Hatfield. *Inorg. Chem.* 16, **1977**, pp. 1572–1574.
- [66] J. A. Barnes, G. W. J. Inman, and W. E. Hatfield. *Inorg. Chem.* 10.8, **1971**, pp. 1725–1727.
- [67] M. C. Kozlowski. *Copper-Oxygen-Chemistry*. Ed. by K. D. Karlin and S. Itoh. 4th ed. New York: Wiley & Sons Inc., **2011**, pp. 131–168.
- [68] C. Würtele, O. Sander, V. Lutz, T. Waitz, F. Tuczek, and S. Schindler. *J. Am. Chem. Soc.* 131, **2009**, pp. 7544–7545.
- [69] C. Würtele, E. Gaoutchenova, K. Harms, M. C. Holthausen, J. Sundermeyer, and S. Schindler. *Angew. Chem. Int. Ed.* 45, **2006**, pp. 3867–3869.
- [70] M. Weitzer, S. Schindler, G. Brehm, S. Schneider, E. Hörmann, B. Jung, S. Kaderli, and A. D. Zuberbühler. *Inorg. Chem.* 42, **2003**, pp. 1800–1806.
- [71] M. Schatz, M. Becker, O. Walter, G. Liehr, and S. Schindler. *Inorg. Chim. Acta* 324, **2001**, pp. 173–179.
- [72] S. Schindler. *Eur. J. Inorg. Chem.* **2000**, pp. 2311–2326.
- [73] G. Zi, L. Xiang, Y. Zhang, Q. Wang, and Z. Zhang. *Appl. Organometal. Chem.* 2.2, **2007**, pp. 177–182.
- [74] R. Belford, D. E. Fenton, and M. R. Truter. *J.C.S. Dalton*, **1972**, pp. 2345–2350.

- [75] H. Remy and H. Laves. *Ber. Dtsch. Chem. Ges.* 61, **1933**, pp. 401–407.
- [76] R. D. Willett and M. L. Larsen. *Inorg. Chim. Acta* 5, **1971**, pp. 175–179.
- [77] S. H. Oakeley, M. P. Coles, and P. B. Hitchcock. *Inorg. Chem.* 43, **2004**, pp. 5168–5172.
- [78] S.-L. Zheng, M. Messerschmidt, and P. Coppens. *Angew. Chem. Int. Ed.* 44, **2005**, pp. 4614–4617.
- [79] M. Angels Carvajal, S. Alvarez, and J. J. Novoa. *Chem. Eur. J.* 10, **2004**, pp. 2117–2132.
- [80] G. M. Chiarella, D. Y. Melgarejo, A. Rozanski, P. Hempte, L. M. Perez, C. Reber, and J. P. J. Fackler. *Chem. Commun.* 46, **2010**, pp. 136–138.
- [81] M. V. Kirillova, Y. N. Kozlov, L. S. Shul’pina, O. Y. Lyakin, A. M. Kirillov, E. P. Talsi, A. J. Pombeiro, and G. B. Shul’pin. *J. Catal.* 268.1, **2009**, pp. 26–38.
- [82] M. Bukowska-Strzyzewska and J. Skoweranda. *Acta Crystallogr. Sect. C* 43, **1987**, pp. 2290–2293.
- [83] R. J. Williams, D. T. Cromer, and W. H. Watson. *Acta Crystallogr. Sect. B* 27, **1971**, pp. 1619–1624.
- [84] J. Giantsidis, M. M. Turnbull, C. P. Landee, and F. M. Woodward. *J. Coord. Chem.* 55, **2002**, pp. 393–402.
- [85] M. Dunaj-Jurčo, J. Kožíšek, A. Ancyškina, G. Ondrejovič, D. Makánová, and J. Gažo. *J. Chem. Soc. Chem. Commun.* **1979**, pp. 654–655.
- [86] R. D. Willett and K. Chang. *Inorg. Chim. Acta* 4, **1970**, pp. 447–451.
- [87] A. Laouiti, M. M. Rammah, M. B. Rammah, J. Marrot, F. Couty, and G. Evano. *Org. Lett.* 14, **2012**, pp. 6–9.
- [88] W. Wu, X. He, Z. Fu, Y. Liu, Y. Wang, X. Gong, X. Deng, H. Wu, Y. Zou, N. Yu, and D. Yin. *J. Catal.* 286, **2012**, pp. 6–12.
- [89] Y. Ito, T. Konoike, T. Harada, and T. Saegusa. *J. Am. Chem. Soc.* 99, **1977**, pp. 1487–1493.
- [90] H. Sun, X. Li, and J. Sundermeyer. *J. Mol. Catal. A* 240, **2005**, pp. 119–122.
- [91] S. Kim and P. H. Lee. *J. Org. Chem.* 77, **2012**, pp. 215–220.
- [92] Y. Liu and J.-W. Sun. *J. Org. Chem.* 77, **2012**, pp. 1191–1197.
- [93] A. El-Toukhy, G.-Z. Cai, G. Davies, T. R. Gilbert, K. D. Onan, and M. Veidis. *J. Am. Chem. Soc.* 106, **1984**, pp. 4596–4605.
- [94] M. A. El-Sayed, A. Abu-Raqabah, G. Davies, and A. El-Thouky. *Inorg. Chem.* 28.10, **1989**, pp. 1909–1914.

9. Bibliography

- [95] Q. Liu, P. Wu, Y. Yang, Z. Zeng, J. Liu, H. Yi, and A. Lei. *Angew. Chem. Int. Ed.* 51, **2012**, pp. 4666–4670.
- [96] M. C. Kozlowski. *Copper Oxygen Chemistry*. Ed. by K. D. Karlin and S. Itoh. 4th ed. New York: Wiley & Sons Inc., **2011**, pp. 361–444.
- [97] E. Boess, C. Schmitz, and M. Klussmann. *J. Am. Chem. Soc.* 134, **2012**, pp. 5317–5325.
- [98] H.-Q. Do, H. Tran-Vu, and O. Daugulis. *Organometallics* 31, **2012**, pp. 7816–7818.
- [99] M. LARGERON and M.-B. Fleury. *Angew. Chem. Int. Ed.* 51, **2012**, pp. 5409–5412.
- [100] C. P. Frazier, J. R. Engelking, and J. R. De Alaniz. *J. Am. Chem. Soc.* 133, **2011**, pp. 10430–10433.
- [101] G. M. Sheldrick. *Acta Crystallogr. Sect. A* 64, **2008**, pp. 112–122.
- [102] T. Horváth, J. Kaizer, and G. Speier. *J. Mol. Catal. A* 215, **2004**, pp. 9–15.
- [103] S. Löw, J. Becker, C. Würtele, A. Miska, C. Kleeberg, U. Behrens, O. Walter, and S. Schindler. *Chem. Eur. J.* 19.17, **2013**, pp. 5342–51.
- [104] A. S. Batsanov, R. L. Giles, and A. Whiting. *Private Communication*, **2005**, CCDC–Number 283548.
- [105] J. Gouteron, S. Jeannin, Y. Jeannin, J. Livage, and C. Sanchez. *Inorg. Chem.* 73, **1984**, pp. 3387–3393.
- [106] M. Bolte. *Private Communication*, **2011**, CCDC–Number: 836368.
- [107] S. T. Rao and M. Sundaralingam. *Acta Crystallogr. Sect. B* 25.12, **1969**, pp. 2509–2515.
- [108] H. W. Smith, D. Mastropaolo, A. Camerman, and N. Camerman. *J. Chem. Cryst.* 24.4, **1994**, pp. 239–242.
- [109] J. R. Black, W. Levason, and M. Webster. *Acta Crystallogr. Sect. C* 51.4, **1995**, pp. 623–625.
- [110] I. Csöreg, P. Kierkegaard, and R. Norrestam. *Acta Cryst.* 2, **1975**, pp. 314–317.
- [111] P. G. Jones and O. Crespo. *Acta Crystallogr. Sect. C* 54.1, **1998**, pp. 18–20.
- [112] J. M. Knaust, D. A. Knight, and S. W. Keller. *J. Chem. Cryst.* 33.11, **2003**, pp. 813–823.
- [113] E. Colacio, R. Kivekäs, F. Lloret, M. Sunberg, J. Suarez-Varela, M. Bardají, and A. Laguna. *Inorg. Chem.* 41.20, **2002**, pp. 5141–9.
- [114] R. R. Gagné, L. M. Henling, and T. J. Kistenmacher. *Inorg. Chem.* 19.3, **1980**, pp. 1226–1231.
- [115] R. R. Gagné, C. A. Koval, and T. J. Smith. *J. Am. Chem. Soc.* 99.25, **1977**, pp. 8367–8368.

- [116] R. R. Gagné, C. L. Spiro, T. J. Smith, C. A. Hamann, W. R. Thies, and A. K. Shiemke. *J. Am. Chem. Soc.* 2.3, **1981**, pp. 4073–4081.
- [117] P. J. van Koningsbruggen, J. G. Haasnoot, H. Kooijman, J. Reedijk, and A. L. Spek. *Inorg. Chem.* 36.11, **1997**, pp. 2487–2489.
- [118] X.-M. Zhang and R.-Q. Fang. *Inorg. Chem.* 44.11, **2005**, pp. 3955–9.
- [119] J.-M. Zheng, S. R. Batten, and M. Du. *Inorg. Chem.* 44.10, **2005**, pp. 3371–3.
- [120] M. Massaux, M. J. Bernard, and M.-T. LeBihan. *Acta Crystallogr. Sect. B* 27, **1971**, p. 2419.
- [121] P. Healy, J. D. Kildea, B. W. Skelton, and A. H. White. *Aust. J. Chem.* 42, **1989**, p. 79.
- [122] R. D. Willett and R. E. Rundle. *J. Chem. Phys.* 40.3, **1964**, p. 838.
- [123] L. F. Kirpichnikova, A. Pietraszko, W. Bednarski, S. Waplak, and A. U. Sheleg. *Kristallografiya (Russ.) (Crystallogr. Rep.)* 49, **2004**, p. 92.
- [124] L. Lu and M. Zhu. *Private Communication*, **2003**, CCDC-Number: 224299.
- [125] F. De Angelis, S. Fantacci, A. Sgamellotti, E. Cariati, R. Ugo, and P. C. Ford. *Inorg. Chem.* 45.26, **2006**, pp. 10576–84.
- [126] A. Kobayashi, K. Komatsu, H. Ohara, W. Kamada, Y. Chishina, K. Tsuge, H.-C. Chang, and M. Kato. *Inorg. Chem.* 52.22, **2013**, pp. 13188–98.
- [127] K. R. Kyle, W. E. Palke, and P. C. Ford. *Coord. Chem. Rev.* 97, **1990**, pp. 35–46.
- [128] C. K. Ryu, K. R. Kyle, and P. C. Ford. *Inorg. Chem.* 30.21, **1991**, pp. 3982–3986.
- [129] P. C. Ford, E. Cariati, and J. Bourassa. *Chemical reviews* 99.12, **1999**, pp. 3625–3648.
- [130] G. Davies and M. A. El-Sayed. *Inorg. Chem.* 22.9, **1983**, pp. 1257–1266.
- [131] M. R. Churchill, I. G. Davies, M. A. El-Sayed, J. P. Hutchinson, and M. W. Rupichic. *Inorg. Chem.* 21, **1982**, pp. 995–1001.
- [132] E. Sugahara, M. Paula, I. Vencato, and C. Franco. *J. Coord. Chem.* 39.1, **1996**, pp. 59–70.
- [133] T. H. Kim, G. Park, Y. W. Shin, K.-m. Park, M. Y. Choi, and J. Kim. *Bulletin of the Korean Chemical Society* 29.2, **2008**, pp. 499–502.
- [134] J. C. Dyason, P. C. Healy, L. M. Engelhardt, C. Pakawatchai, V. A. Patrick, C. L. Raston, and A. H. White. *Chem. Soc. Dalton Trans.* **1985**, pp. 831–838.
- [135] A. Abu-Raqabah, G. Davies, and M. A. El-Sayed. *Inorg. Chim. Acta* 192, **1992**, pp. 31–42.

9. Bibliography

- [136] G. Davies, M. A. El-Sayed, and R. E. Fasano. *Inorg. Chim. Acta* 71, **1983**, pp. 95–99.
- [137] A. Davies, Geoffrey, El-Toukhy, K. D. Onan, and M. Veidis. *Inorg. Chim. Acta* 84, **1984**, pp. 41–50.
- [138] A. El-Toukhy, G.-z. Cai, G. Davies, T. R. Gilbert, K. D. Onan, and M. Veidis. *J. Am. Chem. Soc.* 106, **1984**, pp. 4596–4605.
- [139] K. Z. Ismail, M. A. El-Sayed, A.-M. Al-Kouraty, and G. Davies. *Inorg. Chim. Acta* 217, **1994**, pp. 85–92.
- [140] K. D. Onan, M. Veidis, G. Davies, M. A. El-Sayed, and A. El-Thouky. *Inorg. Chim. Acta* 81, **1984**, pp. 7–13.
- [141] G. Margraf, J. W. Bats, M. Bolte, H.-w. Lerner, and M. Wagner. *Chem. Commun.* 8.8, **2003**, pp. 956–7.
- [142] J. Reim and B. Krebs. *Angew. Chem. Int. Ed.* 33.19, **1994**, pp. 1969–1971.
- [143] J. Reim, R. Werner, W. Haase, and B. Krebs. *Chem. Eur. J.* 4.2, **1998**, pp. 289–298.
- [144] G. F. Endres, A. S. Hay, and J. W. Eustance. *J. Org. Chem.* 28.7, **1962**, pp. 1300–1305.
- [145] M. Hesse, H. Meier, and B. Zeeh. *Spektroskopische Methoden in der organischen Chemie*. 7th ed. Stuttgart: Georg Thieme Verlag, **2005**, pp. 1–32.
- [146] R. Wang, W.-P. Su, R. Cao, Y.-J. Zhao, and M.-C. Hong. *Chin. J. Struct. Chem.* 20, **2001**, p. 37.
- [147] H.-L. Zhu, C.-X. Ren, and X.-M. Chen. *J. Coord. Chem.* 55, **2002**, pp. 667–673.
- [148] G. a. van Albada, I. Mutikainen, U. Turpeinen, and J. Reedijk. *Polyhedron* 23.6, **2004**, pp. 993–998.
- [149] A. S. Komaei, G. A. van Albada, I. Mutikainen, U. Turpeinen, and J. Reedijk. *Polyhedron* 18, **1999**, pp. 1991–1997.
- [150] M. F. Haddow, H. Kara, and G. R. Owen. *Inorg. Chim. Acta* 362.10, **2009**, pp. 3502–3506.
- [151] I. Tiritiris and W. Kantlehner. *Z. Naturforsch., B: Chem. Sci.* 66, **2011**, p. 104.
- [152] M. M. Olmstead, J. U. Franco, and D. Pham. *Private Communication*, **2008**, CCDC-Number: 698121.

A. Publications

Full Papers

- Reactions of Copper(II) Chloride in Solution: Facile Formation of Tetranuclear Copper Clusters And Other Complexes That Are Relevant in Catalytic Redox Processes
S. Löw, J. Becker, C. Würtele, A. Miska, C. Kleeberg, U. Behrens, O. Walter and S. Schindler, *Chem. Eur. J.* **2013**, 19, 5342-5351
- Investigations Concerning $[\text{Cu}_4\text{OX}_6\text{L}_4]$ -Cluster Formation of CuCl_2 with Amines and in Organic Solvents
S. Löw, J. Becker, U. Behrens, S. Schindler, to be submitted to *Inorg. Chem.*
- Synthesis, Structure and Reactivity of the Compound $[\text{Cu}(\text{C}_7\text{H}_7\text{NH}_2)\text{Cl}]_4$
S. Löw, U. Behrens, S. Schindler, to be submitted to *ZAAC*

Oral Presentations

- "Sauerstoffaktivierung mittels mehrkerniger Kupfercluster"
Stipendiatentreffen des VCI, December 2011 (Marburg)
- "Reaktivität und Sauerstoffaktivierung von Kupfer-Cluster-Komplexen"
8. Koordinationschemikertreffen, February 2012 (Dortmund)
- "Copper(II) chloride: A small molecule with huge complexes"
Kooperations-Workshop Gießen-Padua (*with financial support of the DFG*), February 2014 (Padua)

A. *Publications*

Poster Presentations

- "Polynukleare Kupfercluster als Enzymmodelle"
7. Koordinationschemikertreffen, February 2011 (Stuttgart)
- "Simple Copper Clusters as Enzymatic Models?"
Bioinorganic Chemistry Meeting 2013, February 2013 (Costa Teguisse,
Lanzarote)

**Der Lebenslauf wurde aus der elektronischen
Version der Arbeit entfernt.**

**The curriculum vitae was removed from the
electronic version of the paper.**